DTU Library

Absorption and Desorption Modelling United

Fosbøl, Philip Loldrup

Link back to DTU Orbit

2nd ICEPE 2011

International Conference on Energy Process Engineering

BOOK OF EXTENDED ABSTRACTS

June 20 – 22, 2011 · Frankfurt am Main/Germany

Efficient Carbon Capture for Coal Power Plants

www.ICEPE2011.de
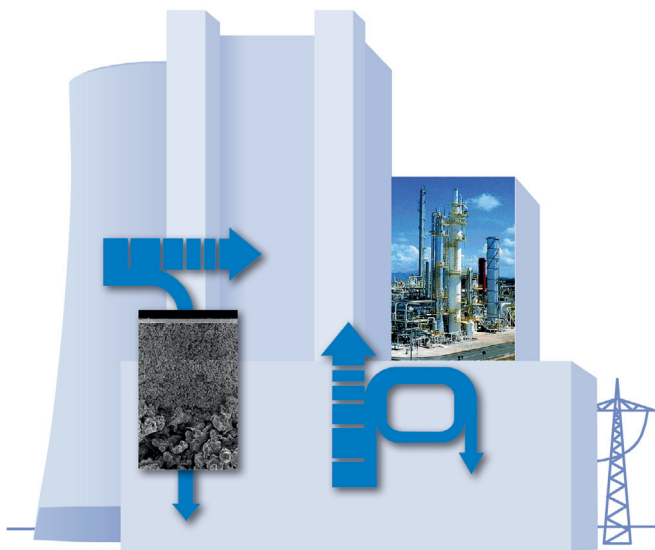
ORGANISED BY

PROCESSNET
EINE INITIATIVE VON DECHEMA UND VDI-GVC

DECHEMA

EFCE
EUROPEAN FEDERATION OF CHEMICAL ENGINEERING

EFCE Event No. 697

IN COOPERATION WITH

VDE · VIK Energie für die Industrie · VGB · AIChE · VDI

COMMITTEES / ORGANIZER
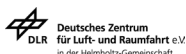
ORGANIZING COMMITTEE

Prof. D. Stolten   Juelich Research Center, Germany (Chairman)
Prof. V. Scherer   Ruhr-University Bochum, Germany (Co-Chairman)
Dr. U. Delfs   VDI e.V., Düsseldorf, Germany
Dr. M. Weber   Juelich Research Center, Germany

HONORARY CHAIRMAN

J. Werther   TU Hamburg-Harburg, Germany

SCIENTIFIC COMMITTEE & SESSION CHAIRS

V. Abetz   Helmholtz-Zentrum Geesthacht, Germany
H.J. Bart   TU Kaiserslautern, Germany
C. Bauer   PSI, Switzerland
B. Epple   TU Darmstadt, Germany
H. Fahlenkamp   TU Dortmund, Germany
M. Gray   American Electric Power, Columbus, USA
M. Grünewald   Ruhr-Universität Bochum, Germany
A. Kather   TU Hamburg-Harburg, Germany
K. Lackner   Columbia University, New York, USA
A. Lyngfelt   Chalmers University Göteborg, Sweden
T. Melin   RWTH Aachen, Germany
W.A. Meulenberg   Juelich Research Center, Germany
M. Modigell   RWTH Aachen, Germany
E. Riensche   Juelich Research Center, Germany
V. Scherer   Ruhr-Universität Bochum, Germany
L. Shen   Southeast University Nanjing, China
H. Spliethoff   TU München, Germany
D. Stolten   Juelich Research Center, Germany
K. Thomsen   TU Denmark, Denmark
E. van Selow   Energy Research Centre of the Netherlands
P. Viebahn   Wuppertal Institute for Climate, Environment
                    and Energy, Germany
M. Weber   Juelich Research Center, Germany
M. Wessling   RWTH Aachen, Germany
F. Wohnsland   VDMA, Germany

ORGANIZER

DECHEMA e.V.

Theodor-Heuss-Allee 25

60486 Frankfurt am Main

Phone   +49 69 7564-125
Fax   +49 69 7564-176
Email: weingaertner@dechema.de

www.icepe2011.de

CONTENTS

LECTURE PROGRAMME

MONDAY, JUNE 20, 2011

09:00	**Registration**	
10:30	**Opening:** D. Stolten, Juelich Research Center, Germany	
10:45	**Address from the IEA: CCS: Global Potential, Status & Challenges:** J. Lipponen, International Energy Agency, France	
11:00	**Industry Perspectives on CCS:** H. Altmann, T. Porsche, Vattenfall Europe Generation AG, Germany	
11:15	**Motivation for and Opportunities of CCS:** K. Lackner, Columbia University, USA	
11:30	**Advanced Power Plant Technology:** H. Spliethoff, TU München, Germany	
11:55	**Carbon Capture Options for Coal Power Plants:** D. Stolten, Juelich Research Center, Germany	
12:20	**Physics and Chemistry of Absorption:** P. Feron, CSIRO, Australia	
12:45	**Lunch**	

P7: Chemical Looping in Power Plants
Session Chair: B. Epple, TU Darmstadt, Germany

14:00	**Review Presentation on Chemical Looping in Power Plants** B. Epple, TU Darmstadt, Germany	
14:30	**Carbon Stripping – A Critical Process Step in the Chemical Looping Combustion of Solid Fuels** M. Kramp, A. Thon, E.U. Hartge, S. Heinrich, <u>J. Werther</u>, TU Hamburg-Harburg, Germany	36
14:55	**Thermodynamic Analysis of a Base Case Coal-fired Chemical Looping Combustion Power Plant** <u>V. Kempkes</u>, A. Kather, TU Hamburg-Harburg, Germany	40
15:20	**High Temperature CO_2 Capture with CaO in a 200 kW_{th} Dual Fluidized Bed Pilot Facility** <u>H. Dieter</u>, C. Hawthorne, M. Zieba, G. Scheffknecht, University of Stuttgart, Germany	41
15:45	**CFD-model of a Fluidized Bed Chemical Looping System: Design of a Heat and Mass Flow Control** <u>H. Kruggel-Emden</u>; S. Wirtz; V. Scherer, Ruhr-Universität Bochum, Germany	45
16:10	**Coffee Break**	

EPL: Economics, Politics & Life Cycle Assessment
Session Chair: P. Viebahn, Wuppertal Institute for Climate, Environment and Energy, Germany

16:40	**Review Presentation on Life Cycle Assessment for Power Plants with CCS** P. Viebahn, Wuppertal Institute for Climate, Environment and Energy, Germany	
17:05	**Carbon Dioxide Capture from Power Generation: Status of Cost and Performance** M. Finkenrath, International Energy Agency, France	
17:30	**LCA of Coal-fired Oxyfuel Power Plants – Cryogenic versus Membrane-Based Air Separation** P. Zapp, Juelich Research Center, Germany	51
17:55 – 18:20	**Emissions from PCC processes** M. Azzi, CSIRO, Australia	
18:30	Get-together, Poster Exhibition (Fingerfood & Beer)	
20:00	End of First Conference Day	

LECTURE PROGRAMME

Page

TUESDAY, JUNE 21, 2011

		Page
09:00	**Physics of Membrane Separation:** M. Wessling, RWTH Aachen, Germany	
09:30	Change rooms	

M2: Materials for Physical Absorption and Chemi-Sorption
Session Chair: M. Grünewald, Ruhr-Universität Bochum, Germany

09:40	**Review Presentation on Physical Absorption Materials** M. Grünewald, Ruhr-Universität Bochum, Germany	
10:10	**Coffee Break**	
10.35	**Ionics Liquids for Carbon Dioxide Capture: Process Selection** J. Albo, J. Cristobal, A. Irabien, University of Cantabria, Spain	108
11:00	**Solubility of CO_2 in Functionalized Ionic Liquid** S. Paul, S. Shunmugavel, A. Riisager, R. Fehrmann, E.H. Stenby, K. Thomsen, TU Denmark, Denmark (t.b.c.)	112
11:25	**Pretreatment of Synthetic Sorbent for Sequentially CO_2 Capture** S. Stendardo, ENEA – C.R. Casaccia, Dept. of Advanced Technologies for Energy and Industry, Italy	113
11:50	**Lunch and Poster Exhibition**	

M3: Inorganic Membranes
Session Chair: W. A. Meulenberg, Juelich Research Center, Germany

13:50	**Review Presentation on Inorganic Membranes** W. A. Meulenberg, Juelich Research Center, Germany	
14:15	**Progress, Performance and Pilot Testing of Post-Combustion CO_2 Capture Membranes at Six Industrial Test Sites** P.H. Raats, M. Huibers, L.A. Daal, KEMA, the Netherlands	
14:40	**Advanced Membrane Design for Oxygen Separation** R. Kriegel, M. Schulz, K. Ritter, L. Kiesel, U. Pippardt, M. Stahn, I. Voigt, Fraunhofer Institute for Ceramic Technologies and Systems, Germany	114
15:05	**Testing of Nanostructured Gas Separation Membranes in the Flue Gas of a Post-Combustion Power Plant** M. Bram, K. Brands, W.A. Meulenberg, H.P. Buchkremer, D. Stöver, Juelich Research Center, Germany; G. Göttlicher, EnBW Energie, Germany; J. Pauls, Helmholtz-Zentrum Geesthacht, Germany	118
15:30	**Coffee break**	

M4: Polymer Membranes for Separation of CO_2
Session Chair: V. Abetz, Helmholtz-Zentrum Geesthacht, Germany

16:00	**Review Presentation on Polymer Membranes for Separation of CO_2 – An overview** V. Abetz, Helmholtz-Zentrum Geesthacht, Germany	
16:25	**Ionic Liquid Coated Zeolite – PDMS Mixed Matrix Membrane for Gas Separation** M. Hussain, A. König, University Erlangen-Nürnberg, Germany	119
16:50 – 17:15	**Functional Materials for CO_2 Separation from Natural and Biogas Streams** C. Staudt, Universität Düsseldorf, Germany	
17:40	End of Conference Day	
19:30	**Conference Dinner with Reception and Poster Award** Dinner Speech: J. Heithoff, RWE Power AG, Germany	

Page

TUESDAY, JUNE 21, 2011

09:00	**Physics of Membrane Separation:** M. Wessling, RWTH Aachen, Germany
09:30	Change rooms

P5: Oxyfuel Combustion with O_2-Transport Membranes
Session Chair: M. Modigell, RWTH Aachen, Germany

09:40	**Review Presentation on Oxyfuel Combustion with O_2-Transport Membranes** M. Modigell, RWTH Aachen, Germany	
10:10	**Coffee Break**	
10.35	**Heat Exchanger Design for an Oxyfuel-Process Utilizing Oxygen from an O_2-Transport Membrane** V. Verbaere, R. Kneer, RWTH Aachen, Germany	125
11:00	**Oxygen Supply for Oxyfuel Power Plants by Oxy-Vac-Jül Process** J. Nazarko, E. Riensche, M. Weber, D. Stolten, Juelich Research Center, Germany	131
11:25	**Pilot Module for Oxygen Separation with BSCF Membranes.** A.Kaletsch, E.M. Pfaff, C. Broeckmann, N. Nauels, M. Modigell, RWTH Aachen, Germany	137
11:50	**Lunch and Poster Exhibition**	

P8: Terrestrial Storage
Session Chair: K. Lackner, Columbia University, USA

13:50	**Review present Presentation on Onshore Storage** K. Lackner, Columbia University, USA	
14:15	**Types and Structures of Onshore CO_2 Deposits** J.P. Gerling, Federal Institute for Geosciences and Natural Resources, Germany	
14:40	**Storage of CO_2 in Saline Aquifers – The ASAP project** R. Luhning, Enbridge Ltd., Canada; J.A.M. Thomson, Norwest Corporation, USA; S. Broek, Hatch Ltd., Canada	144
15:05	**Coupled Processes during CO_2 Storage – Example of the Ketzin Pilot Site** S. Martens, F. Möller, A. Liebscher, S. Lüth, T. Kempka, M. Zimmer, A. Förster, M. Kühn, GFZ Potsdam, Germany	145
15:30	**Coffee break**	

GAS: CCS for Gas Power Plants
Session Chair: C. Bauer, PSI, Switzerland

16:00	**Review Presentation on Results and Methodology of Dynamic Simulation on Hard Coal-, Lignite- and Natural Gas-fired Power Plants** C. Bauer, PSI, Switzerland
16:25	**Hybrid Absorber-Membrane CO_2 Capture** M. Huibers, P.H. Raats, N.A.M. ten Asbroek, KEMA, the Netherlands
16:50	**GT based Power Plants with CO_2 Capture Unit** G.-L. Agostinelli, Alstom Power, Switzerland
17:15	**Approval Procedure for CCS Power Plants** P. Bahlert, PROBIOTIC GmbH, Germany
17:40	End of Conference Day
19:30	**Conference Dinner with Reception and Poster Award** Dinner Speech: J. Heithoff, RWE Power AG, Germany

LECTURE PROGRAMME

POSTER PROGRAMME

New absorbents for an efficient CO_2 separation -EffiCO$_2$-

_Alexander Schraven__, Evonik Degussa GmbH, Marl_; _Thomas Riethmann, Evonik Energy Services GmbH, Essen; Stefanie Rinker, Evonik Degussa GmbH, Marl; Jörn Rolker, Evonik Degussa GmbH, Hanau; Klaus Görner, Universität Duisburg-Essen, Essen; Peter Wasserscheid, Friedrich-Alexander-Universität Erlangen-Nürnberg; Erlangen_

In 2009 the worldwide anthropogenic CO_2 emissions were more than 30 billion tons and the European Union was solely responsible for about 4 billion tons of CO_2 [1]. The energy sector is the biggest industrial CO_2 emitter with roughly 1.5 billion tons of CO_2 within the European Union in 2007[2]. Studies forecast that significant proportions of energy supply will be based on fossil fuels within the next decades[3].

Separation of CO_2 with subsequent usage or storage has a potential for the reduction of CO_2 emissions to the atmosphere in the future and is therefore a promising technology[4]. An efficient process design as well as new and innovative absorbent agents are necessary for reducing the energy losses in e.g. a power plant. These challenges are under examination in the BMBF funded project EffiCO$_2$. Consortium manager of EffiCO$_2$ is the Science-to-Business Center Eco² as part of the strategic research and development department Creavis of Evonik Degussa GmbH. Academic partners in EffiCO$_2$ are the Friedrich-Alexander-University of Erlangen-Nürnberg and the University of Duisburg-Essen. The targets of the project EffiCO$_2$ are the development and the investigation of new and more efficient absorbents for CO_2 separation compared to the state of the art technology (mono ethanol amine, MEA). Within the project new absorbents for CO_2 separation are designed and tailor-made. Within initial screening experiments a structure-activity relationship was derived and new absorbents were designed on the basis of these results.
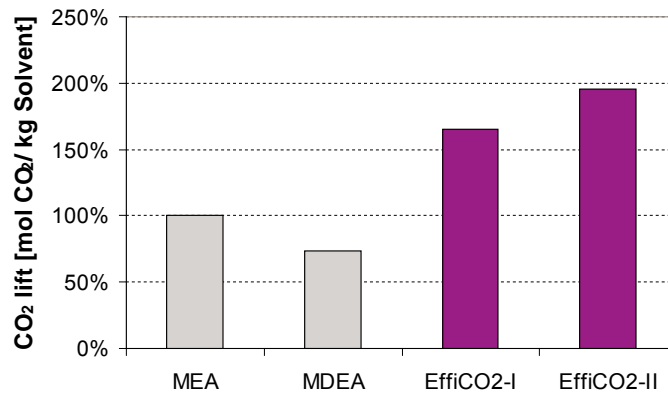
The specific CO_2 lift of state of the art and new absorber solutions (MEA: mono ethanol amine; MDEA: methyl diethanol amine)

Compared to MEA the specific CO_2 lift by solvent weight was approximately doubled. For investigation of the new developed absorption agents with real process conditions a lab scale plant was erected in bypass of a coal fired power plant. Within that test plant thermodynamic and process parameters will be investigated and optimized.

1) Energiedaten –Nationale und Internationale Entwicklung, Bundesministerium für Wirtschaft und Technologie, January 2011

2) CO_2 Emission from Fuel Combustion, International Energy Agency, 2010

3) *International Energy Outlook 2010, U.S. Energy Information Administration, 2010*

4) *Utilisation and Storage of CO_2 , Position paper, DECHEMA,VCI, Frankfurt 2009.*

A rational approach to amine mixture formulation for CO_2 capture applications

Graeme Puxty, CSIRO Energy Technology, PO Box 330, Newcastle NSW 2300, Australia

The desirable properties for an aqueous amine based CO_2 capture solvent are rapid CO_2 mass transfer, large CO_2 absorption capacity and small energy requirement for regeneration. No single amine can deliver good performance in all of these areas as from a chemical perspective these are competing objectives. As a consequence modern amine based solvents are mixtures of amines, each having good performance in at least one of these areas. It is hoped that overall performance of the resulting mixture is an improvement over any of its constituent amines. There is often a synergism between the amines that results in performance better than would be predicted if the individual amine properties were simply "added" together.

The question answered in this work is, given the properties of a range of amines how do you rationally identify which amine mixtures will yield the best performance? A number of parameters define an amine's performance in each category:

Mass transfer –amine-CO_2 reaction rate; CO_2 and amine diffusion; and CO_2 equilibrium partial pressure (p_{CO2}) at absorber conditions (driving force)
Absorption capacity – CO_2 equilibrium partial pressure (and loading) at absorber conditions
Regeneration energy – enthalpy of absorption; CO_2 equilibrium partial pressure (and loading) at absorber conditions; and CO_2 equilibrium partial pressure and loading at desorber conditions

Aqueous amine solutions generally cover a small range of viscosities and thus diffusion coefficients. So if diffusion is neglected amines can be categorised by their performance for each parameter and structural class as follows:

Table 1 Categorisation of amines according to performance for each parameter. Shading indicates desirable performance.

Parameter	Primary and Secondary Amines	Tertiary and Sterically Hindered Amines
Reaction Rate	Fast	Slow
Absorption Capacity	Small	Large
p_{CO2} in Absorber	Small	Large
p_{CO2} in Desorber	Small	Large
Absorption Enthalpy	Large	Small

Table 1 demonstrates why a mixture can yield improved overall performance relative to any single amine. However, this is not always the case and depends upon the priority given to each parameter. Given performance information for a range of individual amines, how is it possible to determine which amines will yield an optimal mixture and desirable trade-off between the parameters? Answering this question is complex and requires taking the details of amine-CO_2 chemistry into account.

In this presentation it will be detailed how meaningful quantitative values can be derived from the amine-CO_2 chemical mechanism to describe the performance of individual amines and amine mixtures for the parameters listed in Table 1. The values are summarised below:

Table 2 The quantitative values used to describe each parameter.

Parameter	Value
Reaction Rate	k – second-order amine-CO_2 reaction rate constant
Absorption Capacity	$K_{AmCOO} = \dfrac{c_{AmCOO}c_H}{c_{CO2}c_{Am}}K_B$, $K_{HCO3} = \dfrac{c_{HCO3}c_H}{c_{CO2}c_{H2O}}K_B$, $K_B = \dfrac{c_{BH}}{c_B c_H}$
p_{CO2} in Absorber	- overall equilibrium constants of carbamate and bicarbonate formation and base protonation
p_{CO2} in Desorber	$\Delta H_{abs} = (\dfrac{c_{AmCOO}}{c_{CO2,tot}})\Delta H_{AmCOO} + (\dfrac{c_{HCO3}}{c_{CO2,tot}})\Delta H_{HCO3} + \Delta H_{CO2}$
Absorption Enthalpy	

This then provides a pathway for the rational design of amine mixtures based on the properties of individual amines. This approach will be described and discussed with examples for a range of amine mixtures. The primary two conclusions that result from this rational design process are:

1) When formulating an amine mixture to maximise rate and capacity it is crucial that the basicity and/or concentration of any tertiary or sterically hindered amine is such that it is the primary proton acceptor in the system. This maximises the CO_2 loading to which primary or secondary amines remain unprotonated and reactive towards CO_2.
2) As has been previously indicated[i], focusing on simply reducing the enthalpy of reaction does not necessarily result in a reduction of regeneration energy requirement. This energy requirement consists of contributions from the enthalpy, solvent heat capacity, CO_2 loading and the CO_2 partial pressure at desorption conditions. Of particular note is that decreasing the enthalpy also decreases p_{CO2} in the desorber and this effect can offset any benefit.

[i] Oexmann, J.; Kather, A., *International Journal of Greenhouse Gas Control* 2010, 4, 36-43.

Carbon Capture with low environmental impact: Siemens PostCap Technology

Björn Fischer; Diego Andrés-Kuettel; Dr. Ralph Joh, Dr. Markus Kinzl, Dr. Rüdiger Schneider, Dr. Henning Schramm

Siemens AG, Energy Sector, Industriepark Hoechst, Frankfurt am Main, Germany

1. Summary

Siemens has developed a proprietary post-combustion carbon capture process (PostCap^{TM}) for the separation of carbon dioxide from power plant flue gases. This absorption-desorption process is based upon an amino acid salt solvent, and is ready for large-scale demonstration.

Amino acid salts have numerous benefits as CO_2-absorption solvents, which are mainly outlined in this report. These positive properties have been validated by more than 4,000 operation hours in CO_2-capture pilot plant retrofitted to a coal-fired power plant, as well as by a vast laboratory research program.

2. Use of AAS for CO_2 removal

Amino acid salts (short: AAS) are the salt form of natural amino acids. They are therefore formed by neutralizing an amino acid compound with an alkali metal hydroxide (see Figure 1). Thus the alkalinity of the amine group is increased, i.e. the amino acid is "activated" and reacts selectively with acid gases such as CO_2. Due to their ionic nature, both AAS and their absorption products are conveniently nonvolatile.
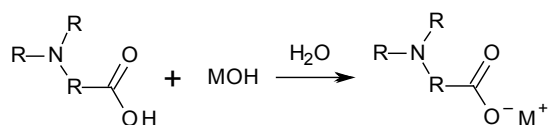
Figure 1: From amino acids to amino acid salts

Amino acids derive from ammonia, from which one, two or three hydrogen atoms are substituted by alkyl and / or aryl groups. At least one of the substituents comprises a acidic group. All aqueous solutions of amines are of alkaline nature. Hence, they react with acid gases through their free electron pair. Amino acids are normally found in detergents, fertilizers and cosmetics.

As shown by Eide-Haugmo et al. (2009) [1], AAS have a high biodegradability. The AAS ecotoxicity is an order of magnitude lower than any of the other alkanolamines, piperazine or ammonia, which are also often discussed as solvents for CO_2 capture.

To sum up, the main advantages from AAS are:

- Fast CO_2 absorption kinetics.
- Low energy demand (demonstrated by current Siemens investigations).
- Zero vapor pressure of the active substance, which yields neither solvent loss due to evaporation, nor an extra wash unit at the top of the absorber.
- High biodegradability and zero toxicity.
- High stability in degrading environments.
- Mainly nonvolatile degradation products, which remain at all times in the liquid phase.
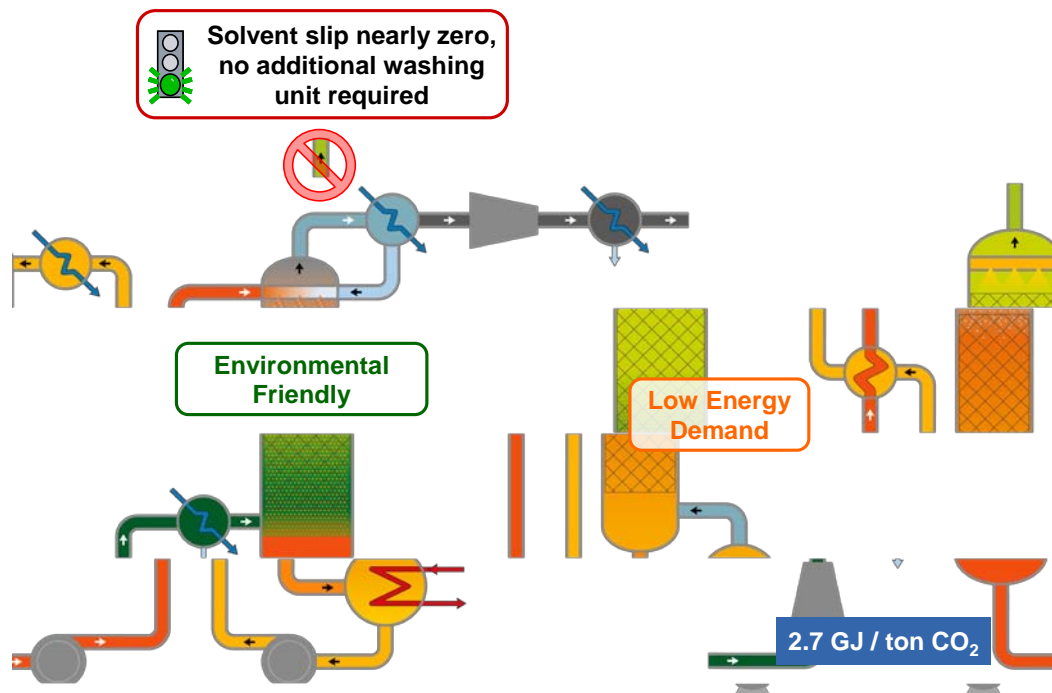
Figure 2: Siemens CO_2 capture process (PostCap) based on amino acid salts

3. Pilot Plan Operating Experiences and Conclusions

The Siemens PostCap™ CO_2-capture process experiences in general have validated the numerous benefits amino acid salt based solvents potentially possess for the separation of CO_2 from power plant flue gases. Due to the ionic nature of AAS, the PostCap™ process does not have either solvent or reaction product emissions during

[1] Eide-Haugmo, I. et al.: Invironmental impact of amines. *Energy Procedia 1*, **2009,** p. 1297–1304

the operation of the capture plant. This significantly reduces the OpEx in comparison to standard ethanolamine processes.

Laboratory research has also determined that AAS is resistant to oxidative and thermal degradation, as well as to degradation by means of carbamate polymerization. The formation of heat-stable salts due to the impurities in the flue gas current is not a handicap for the PostCap^{TM} process. These HSS can be regenerated in an already demonstrated Siemens proprietary reclaiming process.

The more than 4,000 operation hours of the PostCap^{TM} pilot plant experiences have demonstrated not only the aforementioned benefits of AAS, but also the appropriate use of AAS solvent, when considering CO_2-capture performance. A low energy demand of 2.7 GJ/ton CO_2 is achieved. For fossil-fired power plants, this means that the power plant efficiency decreases by only < 6% points.

Now that the Siemens PostCap^{TM} process has been thoroughly validated in pilot operation, it is ready for large-scale implementation.

Development of Thermomorphic Biphasic Solvents for Low-Cost CO$_2$ Absorption Process

Jiafei Zhang, *Yu Qiao, David W. Agar*
Technische Universität Dortmund, D-44227 Dortmund, Germany

1. Introduction

Post-combustion capture (PCC) with chemical absorbents is probably one of the most feasible and dominated technologies for controlling greenhouse gas emission from fossil fuels combustion. Monoethanolamine (MEA) is the most common commercial absorbent widely used for fuel gas scrubbing. However, the unfavourable economics, primarily due to the energy required for solvent regeneration, is a major shortcoming for the alkanolamine-based CO$_2$ capture process [1,2]. Development of new solvents is hence crucial for improving the absorption efficiency and reducing energy consumption in the carbon capture process. Some proprietary solvents, which can allegedly cut the regeneration energy by 20-34% compared to MEA, have been reported, but the desorption still needs to be carried out at 120 °C [3-5]. Thermomorphic biphasic solvent (TBS), comprising lipophilic amine as activated component, has been proposed to ameliorate such problem [6]. Potential advantages of using TBS absorbent for PCC, especially in low regeneration temperature and high cyclic CO$_2$ loading capacity, have already been proven [7,8]. Due to the limited aqueous solubility, a thermomorphic (i.e. thermally induced) miscibility gap can be induced during regeneration. Extensive CO$_2$ desorption is thus achieved at temperatures only slightly in excess of the critical phase transition temperatures, typically 60-80 °C, enabling the utilisation of low grade or waste heat for solvent regeneration. Concerning the advantages provided by liquid-liquid phase separation (LLPS), a new CO$_2$ capture technology - DMX^{TM} process - has also been developed by IFP Energies nouvelles to reduce the operating cost by demixing and phase splitting in decanter before thermal regeneration with steam stripping [9].

2. Lipophilic amine and phase transition

Lipophilic amine is a hybrid molecule with hydrophilic and hydrophobic functional groups, for example, Hexylamine (I), Dipropylamine (II) or N,N-Dimethylcyclohexylamine (III) . Due to the restricted miscibility, the characteristics of lower critical solution temperatures (LCST) behaviour were observed in mixtures of lipophilic amine and water [10]. The aqueous solubility of amine decreases with increasing temperature and the solution thus exhibits LLPS upon heating. At concentrations of 20-40 wt%, the LCST of aqueous fresh amine solutions is between 5 and 30 °C (see Figure 1). It can be increased by not only the enhancement of concentration but also the solubilisation effect of CO$_2$ (see Figure 2), since the formatted aqueous soluble carbamate, carbonate and bicarbonate play a role of solubiliser for dissolving all the nonprotonated amines into water, which significantly provides more technical feasibility for regulating the phase transition behaviour in absorption process.
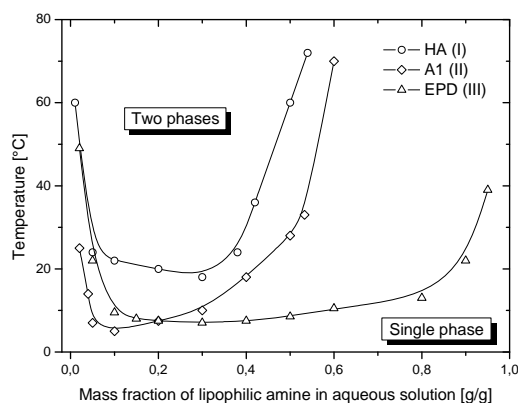
Figure 1. LCST of lipophilic amine solutions
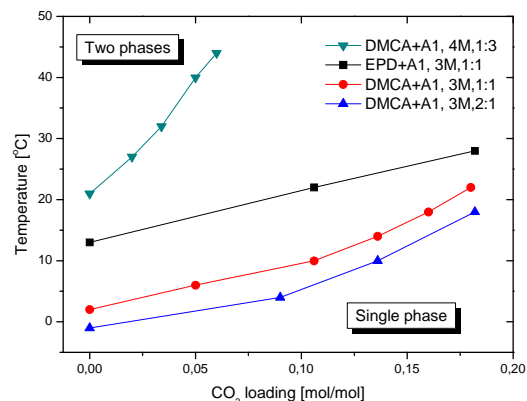
Figure 2. Influence of loaded CO$_2$ on LCST

The novel lipophilic amine solvents were mainly investigated as a means to circumvent the exergy demands through thermomorphic LLPS during regeneration. The regenerated aqueous lipophilic amine solutions exhibit biphasic behaviour at concentrations of 2-4 M and temperatures of 60-80 °C. The heterogeneous solution becomes homogeneous upon cooling after achieving the LCST. This process therefore permits to exploit the low value heat from network energy recovery system for desorption purpose.

3. Solvent selection

Absorption of CO_2 into lipophilic amine solvents was initially developed by observing the miscibility of organic and aqueous phases and temperature dependent phase transition behaviour. According to the theoretical study and experimental measure on the physical and chemical properties, in total over fifty available lipophilic amines were preliminarily selected for test tube experiments. The overall screening among those amines is based on the comprehensive performance in absorption and regeneration, primarily including CO_2 capacity, reaction rate, phase separation temperature and regenerability. The selected amines have been classified into two categories: absorption activators, such as DPA (II) and A1 (II), with rapid reaction kinetics, and regeneration promoters, for example, EPD (III) and DMCA (III), exhibiting outstanding regenerabilities.

3.1 Physical properties

In order to find adequate amines as alternative absorbents, the structural influence on the parameters of boiling point, basicity, solubility and viscosity, has been studied for prediction and selection. The investigation has been conducted with different aliphatic amines by varying hydrophobic substituents, such as primary, secondary and tertiary amines, linear and branched chains, cycloalkyl and cyclic structures. Most of the primary amines are unfavourable, due to either lower boiling point or high viscosity, e.g., gel formation was found when mixing Heptylamine or Octylamine in water. Secondary amines are preferred for attaining rapid absorption rate because of the higher basicity (pK_{aH}) compared to other amines [12]. Tertiary amines are also recommended for enhancing CO_2 desorption owing to their good regenerability and chemical stability. Solubility is a two-edged sword in the absorption and desorption performance. When a lipophilic amine has high aqueous solubility, fast absorption rate can be obtained, but its regenerability will be depressed.

Primary amine (I)	$pK_{aH} = 10.6 \pm 0.2$	(1)
Secondary amine (II)	$pK_{aH} = 11.1 \pm 0.1 - n \times 0.2$	(2)
Tertiary amine (III)	$pK_{aH} = 10.5 \pm 0.2 - n \times 0.2$	(3)

where pK_{aH} means value of the conjugated acid and derived from molecular simulation. As a reference, pK_{aH} (NH_3) = 9.3.   n is the number of methyl groups bound to the basic nitrogen atom and the max. value is 3.

3.2 Absorption

The absorption rate is significantly influenced by aqueous solubility, surface tension and basicity of amine. According to the reaction mechanism, CF is the main reaction in primary and secondary amines and takes place very fast [13]. Rapid reaction rate has been obtained in amine solutions such as HA, A1, DPA, etc. (see Figure 3). Therefore, the highly reactive primary or secondary amines are typically considered as activators for absorption; while the moderate reactive tertiary amines can be used as regeneration promoter due to their remarkable regenerability enhanced by LLPS. In primary and secondary amine solutions, the loading capacity can be enhanced by CR after approaching 0.5 mol_{CO2}/mol_{sol} for corresponding amine solvent when more and more carbamates get accumulated.

Carbamate formation (CF)	$CO_2 + 2RNH_2 \Leftrightarrow RNH_3^+ + RNHCOO^-$	(4)
Bicarbonate formation (BF)	$CO_2 + RNH_2 + H_2O \Leftrightarrow RNH_3^+ + HCO_3^-$	(5)
Carbamate reversion (CR)	$CO_2 + RNHCOO^- + 2H_2O \Leftrightarrow RNH_3^+ + 2HCO_3^-$	(6)
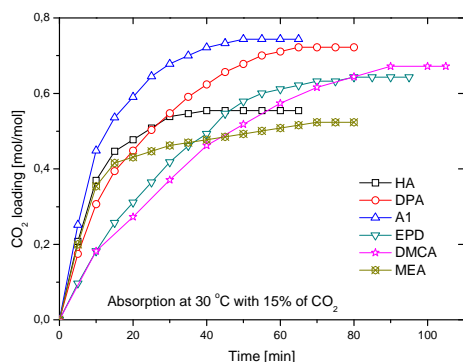
Figure 3. CO$_2$ absorption in 3 M lipophilic amine solutions
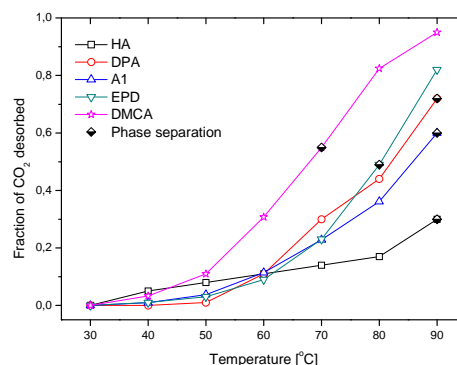
Figure 4. CO$_2$ desorbed from 3 M loaded lipophilic amine solutions

3.3 Regeneration

High temperature (>120 °C) required for solvent regeneration is an evident weakness in the alkanolamine-based CO$_2$ capture process, since it induces solvent degradation and energy consumption with steam stripping. However, lipophilic amine can solve this problem dramatically with thermomorphic LLPS, which is the most favourable phenomenon in the regeneration process. Table 1 demonstrates LLPS was found in the most of tertiary amines (III), some of secondary amines (II) and few primary amines (I) in the screening experiment. According to the comparison of cyclic CO$_2$ capacity, DMCA and EPD have performed the most remarkably and become the most considerable solvents as regeneration promoter for further study. The regenerability of DMOA, MPD and DBA was also outstanding, unfortunately, extremely slow absorption rate, high volatility loss, or precipitation, respectively, was observed in such aqueous amine solutions.

Table 1. Phase separation temperature and net loading capacity (25-80 °C) of lipophilic amine solutions

Amine (*3M*)		Type	LLPS temperature °C	Net loading capacity *g/L*
Hexylamine	(HA)	I	90	29.3
A1		II	90	42.2
Dipropylamine	(DPA)	II	90	54.3
Dibutylamine	(DBA)	II	50	61.5
Di-*iso*-butylamine		II	50	56.3
Di-*iso*-propyl ethylamine		III	50	~ 10
N,N-Dimethyl butylamine		III	80	~ 40
N-Methylpiperidine	(MPD)	III	80	57.6
N-Ethylpiperidine	(EPD)	III	80	73.6
N,N-Dimethyl cylcohexylamine (DMCA)		III	70	76.3
N,N-Dimethyl octylamine		III	50	62.9

Figure 4 illustrates that the solvent regenerability gets enhanced after the LLPS takes place and very deep regeneration is obtained in tertiary amine solutions such as DMCA. The major advantage of using lipophilic amines with regeneration involving LLPS to a multiphase system is that the desorption can be carried out at a modest temperature, i.e. 80 °C or even lower, which is much less than the temperature employed in industrial process using alkanolamines. Together with the high cyclic loading capacity of such amines, the TBS absorbent has offered more degrees of freedom for cost reduction with respect to the quality of energy requirement.

4. Solvent formulation and TBS process

Since none of single lipophilic amine is able to meet all the selection criteria in both reactivity and regenerability. Study on optimisation of absorbent formulations has thus been carried out for demonstrating the technical viability of such novel solvent and enhancing the energy efficiency of PCC process. The absorption was initially performed in a 100 mL bubble column with varying operating parameters. After amelioration, it has been scaled up and conducted

in a 1 m height parked column. The new formulated absorbent, blending of activator and promoter, for instance A1+DMCA, has performed rapid absorption rate, high net CO_2 loading capacity (~3.2 mol/kg), low regeneration temperature (~80 °C) and good regenerability (>95%), which are superior to the benchmark 30wt% MEA solution (see Figure 5). The experimental study has also focused on the influences of CO_2 loading on the phase separation behaviour and temperature on solvent regenerability. By optimising the solvent formulations and processing conditions, the regenerated TBS solution has successfully achieved homogeneous by cooling to the LCST around 40 °C, and the loaded solution has converted to two phases upon heating at 80 °C, which enables the use of low value heat at approx. 90 °C in regeneration. For assessing the technical feasibility in further evaluation work, we have developed the TBS absorbents with LLPS and process without steam stripping for desorption (see Figure 6), it cuts the energy consumption by more than 35% in comparison to the conventional alkanolamine solvents.
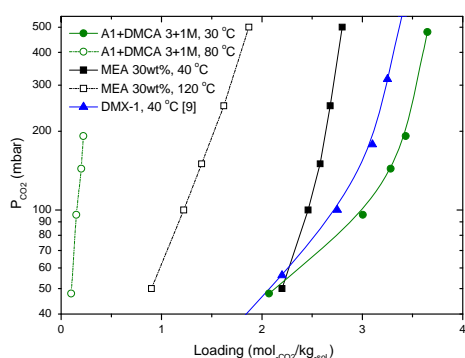
Figure 5. Vapour-Liquid Equilibrium of TBS
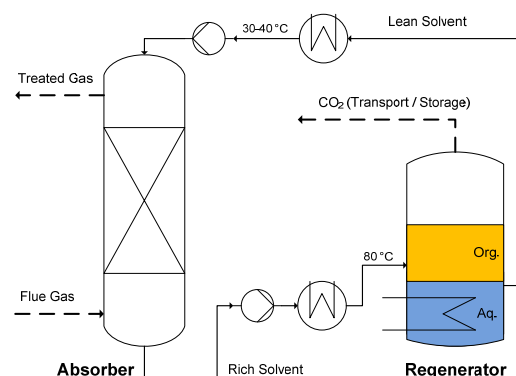
Figure 6. Flow sheeting diagram of TBS process

5. Conclusions

The selected biphasic solvent system exhibiting thermomorphic LLPS by integrating with extractive behaviour potentially enables an extensive regenerability at 80 °C, thus permits a more flexible and expedient thermal integration of the CO_2 capture process. The performance of such solvents observed is superior to that of conventional alkanolamines, especially in high net CO_2 loading capacity and low energy consumption.

References

[1] Kohl, A.L. and Nielsen, R.B., 1997, *Gas Purification*, 5th ed., Gulf Publishing Co., Houston, Texas.
[2] Rochelle, G.T., 2009, Amine scrubbing for CO_2 capture. *Science*, 325: 1652-1654.
[3] Notz, R.; Asprion, N.; Clausen, I. and Hasse, H., 2007, Selection and pilot plant tests of new absorbents for post-combustion carbon dioxide capture. *Chem. Eng. Res. Des.*, 85: 510-515.
[4] Goto, K.; Okabea, H.; Shimizua, S.; Onodaa M. and Fujioka, Y., 2009, Evaluation method of novel absorbents for CO_2 capture. *Energy Procedia*, 1: 1083-1089.
[5] Tatsumi, M.; Yagi, Y.; Kadono, K, et al., 2011, New energy efficient processes and improvements for flue gas CO_2 capture. *Energy Procedia*, 4: 1347-1352.
[6] Agar, D.W., Tan, Y.H. and Zhang, X., Patent WO/2008/015217.
[7] Zhang, J.; Agar, D.W.; Zhang, X. and Geuzebroek, F., 2010, CO_2 Absorption in biphasic solvents with enhanced low temperature solvent regeneration. *Energy Procedia*, 4: 67-74.
[8] Zhang, J.; Nwani, O.; Tan, Y. and Agar. D.W., 2011, Carbon dioxide absorption into biphasic amine solvent with solvent loss reduction, *Chem. Eng. Res. Des.*, in Press, DOI: 10.1016/j.cherd.2011.02.005.
[9] Raynal, L.; Alix, P.; Bouilon P., et al., 2011, The DMX[TM] process: an original solution for lowering the cost of post-combustion carbon capture. *Energy Procedia*, 4: 779-786.
[10] Yalkowski, S.H., 1999, *Solubility and Solubilization in Aqueous Media*, American Chemical Society, Washington, DC.
[12] Perrin, D.D.; Dempsey, B. and Serjeant, E.P., 1981, *pKa Prediction for Organic Acids and Bases*. Chapman and Hall, London.
[13] Astarita, G., 1983, *Gas Treating with Chemical Solvents*. Wiley-Interscience Publication, New York.

The CO_2 post-combustion capture development programme at Niederaußem

Peter Moser, RWE Power AG, New Technology, Essen, Germany;

Sandra Schmidt, RWE Power AG, New Technology, Essen, Germany;

Georg Sieder, BASF SE, Ludwigshafen, Germany;

Hugo Garcia, BASF SE, Ludwigshafen, Germany;

Torsten Stoffregen, Linde-KCA Dresden, Dresden, Germany;

Frank Rösler, Linde-KCA Dresden, Dresden, Germany

Introduction

In spite of the ongoing massive expansion of renewable energy, CO_2 mitigation at fossil-fired power stations will be a key lever for climate protection since power production from fossil-based fuels will remain the backbone of global power production in the next decades. Up to 30% of the specific CO_2 emissions from lignite-based electricity generation can be avoided by building new power stations equipped with state-of-the-art technology (net efficiency >43%) to replace the oldest units still in operation (net efficiency approx. 32%). An example of this CO_2 mitigation approach is the construction of the BoA[1] 2&3 power station in Neurath. After commissioning the two 1,100 MW_{el} units will replace 16 units with 150 MW_{el} each by end-2012. A further reduction in CO_2 emissions can be achieved by employing innovative techniques for increasing efficiency, e.g. the WTA lignite pre-drying process or the increase of steam parameters to 700°C. To enhance this mitigation effect, carbon capture and storage (CCS) technologies must be applied.

The combination of post-combustion capture (PCC) with these newly developed technologies for increasing power plant efficiency allows more than 90% of the CO_2 to be captured at a power plant efficiency of app. 40%. Despite the use of CCS, this efficiency is higher than today's average power plant efficiency. Thus, combining highly efficient CCS and power generation technology both helps spare resources and offers a cost-efficient method of climate protection. In the 450 scenario of the IEA, which describes a strategy for limiting global warming to 2°C, CCS is of equal importance to the reduction of CO_2 emissions in the EU as renewables and CCS can

---

[1]Lignite-fired power plant with optimized plant technology

be used at significantly lower costs than renewables. In addition, working group three of the IPCC regards CCS as a key technology for climate protection.

Development of a full-scale PCC plant

The CO_2 scrubbing technology using amines has been a well-known technology for producing CO_2 in the chemical industry and in the soft drink industry for decades, but it has not been employed in fossil-fired power plants to reduce their CO_2 emissions. To develop a highly efficient PCC technology with a CO_2 capture rate of 90% for a full-scale 1,100 MW_{el} power plant, a holistic approach is important. Thus, it is necessary to simultaneously assess the capture process, the engineering work, the equipment and the integration of the capture plant into the power plant process with regard to efficiency, profitability, operating behaviour and process and solvent performance. The interdisciplinary cooperation of chemical company BASF, engineering company Linde and utility RWE is perfectly in line with this holistic approach.

In the first stage of the development programme, more than 400 substances were screened on the basis of available data. Comprehensive lab tests were conducted on 180 of the most appropriate substances and their blends before trialling the best 15 candidates in a "mini plant". The criteria used for ranking the solvents and pre-selecting the most promising ones included: a low energy demand for solvent regeneration, high stability against oxygen and thermal degradation, low emissions, low solvent loss, high cyclic capacity, sufficiently fast reaction kinetics and industrial availability of the solvent [1].

In the second stage of the development programme, the two best solvent candidates were tested for six months each in the pilot plant at Niederaußem under the real conditions of the power plant. The testing programme at the pilot plant was mainly determined by the necessity to validate the basic capture process data for the preliminary design of the full-scale PCC plant. The boundary conditions regarding CO_2 transport and storage also played an important role for this design and the testing programme (Figure 1). A multitude of different optimization approaches to decrease the cost and energy demand of the PCC process and its integration into the power plant process were evaluated as part of the testing programme at the pilot plant, e.g.: interstage cooling, cost-efficient flue gas conditioning, waste heat recovery by integrating PCC into the power plant process, interaction between low

pressure steam for regeneration, pressure of the desorber column and compressor performance, cost/temperature difference of the solvent/solvent heat exchanger and cost-efficient materials.
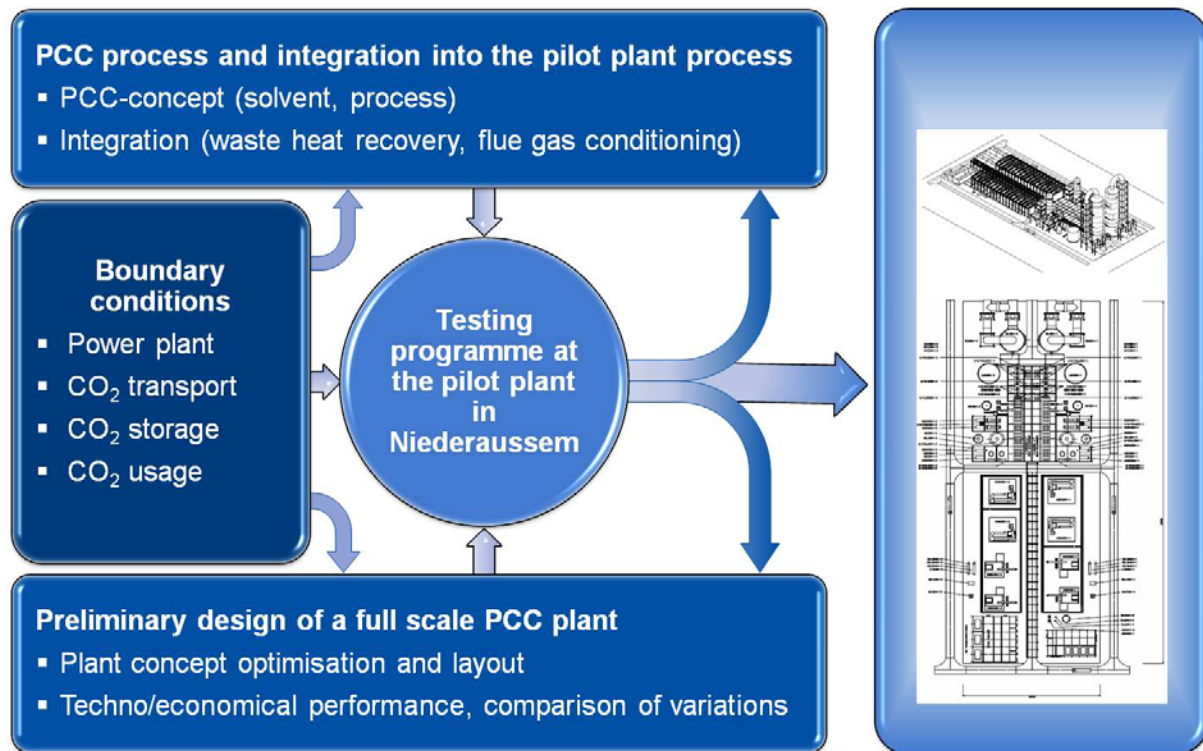
Figure 1:   Development over the pilot plant to a full scale PCC plant

The last step of technology development before commercial application is the demonstration of the technology, which comprises all topics that cannot be investigated on a pilot plant scale, such as: site fabrication of the columns and resulting tolerances, logistics for the internal packings and uniformity of gas and solvent distribution over the column cross-section for such large columns. Assuming that a detailed understanding of the process, solvent and material behaviour and the integration concept can be attained during the trials and plant engineering only a single intermediate scale-up step from pilot to commercial scale will be necessary.

Pilot CO_2-scrubbing plant in Niederaußem

The location of the pilot CO_2-scrubbing plant, which forms part of the so-called Coal Innovation Centre, at the 1,000 MW_{el} lignite-fired BoA 1 unit has many advantages. On the one hand, BoA 1, being a base-load unit, offers the preconditions required to conduct reproducible and transferable test series at a high level of availability. On the other hand, various prototype and pilot plants that can also be run in combination are

being operated at the BoA 1 plant. For instance, a WTA prototype is used to replace up to 30% of the furnace thermal rating of the BoA 1 plant by combusting dry lignite and to utilize the waste heat produced by lignite drying in the power plant process, increasing the efficiency of the unit by > 1 percentage point [2]. In addition, a high-performance FGD plant known as "REAplus" is operated with the aim of reducing the SO_2 contents in the flue gas from the current maximum of 200 mg/m³$_N$ to 10 mg/m³$_N$. This is an important prerequisite for the future use of CO_2 scrubbing since SO_2 leads to increased degradation of the CO_2 scrubbing solvent. The combined operation of these prototype and pilot plants at the BoA1 unit permits the CO_2 scrubbing technology to be tested under the conditions of future applications. Some of the CO_2 from the pilot plant is currently stored in vessels for research projects on CO_2 usage and made available to Bayer or RWTH Aachen University among others [3].

With an absorber diameter of 600 mm and a plant height of 40 m, the pilot plant provides ideal conditions for a scale-up of the process as the carbon capture rate and dwell times will be comparable with those of a large-scale plant. More than 250 measuring points, an online gas analysis system, sampling points for solvent, condensate and gas samples in the whole process, an extensive analysis programme for emissions and trace elements and 14 testing points for innovative materials in the CO_2 scrubbing process provide good prerequisites for obtaining robust data for the design studies and the design of the large-scale and demonstration plants from the pilot-plant testing programme. The first test phase, whose aim was to select the optimum CO_2 scrubbing solvent for use in power plants, was completed in mid-March 2011. We started with 30% wt monoethanolamine (MEA) solution as a benchmark, which was used to test the operating behaviour of the plant and the comparability of the test results with results obtained from simulations. This was followed by two new CO_2 scrubbing solvents called Gustav 200 and Ludwig 540. Each of these three test phases was subdivided into parameter studies and long-term tests. During the parameter studies, the ideal operating conditions were determined and a sensitivity analysis was performed to establish the dependence of the process behaviour on changes in the various parameters. During the long-term tests, solvent performance (solvent loss, degradation, emissions and stability) and the operating behaviour of the plant under different boundary conditions (load change of the power plant, combined operation of the CO_2 scrubbing plant with the REAplus and/or WTA plant, etc.) were investigated (Figure 2).
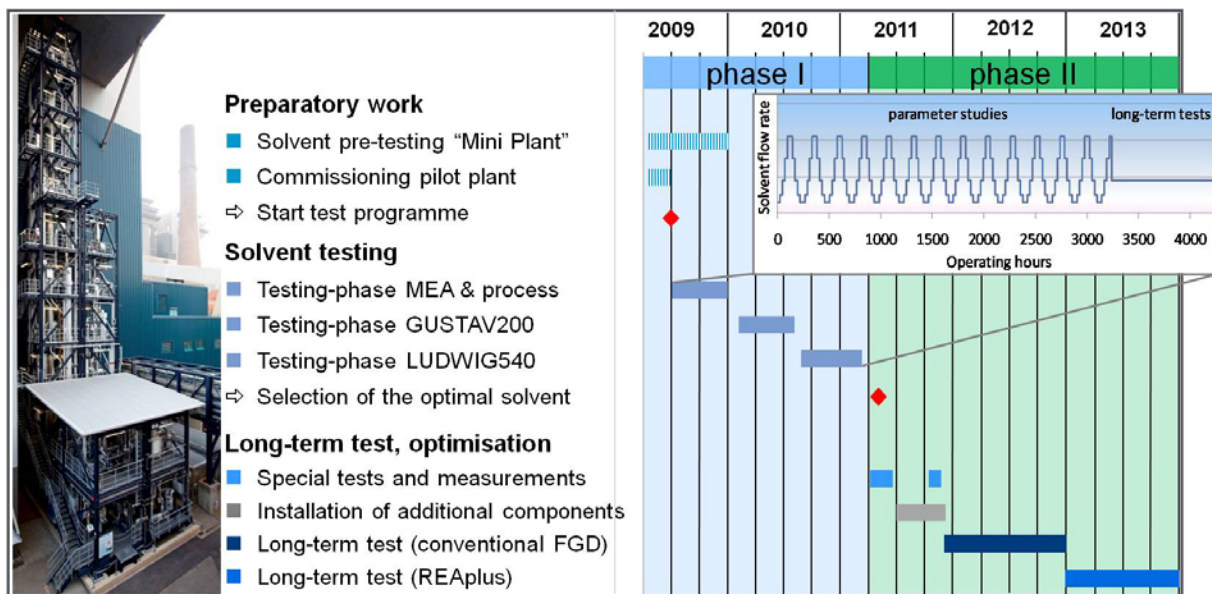
Figure 2: Testing programme at the CO_2-scrubbing pilot plant at Niederaußem

During the three test sections in phase one of the testing programme (MEA, Gustav 200 and Ludwig 540), some 2,680 tons of CO_2 were captured with the CO_2 scrubbing plant. With 9,710 hours in operation, the pilot plant achieved an availability level of 97%. The evaluation of all results obtained with the two new optimised solvents as regards materials, emissions, degradation and solvent loss took several months. The already available results are very promising.

With only 0.3 kg_{MEA}/kg_{CO2}, the solvent consumption of MEA was significantly lower than data given in the literature (e.g. 1.4 – 2.1 kg_{MEA}/kg_{CO2} for the Esbjerg pilot plant) [4]. The specific energy demand for the regeneration of the new scrubbing solvents Gustav 200 and Ludwig 540 is < 2.8 MJ/t_{CO2} and, hence, 20% better than the best case of an optimized MEA process. Apart from this, the solvent flow rate is lower and the possible temperature range for regeneration is wider than for MEA.

One of the two new scrubbing solvents was chosen for the second phase of the development programme. In this phase, the pilot plant will be modified by installing high-performance column internals in the absorber, an improved emission control system at the top of the absorber and additional online gas analysis equipment. In two long-term tests – each lasting approx. one year, the first with flue gas feeding from the conventional FGD plant, the second with flue gas feeding from the high-performance FGD plant – the long-term behaviour will be tested in particular with regard to degradation, reclaiming and emission behaviour.

Conclusion

The results of the testing programme show that the goal of an efficiency loss of less than 10 percentage points for a power plant with CCS is achievable by the innovative capture technology that is tested in Niederaußem. The pilot plant results significantly reduce the design uncertainties for a full-scale PCC plant. A demonstration plant could be implemented on the basis of the available results.

Nevertheless, the implementation of a demonstration project requires the prior establishment of a regulatory framework and the gaining of public acceptance of CCS in Germany.

Acknowledgements

References

[1] G. Sieder, A. Northemann, T. Stoffregen, B. Holling, P. Moser, S. Schmidt: Post Combustion Capture Technology: Lab scale, Pilot scale, Full-scale Plant. Sour Oil & Gas Advanced Technology Conference 2010, Abu Dhabi, United Arab Emirates (2010)

[2] H.J. Klutz, C. Moser, D. Block: Stand der Entwicklung der WTA-Wirbelschicht-trocknung für Braunkohle bei der RWE Power AG. 42. Kraftwerkstechnisches Kolloquium, Kraftwerkstechnik – Sichere und nachhaltige Energieversorgung – Volume 2 (2010)

[3] A. Bazanella, D. Krämer, M. Peters: CO_2 als Rohstoff. Nachrichten aus der Chemie, 58, pp. 1226 et seq. (2010)

[4] J. Knudsen, J. Jensen, P.-J. Vilhelmsen, O. Biede: Experience with CO_2 capture from coal flue gas in pilot-scale: Testing of different amine solvents, Energy Procedia 1, 783–790 (2009)

Mass Transfer Coefficients - Experimental Evaluation of CO_2 Capture with Structure Packing

Rosa-Hilda Chavez, Instituto Nacional de Investigaciones Nucleares (ININ), Carretera México-Toluca S/N, La Marquesa, Ocoyoacac, 52750, México, MEXICO; Javier de J. Guadarrama,Instituto Tecnológico de Toluca, Av Instituto Tecnológico de Toluca S/N, Metepc, 52140, México, MEXICO

Abstract

The objective of this work is to study CO_2 absorption by experimental absorption column, using metal structured packing material named ININ18. This material was developed by Mexican National Institute of Nuclear Research (ININ by its acronym in Spanish). The system studied was Monoethanolamine (MEA) at 30 weight percentage in aqueous solution countercurrent with CO_2 flue gas. The capture process was carried out in an absorption column with dimensions of 4.0 meters of height and 0.3 meters of diameter. Mass transfer coefficient and height of mass transfer were evaluated. The results showed volumetric mass transfer coefficient of $3.76s^{-1}$ and height of mass transfer equivalent unit of 0.317m, and absorption efficiency of 90%.

Introduction

The Kyoto protocol is an essential step to mitigate the emission of pollutants and the CCS technologies are the instruments of CO_2 capture and sequestration (Thitakamol et al., 2007). The difference between categories for capturing CO_2 from power plants is depended on fuel treatment, its oxidation, CO_2 concentration, and gas pressure (Rubin and Rao, 2002). The general method involves contacting a gas stream to an aqueous amine solution which reacts with the CO_2 by acid-base neutralization reaction to form a soluble carbonate salt. This reaction is reversible, allowing the CO_2 gas to be liberated by heating in a separate stripping column (Leites et al., 2003).

Methodology

Carbon dioxide was absorbed into 30 weight% MEA solution in a packed absorption column with a diameter of 0.3m and packing height of 3.5m (Figure 1 and 2). The column was packed with ININ18 structured packing (Table 1), with gas and liquid distributors located at the bottom and top of the column respectively (Chavez and Guadarrama, 2010). The inlet solution (CO_2 lean) was taken from a container and pumped to the top of the column with the geared solution delivery pump. The exit (CO_2 rich) solution was recycled to the tank. The inlet pump was fitted with flow meters enabling accurate flow rate measurements as well as variable pump speed controllers to modulate solution flow to the desired rate. The solution level within the column was maintained at the desired level by

controlling the inlet solution flow rate. The carbon dioxide and air inlet gases were supplied from regulated compressed gas tanks via respective volumetric flow controllers. This gas was then passed through a mixing manifold that contains a stationary mixing element to promote optimal gas mixing prior to its feed to the absorption column.

Table 1. Characteristic of ININ18 structure packing

Type	stainless steel
Wire gauge	18
Porosity (ε)	0.9633
Geometric area a_p	418 m^2/m^3
Diameter	0.252 m
Height	0.19 m
Corrugated angle (θ)	45°

feed to the absorption column.Downstream of the manifold was a mixed gas flow meter which was used to verify the flow of gas through the pure gas flow meters.

Figure 1. Real experimental column
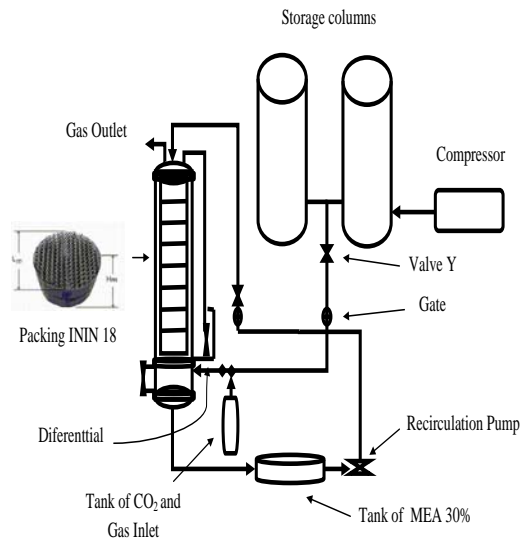
Figure 2. Process study system

Inlet and outlet gas samples were determined by gas chromatography technique, using a thermal conductivity detector. Gas chromatograph equipment is Varian 3760 with two detectors: flame ionization and thermal conductivity and three chromatographic columns used on the type of combustion gases: CH_4, C_6H_{14}, CO_2 and CO. The chromatograph is provided by HP-5MS column of 30 meters long with a diameter of 0.25μm, samples of 3cm^3 were injected manually and the temperature was analysis carried at 35°C and 5 minutes of routine. The results given were a series of chromatograms shown in time retention of each compound as well as the concentration were determined by comparing with standard area from standard known composition.

On the bases of conventional definitions of mass transfer units, the height of a gas phase transfer unit and the height of a liquid phase transfer unit respectively are:

$$H_G = HTU_G = \frac{U_G}{K_G a_e \rho_G} \quad (1)$$

$$H_L = HTU_L = \frac{U_L}{K_L a_e \rho_L} \quad (2)$$

The two-film model is based on the number of mass transfer global units, NTU, of both gas and liquid resistance, and it involves the efficiency in terms of the height of mass transfer global unit $HETP$. In this work, gas is high soluble in the liquid and Henry constant is small. Liquid side resistance is negligible. The relative magnitude of the individual resistance evidently depends on gas solubility, as represented by the Henry's law constant. The gas side resistance is controlling mass transfer when a relatively soluble gas is absorbed (Leites et al., 2003).

$$NTU = \frac{y_1 - y_2}{(y - y^*)_M} \qquad (3)$$
$$Z = HETP * NTU \qquad (4)$$

Results

Figure 3 and Table 2 present the results obtained from chromatographic analysis, during 60 minutes, countercurrent flows, in closed system. From absorption evaluation there were possible to determine mass transfer parameters and absorption efficiency of 90%. The gas composition was chosen because it best represents the flue gas composition found in power stations; the target process for this method of CO_2 capture. These results were considered reasonable due to the complex nature of the electrolyte solution and numerous possible reactions involved.

Figure 4 and 5 show pressure drop and liquid holdup with respect gas flow at different liquid flows. Height of mass transfer unit in gas and liquid phases, at different liquid flows are shown in Figures 6 and 7.

Conclusions

This study is feasible to scale up columns with bigger gas treatment flows and different dimension columns. The results of CO_2 capture system were found to be relatively accurate and reproducible. This increase in k_Ga indicates the speed increase in which the solute is transferred into the liquid phase, the highest value of k_Ga in the region is loaded with a range of 80 to 90% compared to the flooding system.
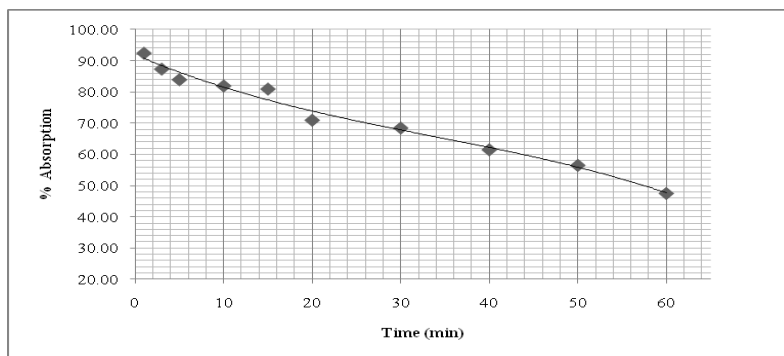
Figure 3. Measurement of CO_2 absorption

Table 2. Mass transfer results

HTU_{OG}	m	0.317
HTU_{OL}	m	0.0273
$k_G a_e$	s^{-1}	3.76
$k_L a_e$	s^{-1}	0.2978
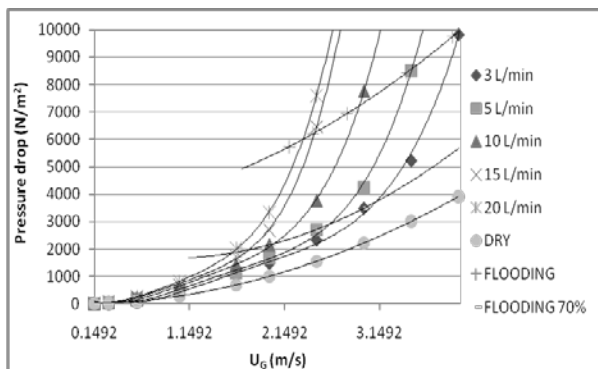
Figure 4. Pressure drop versus gas velocity of ININ18 packing
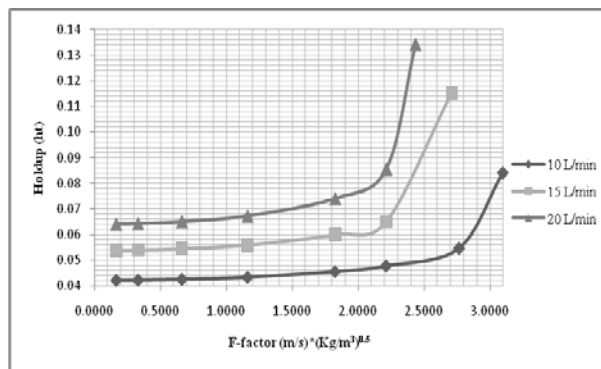
Figure 5. Liquid holdup versus F-factor of ININ18 packing
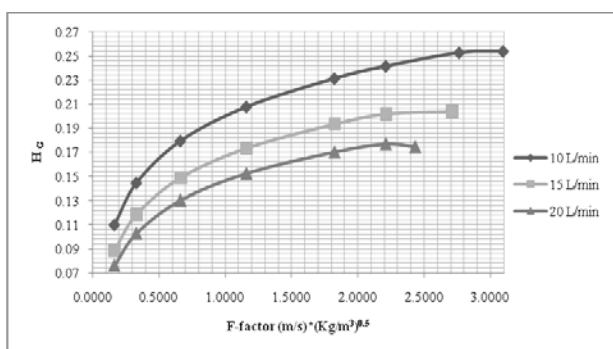
Figure 6. Height of mass transfer unit in gas phase
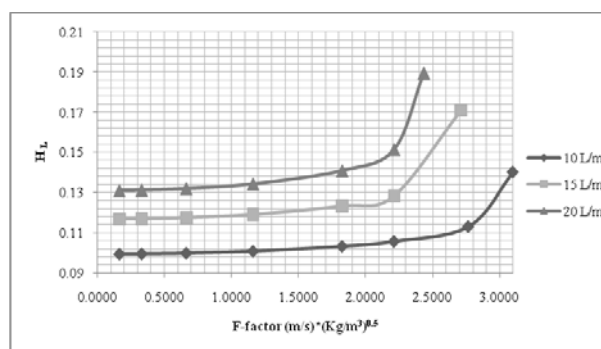
Figure 7. Height of mass transfer unit in liquid phase

Acknowledgments

Nomenclature

a_e	Effective interfacial area [m^2/m^3]	U_G, U_L	Superficial gas and liquid velocity through a packed bed [m/s]
k	Mass transfer coefficient [m/s]	Z	Total height of packing [m]
ka_e	Volumetric mass transfer coefficient [s^{-1}]	ρ	Density [kg/m^3]

References

Chavez R.H., Guadarrama J.J., Comparison of structured packing in CO2 absorber with chemical reactions, Chemical Engineering Transactions, 21, 577-582.

Leites I.L., Sama D.A., Lior N., 2003, The theory and practice of energy saving in the chemical industry: some methods for reducing thermodynamic irreversibilities in chemical technology processes, Energy 28, 55-97.

Rubin E.S., Rao A.B., 2002, A technical, economic and environmental assessment of amine-based CO2 capture technology for power plant greenhouse gas control", DOE/DE-FC26-00NT40935.

Thitakamol B., Veawab A., Aroonwilas A., 2007, Environmental impacts of absorption-based CO2 capture unit for post-combustion treatment of flue gas from coal-fired power plant, International Journal Greenhouse Gas Control, 318-342.

Pilot plant studies of new solvents for post combustion CO_2 capture

Inga Tönnies, Hari Prasad Mangalapally, Hans Hasse

Laboratory of Engineering Thermodynamics, University of Kaiserslautern

Reactive absorption is the most promising process for post combustion carbon capture (PCC). The process with the standard solvent monoethanolamine (MEA), however, suffers from a high regeneration energy which leads to a significant drop in the power plant efficiency. Significant progress can be achieved by using new tailored solvents. After a screening, promising solvents must be investigated in pilot scale plants with the aim to reliably determine their potential before using them in large scale test facilities. The present work reports on such studies. Both the methodology of the studies as well as results obtained for a number of new solvents are discussed.

The studies were carried out in the pilot plant at TU Kaiserslautern. Results for three new solvents from the EU-project CESAR, which all belong to the class of aqueous amine solutions, are presented in detail. They were studied in the same systematic manner: In the first set of experiments, the solvent flow rate is varied at constant CO_2 removal rate. From the results, the optimum solvent to gas flow ratio (L/G) and the corresponding minimum regeneration energy are obtained. In the second set of experiments, the gas flow is varied at constant L/G and constant CO_2 removal rate. This allows the identification of the influence of kinetic limitations. It is also, together with the fact that all results are normalized to those for MEA, the key to obtaining generic results which are largely independent of the specific plant design. The pilot plant results are compared with those from a short-cut method for solvent screening which is shown to yield the correct ranking of the solvents [1]. The most promising solvent, CESAR C1, results in a reduction of the minimum regeneration energy by 20% and a reduction of the solvent flow rate by 50% compared to MEA.

[1] R. Notz, I. Tönnies, H. P. Mangalapally, S. Hoch, H. Hasse. A short-cut method for assessing absorbents for post-combustion carbon dioxide capture, International Journal of Greenhouse Gas Control, 2011 (in press).

Carbon Stripping - A Critical Process Step in the Chemical Looping Combustion of Solid Fuels

Marvin Kramp, Andreas Thon, Ernst-Ulrich Hartge, Stefan Heinrich, Joachim Werther

Institute of Solids Process Engineering and Particle Technology,

Hamburg University of Technology, Denickestrasse 15, 21073 Hamburg, Germany

Introduction

Chemical Looping Combustion (CLC) of solid fuels can be realized in two interconnected fluidized bed reactors, where the solid fuel is directly introduced into the fuel reactor. Such a process has an increased complexity compared to CLC with gaseous fuels. Solid fuels can usually only react with the solid oxygen carriers (OC) if the char is gasified before. This process is slow compared to the reaction of oxygen carrier particles with the gasification products H_2 and CO ([1]). It is favorable if the char has a long residence time in the fuel reactor, while the large flow of OC particles needs only a short residence time. In order to limit the size of the fuel reactor the mixed flow that leaves the fuel reactor is introduced into a carbon stripper where a carbon rich fraction is separated from the OC and is then recycled into the fuel reactor. The most effective separation of two flows is the classification according to settling velocity, hence coal and OC have to differ significantly in particle size. In the current work a fine ground coal and coarse OC particles are used. The carbon slip from the fuel reactor to the air reactor has to be kept at minimum in order to prevent CO_2 emissions from the air reactor. In the present work process simulation is applied to investigate how carbon slip and consequential CO_2 capture rate are influenced by the carbon stripper. Furthermore the importance of fuel choice is demonstrated.

Theory

Fuel Reactor Model

The fuel reactor is a bubbling fluidized bed. It is described in a first approach as an ideally mixed reactor. Different residence times of gas and solids in the fluidized bed reactor are taken into account. For the solid fuel instantaneous devolatilization is assumed. The composition of the volatiles is calculated according to a slightly modified model of Jensen ([2]) that neglects the formation of NO_x and the sulfur content of the fuel. During gasification the size reduction of char particles is considered to be a process of external surface reaction. The new particle size distribution of the char is calculated according to Levenspiel ([3]).

In CLC it is self-evident to recycle apart of the off-gas (CO_2 and H_2O) from the fuel reactor in order to gasify the char. For simulation purposes a set of kinetic equations suggested by Matsui et al. ([4,5]) was chosen. In steam gasification Matsui et al. ([4]) introduced the factor β that describes the ratio of CO_2 production to CO production. For this investigation the factor was set to 1.2 ([4]). Since the OC reaction with the gasification products is fast compared to the gasification itself, the concentrations of CO and H_2 are assumed to be zero.

Carbon Stripper Model

To characterize a classification process usually the grade efficiency

$$G\left(u_{t,i}\right)=\frac{\text{mass of solids with settling velocity } u_{t,i} \text{ in the coarse fraction}}{\text{mass of solids with settling velocity } u_{t,i} \text{ in the feed}} \qquad (1)$$

is used. In the current work the Rogers expression ([6]), has been used to calculate the grade efficiency of the carbon stripper. The sharpness of the separation is defined by:

$$\chi = \frac{u_{t,25}}{u_{t,75}}, \tag{2}$$

where $u_{t,25}$ and $u_{t,75}$ are the terminal velocities that belong to the values of the grade efficiency curve at $G(u_{t,i}) = 0.25$ and 0.75, respectively. An ideal separation would have a value of $\chi = 1$ (usual technical sharpness: $0.3 < \chi < 0.6$, technically sharp: $0.6 < \chi < 0.8$, analysis sharp: $0.8 < \chi < 0.9$ according to 7). Reactions are not considered in the carbon stripper.

Simulation Environment

The simulations have been carried out with SolidSim (8), a steady-state flowsheet simulation system for solids processes.

Results and Discussion

Test Case

The flowsheet of the test case is shown in Figure 1. The carbon stripper (classifier) is located downstream of the fuel reactor. The fine ground solid fuel is introduced into the fuel reactor, whereas the OC particles are larger in size. The stream of coarse particles leaving the carbon stripper is sent to the air reactor whereas the fine stream is reintroduced into the fuel reactor. The OC refill stream in Figure 1 is necessary to achieve the desired target circulation flow rate of OC during the iterative solution procedure. It will approach zero at steady-state.

Two different fuels are used in the simulations: The Columbian hard coal "El Cerrejon" and the Turkish lignite "Soma". Fuel data is given in Table 1 (9,10). For both types of coal the feed has been adjusted to 100 MW$_{th}$ at complete combustion. The initial particle size distributions of the coals are like those a state of the art mill for pulverized coal boilers produces (11). The impregnated oxygen carrier particles are composed of 10 wt.-% CuO and inert Al$_2$O$_3$ (Puralox NWa155 from Sasol, Germany). The particle size of the oxygen carrier is defined by the inert support, therefore a measurement via laser diffraction was carried out on the Puralox. For 900°C and a mixture of CO_2 and H_2O the

Figure 1: Simulated Flowsheet

Table 1: Fuel data

	El Cerrejon	Soma
app. density of char [kg/m³]	1500	750
LHV [MJ/kg] (raw)	28.00	16.08
water [wt.-%] (raw)	15.39	17.10
ash [wt.-%] (wf)	10.30	19.80
volatiles [wt.-%] (waf)	41.90	64.10
C [wt.-%] (waf)	81.00	62.47
H [wt.-%] (waf)	6.01	5.11
O [wt.-%] (waf)	10.70	28.68
N [wt.-%] (waf)	1.50	1.12
S [wt.-%] (waf)	0.79	2.62

settling velocity distributions are shown in Figure 2 (apparent density of OC is 1800 kg/m³ in oxidized state). Due to their different apparent densities both coals have a slightly different settling velocity distribution even through they have the same particle size distribution. Assuming 50 % oxygen carrier conversion, circulation flows of 706 kg/s and 779 kg/s OC have to be maintained for El-Cerrejon hard coal and Soma lignite, respectively. The fuel reactor is operated at 900 °C and the porosity in the reactor is calculated as 0.55. The

average solids residence time in the fuel reactor based on the OC circulation flow and the fuel feed is 240 s.
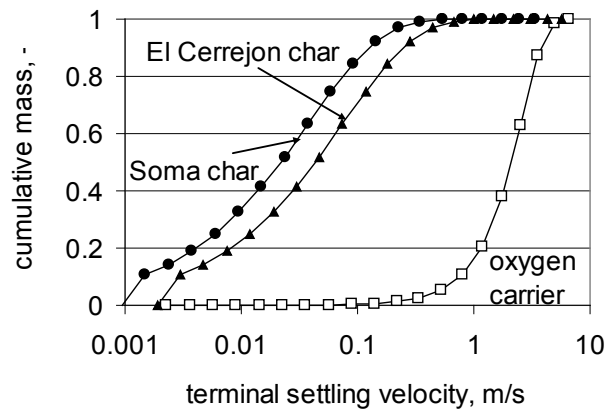
Figure 2:Settling velocity distributions for Soma char (dots), El Cerrejon char (triangles) and oxygen carrier (empty squares) in the range of overlap

Simulation Results

The simulation results are compared on basis of the CO_2 capture rate CCR:

$$CCR = \frac{CO_2 \text{ flow from fuel reactor}}{\text{total } CO_2 \text{ flow based on fuel input}} \quad (3)$$

The CCR is lower than 100 %, if char is transported with the flow of coarse OC particles from the carbon stripper to the air reactor, since the char would combust and form CO_2 there. Char slip cannot be reduced to zero because the separation of OC and char particles in the carbon stripper is not ideally sharp and there is a certain overlap of the settling velocity distributions of char and OC (Figure 2).

Figure 3 shows the result of the variation of the cut velocity for a separation sharpness of $\chi = 0.5$. It can be observed that the char flow towards the air reactor

Figure 3: Char flow towards air reactor and corresponding total flow of solids entering the carbon stripper in dependence of cut velocity (χ=0.5). Empty dots denote El Cerrejon and filled dots denote Soma coal.

decreases with increasing cut velocity, while the solid flow to the sifter increases. The char flow to the air reactor has a minimum at approximately 2 m/s cut velocity. The increased flow that is returned to the reactor dilutes the char and thereby causes the minimum in the char flow to the air reactor. Since Soma lignite has a higher volatiles content compared to the El Cerrejon coal, the char flow is in general lower. Furthermore the lower char density of Soma lignite facilitates the separation in the carbon stripper. The solids flow to the classifier is increasing considerably when the cut velocity is increased. For example at 3 m/s the flow entering the sifter is approximately 3.3 times the flow of OC particles circulating between the reactors. Such high circulation rates would necessitate a rather large carbon stripper.

In Figure 4 and Figure 5 the CCRs for El Cerrejon hard coal and Soma lignite are shown in dependency of the cut velocity. Without carbon stripper, only CCRs as low as 0.41 and 0.56 are calculated for El Cerrejon and Soma coal, respectively. For $\chi = 0.5$ the maximum CCR of 90.6 % (92.9 % for Soma) is reached at roughly 2 m/s cut velocity. The influence of the

separation sharpness is demonstrated by a variation between $\chi = 0.5$ (usual technical sharpness) and $\chi = 0.8$ (technically sharp separation). If a separation sharpness as high as $\chi = 0.8$ can be realized, the CCR can reach values as high as 98.3 % (98.8 % for Soma).

Even if a separation sharpness higher than 0.5 cannot be achieved, there is still potential for improvements in the CCR. Especially by influencing parameters like: particle size distributions of the coal and OC particles, temperature in the fuel reactor, fuel reactor size / residence time, steam enrichment of the gasification gases and the reactivity of the char.
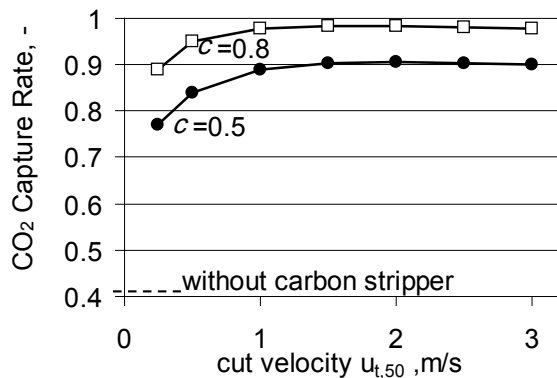
Figure 4: CCR in dependency of the cut velocity for El Cerrejon coal and separation sharpnesses of $\chi = 0.5$ and $\chi = 0.8$
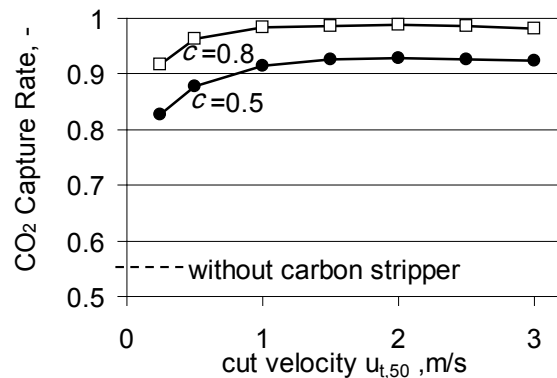
Figure 5: CCR in dependency of the cut velocity for Soma coal and separation sharpnesses of $\chi = 0.5$ and $\chi = 0.8$

Conclusions

The influence of the carbon stripper on the CO_2 capture rate of a CLC process for solid fuels was investigated. It was demonstrated that the carbon stripping step is of great importance if high CO_2 capture rates are to be achieved. Without carbon stripping the CO_2 capture rate can, depending on the fuel, be below 50 %. An increase in the cut velocity of the carbon stripper lowers the carbon slip to the air reactor (until a minimum is reached at approximately 2 m/s) but on the other hand increases the load on the carbon stripper.

Acknowledgement

References

1. Berguerand N., Lyngfelt A. (2008), Int. J. Greenh. Gas Con. 2, 2, 169–179.
2. Jensen A. (1996), Nitrogen Chemistry in Fluidized Bed Combustion of Coal. Ph.D. thesis. Technical University of Denmark. Lyngby, Denmark.
3. Levenspiel O. (1989), The chemical reactor omnibook, OSU Book Stores. Corvallis, Or.
4. Matsui I., Kunii D., Furusawa T. (1985), J. Chem. Eng. Jpn. 18, 2, 105–113.
5. Matsui I., Kunii D., Furusawa T. (1987), Ind Eng. Chem. Res. 26, 1, 91–95.
6. Rogers R. S. C. (1982), Powder Technol. 31, 1, 135–137.
7. Rumpf H. (1990), Particle technology, Chapman and Hall. London.
8. SolidSim Engineering GmbH (2010), SolidSim. http://www.solidsim.com/.
9. Ratschow L. (2009), Three-dimensional simulation of temperature distributions in large-scale circulating fluidized bed combustors, Shaker. Aachen.
10. Küçükbayrak S., Kadioğlu E. (1989), Thermochimica Acta 155, 1–6.
11. Baumeister W., Bischoff W., Pannen H. (2002), VGB PowerTech 82, 9, 54–60.

Thermodynamic analysis of a base case coal-fired Chemical Looping Combustion power plant

Dipl-Ing V Kempkes, Prof Dr-Ing A Kather

Institute of Energy Systems, Hamburg University of Technology, Denickestrasse 15, Hamburg, Germany

Introduction

The Chemical Looping Combustion (CLC) process is commonly realized as a coupled fluidised bed system which consists of two reactors, the air reactor and the fuel reactor. Both reactors are connected by a circulating stream of solid oxygen carrier [1, 2]. The solid oxygen carrier reacts particularly well with gaseous fuel components. For this reason, solid fuel components have to be gasified with CO_2 and H_2O to generate CO and H_2, which can then be oxidised by the solid oxygen carrier in the fuel reactor. To secure a certain amount of CO_2 and H_2O the fuel reactor is fluidised by recirculated flue gas or – to enhance gasification kinetics – by pure steam or steam-enriched flue gas. Eight different cases are modelled, to investigate the impact of different fluidisation requirements, steam addition and air ingress on the overall process behaviour of a base case CLC system.

Modelling approach

CLC Process
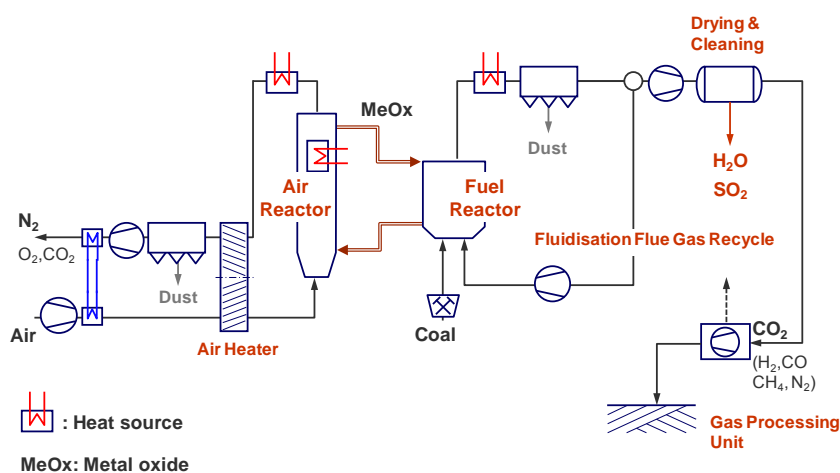
Figure 1: *Simplified scheme of the base case process of Chemical Looping Combustion*

The general setup of the CLC process has been modelled in Aspen Plus® and is shown in Figure 1. The fuel reactor is hard-coal fired and has a thermal input of 1000 MW. The air and the fuel reactor are modelled with an equilibrium approach. Air fluidises the air reactor and oxidises the reduced oxygen carrier. The oxygen-depleted air is separated from the oxygen carrier particles with a cyclone unit downstream of the air reactor. The oxygen carrier is transported to the fuel reactor via a loop seal, while the oxygen-depleted hot air is cooled down to 353 °C in a heat recovery system. The remaining heat is used to preheat fresh air within a regenerative air heater and an additional heat recovery system. Dust is removed by an electrostatic precipitator (ESP) downstream the regenerative air heater. In the fuel reactor the solid fuel is pyrolysed and subsequently gasified by H_2O and CO_2. The gasification products reduce subsequently the solid oxygen carrier. Almost all nitrogen and sulphur content of the fuel is converted to N_2 and SO_2. A carbon stripper is used to increase the solid fuel conversion in the fuel reactor by separating char particles and the solid oxygen carrier at the exit of the fuel reactor. The

High Temperature CO_2 Capture with CaO in a 200 kW$_{th}$ Dual Fluidized Bed Pilot Facility

C. Hawthorne, H. Dieter, H. Holz, T. Eder, M. Zieba, G. Scheffknecht

IFK, University of Stuttgart, Stuttgart, Germany

1. Introduction

The Calcium Looping (CaL) process is a promising post-combustion technology for the capture of CO_2 from coal-fired power plant flue gases [1]. The Calcium Looping process is based on the reversible reaction including calcium carbonate, calcium oxide, and carbon dioxide ($CaO_{(s)} + CO_{2(g)} \leftrightarrow CaCO_{3(s)} + Heat$). Carbonation occurs at temperatures between 600-700°C, and CO_2 is released by the calcium carbonate particles around 850-950°C at a sufficiently high rate depending on the bulk CO_2 partial pressure. Utilizing this reversible reaction, the Calcium Looping process is conducted in a Dual Fluidized Bed (DFB) system, consisting of a carbonator where CO_2 from flue gas is captured, and a regenerator where CO_2 is released. Coal is combusted with oxygen (mixed with re-circulated flue gas) in the Regenerator to supply the heat for calcination, producing a CO_2-rich flue gas (>95 vol.-%) for compression and storage. The process employs widely available natural limestone and offers high CO_2 capture rates with electric efficiency penalties comparably lower than competing capture technologies such as amine scrubbing. Furthermore, the heat released in the carbonator due to CO_2 capture, as well as the carbonator and regenerator convective pass, can be used efficiently in an additional steam power cycle, thereby increasing the overall electric output [2]. This paper shows the first ever pilot plant results of the Calcium Looping process from the newly commissioned 200 kW$_{th}$ facility at IFK.

Figure 1: The Calcium Looping (CaL) process.

F_{CO2}	CO_2 molar flow rate
F_0	$CaCO_3$ molar make-up rate
F_{Ca}	Calcium molar looping rate
E_{CO2}	CO_2 Capture efficiency
X_{carb}	Carbonation conversion
F_{Ca}/F_{CO2}	Calcium Looping ratio
F_0/F_{CO2}	Make-up ratio

2. Experimental

The technical feasibility of the CaL process was demonstrated on a 10 kW$_{th}$ (flue gas equivalent) electrically heated dual fluidized bed lab-scale facility at IFK achieving CO_2 capture efficiencies above 90% [3]. Therefore, a joint industrial-university research and development project was initiated to design and operate the Calcium Looping pilot plant to be used to scale up the process to a pilot size of 20 MW$_{th}$ [4]. The IFK pilot plant [4] was designed to: a) process real coal combustion flue gas as well as synthetic flue gas, b) investigate the thermal and chemical dynamic behavior of the plant for scale-up, and c) investigate long-term sorbent behavior, especially with respect to regeneration in an oxyfuel atmosphere in the presence of coal ash and sulfur. The carbonator, and associated equipment, is sized to process a combustion flue gas equivalent in flow rate to a 200 kW$_{th}$ coal-fired boiler. The 200 kW$_{th}$ pilot facility consists of three interconnected fluidized bed reactors which, as shown in figure 2, can be operated in two different Calcium Looping DFB configurations. In the (1) first configuration (reactor (C) – CFB carbonator, reactor (B) – CFB regenerator), the reactors are connected via two crosses in which the material flow rates are controlled by two cone valves, as described by Hawthorne et al. [4]. The (2) second configuration (reactor (A) – turbulent FB carbonator, reactor (B) – CFB regenerator) controls solid circulation via one L-valve and the two fluidized beds are hydraulically linked by a loop

seal at the bottom of reactor (A). Since a CFB carbonator is superior to a turbulent FB in terms of optimizing CO_2 capture costs (good CO_2 capture at higher flue gas throughputs), configuration (2) could in principle be outfitted with a CFB carbonator without altering DFB functionality. Therefore, both configurations are potentially feasible options for commercialization of the Calcium Looping process. This paper details the operation and experimental results of configuration (2) on a pilot scale.

The turbulent FB carbonator circulates sorbent internally and has a diameter of 33 cm and a height of 6 m. The entrained sorbent removes CO_2 from the flue gas and is separated from the exiting flue gas by the primary cyclone, returning to the bed by means of the upper loop seal. The internal circulation of sorbent achieves a uniform temperature throughout the entire vertical height of the carbonator ensuring controlled experimental conditions. The carbonator temperature was varied between 620 and 700 °C. The partially carbonated sorbent leaves the carbonator and enters the regenerator (21 cm diameter, 10 m high) by way of the lower loop seal where it is fully calcined to CaO. The rate of solid discharge from the L-valve determines the circulation rate of the system and the lower loop seal fluidization rate regulates the distribution of total solid inventory between the two reactors. In this experimental campaign, the required energy for heating up and calcining the incoming solids is provided by the combustion of wood pellets under oxygen-enriched conditions. Wood pellets were chosen as the fuel since it was desired to test the process without the effects of coal ash and sulfur on sorbent activity. Upcoming publications will focus on the effect of the coal matrix on the Calcium Looping process.

Figure 2: The 200 kW$_{th}$ Pilot Plant DFB Configurations.

The pilot plant is equipped with numerous pressure transducers and thermocouples and all inlet and outlet gas flows are continuously recorded. The inlet and outlet concentrations of the carbonator are continuously recorded by online analyzers, as is the outlet concentration of the regenerator. The internal reactor specific solids circulation rate and the sorbent looping rate (circulation rate between reactors) are measured by means of a solids measurement unit. Additionally the solid flow can be measured continuously by means of a special solid flow sensor adapted to high temperatures. In all, over 250 process measurements are recorded every second by the process control system.

The limestone used in these experiments is a local limestone from the Swabian Alb with a particle size of 300-600 μm. A synthetic flue gas (air & CO_2) was fed to the carbonator with a CO_2 concentration of either 10 or 15 vol.-%. These experiments collected data from numerous steady-states in which the carbonator temperature and gas concentrations remained constant for a fixed period of time. After the steady-state measurement was completed, solid samples of the carbonator and regenerator bed were taken in order to measure their carbonated fraction and their rate of CO_2 uptake. The sorbent looping rate was also measured with the solids measurement unit. Furthermore, to quantify the rate of material loss due to attrition, the amount of dust collected in the secondary cyclone and filters was measured every hour.

3. Results

The facility operated stably over several days and the first experimental calcium looping campaign with the new 200 kW$_{th}$ Calcium Looping facility was concluded successfully. The pertinent carbonator and regenerator process parameters such as bed inventory and sorbent

looping rates required for Calcium Looping were achieved. As suggested by previously conducted scaled cold modeling work, the DFB system proved to be a robust and smooth system. Furthermore, it was capable of changing from one steady-state to another (e.g. carbonation temperature, circulation rate) with relative ease and usually within 15 minutes. The carbonator temperature profile was very uniform and stable over time.

The oxygen-fired regenerator combusting wood pellets with an oxygen-air mixture as high as 50 vol.-% at exit temperatures between 875-930 °C, proved to be a very stable and efficient sorbent calciner, already logged over 250 hours of operation. The temperatures and sorbent residence time in the regenerator are sufficient to achieve full sorbent calcination as confirmed by subsequent thermo gravimetric analysis of the bed samples taken during experimentation. The effect of sorbent attrition was found to be minimal with regard to process operation. The mean particle diameter dp_{50} decreased during one week of operation by 100-150 µm. Preliminary results based on the dust collected over many days of operation from the filtration system indicates sorbent loss (as a fraction of total solids inventory) due to attrition occurs at a rate of 5 wt.-%/h. This result demonstrates that attrition of the limestone sorbent is not a major obstacle to process commercialization. Furthermore, there remains preventative measures to reduce this measured rate of attrition.
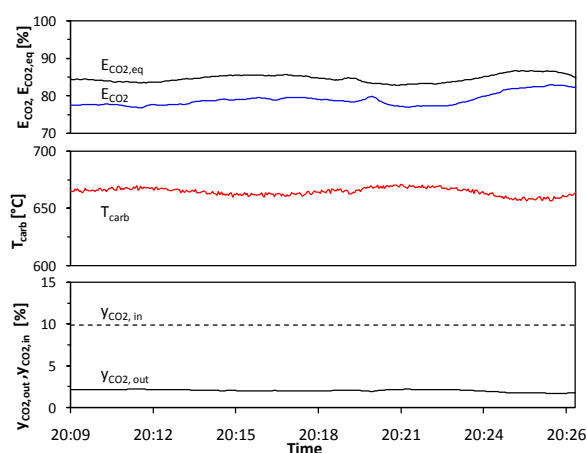
Figure 3: Steady state operation: E_{CO2}, $E_{CO2,eq}$, T_{Carb}, $y_{CO2, in}$ and $y_{CO2,out}$ are plotted vs. time.

A 20 minute steady state at 650 °C with an CO_2 inlet concentration of 10 vol.-% is shown in Figure 3. The CO_2 outlet concentration is in the range of 2.1 vol.-% which results in a CO_2 capture efficiency above 80 %, close to equilibrium. Small changes in carbonator temperature of less than 10 °C are attributed to fluctuations in the solid circulation rate and are typical of DFB systems. Improvements have since been undertaken to minimize future fluctuations and their effect on temperature.

The effects of a change in CO_2-inlet concentration from 10 to 15 % at constant gas flow and sorbent looping rate is plotted in Figure 4. Despite an increase in the inlet CO_2 concentration (and molar CO_2 input), the carbonator temperature and outlet CO_2 concentration remains at first constant meaning more CO_2 is being captured, resulting in a temporary increase in capture efficiency of 6-7 % with the equilibrium capture efficiency likewise increasing. However, since more CO_2 is being captured, the additional heat from the exothermic carbonation reaction is released raising the carbonator bed temperature from 650 °C to 680 °C in around 5 minutes. Since the equilibrium CO_2 concentration increases with temperature, less CO_2 is subsequently captured and the capture efficiency sinks back to near its initial value.

Figure 4: Transition between $y_{CO2,in}$=10 and 15 vol.-%.

The results shown here focus on temperature variation and the corresponding change in CO_2 capture in the pilot plant. Figure 5 shows the measured carbonator CO_2 outlet concentrations of various steady states in a temperature range between 620-700 °C and for CO_2 inlet concentrations of 10 and 15 vol.-%. As mentioned previously, the equilibrium CO_2 concentration rises with increasing temperature, thereby limiting the maximum capture possible. Although the experiments were conducted with two different CO_2 inlet
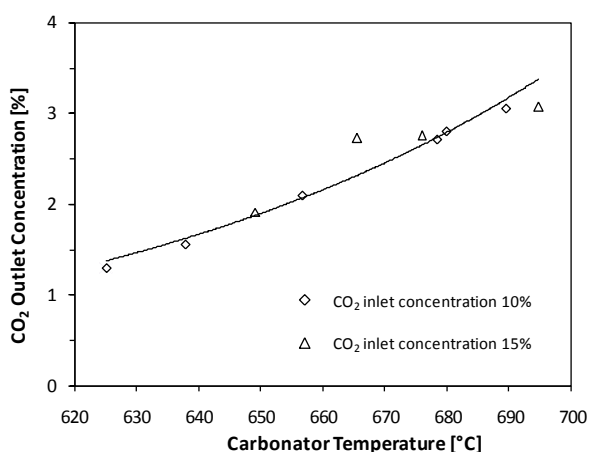
Figure 5: Carbonator outlet Concentration vs. Carbonator Temperature.
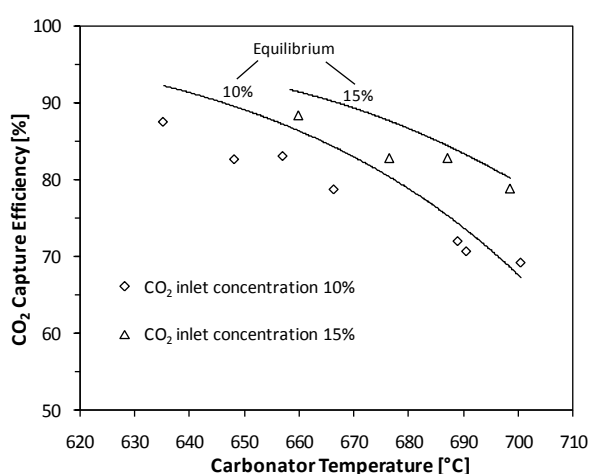
Figure 6: Capture efficiency with different CO_2 inlet concentrations.

concentrations, the measured values follow the expected exponential trend indicating that the CO_2 capture efficiency is close to equilibrium.

Figure 6 shows the steady state capture efficiency values classified according to either an inlet CO_2 concentration of 10 or 15 vol.-%, along with their respective equilibrium capture efficiencies. The measured capture efficiencies generally lie in close proximity to their respective equilibrium curves which indicates good gas-solid contacting in the turbulent fluidized bed carbonator. Carbonator temperatures below 680 °C in this data set were normally associated with lower solid looping ratios, which is the ratio of the mol of fresh CaO coming from the regenerator to the molar flow of CO_2 fed to the carbonator (see figure 1), and led to an increased carbonated fraction in the bed and thus reduced CO_2 uptake rates. Therefore, the capture efficiency values are not as close to equilibrium as those at high solid looping ratios (since less CaO was carbonated). The carbonated bed fraction in the carbonator was determined with thermo gravimetric lab analysis. Most importantly, for concentrations between 10 and 15 vol.-%, CO_2 capture efficiencies as high as 88 % were achieved between temperatures of 630 °C and 660 °C during continuous operation of the new 200 kW$_{th}$ Calcium Looping pilot plant.

4. Conclusions

For the first time ever, the Calcium Looping process was demonstrated in continuous operation under realistic process conditions on a 200 kW$_{th}$ pilot plant. The process and pilot plant operation proved to be robust, stable, and easy to control. Full calcination of carbonated sorbent and fresh limestone was achieved in an oxygen-fired regenerator with inlet oxygen concentrations as high as 50 vol-%. The rate of total solids inventory loss due to sorbent attrition over many days was measured to be 5 wt.-%/h, thereby posing no serious obstacle to commercialization. Carbon dioxide capture efficiencies close to the thermodynamic equilibrium were achieved over a wide range of temperatures, calcium looping ratios, for CO_2 inlet flue gas concentrations of 10 and 15 vol-%. Capture efficiencies as high as 88 % were achieved at temperatures between 630 °C and 660 °C.

5. Acknowledgements

6. References

1. Abanades, J. C., Rubin, E. S., Anthony, E. J., 2004. Sorbent cost and performance in CO_2 capture systems. Ind. Eng. Chem. Res. 43, 3462-3466.
2. Hawthorne, C., Trossmann, M., Galindo Cifre, P., Schuster, A., Scheffknecht, G., Simulation of the carbonate looping power cycle. *Energy Procedia*. 2009, 1(1), 1387-1394.
3. Charitos, A., Hawthorne, C., Bidwe, A.R., Sivalingam S., Schuster, A., Spliethoff, H., Scheffknecht, G., Parametric investigation of the calcium looping process for CO_2 capture in a 10 kW$_{th}$ dual fluidized bed. *Int. J. Greenh. Gas Con.* 2010, 4(5), 776-784.
4. Hawthorne, C., Dieter, H., Bidwe, A., Schuster, A., Scheffknecht, G., Unterberger, S., Käß, M., CO_2 Capture with CaO in a 200 kW$_{th}$ Dual Fluidized Bed Pilot Plant. *Energy Procedia, 2011, (4) 441-448.*

CFD-model of a fluidized bed chemical looping system:
Design of a heat and mass flow control

H. Kruggel-Emden; S. Wirtz; V. Scherer

Department of Energy Plant Technology, Ruhr-University Bochum,

Universitätsstraße 150, D-44780 Bochum, Germany

Abstract

Carbon capture through chemical looping combustion is a technological and eco-nomical feasible option applicable to a wide range of fossil fuels. Within the chemical looping process the oxygen required for the fuel conversion is provided by a solid carrier material which is alternately oxidized and reduced in a spatially or temporally detached process. The oxidation of the carrier is strongly exothermic and the conver-sion of oxidation and reduction need to be balanced for temporally stable operation of the process.

Modeling of the transient behavior of a chemical looping system is possible through multiphase CFD in an Eulerian-framework. To reach steady state operation within simulations cooling of the reactors and carrier mass flow must be adequately ad-justed. Therefore an interconnected multiphase CFD-model is extended by an ad-justment control. Results obtained are relevant for experimentally investigated chemical looping systems where an adjustment control is essential in case of tran-sient operation.

1 Introduction

In order to reduce the impact of global warming conversion of fossil fuels in combina-tion with carbon capture poses a suitable option. Different technologies like pre-combustion, oxy-fuel combustion or post-combustion are available. Among these technologies chemical looping combustion has a high potential, due to its comparably low energy penalty [1]. Different modes of operation are applicable for chemical loop-ing combustion systems with fluidized bed technology being often favored due to its comparable easy solids handling characteristics.

Over the past 10 years chemical looping combustion has been intensively investi-gated, but it is yet not a commercially applicable technology. Demonstration proc-

esses of up to 1MW$_{th}$ are at present in operation [2] with the aim to increase system size further. Robust simulation tool are needed for system design and scale up.

Multiphase fluid dynamics models have been applied to chemical looping combustion in several cases e.g. [3,4]. A reacting, two dimensional chemical looping model in which the piping between the fuel reactor and the air reactor is represented in a simplified way was proposed recently by Kruggel-Emden et al. [5]. A limitation of the model and not discussed anywhere else in literature is that solid mass flow and temperature in the CFD-model are not controlled which results in non-stable operation. Therefore the model [5] is extended in this paper with a suitable adjustment control for mass flow and temperature.

2 Interconnected chemical looping CFD-model

The underlying chemical looping model is based on the two-phase Euler-approach implemented into the computational fluid dynamics software FLUENT. Balance equations are solved for the gas and solid phase. A sketch of the model is shown in figure 1. Air and fuel reactor are simulated in separated fluid dynamics simulations. Further details can be found in [5].

Figure 1: Outline of the modeling framework for chemical looping combustion.

If a predefined temperature level is desired in a chemical looping system heat needs to be extracted. Highest temperatures are reached in the air reactor therefore this vessel provides the best location to extract excess heat. Oxidation and reduction re-action are balanced by maintaining a sufficient solid circulation rate. For the purpose of control the heat flux density $\dot{q}$ and mass flow rate $\dot{m}_{s,buf}$ are the manipulated and the solid outlet temperature $T_{s,ox}$ and the degree of reduction $X_{s,red}$ ($X=1$ carrier fully reduced; $X=0$ carrier fully oxidized) are the controlled variables (figure 1).

3 Design of the temperature control

For the temperature control in the chemical looping system a controllable heat sink in form of a cooling jacket attached to the air reactor side walls is used. Solid and gas air reactor outlet temperatures $T_{s,ox}^{act}$, $T_{g,ox}^{act}$ are monitored and the excess heat flux $\dot{Q}$ with regard to a setpoint temperature $T_{g,ox}^{set} = T_{s,ox}^{set}$ is calculated:

$$\dot{Q} = c_{p\,s,ox} \cdot \dot{m}_{s,ox} \cdot \left(T_{s,ox}^{set} - T_{s,ox}^{act}\right) + c_{p\,g,ox} \cdot \dot{m}_{g,ox} \cdot \left(T_{g,ox}^{set} - T_{g,ox}^{act}\right) \tag{1}$$

The heat flux density for the air reactor is calculated according to a proportional-integral controller where Kp is the proportional and $1/Tn$ is the integral gain which are both controller tuning parameters:

$$\dot{q} = Kp / A_{surf} \cdot \left(\dot{Q} + 1/Tn \cdot \int_{\tau=0}^{\tau=t} \dot{Q}\, d\tau \right) \tag{2}$$

Tuning of Kp and Tn is achieved through a system characterization by investigating the open loop step response [6] of the air reactor to a predefined cooling. Tuning pa-rameters derived vary for different carrier mass flow rates (table 1).

$\dot{m}_{s,buf}$ [kg/s]	Kp [-]	Tn [s]
2	1.85	3.24
4	2.25	3.24
6	2.58	3.24

Table 1: Parameters of a PI-temperature controller derived according to an open loop step response [6] for a carrier of Mn_3O_4/MnO.

4 Design of the mass flow control

For the mass flow control the carrier material flux $\dot{m}_{s,buf}$ entering the air reactor is adjusted by a PI-controller:

$$\dot{m}_{s,buf} = -Kp \cdot \left((X_{s,red}^{set} - X_{s,red}^{act}) + 1/Tn \cdot \int_{\tau=0}^{\tau=t} (X_{s,red}^{set} - X_{s,red}^{act}) \, d\tau \right) \tag{3}$$

The proportional gain Kp and the integral gain $1/Tn$ are tuning parameters and are derived from a simplified external model of the fuel reactor. In the simplified model the fuel reactor is assumed to be an ideal mixer with constant solid volume in which the total fuel mass flow entering the reactor is converted. Kp and Tn are calculated based on an optimization of the transient overshooting of $X_{s,red}^{act}$ from its setpoint:

$$f(Kp, Tn) = \left| \int_{t=0}^{t=\infty} (X_{s,red}^{set} - X_{s,red}^{act}) dt \right| \tag{4}$$

Results for $f(Kp, Tn)$ are dependent on t_{del} which is the delay time the solid material needs to be passed through the air reactor. t_{del} is not calculated in the simplified external model. Results for Kp and Tn are given in table 2.

t_{del} [s]	Kp [-]	Tn [s]
3	52.1	9.7
4	39.5	11.5
5	31.9	13.5

Table 2: Optimized parameters of a PI-mass flow controller for a carrier of Mn_3O_4/MnO.

5 Simulation of chemical looping combustion in a controlled model

As a test case of the extended CFD-model a chemical looping system with Mn_3O_4/MnO as carrier material is operated at full load of P=0.5 MW and powered down to part load of 0.4MW and further down to 0.3 MW. The air reactor solid outlet temperature is set to $T_{s,ox}^{set}$=1270 K and the fuel reactor carrier conversion is set to $X_{s,red}^{set} = 0.55$. Carrier mass flow rates (figure 2A) are declining with decreasing load

level. Carrier mass flow rates leaving the fuel reactor reveal strong fluctuations and are influenced by the bubble characteristics in the bed. Carrier solid temperatures (figure 2B) stabilize quickly after each load change. In case of P=0.3MW no cooling of the air reactor is necessary (figure 3C). The related mass flow rate in this case is not sufficient to maintain the setpoint temperature of T=1270K for the air reactor outlet. The applied mass flow control effectively stabilized the degree of conversion of the carrier material in the system (figure 2D).
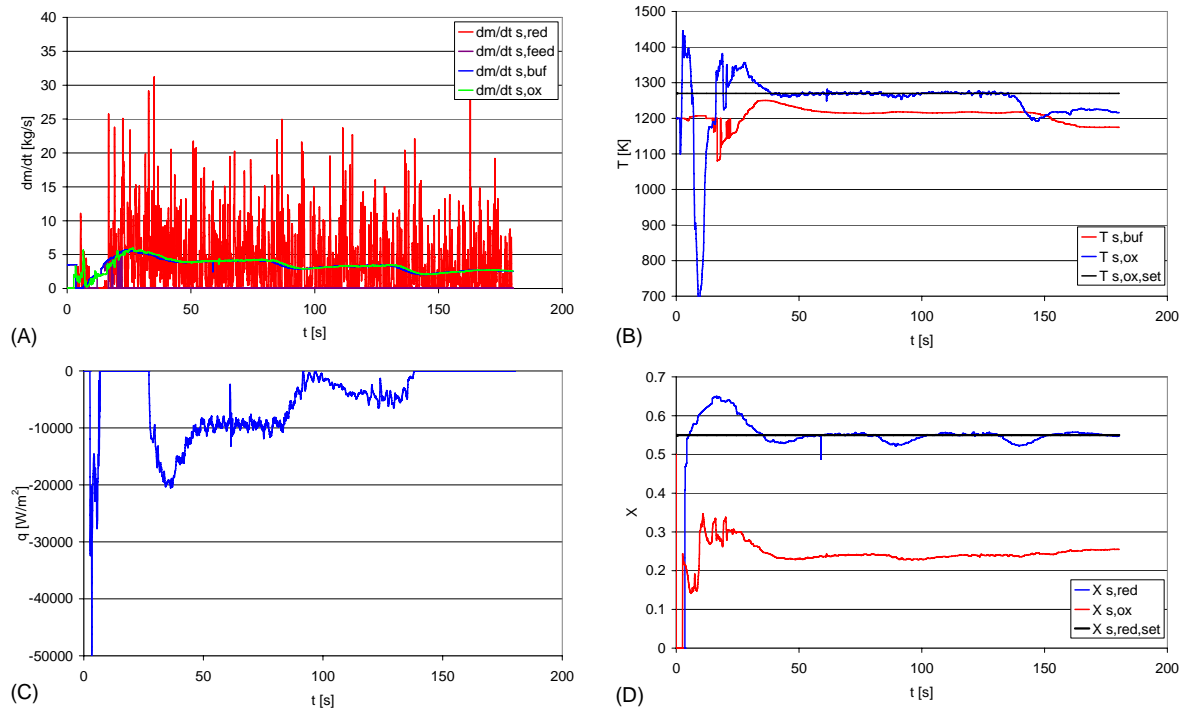
Figure 2: Performance of the chemical looping system operated at P=0.5MW for t<80s, P=0.4MW for 80s<t<130s and P=0.3MW for t>130s. (A) Solid mass flow, (B) temperatures, (C) heat flux density and (D) degrees of reduction of the different solid flows. $T_{s,ox}^{set}$=1270K and $X_{s,red}^{set}=0.55$.

6 Conclusions

A multiphase CFD-model was successfully extended with a temperature and mass flow control. PI-controllers were used and their control parameters were derived by analyzing an open loop step response in case of the temperature control and by utilizing an external model and applying an optimization routine in case of the mass flow control. For a test case where the system load was varied the control system allowed steady state operation of the chemical looping system within the multiphase CFD-model. For the future the derived control system allows detailed insight into the dynamics of chemical looping systems with varying carrier materials and system condi-

tions. The derived control parameters are also applicable to controllers in experimentally investigated chemical looping systems and are necessary for their effective operation.

References

[1] A.B. Rao, E.S. Rubin, *Environmental Science & Technology* **2002,** 36, 4467.

[2] B. Epple, J. Stroehle, *VGB Powertech* **2008**, 11, 85.

[3] J. W. Jung, I. K. Gamwo, *Powder Technology* **2008**, 183 (3), 401.

[4] W. Shuai, Y. Yunchao, L. Huilin, W. Jiaxing, X. Pengfei, L Guodong, *Chemical Engineering Research and Design*, in press. DOI:10.1016/j.cherd.2010.11.002

[5] H. Kruggel-Emden., S. Rickelt, F. Stepanek, A. Munjiza, *Chemical Engineering Science* **2010**, 65 (16), S. 4732.

[6] K. L. Chien, J. A. Hrones, J. B. Reswick, in: *Transactions of the American Society of Mechanical Engineers*, Vol. 74, Cambridge **1952**

LCA of coal-fired oxyfuel power plants

-cryogenic versus membrane-based air separation-

Petra Zapp, Andrea Schreiber, Josefine Marx
Forschungszentrum Jülich, Institute of Energy and Climate Research, Systems Analysis and Technology Evaluation (IEK-STE), 52452 Jülich, Germany

1. Introduction

The environmental performance of carbon capture and storage (CCS) beyond the reduction of climate effective CO_2 emissions has become more and more subject of a wider discussion. Among the different CCS concepts for power plants, oxyfuel combustion is a promising candidate for carbon capture. Taken from other oxygen demanding technologies, cryogenic air separation is an already available state-of-the-art technology to produce the high tonnage of oxygen per day necessary for commercial-scale oxyfuel power plants. However, the high energy demand is associated with a considerable loss in efficiency of up to roughly 10 %-points. This yields in an additional demand of fuel and related emissions. To reduce these effects, efforts are made to find new technology options with lower efficiency losses and lesser environmental impacts. One option is the development of high temperature ceramic membranes. For the analysis promising membranes produced from $Ba_{0.5}Sr_{0.5}CO_{0.8}Fe_{0.2}O_{3-\delta}$ (BSCF) perovskite material are considered.

Although some studies evaluate the environmental effects of oxyfuel processes using cryogenic air separation [1-4], none exists so far looking at membranes. This paper compares the environmental impacts of both air separation concepts in the context of an oxyfuel process using life cycle assessment (LCA) methodology. Beside global warming potential other environmental effects like acidification, eutrophication and human toxicity are considered. The results are reflected to the environmental effects of conventional power production without CCS.

2. Power plant concepts

For all concepts the same basic assumptions have been used to make the results comparable. Basis for the comparison is a German state-of-the-art super critical (SC) hard coal power plant without any CO_2 capture. Its technical conditions provide also the basis for modeling both oxyfuel concepts. Figure 1 outlines the structure considered in the life cycle investigations.
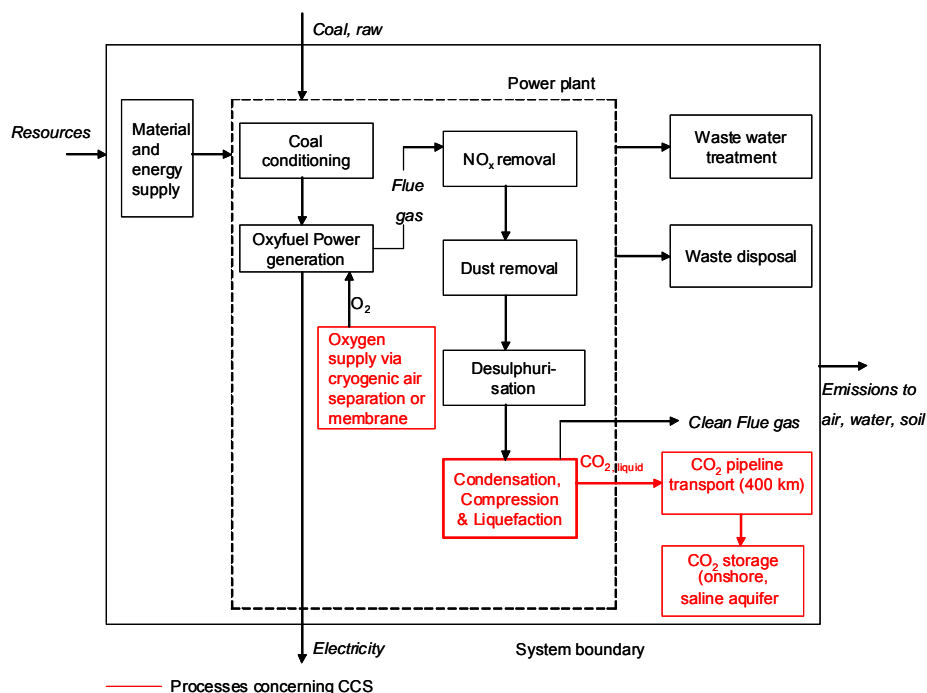
Figure 1: LCA system boundaries of a conventional power plant without CCS and an oxyfuel plant with air separation (red boxes)

2.1. Reference Power Plants without CCS

In 2004 a consortium of industry and science defined basic parameters to describe a SC power plant [5]. This SC reaches a net efficiency of nearly 46% surpassing the average net efficiency of German power plants. To reduce complexity the plant information are transformed into LCA structure. Basic processes of the system are "Coal conditioning", "Power generation", "NO_x removal", "Dust removal", "Desulphurization" (see fig. 1). The separation efficiency of the flue gas cleaning system represents advanced conditions under the current limits presented by German legislation [6] (SO_x: 150 mg/Nm^3 ≤ 200 mg/Nm^3, NO_x: 100 mg/Nm^3 ≤ 200 mg/Nm^3). For the analysis the South African coal "Kleinkopje" is considered.

2.2. The oxyfuel process

In addition to the basic processes the oxyfuel concepts include the "oxygen supply via air separation", "H_2O condensation, CO_2 compression & liquefaction", "CO_2 transport" via pipeline (400 km onshore) and "CO_2 storage" in a deep saline aquifer (800 m) (see also fig. 1). Air leakages of 3% are considered. The necessary oxygen is supplied by two different technologies for the air separation unit (ASU), cryogenic and membrane-based.

2.2.1. Cryogenic air separation

Cryogenic air separation (C-ASU) is a state-of-the-art technology suitable for high tonnage oxygen production for power stations. While energy consumption increases with higher O_2 purity requirements, a higher O_2 purity lowers the energy demand in the CO_2 compression and purification step. In compliance with other studies [7, 8] 95% purity is chosen for the investigation (containing 3.8% Ar and 1.2% N_2 [9]), as optimum value between additional energy necessary for further O_2 purification and savings obtained during the CO_2 compression. A specific energy consumption of 200 kWh/$tonO_2$ is estimated. The net plant efficiency amounts to 36.4%.

2.2.2. Membrane-based air separation

In recent years great efforts are undertaken to improve the efficiency of oxyfuel power plants by development and integration of novel gas separation membranes [10]. One possibility to provide oxygen is the use of high temperature ceramic membranes (HTM-ASU). A favored membrane material is $Ba_{0.5}Sr_{0.5}Co_{0.8}Fe_{0.2}O_{3-\delta}$ (BSCF) since its permeation rate is high because of its high ionic and electronic conductivity [11]. As this material still faces severe problems of chemical stability in a four-end concept, a three-end mode is chosen for this analysis. Thermodynamic modeling of a highly integrated membrane module [12] showed a required membrane area of 254 thousand m² assuming a membrane thickness of 0.6 mm and an average oxygen permeation rate of 1.75 ml/(min*cm^2). Applying membrane-based technology a plant efficiency of 39.6% is reached. In a first calculation a life time of 40 years for membranes and modules is assumed.

2.2.3. Performance parameter for the LCA analysis

The comparison of the different power plant types is performed on a basis of 1 kWh electricity produced (functional unit in LCA). In table 1 the main performance data of the three plants investigated are summarised.

Table 1: Performance data of the reference plant (RP SC) and of oxyfuel plants with cryogenic (C-ASU) and membrane (HTM-ASU) air separation

Plant parameter	RP SC	C-ASU	HTM-ASU
Plant net output [MW]	555.3	440.9	479.5
Net plant efficiency LHV [%]	45.9	36.4	39.6
Efficiency drop [%-points]	-	9.5	6.3
Membrane area [thousand m^2]	-	-	254
CO_2 recovery rate [%]	-	90.2	90.1

3. Environmental analysis of the power plant concepts

For the environmental analysis the total life cycle of the power plants is considered [13]. All life stages from the mining of the necessary materials and energy carriers, the production and operation of power plants and the final disposal after its life time are taken into account to avoid problem shifting between stages. Therefore, the described power plant systems are extended by upstream processes such as fuel or operation material supply and downstream processes like waste disposal or waste water treatment. Also construction and dismantling of components of the power plants and air separation facilities are included in the analysis.

In the life cycle inventory (LCI) a full inventory is set up for each power plant type by describing all relevant environmental inputs and outputs for each process step using the calculation software GaBi 4.4. Input and output data for the power plants are taken from detailed thermodynamic modeling [12] and transformed to LCA data, membrane data derive from partners of the MEM-BRAIN project [14]. Data for background systems such as fuel supply or waste treatment originate from the comprehensive ecoinvent database [15] and information about transport and storage are taken from one study [16].

In the Life Cycle Impact Assessment (LCIA) the gathered and aggregated inputs and outputs of the system are categorized and allocated to impact categories. Considered are the potential of global warming (GWP), acidification (AP), eutrophication (EP), human toxicity (HTP) and photochemical ozone creation (POCP). Characterisation of environmental impacts is based on CML 2001, updated in November 2009 [17]. The final normalisation step relates the results of the impact assessment to the total amount of the corresponding impact category in Germany.

3.1. Results of the inventory

For the three concepts the inputs and outputs along the entire life cycle are calculated. Table 2 shows important inputs (coal, limestone, NH_3) and outputs (CO_2, SO_2, NO_x, CO, particles, gypsum) for all power plants relative to 1 kWh electricity produced.

Table 2: Major inputs and outputs per kWh_electricity produced_ of the power plants (incl. upstreams and downstreams)

		RP SC	C-ASU	HTM-ASU
Input				
coal	g/kWh	313.8	395.3	363.5
limestone	g/kWh	5.2	7.1	6.6
ammonia	g/kWh	0.9	0.2	0.15
Output				
CO_2	g/kWh	803	174	150
CO_2 captured	g/kWh	-	886.7	811.9
SO_2	g/kWh	0.74	0.50	0.43
NO_x	g/kWh	0.90	0.89	0.79
CO	g/kWh	0.15	0.20	0.20
particle	g/kWh	1.2	1.5	1.4
gypsum	g/kWh	8.9	12.3	11.3

When CCS technology is applied CO_2 emissions released decrease significantly as intended. In oxyfuel processes NO_x is decreased due to the changed process management which correlates to a reduction in ammonia demand. However, coal input and some other emissions, such as CO or particles increase due to the loss in efficiency. A decrease in SO_2 emissions is gained by a higher use of limestone, producing more gypsum.

3.2. Results of the impact assessment

Beside the emissions presented above, all other emissions are also considered when evaluating the environmental effects of the systems. Figure 2 shows five impact categories, expressed in the specific equivalent of the particular category again per kWh electricity produced. It gives also the portion of upstream and downstream processes.
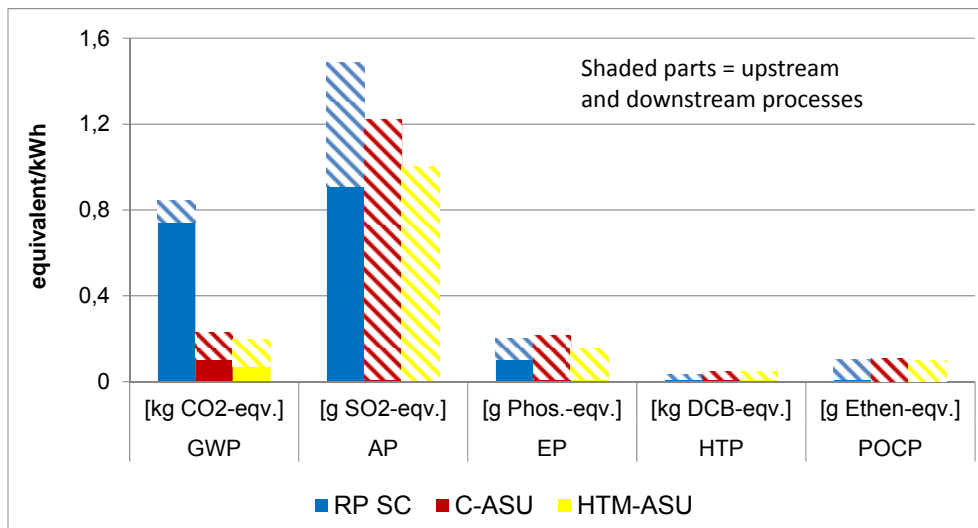
Figure 2: Selected environmental impacts of power plants per kWh$_{electricity\ produced}$ (incl. upstreams and downstreams)

The results show, that for both oxyfuel power plants the GWP and AP decrease compared to conventional power plants, while other impacts such as EP and POCP are hardly affected. However, HTP increases from 32.8 for the reference plant to 48.2 kg DCB-equivalent/kWh for the membrane ASU. While in most impact categories the membrane technology shows a better performance, mainly due to lesser efficiency losses, the human toxicity increases stronger. One reason for this is the high amount of steel in the membrane module.

Due to the efficiency losses the upstream coal process chain (mining and ocean coal transport) as well as downstream waste processes for ashes account mainly for the overall environmental effects. Whereas human toxicity is dominated by the production of the membrane module, especially the housing of the module, as described above. The results for the membrane-based air separation rely strongly on the assumed life time of the module and the membranes themselves. Sensitivity analysis show a strong increase in HTP at lower life times (117 kg DCB-equivalent/kWh for a life time of 5 years).

To evaluate the importance of different effects, each impact is benchmarked against the known total effect for this class, such as the total impacts of Germany. In table 3 it is assumed that the total electricity production by hard coal in 2007 (142 TWh, [18]) was generated using one of the three technologies considered. It is then related to the total German impact of that year.

Table 3: Total German impacts [19] and share of normalised impacts for 2007

Total German impacts [19] [kg-equiv.]		RP SC [%]	C-ASU [%]	HTM-ASU [%]
GWP	1.144 E12	10.4	2.7	2.4
AP	3.984 E9	5.3	4.4	3.6
EP	3.418 E9	0.83	0.88	0.62
HTP	1.014 E12	0.5	0.6	0.7
POCP	1.281 E9	1.1	1.2	1.05

As intended by CCS, the GWP could be reduced drastically from more than 10% without capture to 2.7% using cryogenic ASU and even to 2.4% with membrane technology. Also the contribution to the acidification potential could be reduced from more than 5% to less than 4%. To all other impacts the contribution of hard coal electricity production is quite low and changes are neglectable.

Conclusion and perspectives

Oxyfuel technology can contribute significantly to an environmentally friendlier electricity production. However, the resource demand for hard coal will increase by 25% for cryogenic and 15% for membrane-based air separation, due to its efficiency losses. The contribution to the total German GWP of hard coal based oxyfuel power generation could be reduced to 2.4%. Also, the AP is decreasing. Other impact categories are hardly affected by a change in technology. The slight increase in emissions which cause human toxicity do not rise today's low share of this sector to a concerning one. As efficiency decrease is the driving force of most changes and no chemicals or other substances are involved in the capture process, technologies with lesser effects on the efficiency are favorable. The efforts in the development of membrane based air separation show a good way to improve the environmental performance. However, further research demand can be defined. Long term tests under operating conditions must prove the modeled performance data used for these calculations. Especially the life time and size of the housing of the membrane module play a decisive role. Effects on humans, although still marginal in a German overall view, are mainly driven by these factors. The performance of the membrane itself affects also the amount and supply of sophisticated materials. This subject has not been covered in this paper, but needs further investigation.

References

[1] M. E. A. Fischedick, et al. Comparison of carbon capture and storage with renewable energy technologies regarding structural, economic, and ecological aspects in Germany. International Journal of Greenhouse Gas Control 2007, 1, 121-133.

[2] C. Bauer, et al. NEEDS (New Energy Externalities Developments for Sustainability). Final report on technical data, costs, and life cycle inventories of advanced fossil power generation systems. Paul Scherrer Institut (PSI) Ch und Institut für Energiewirtschaft und Rationelle Energieanwendung, Univ. Stuttgart (IER) D, 2009.

[3] A. Korre, et al. Life cycle modeling and comparative assessment of the environmental impacts of oxy-fuel and post-combustion CO2 capture, transport and injection processes. Energy Procedia 2011, Vol. 4, 2510-2517.

[4] B. Singh, et al. Comparative impact assessment of CCS portfolio: Life cycle perspective. Energy Procedia 2011, Vol. 4, 2486-2493.

[5] VGB-PowerTech e.V. (ed). Konzeptstudie Referenzkraftwerk Nordrhein-Westfallen (RKW NRW) 2004. Report 85.65.69-T-138, 123, VGB PowerTech service GmbH: Essen, February.

[6] Thirteenth Ordinance on the Implementation of the Federal Immission Control Act: Ordinance on Large Combustion Plants and Gas Turbine Plants -13. BImSchV. Federal Law Gazette I, p.1717, Bundesanzeigerverlag 2004: Cologne, 20 July.

[7] D. J. Dillon, et al. Oxy Combustion Processes for CO2 Capture from Power Plants 2005. IEA Greenhouse Gas R&D Programme, Report 2005/9.

[8] W. F. Castle. Air separation and liquefaction: recent developments and prospects for the beginning of the new millennium. International Journal of Refrigeration 2002, 25(1), 158-172.

[9] A. Kather and S. Gunter. The oxycoal process with cryogenic oxygen supply Naturwissenschaften 2009, 96(9), 1-18.

[10] M. Czyperek, et al. Gas separation membranes for zero-emission fossil power plants: MEM-BRAIN. Journal of Membrane Science 2010, 359(1-2), 149-159.

[11] S. Engels, et al. Simulation of a membrane unit for Oxyfuel-Power-Plants under consideration of realistic BSCF-membrane properties, Journal of Membrane Science 2010, 359(1-2), 93-101.

[12] R. Castillo. Thermodynamic evaluation of membrane based oxyfuel power plants with 700 C technology. Energy Procedia 2011, Vol. 4, 2026-2034.

[13] ISO 14040/14044 Environmental management - Life cycle assessment - Principles and framework, - Requirements and guidelines. (2006),

[14] MEM-BRAIN, www.helmholtz.de/allianz-mem-brain

[15] Ecoinvent Centre 2007. Ecoinvent data v2.0, 2007. Swiss Centre for Life Cycle Inventories. www.ecoinvent.ch.

[16] C. Wildbolz. Life cycle assessment of selected technologies for CO2 Transport and Sequestration. Diploma Thesis July 2007 No. 2007MS05 Swiss Federal Institute of Technology, Zurich.

[17] J. Guinée, et al. Handbook on Life Cycle Assessment: Operational Guide to the ISO Standards. Kluwer Academic Publishers 2002., Dordrecht.

[18] Zahlen und Fakten - Energiedaten. Federal Ministry of Economics and Technology Germany, BMWi, 2011, http://www.bmwi.de/BMWi/Navigation/Energie/Statistik-und-Prognosen/energiedaten.html

[19] GaBi 4.4, Software-System and Databases for Life Cycle Engineering. 2011, PE International, http://gabi-software.de

Dynamic Simulation of Oxyfuel Power Plants

A. Kröner, M. Pottmann

Linde AG, Linde Engineering, Dr.-Carl-von-Linde-Str. 6-14, Pullach, Germany

Introduction

As a leading international engineering and contracting company, the Engineering Division of The Linde Group designs and builds turnkey process plants for a wide variety of industrial users and applications. Dynamic simulation of process plants plays a key role in the engineering workflow, especially in the area of process innovation. This paper illustrates concepts for dynamic simulation of compound oxyfuel power plants.

Linde Engineering has been developing technical solutions for Carbon Capture and Storage (CCS) in power generation, both as proprietary developments and in collaboration with industry partners. Among them are CO2 scrubbing units for post-combustion power plants [1], IGCC precombustion techniques [2], innovative concepts for high pressure oxyfuel [3], and the efficient integration of atmospheric pressure oxyfuel process sections.

In an atmospheric oxyfuel power plant as shown in Figure 1, coal is combusted in the furnace in an atmosphere of gaseous oxygen (GOX), produced by an air separation unit (ASU), and CO_2. The CO_2-rich furnace outlet is cleaned in a flue gas treatment unit (FGT) from which the cleaned flue gas stream (FG) is transferred to the gas processing unit (GPU) for further concentration and compression. The GPU separates FG into a high-pressure CO_2 stream (CO2) ready for underground storage and inerts i.e. N_2, Ar, and O_2 vented to atmosphere (Vent). Parts of both raw flue gas and cleaned flue gas are recycled to the furnace to make up the burner atmosphere.

Tight dependencies within and among these process sections w.r.t. energy and mass flows, render a complex compound process. Based on long term experiences in air separation and CO_2 handling Linde Engineering is a competent provider of ASUs and GPUs for atmospheric oxyfuel power plants. Furnace, FGT, boiler, and steam cycle (of which the latter two are not shown in Fig. 1), are power plant specific units originating from industry partners.

The basis of steady state design are - among others - initial steady-state conditions of feed streams AIR and COAL, and of the GOX and FG streams connecting process

sections. Each project partner selects the most appropriate process technology and determines the most economic steady state design for his process section.
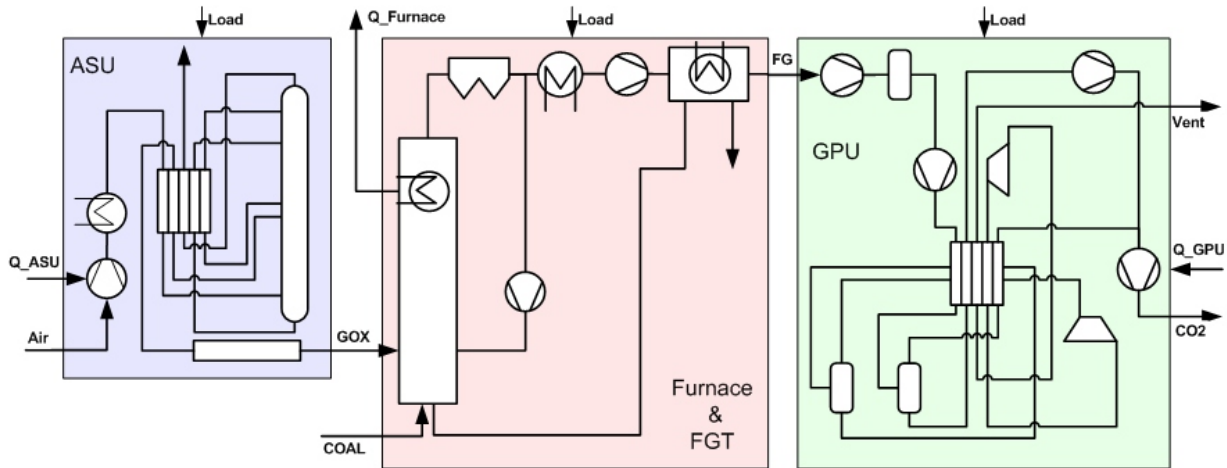
Figure 1: Schematic of an atmospheric oxyfuel power plant

Dynamic simulation

Once an optimal static process has been fixed, its flexibility in transient operation must be examined and adequate control schemes must be designed. This is a crucial issue as modern power plants are exposed to increasingly fluctuating electrical power demand. The dynamic behavior of process sections is investigated independently based on standard operating scenarios such as the one shown in Table 1. In order to cope with a change in electricity demand the COAL and GOX feed rates to the furnace shall be reduced from nominal 100% to 85% within 3 minutes. During this transition, the GOX pipeline pressure must remain within ±0.05 bar and the GOX O_2 concentration must remain within ±1.0%-points around their nominal values.

	COAL	GOX	CO2
flowrate (nominal)	100%-85% in 3 min	100%-85% in 3 min	-
pressure	-	±0.05 bar	100 bara
composition	-	±1.0 % O2	>95% CO2; <1% O2

Table 1: Typical load change conditions for COAL, GOX, and CO2 streams

At Linde Engineering dynamic simulation models are developed within software tools also used for steady state design. For ASUs an equation-based in-house simulator is used whereas GPUs are modeled with a commercial process simulator [4,5]. The basic control schemes are designed and tested with the section models using above standard disturbances introduced as step or ramp changes. Similar approaches are pursued by

project partners for investigation of their process sections. However, this only facilitates tests of the individual units without any feedback from interconnected process sections.

The compound oyxfuel process model

A compound oxyfuel power plant model is required to investigate dynamic interactions between the process units and their impact on process operability. For instance, the impact of flue gas recycle and energy integration on load change and disturbance responses of the interconnected process sections is of interest. As contributing partners use individual modeling and simulation software, a heterogeneous model collection needs to be integrated. This can be achieved if two conditions are satisfied [4]: i) the models are compatible at points of interchange, i.e. at source and sink of streams like GOX and FG, ii) the models are transferred to a common mathematical representation.

Model reduction and model identification is applied to the first-principle based dynamic section models including controllers. The reduced models are transferred to a general-purpose dynamic simulation software and connected to give the compound oxyfuel model.

The compound model is subjected to a load change as specified in Table 1. The following figures show the dynamic responses of relevant stream properties as deviations from their initial steady state values.
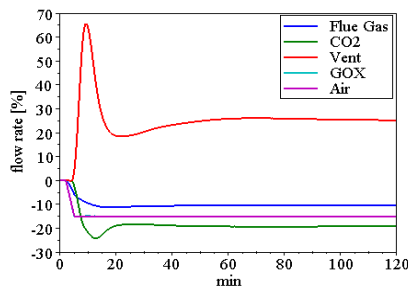
Figure 2: Flow rate deviations   Figure 3: CO2 mass fraction deviations
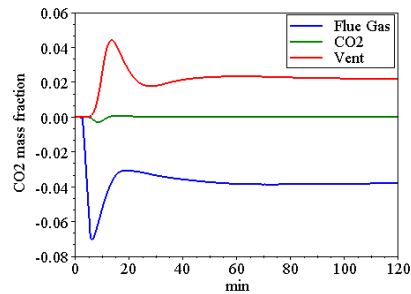
In Fig. 2 GOX and Air flow rates (as well as COAL feed not shown) behave almost identical due to controllers receiving setpoints proportional to the Load signal. The ASU is able to keep the O_2 concentration in the GOX stream within the required bounds of ±1% (Fig. 4). Even though the CO_2 content in the flue gas (FG) decreases significantly by 4%-points, very small concentration variations in the GPU CO_2 stream are observed. The decrease of the flue gas by less than 15% (Fig. 2) is due to a higher air leakage flow entering the furnace during part load and thus increasing the total vent flow. In the partial load case CO_2 and Ar in the flue gas (FG) are replaced by N_2 and water (not shown).

Finally, the pressure control scheme is capable to keep the GOX transfer line pressure fluctuations below 50 mbar. The GPU header pressure is held essentially constant due to suction pressure control at the GPU raw gas compressor (Fig. 7).
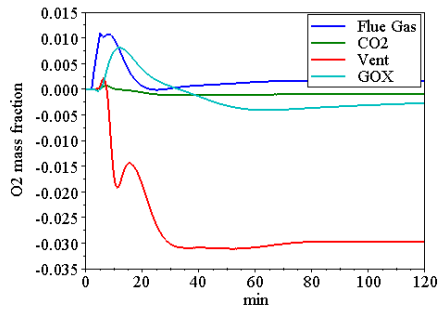
Figure 4: O_2 mass fraction deviations   Figure 5: N_2 mass fraction deviations
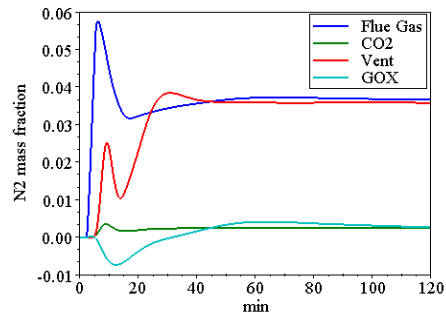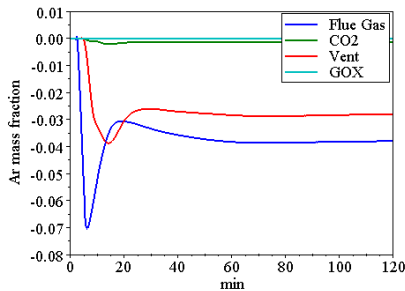
Figure 6: Ar mass fraction deviations   Figure 7: Pressure deviations
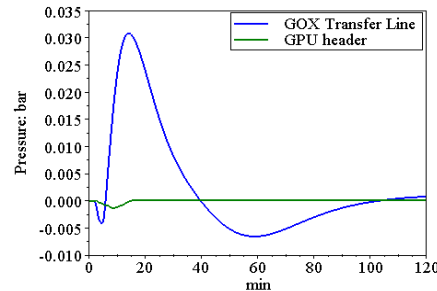
This dynamic simulation study of an atmospheric oxyfuel power plant proves the formerly introduced concept [4] based on stand-alone dynamic model development by different project partners, model reduction and identification and the combination of reduced models in an independent simulation environment. The compound model indicates feasibility of the design, and can be the basis for further process and control strategy improvements.

Literature

[1] RWE Power AG, BASF AG, Linde AG, 2008, press release, access 07.04.2011, http://www.rwe.com/web/cms/de/107138/rwe/verantwortung/im-dialog/aktuelles.

[2] Linde AG, 2009, Linde Annual Report 2009, München.

[3] Tautz, H., High pressure oxyfuel process, this conference.

[4] Engl, G. et al., Proceedings of ESCAPE 20, pp 451-456, Elsevier, 2010.

[5] Pottmann M. et al., Energy Procedia 4 (2011), pp 951-957.

CO₂-Capture from Cement Plants Applying Oxyfuel Concepts

Dipl-Ing S Oberhauser, Prof Dr-Ing A Kather, Hamburg University of Technology,

Institute of Energy Systems, Hamburg, Polysius AG, Beckum

1. Introduction

Carbon Capture from fossil fuel fired power plants has attracted growing interest in the field of CO_2 mitigation strategies over the past few years. Among the large stationary CO_2 sources, cement production contributes about 7% to the overall worldwide CO_2 emissions. Part of these CO_2 emissions is caused by the fuel required for the calcination reaction and to heat the raw material up to a temperature of 1400℃ . The largest part of the CO_2 emissions, however, is caused as a product of the calcination process. This part cannot be avoided by using less CO_2 intensive energy sources. Therefore, only CCS techniques seem to provide a promising CO_2 mitigation option for the cement industry.

Generally all of the 3 main CCS routes (oxyfuel, post-combustion and pre-combustion) could be applied to cement plants. In the case of post-combustion, a good CO_2 capture rate seems to excessively increase the fuel requirement needed for the regeneration of solvents like Monoethanolamine (MEA). However, the additional heat demand can be reduced by the development of less regeneration heat intensive solvents and improvements in heat integration. Pre-combustion, in its usual meaning, would only be suitable to capture the CO_2 emitted from the fuel, not from the calcination reaction. Compared with a power plant, the calcination reaction in an air-operated cement plant increases CO_2 concentration to a higher level. This indicates that the oxyfuel route seems to be a very appropriate concept for applying CCS to cement industries.

The aim of this work is to evaluate and compare several promising oxyfuel concepts for cement plants based on rigorous thermodynamic models in Aspen Plus®, taking into account realistic boundary conditions for both the oxyfuel and the reference air case. The influences of modified flue gas conditions on the key reactions are considered in detail. The selection criterion for choosing the concepts studied here is mainly the practical feasibility of the required process modifications. In a further step suggestions and corresponding simulations are shown to further improve these concepts in terms of fuel demand, electrical power duty and CO_2 capture rate.

2. Basic Information on Cement Plants

The raw material for cement production mainly consists of calcium oxide (CaO), silicon dioxide (SiO_2), aluminium oxide (Al_2O_3) and ferric oxide (Fe_2O_3). Additionally, small amounts of magnesium carbonate and other components containing alkali elements and sulphur can occur within the raw meal. The conditions required by two main reactions have to be provided within the cement plant. The first is the calcination of the raw meal according to equation (1) with a conversion rate of 100% at 880°C to 900℃.

$$CaCO_3 \rightarrow CaO + CO_2 \qquad (1)$$

The second important conversion is the recombination of CaO, SiO_2, Al_2O_3 and Fe_2O_3 to the clinker phases $2CaO·SiO_2$ (C2S), $3CaO·SiO_2$ (C3S), $3CaO·Al_2O_3$ (C3A) and

$4CaO \cdot Al_2O_3 \cdot Fe_2O_3$ (C4AF), which yield the characteristic behaviour of cement. Therefore, calcinated hot raw meal has to be heated up further to 1400°C - 1450°C. In a cement plant this step is provided by a rotary kiln in which the primary combustion occurs (see Figure 1)
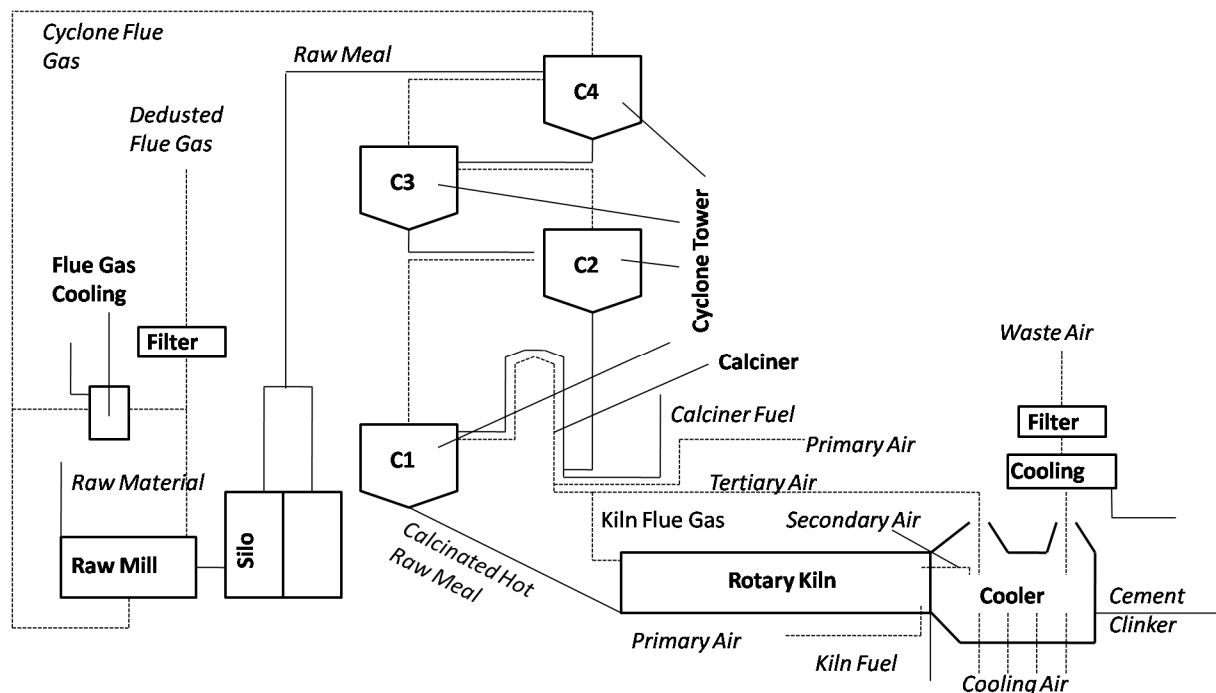
Figure 1: Flow Sheet of a Conventional Cement Plant with a Preheater of 4 Cyclones

The flue gas of the rotary kiln is used to preheat the raw meal in several cyclone preheater stages. Here the raw meal is mixed with flue gas to be heated up and directly afterwards, to be separated again from the flue gas. Conventional cement plants have 3 to 5, or occasionally 6 preheater stages. In modern cement plants the degree of calcination reaches an extent of more than 90% in the calciner loop before the rotary kiln. A secondary combustion and the rotary kiln flue gas provide the energy for this reaction. The secondary combustion causes more than 50% of the overall fuel demand. Before preheating, the raw meal is ground and pre-dried in the raw mill and enters the raw meal silos, which ensure high homogeneity in the feed stream to the upper cyclone. To fill up the silos the raw mill is designed for a higher supply rate than the required feed rate to the upper cyclone. Therefore an integrated operation mode exists in which the raw mill is running, the silos are filled up and the cyclone flue gas pre-dries the raw meal (compound mode). For a certain period of time the raw mill is out of operation, the silos are emptied and the cyclone flue gas is sent directly to a flue gas cooler and subsequently to the filter (direct mode). These particular operation characteristics also have to be taken into account for designing the oxyfuel operation.

3. Oxyfuel Concepts

The most obvious concept for the oxyfuel operation of a cement plant can be described as follows (see Figure 2).

Hot ESP   *CO2 Rich Flue Gas*

Raw Meal   C4   *Secondary, Tertiary Oxygen*

Dedusted Flue Gas   C3

Waste Air

C2   Cyclone Tower   *(Gas-Gas Heat Exchanger)*   **Filter**   **Cooling**

Calciner

Calciner Fuel

Primary Oxygen

Filter

Raw Material   C1   *Kiln Flue Gas*

Calcinated Hot Raw Meal

Raw Mill   **Silo**   **Rotary Kiln**   **Cooler**   *Cement Clinker*

Primary Oxygen   *Kiln Fuel*   *Cooling Air*
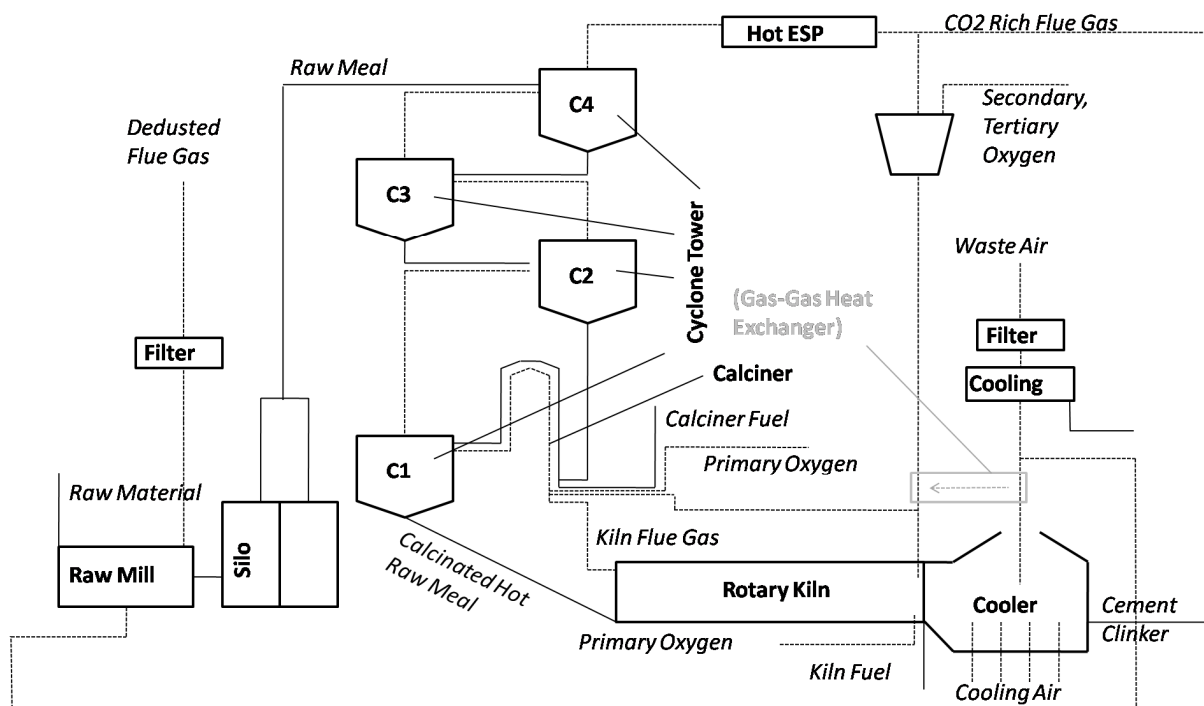
Figure 2: Flow Sheet of a Full Oxyfuel Cement Plant with a Preheater of 4 Cyclones

An air separation unit (ASU) is installed to supply both primary and secondary oxygen for combustion. The oxygen excess is held to be the same as in the reference case, 1.15 for the primary and 1.30 for the secondary combustion. The flue gas of the upper cyclone preheater is dedusted in a hot ESP. More than 50% of the flue gas has to be recycled to provide the same adiabatic flame temperature in the primary combustion as well as the same flow regime (same solid loadings) in the calciner loop. The latter has the more important contribution but is a conservative estimation. The recycled flue gas can be reduced if higher loadings are possible resulting in lower temperatures at the recycle split and therefore lower heat losses. The remaining flue gas is cooled, desulphurised, and treated in a CO_2 purification and compression unit. Instead of flue gas, hot air from the clinker cooler has to be used to pre-dry the raw meal in the raw mill in order to avoid air inleakage. The air from the cooler cannot be used as combustion air which causes a large amount of heat that is not reused. Nonetheless, part of the heat of the clinker cooler could be reused by a gas-gas heat exchanger or by supplying part of the cooling duty by means of recirculated flue gas, thus sending the flue gas directly through the cooler with air inleakage.

It could be preferable to operate the rotary kiln of the new oxyfuel plant applying conventional air combustion. The reason for this is the huge experience in achieving the required clinker quality under various raw meal and fuel conditions and the unknown impact of oxyfuel operation on clinker quality. In this case (see Figure 3) a concept exists where the ASU only supplies oxygen to the calciner. The flue gas of the conventional rotary kiln is separated from the calciner and the oxyfuel preheating tower. To reuse the heat of the rotary kiln flue gas a second tower of cyclone preheater stages has to be installed in which a part of the raw meal is preheated. A small part of the hot air from the clinker cooler can be used in the primary combustion. For the remaining heat the same considerations can be made as in the full oxyfuel case, either to reuse the heat of the hot air in a gas-gas heat exchanger for preheating the recirculated flue gas or to directly use the recycled flue gas for clinker cooling.
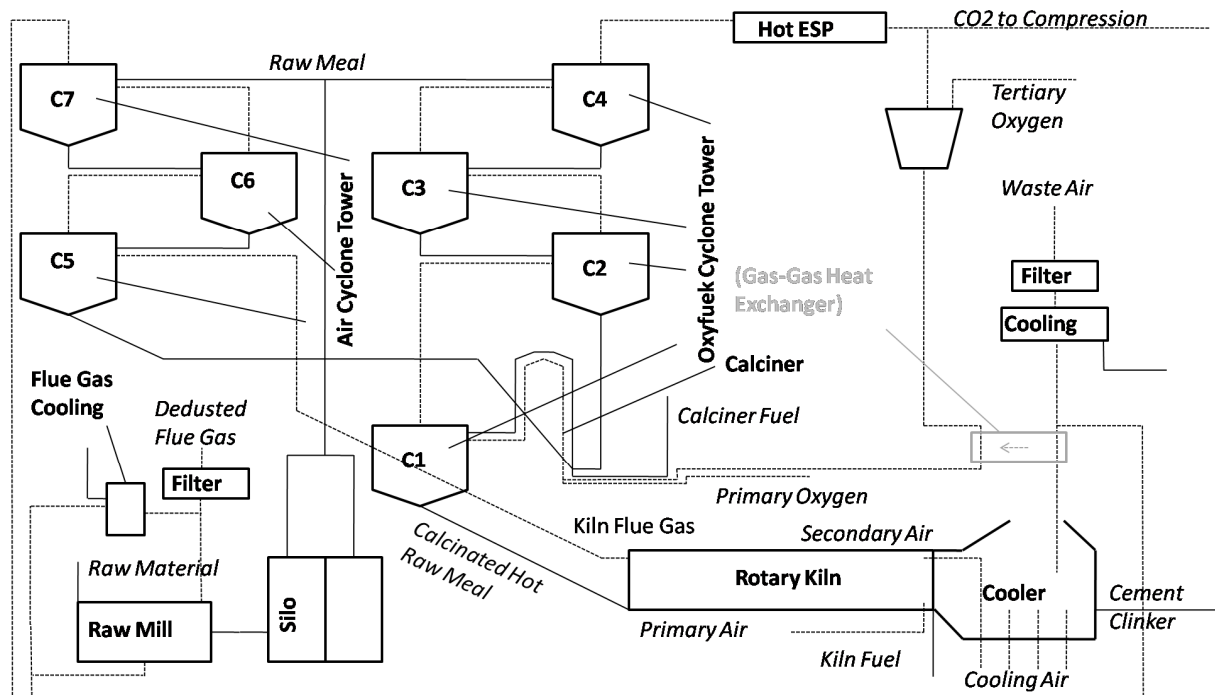
Figure 3: Flow Sheet of a Partial Oxyfuel Cement Plant with 2 Preheater Towers

Figure 4 shows the first results regarding the fuel energy demand and the electrical power demand of the 3 introduced full oxyfuel concepts and the 3 introduced partial oxyfuel concepts with reference to the air case. Figure 5 shows the corresponding CO_2 emissions of the introduced concepts.
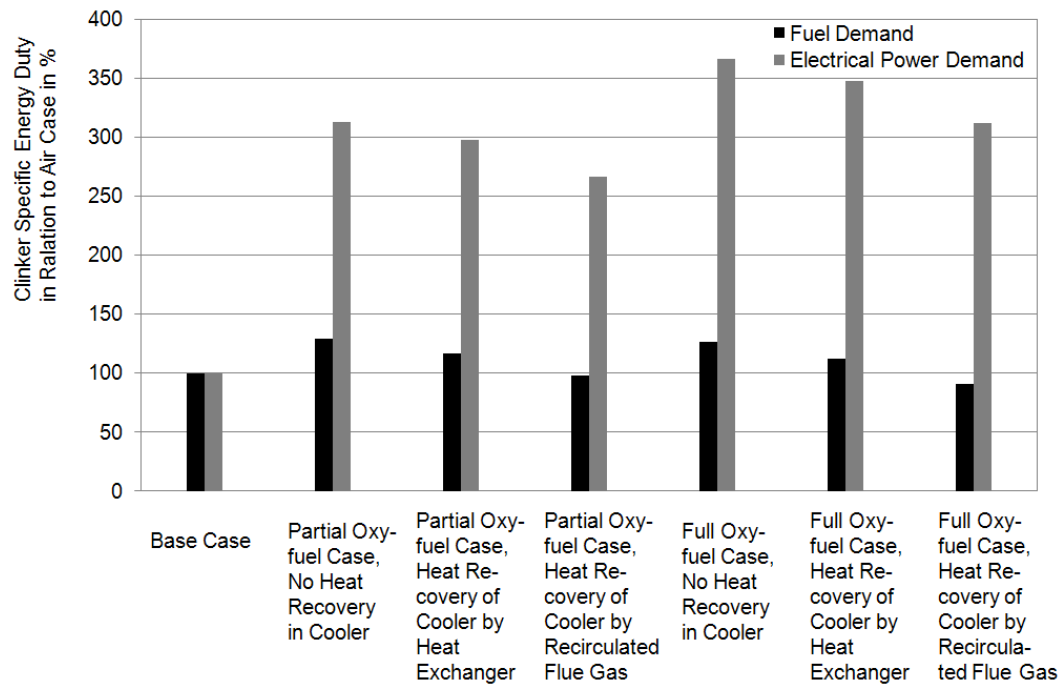
Figure 4: Fuel Energy Demand and Electrical Power Demand of Introduced Concepts
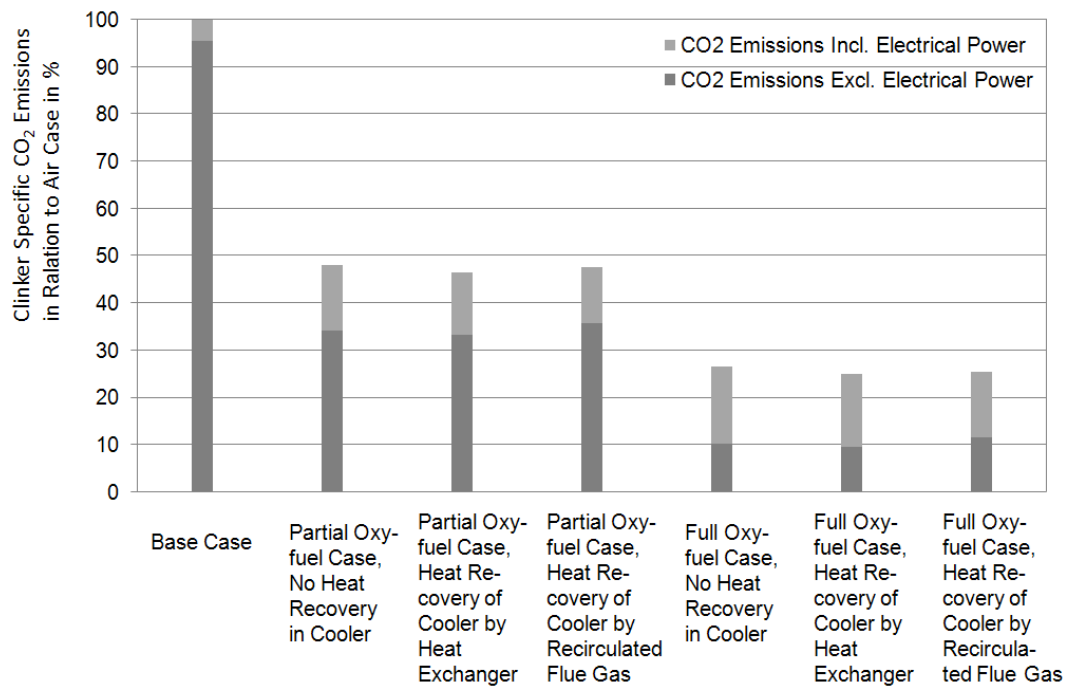
Figure 5: CO_2 Emissions of Introduced Concepts

All of the introduced oxyfuel concepts show significant reduction in CO_2 emissions but indicate a massive increase in the electrical power demand resulting from the additional power required by the ASU and the CO_2 purification and compression. Furthermore, the fuel energy demand significantly increases except in the case of a direct recovery of heat from the clinker cooler to the recycled flue gas. Therefore, this work will also show strategies to increase the overall CO_2 capture rate and to reduce the electrical power and the fuel energy demand.

High pressure oxyfuel process with staged combustion

Hanno Tautz*, *Linde Engineering, 82049 Pullach, Germany*

1   Introduction

The application of pure oxygen for the combustion of coal provides the advantage to reduce the flue gas flow significantly and to operate the combustion and steam production at higher pressure. This results in higher electrical net efficiency and a reduction of investment costs.

2   High pressure oxyfuel process concept

There are already different oxyfuel processes under investigation. One approach is to keep the technology as close as possible to the existing atmospheric boiler concept. In this case the combustion temperature of coal with oxygen has to be limited by dilution of the pure oxygen with a recycled CO_2 flow.

Another approach is the application of elevated pressure to the combustion process. In this case although a recycle flow of CO_2 or condensed water or a mixture of this is necessary to limit the combustion temperature.

To overcome the problem of intensive cooling of coal combustion with oxygen in the new process, the oxidation is separated in two steps. First there is a gasification of the coal with pure oxygen and in a second step the produced syngas is burnt in several stages in the heat exchangers for the steam production. Between both steps there is a cyclone and hot gas filter system for gas cleaning from solids.

With this the recycle of CO_2 can be avoided and the application of cooling water is limited to an extend, which can be useful applied in the preheating of boiler feed water. As the combustion is mainly in reducing atmosphere the NOx formation is strongly reduced. At the pressure of 80 bara first the water can be condensed at about 50 °C. With a further reduction of the temperature to 30 °C CO_2 is condensed in a relatively pure condition and need no further cleaning step for compression to 120 bara with a pump. The desulphurization can be done in the water phase by neutralization of H_2SO_4 with caustic, see figure 1.
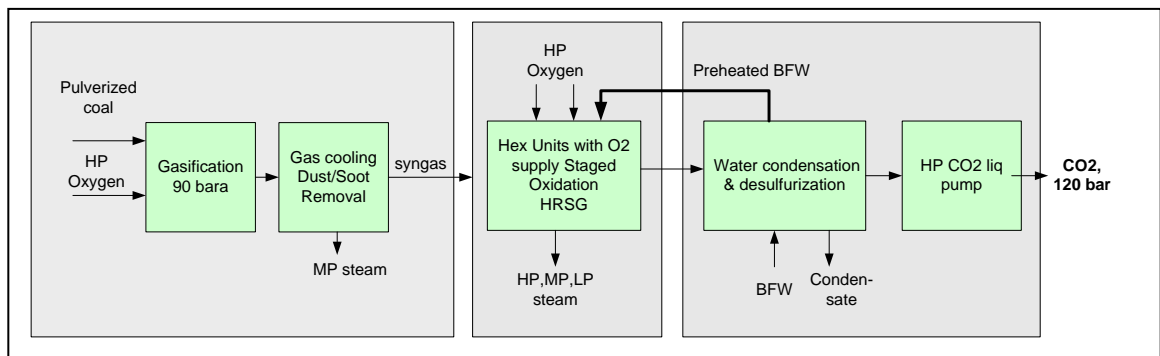
Figure 1: Process principle for high pressure oxyfuel process with staged combustion

3 Thermodynamic background

3.1 Increase of thermal energy input by condensation energy

From the thermodynamic background the combustion of coal at elevated pressure has the advantage, that the thermal energy of water condensation can be used at reasonable temperatures for the preheating of boiler feed water.

The difference of this thermal energy is shown in a QT diagram in figure 2. The values are calculated for the combustion of predried lignite with a ash free lower heating value of about 22000 kJ/kg for a power plant with 2200 MW thermal energy input.

At 80 bara the condensation starts at a temperature of about 145 °C compared with about 80 °C at atmospheric pressure. With this higher condensation temperature the boiler feed water can be preheated to about 160 °C instead of 100 °C and about 110 MW more thermal power can be used for the process.
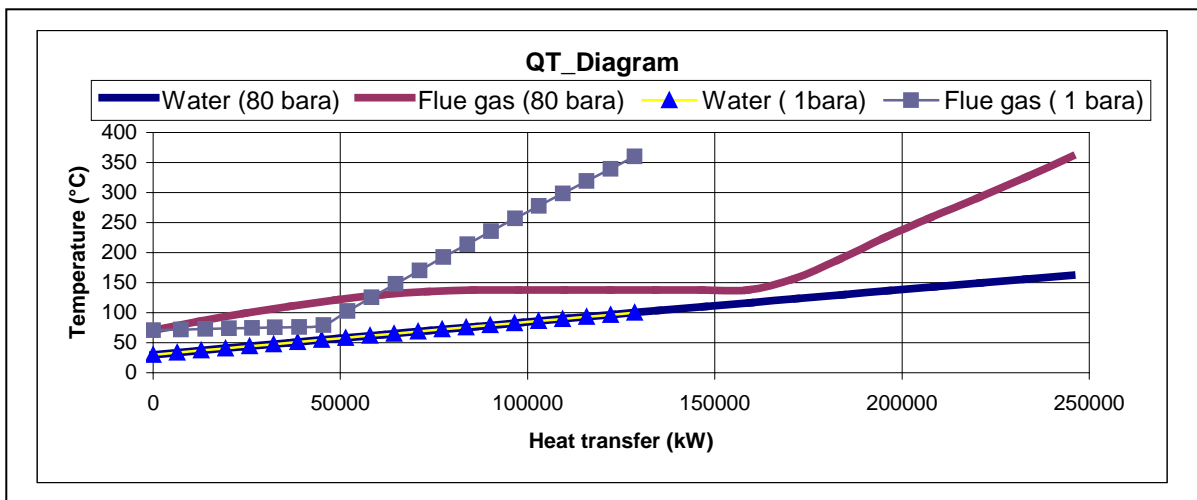
Figure 2: QT-diagram for atmospheric and high pressure flue gas case.

3.2 Increase of turbine efficiency with higher steam temperature

There are intensive investigations to develop high temperature materials, which can be applied in steam boilers for steam generation up to 700 °C at 350 bar. With the current available materials the introduction of these operation conditions is not expected within the next few years in atmospheric boiler plants.

The high pressure oxyfuel process gives the opportunity to apply these process parameters already with existing materials.

For this there are the following reasons:

- Reduction of differential pressure between steam and flue gas by 80 bara.
- Increased heat transfer because of elevated pressure
- Reduction of heat and fouling resistance because of gas cleaning in front of heat exchanger section

Therefore the flue gas and material temperature and the tube material wall thickness in the heat exchangers can be lower than in atmospheric boilers for the same heat transfer power.

The expected increase of electrical efficiency with the 700 °C technology and equipment optimization is 4 % points /1/.

4   Key equipment for steam production

The production of high pressure steam at temperatures above 500 °C needs special heat exchanger constructions.

Typical used tube sheets would become too thick at the high temperatures and pressures. A suitable construction for high pressure flue gas and staged combustion can be a spiral wound heat exchanger, see figure 3.

The steam can be overheated in tube bundles, which are connected over different tube baffles to the high pressure pipes. With this the diameter and the mechanical load of the tube sheets can be reduced. Additional burning or oxidizing gases can be introduced in the heat exchanger.
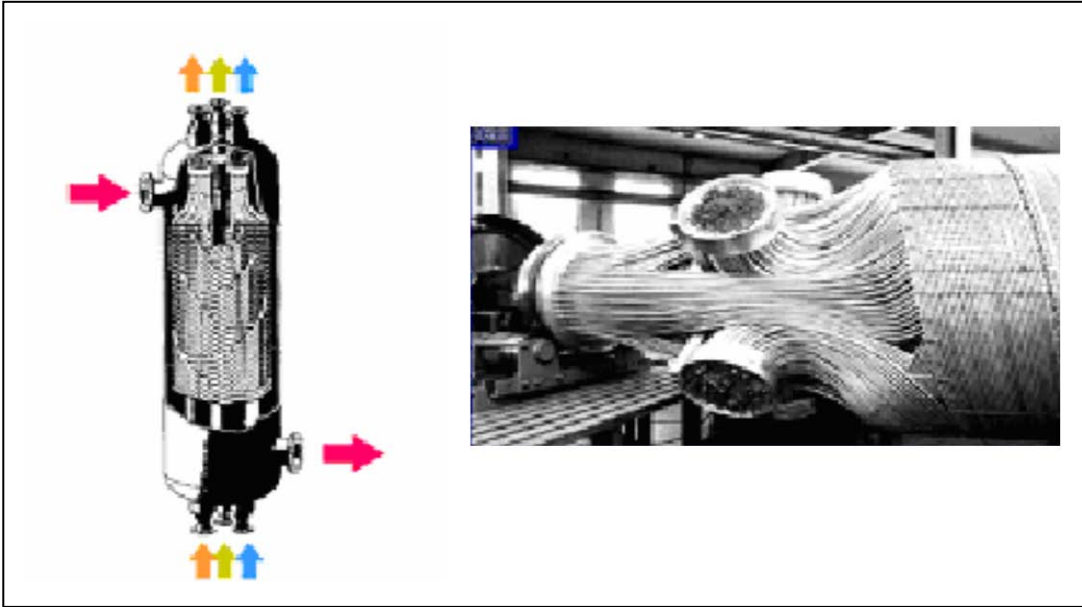
Figure 3: Spiral wound heat exchanger for high temperature steam production.

5   Results of process simulation

A detailed process simulation was conducted for the calculation of the electrical efficiency of the high pressure oxyfuel process and is compared with published data for the atmospheric oxyfuel process and an IGCC process with CO2 capture. The results can be seen in table 1:

Table 1: Efficiencies of oxyfuel processes with CCS.

	Atmospheric Oxyfuel	IGCC & CCS	HP Oxyfuel 600 °C steam	HP Oxyfuel 700 °C steam
Net efficiency (%)	40 /3/	35 /2/	42	42+4=46
CO2 capture (%)	90	90	99	99

6   Process concept and construction

The high pressure oxyfuel process shows a strong reduction of effective gas flow. This results in a quite compact plant layout, which can be seen in figure 4 and 5.
A preliminary estimation of tonnage shows a strong reduction of material for the boiler construction.
The main equipment can be pre fabricated in a workshop, transported and directly installed at the construction site. With this the erection time and costs can be reduced significantly.
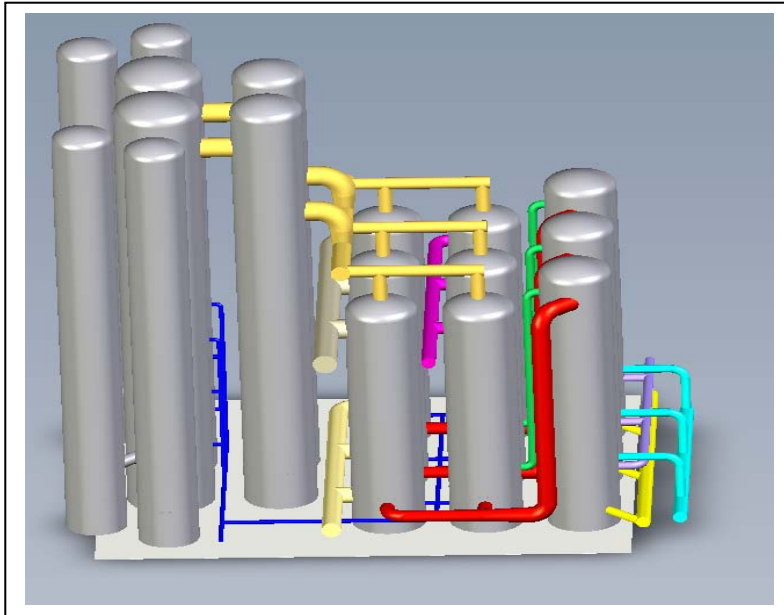
Figure 4: Sketch of high pressure oxyfuel process
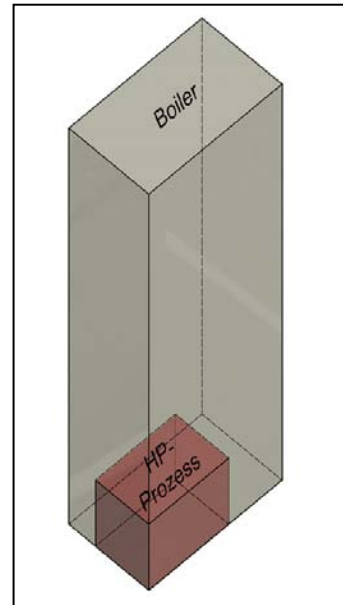
Figure 5: Size proportion Boiler plant and HP oxyfuel

7   Summary

- o Higher electrical efficiency by > 2-6 % points compared to atmospheric oxyfuel process.
- o   Strongly reduced cost reduction by unit standardisation, prefabrication and material reduction.
- o   Strong reduction of boiler size and material demand.
- o   Simplified gas cleaning and CO2 capture
- o Option for 700 °C steam technology possible
- o The production of syngas gives the possibility to use the gasification for polygeneration processes in times of lower electricity demand.

8   Literature

/1/ Leuchtturm COORETEC, Forschungsbericht Nr. 566
/2/ www. Life Needs Power 2008.de
/3/ Kraftwerkstechnisches Kolloquium 2004, V39

Vattenfall's CCS-Strategy

Author: Dipl.-Ing. Uwe Burchhardt, Vattenfall Europe Generation AG, Cottbus

Introduction
In connection with Vattenfall's goal to be a leading European energy supplier, the strategic target to reduce CO_2 emissions from power and heat generation by 50% by the year 2030 was set. Furthermore, Vattenfall wants to provide heat and electricity climate-neutral by 2050. Additionally, absolute CO_2 emissions are to be decreased from currently 90 million tons per year to about 65 million tons by 2020. These reduction goals correspond with the targets given by the European Union and even exceed them.
Apart from a significant increase in power generation from renewables, Carbon Capture and Storage is a major corner stone of our technical strategy to reach our ambitious reduction goals. Within the Vattenfall Group, all three technologies currently competing for the lead in CO_2-capture are being researched: these are Oxyfuel, pre-combustion capture (IGCC) and post combustion capture (PCC).

1. Since 2008, tests to research the entire capture technology-chain have been run at the Oxyfuel pilot plant in Schwarze Pumpe (Germany) (from coal feeding to the final CO_2-product).
2. At the IGCC-power plant in Buggenum (the Netherlands), a pilot plant for CO_2 shift and removal processes is being tested in the bypass for the fuel gas treatment since 2010.
3. After participating in the Castor project for testing and selection of solvents suitable for post combustion processes, Vattenfall have engaged in on-going cooperations for further testing in the Castor pilot but also for testing of optional technologies and solvents in a larger pilot at 100 tpd scale. This is the CCPilot100+ project in Ferrybridge UK, to be commissioned 2011.

Practical experience gained in these projects is to support the selection of future CCS-technologies for commercial utilization. Below, the experience gained so far will be presented in detail and an outlook on the Oxyfuel technology will be given.

Results and Knowledge Gained during Test Operation of the Oxyfuel Pilot Plant
At the 30 MW (thermal) Oxyfuel-pilot plant in Schwarze Pumpe (see chart 1), the following aspects could be proved on a pilot level for the first time:
  - The permission procedure for a CCS-power plant
  - The combustion behavior of lignite under Oxyfuel conditions
  - The compliance with emission requirements
  - The interaction of components originating from the chemical industry with power plant technology (air separation – boiler – flue gas cleaning – CO_2-plant)
  - The CO_2-purity necessary for transport and storage.

Chart 1: Oxyfuel-pilot plant in Schwarze Pumpe

Since the commissioning in September 2008, the plant has been in operation for more than 12,000 hours. During this time, more than 8,900t of CO_2 could be captured and liquefied. At this pilot plant the sulphur-rich recirculation was tested (downstream of the electrostatic precipitator, but upstream of the flue gas desulphurization). Experience on the pre-mixed operation mode (O_2 fed into the recirculation) and the expert operation mode (O_2 fed into individual burner ports) could be gained.

So far, three burners have been tested; a combined jet-/swirl burner and two pure swirl burners. Different ignition burner concepts on a gas basis have been researched. Besides the conventional, separately arranged ignition burners, especially the ignition burners integrated into the main burner have been proved to be effective.

The combustion behavior under Oxyfuel conditions has permanently been improved. Vattenfall wanted to keep the remaining amount of excess oxygen at the end of the boiler smaller than 5% to reach a possibly high O_2 amount in the oxidant (combustion gas enriched with O_2). While a low O_2 surplus in the waste gas can reduce the oxygen demand for the combustion process, a high amount of excess oxygen in the oxidant results in a low recirculation rate. Both arrangements have direct impact on the efficiency of the Oxyfuel process. Values reached during different test campaigns (TC 3-5) are displayed in chart 2 and 3.
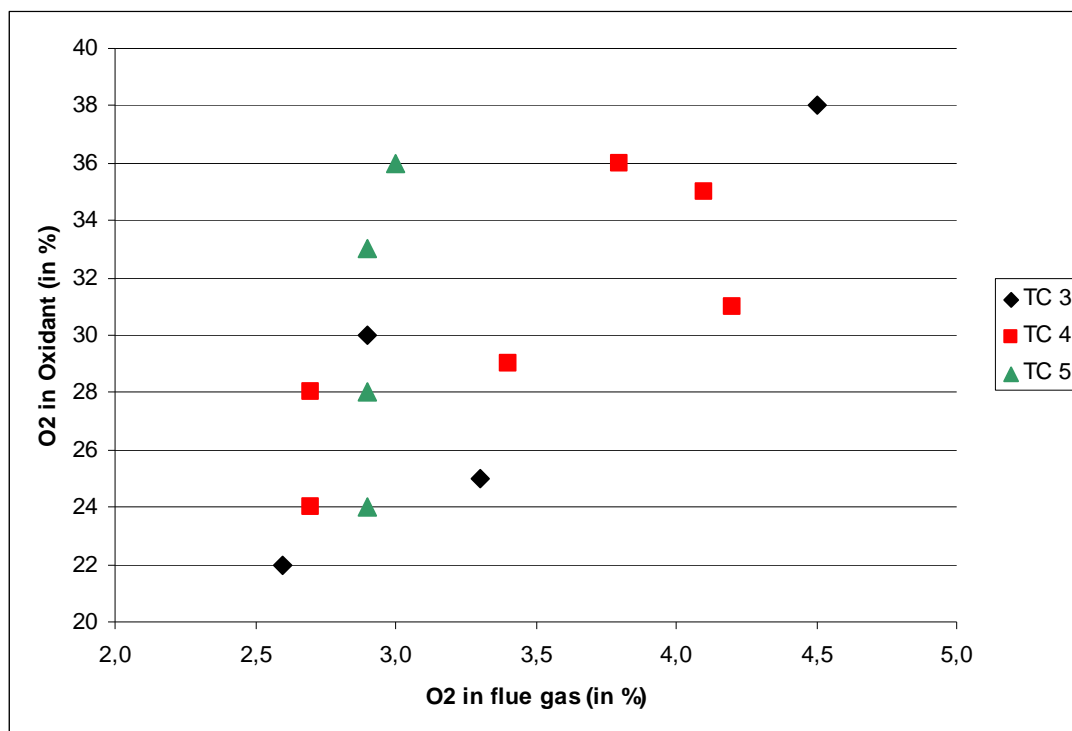
Chart 2: Diagram of tested operating points
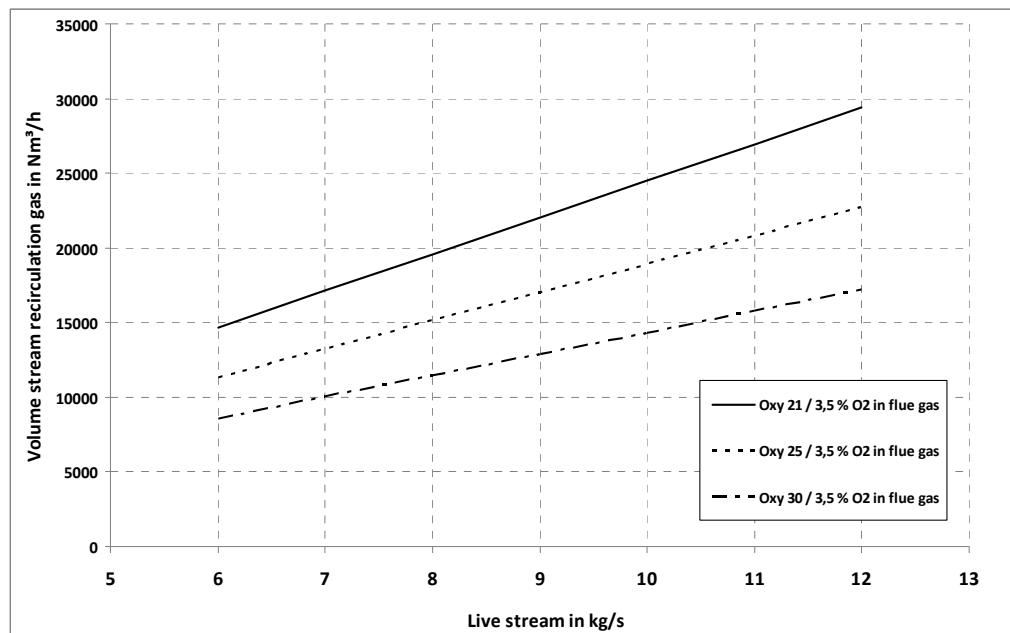
Chart 3: Impact of the O_2-content in the oxidant on the recirculation rate

Additionally to the researched combustion behavior and the heat transfer in the Oxyfuel boiler, the flue gas cleaning process, using an electrostatic precipitator, a flue gas desulphurization plant and a flue gas condenser to provide the required flue gas composition for the CO_2 process, has been researched, as well. The suitability of conventional power plant components was proved, and required removal rates (dust and SOx) could be achieved.
Special focus was on NOx-reduction in the Oxyfuel process. Here, the following alternatives were researched and evaluated.
1. High-dust-DeNOx (SCR) in the boiler
2. Low-dust-DeNOx (SCR) downstream the electrostatic precipitator
3. Combined DeSOx- and DeNOx-processes during flue gas cleaning
4. DeNOx in the CO_2-compression process (cold DeNOx)
5. DeNOx in the vent gas discharge of the CO_2 plant

Vattenfall is focusing on the options 1, 3 and 4 and will run further practical tests.

In the CO_2-process, practical experience could be gained on the following aspects:
- Compression process (vibration behavior when using CO_2-rich flue gas)
- Operation behavior of activated carbon filters
- Drying processes of molecular sieves
- Vent gas composition and how to use it
- Aspects influencing the CO_2-quality

In the CO_2-plant, a CO_2 retention rate of 93% could be achieved. Therefore, a CO_2-removal rate of higher than 90% for the entire process could be proved in practice.
The current results gained from the Oxyfuel pilot plant are sufficient to take the next step and set up a demonstration plant.

Concept of the CCS-Demonstration Plant in Jänschwalde
Based on the lessons learnt from the Oxyfuel pilot plant and our PCC projects so far as well as from the feasibility study carried out in the year 2009, the scale-up behavior to a demonstration plant can be calculated.

In 2010, Vattenfall decided to set up a CCS-demonstration plant at the power plant site in Jänschwalde (6x500 MWel) and benefit from EU funds available (EEPR and NER 300).

Chart 4: The demonstration plant at the site in Jänschwalde

The concept is based on lignite and includes a separate Oxyfuel unit with a capacity of 250 MWel and the retrofit of an existing unit with post combustion scrubbing with a capacity of 50 MWel. The plant layout can be seen in chart 5.
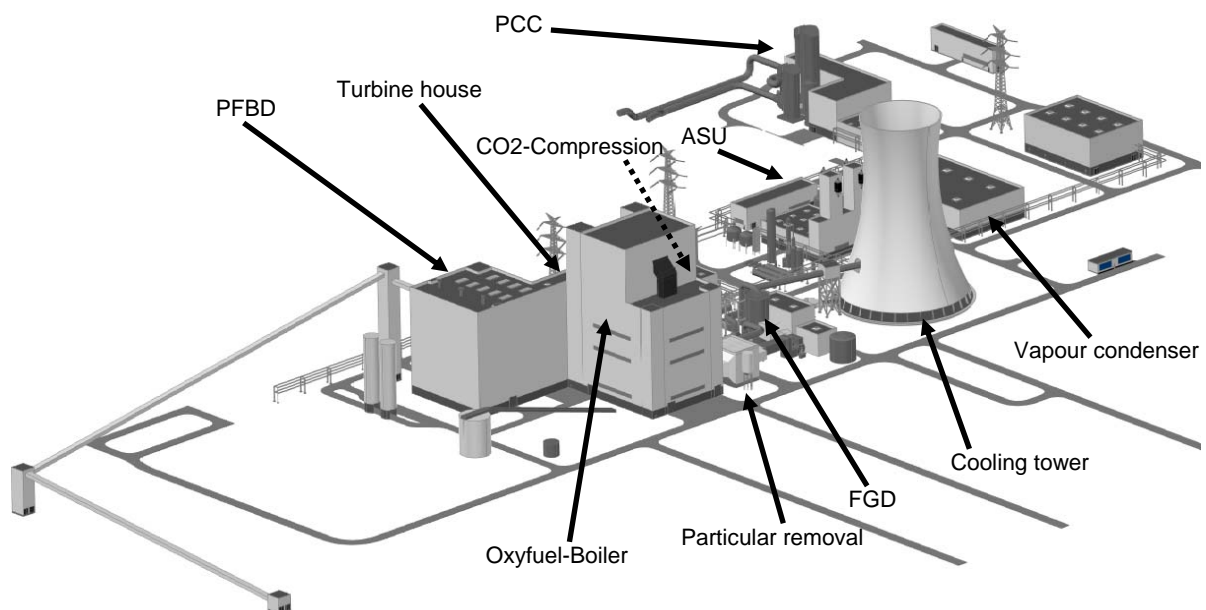
Chart 5: Layout of the 250 MWel Oxyfuel-unit in Jänschwalde

For the design of the Oxyfuel boiler the following principles have been taken into account:
- Integration of a coal drying and an air separation unit into the power plant concept
- State-of-the-art live steam parameters
- Boiler and flue gas cleaning based on concepts tested
- Making use of condensate from coal drying, flue gas condensation and the CO_2 process for internal processes
- Optimization of the O_2 purity (air separation unit) with respect to the operating cost of the entire process
- Reaching a CO_2 purity required for transport and storage
- CO_2 process with direct compression for pipeline transport

In contrast to the pilot plant, the Oxyfuel demonstration concept will use a sulphur-poor recirculation (downstream the flue gas desulphurization plant) due to reasons of availability. For coal drying, a pressure charged steam fluidized bed drying (PFBD) will be used. It is designed three-line with direct feeding of dried lignite to the burners and it will be integrated into the boiler concept right next to the boiler house. The air separation unit will be designed energy-optimized (without backup system) and it will have an oxygen-purity above 95 % and a load change rate of +/- 5% per minute. The CO_2 plant will have a material-optimized and energy-optimized design. CO_2 purity will be above 95% and the ultimate pressure is calculated until 140 bar.

		Unit G Oxyfuel	Unit F with PCC	Unit F (conventional)
Operating mode		Demo	Base load	Base load
Fuel		Dried lignite	Raw lignite	Raw lignite
Gross output	MW	250	519	530
Auxiliary power	MW	83	37	30
Net efficiency	%	36	36.5	37.9
Availability	%	> 91		
Live steam temperature	°C	600	535	535
Reheating temperature	°C	610	545	545
Demand for lignite	million t/a	1.5	4.1	4.1
Specific CO_2-emissions	g/kWh$_{net}$	78	933	1,004
CO_2 captured (for 7,700 operation hours /year)	million t/a	1.3	0.385	-

Table 1: Basic data of the demonstration power plant in Jänschwalde

From the Oxyfuel and the PCC plants, the captured CO_2 will be compressed together at a CO_2 plant (without intermediate storage) and transported to possible storage sites not further than 300km away. For possible storage, two saline aquifers and a depleted gas field are currently being researched.
The demonstration project in Jänschwalde has already been subsidized with €180m by the European Union through the European Energy Program for Recovery (EEPR). A further application for granting subsidies from the Program for the promotion of new technologies to reduce CO_2 emissions from power generation significantly (NER 300) has been submitted for the demonstration project in Jänschwalde.

Outlook and Potential
Future developments of the CCS-technology will mainly aim at an increased efficiency and an improved availability as well as at a better coordination of CCS power plant and pipeline transport and storage. CO_2 storage in saline aquifers and the CCS-technology's efficiency has to be proved in the real world. The regulation control behavior of the entire CCS-chain in compliance with market demands is of importance.

At the Oxyfuel pilot plant, the following tests have been scheduled for the next few months.
- Load change behavior of the air separation unit with a connected burner
- Tests to be run with different coal qualities
- Material tests in an Oxyfuel atmosphere (on-line and pressure loaded probes)
- Additional tests for the "Cold DeNOx" (regeneration and alternative reducing agents)
- Alternative flue gas cleaning and CO_2-processes

For testing of an alternative flue gas cleaning method, a separate pilot plant in the Oxyfuel pilot plant's bypass was designed. This is to simplify the flue gas cleaning by combining the desulphurization, denitrification and CO_2-process.

Chart 6: The alternative CO_2-plant in the Oxyfuel-pilot plant

From Vattenfall's point of view, further potentials as well as additional research demand is especially given with respect to:

- The optimization of individual components (air separation unit, CO_2-plant) and systems (synergies in cooling processes and utilization of waste heat)
- The utilization of a sulphur-rich recirculation (requirements on material)
- Alternative flue gas cleaning processes (the purity of the captured media and their industrial utilization)
- Use of the membrane technology (ASU, CO2 plant)
- The integration of the pressure charged steam fluidized bed drying (DDWT) with vapor compressor (further development of rotary vane feeders and tests of a vapor compressor for an exegetical utilization of vapor within the power plant)

A further aspect for the introduction and acceptance of CCS-technologies is the industrial application of the captured CO_2. CO_2 qualities of all capture processes are suitable for utilization in water treatment plants, technical gases, fire extinguishers etc. We can see further potential for CO_2 applications in algae breeding or the synthesis of plastics, chemicals or fuels. However, this will require further comprehensive research by universities, institutes and the chemical industry. Vattenfall is willing to support this research by providing "real Oxyfuel CO_2".

Summary
Oxyfuel works successfully on a pilot level; all emission limits could be complied with and the required CO_2 purity was reached. CO_2 capture within the IGCC process has been proved in practice and several post combustion projects could meet their targets. For CO_2 transport, experience gained with pipelines worldwide can be referred to. The first CO_2 storage in a saline aquifer in Ketzin (Germany) has been running successfully for years. CO_2 storage in depleted oil and gas fields is state-of-the-art. The conditions to test the complete CCS-chain (capture, transport and storage) are present. Financial subsidies by the European Union are possible.

Nevertheless, Vattenfall had to find out that not the technical solution is greatest challenge. To gain public and political acceptance is of far greater importance for the introduction of CCS-technologies and in this process Vattenfall will continue to contribute.

Corrosion aspects of materials Selection for

CO$_2$ Transport and Storage

D. Bettge, A.S. Ruhl, R. Bäßler, O. Yevtushenko, A. Kranzmann, Federal Institute for Materials Research and Testing, Berlin, Germany

Introduction

The geological storage of carbon dioxide (Carbon Capture and Storage, CCS) in depleted gas reservoirs or in saline aquifers is a widely discussed issue. Carbon dioxide may induce corrosion on the piping steels during compression, transportation and injection. Therefore, selection of appropriate piping steels is a key factor in order to increase the safety and reliability of the CCS technology, and to keep the processes cost-effective.

The here described subproject of the COORAL project (German acronym for "CO2 purity for capture and storage") deals with the levels of impurities in the CO$_2$ stream that will be acceptable when using specific steels. Material exposure to carbon dioxide (CO$_2$) containing specific amounts of water vapor, oxygen (O$_2$) sulfur dioxide (SO$_2$), nitrogen dioxide (NO$_2$), carbon monoxide (CO) can be a challenge to steels. Within this subproject 13 different steels are tested for suitability as materials used for compression, transportation and injection units within the CCS chain.

Corrosion Caused by Condensation in CO$_2$ Containing Impurities

Sample coupons are fixed to Teflon mountings in air tight reaction vessels. The vessels are continuously fed with on-site prepared gas mixtures for 120 to 600 hours. Reaction vessels are positioned in climate chambers to simulate different temperatures, ranging from 5 °C to 170 °C. Humidity is added by directing a fraction of the CO$_2$ flux through a washing bottle. Water vapor concentrations are varied between 0 and 2.5 %, O$_2$ up to 1.8 %, SO$_2$ up to 220 ppm, NO$_2$ up to 1,000 ppm and CO up to 750 ppm.

The results indicate that under these circumstances corrosion increases with decreasing temperature. Dew point dependent condensation of sulfuric and nitric acids can lead to severe corrosion. At temperatures above 60 °C only slight corrosion and discolorations occur even at elevated concentrations of water, SO$_2$, O$_2$ and NO$_2$. At 5 °C condensation and liquid film formation on steel surfaces with dissolution of metals and precipitation of ferrous and ferric minerals were observed. Surfaces seemed to be uniformly corroded. Cleaned surfaces after removal of corrosion products by ultrasonic reveal that corrosion pits also formed.

Fig. 1: Example images of coupons made of „compressor steels" (from left to right: 1.4006, 1.4313, 1.4542) after 600 hours at 170 °C in continuous CO$_2$ stream at atmospheric pressure.

Fig. 2: Example images of coupons (from left to right, 1.4006, 1.4313, 1.1018) after 600 hours at 170 °C in continuous CO_2 stream at atmospheric pressure, elevated amounts of impurities.

Fig. 3: Example images of coupons (from left to right, 1.4006, 1.4313, 1.1018) after 600 hours at 60 °C in continuous CO_2 stream at atmospheric pressure.

Fig. 4: left: Generation of bubbles on coupon surfaces due to condensation of acids and gas generation at 5 °C and 0.8 % water, 1,8 % oxygen, 760 ppm CO_2, 1000 ppm SO_2 and 220 ppm SO_2. right: Corrosion of low alloyed pipeline steels after 120 hours at 5 °C in CO_2 containing 2 % H_2O, 0.6 % O_2 and 650 ppm SO_2.

Corrosion in CO_2 Saturated Brine

Electrochemical experiments were carried out on piping steels exposed to CO_2 and artificial saline brine ("Stuttgart" aquifer). The corrosion of 1.4021, 1.4162 and 1.7225 (AISI 4140) steels, which are considered for injection, was investigated. The specimens were exposed to the CO_2 saturated brine for 24 h up to 336 h. Electrochemical and metallographic analyses have been carried out.

Some results are shown in the figure below. For example, the steel 1.4021 exhibits pitting corrosion and is therefore not recommended for the use in injection wells. After 14 days 1.4162 does not show any indications of pitting corrosion. The diagram indicates that passive layers are formed. Therefore local corrosion is not likely to occur during longer expositions.

1.7225 shows uniform corrosion. After 5 days of exposition a constant corrosion rate is established. The corrosion rate is about 1.9 mm/year measured by mass loss.
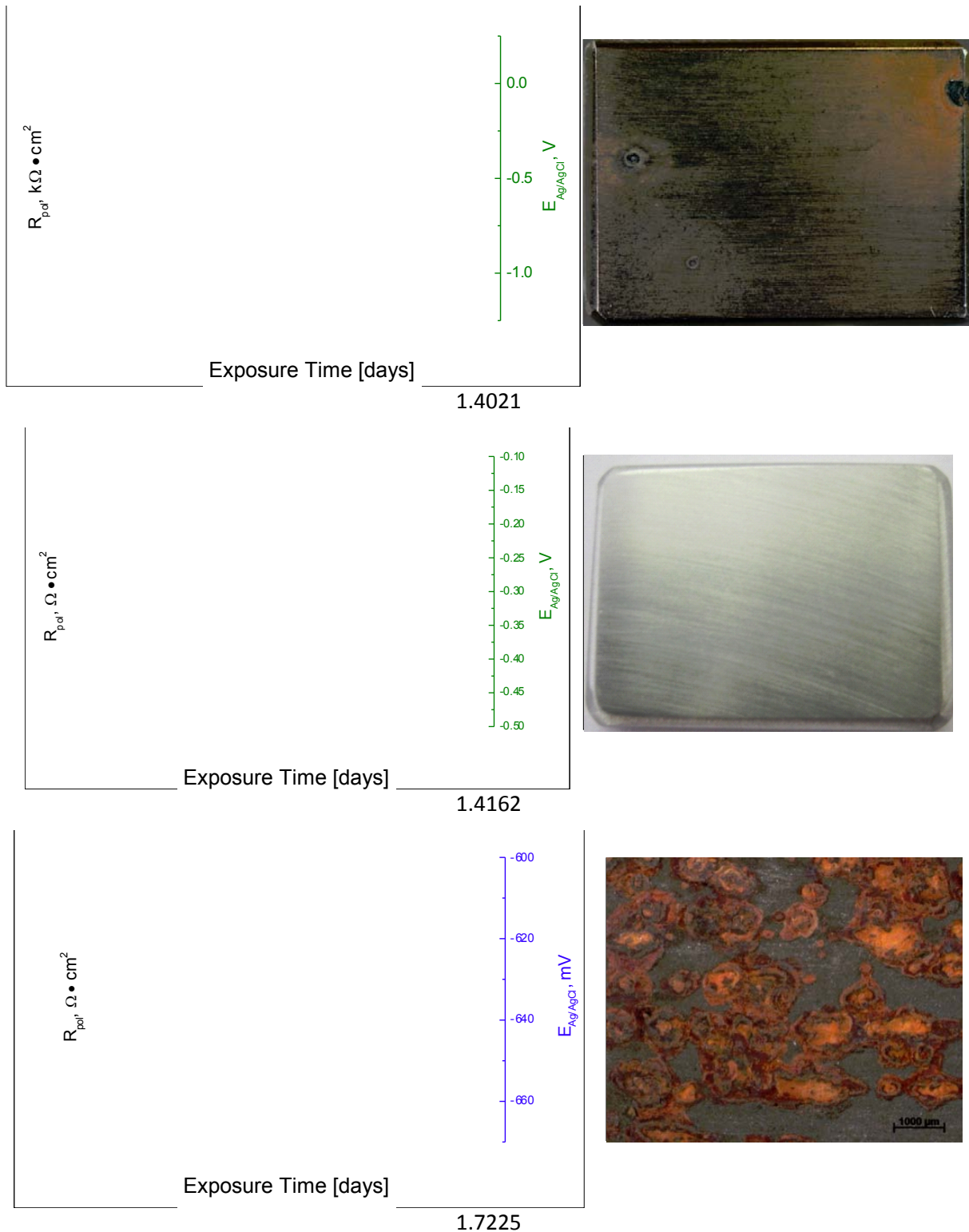
1.4021

1.4162

1.7225

Fig. 5: Examples for corrosion of steels in CO_2 saturated brine, steels 1.4021, 1.4162 and 1.7225. Left: polarization resistance and free corrosion potential over time. Right: Surfaces of coupons after 336 hours. 1.4021: pitting corrosion, 1.4162: no corrosion, 1.7225: uniform corrosion.

Aspects of CO_2-Pipelinetransport
U. Lubenau, DBI Gas- und Umwelttechnik GmbH

Carbon capture and storage offers the opportunity to reduce CO_2 emissions while using fossil fuels. Concerning the current situation of energy generation and assuming that fossil fuels will play an important role on the way to a sustainable energy supply it is expected that CCS will be further considered as a bridge into the future.

As CO_2 point sources and suitable sinks are often located in different regions (figure 1), transport routes are essential. The transport of huge amounts of gases is state of the art and managed by pipelines. Solely in Europe the existing Natural Gas System has a length of 1.2 million km. The engineering of transport and distribution systems is well developed concerning hydraulic and material aspects. Transportation of CO_2 is different in comparison to natural gas for several reasons. Firstly the thermodynamic properties are significantly different to natural gas, resulting in different head losses, even when CO_2 is transported in its gaseous state. Moreover the critical point is relatively low regarding temperature and pressure.

This offers transportation in the supercritical phase, which is challenging but allows transport in a relatively dense state. The thermodynamic properties of CO_2 necessary for hydraulic calculations are available. Furthermore pure CO_2 is not known for initiating or propagating material degradation mechanisms. But the situation is different for CO_2 containing impurities and it is known that the flue gases of coal fired power plants will contain significant shares of impurities.

These impurities can be removed but the treatment is costly and therefore it is necessary to find a compromise for solving the problems before transporting (by removal of impurities) or making the transport system fit for CO_2 with significant shares of impurities. To solve this problem it is necessary to determine the thermodynamic properties for realistic flue gas compositions and then calculate the head losses for different transport scenarios (regarding distances and transport state of the CO_2).

Furthermore it is important to evaluate if standard carbon steel (e.g. line pipe steel used in the oil and gas business as X 42, X 70 or X 80) can be used for the transportation of impure CO_2.

In the project COORAL (funded by the Bundesministerium für Wirtschaft und Technologie) these questions will be answered and moreover the whole chain of a safe and stable underground storage of CO_2 from the production process to the reservoir will be addressed (http://www.bgr.bund.de/nn_1633894/DE/Themen/Geotechnik/CO2-Speicherung/COORAL/Startseite/startseite__node.html?__nnn=true). Concerning the transportation several scenarios will be investigated and economical evaluated. Furthermore the effect of the equations used for the head loss calculation is going to be investigated.
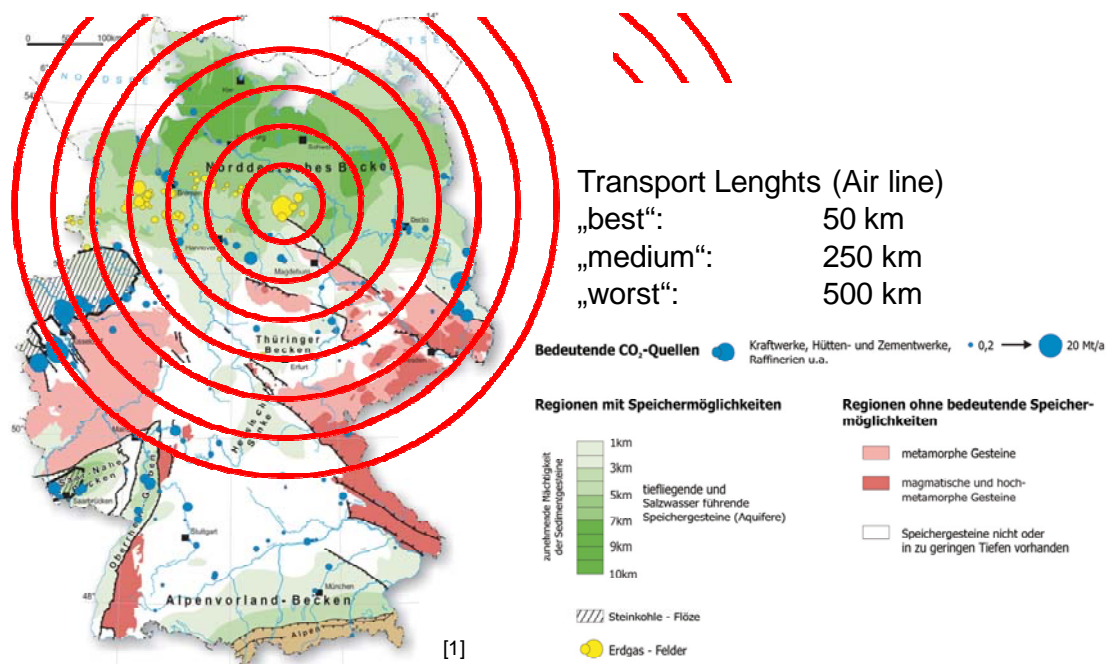
Figure 1: Distances between CO_2 Sources and Sinks

Tuesday, June 21, 2011

Post-combustion processes employing polymeric membranes

Torsten Brinkmann, Helmholtz-Zentrum Geesthacht,Institute of Polymer Research, 21502 Geesthacht, Germany; Thorsten Wolff, Helmholtz-Zentrum Geesthacht, Institute of Polymer Research, 21502 Geesthacht, Germany; Jan-Roman Pauls, Helmholtz-Zentrum Geesthacht, Institute of Materials Research, 21502 Geesthacht, Germany

Gas permeation employing CO_2-selective polymeric membranes is a promising alternative to absorption processes. Its suitability for the removal of CO_2 from flue gases of fossil fuel fired power plants will be investigated and rated. The newest performance data of polymeric membrane developments will be considered for process simulations. Based on the membrane's performance, process designs with different possible plant layouts will be discussed. The influence on the power plant efficiency will be quantified. By varying parameters as e.g. feed to permeate pressure ratio or process stage arrangement, the demand of energy for pumps and cooling devices shall be minimised and related to the purity of CO_2 in the permeate and the over all power plant efficiency.

Next to the process design studies, additional aspects of applying gas permeation to post-combustion will be discussed. One important point is the design of membrane modules tailored towards this application. The module concepts discussed will focus on flat sheet membrane configurations with a minimised pressure drop on the permeate side to facilitate an optimised withdrawal of the CO_2 enriched permeate. Furthermore, the pre-treatment of the flue gases is important since it will have a large influence on the membrane life time. The required driving force of the process has to be applied by blowers, compressors and vacuum pumps or combinations thereof. Due to the large flowrates involved, the selection and availability of these components is of a large importance.

Carbon Molecular Sieve Membranes for Carbon Capture

Bee Ting Low and *Tai-Shung Chung, National University of Singapore, Singapore*

Introduction and Objectives

Power generation via fossil fuel combustion produces carbon dioxide which is often deemed as the primary cause for global warming. The removal of carbon dioxide from flue gas is thus of paramount importance [1]. In recent years, advances in membrane separation make it competitive with the conventional amine absorption in flue gas treatment [1]. The design of membrane material is a critical aspect in the development of membrane technology for post-combustion carbon capture. Carbon molecular sieve membranes (CMSMs) represent a special category of inorganic membranes that shows promising CO_2/N_2 separation performance. The motivation for transforming a polymeric membrane to a highly size-selective inorganic CMSM is to circumvent the permeability-permselectivity tradeoff relationship shown by most polymers [2-4].

The molecular frameworks of thermosetting polymers (e.g. polyimides) can be retained after carbonization and hence are ideal for fabricating CMSMs [2]. Recently, Low et al. studied the formation of pseudo interpenetrating polymer networks (IPNs) by the in-situ reaction of 2,6-bis(4-azidobenzylidene)-4-methylcyclohexanone (azide) within pre-formed linear polyimide frameworks [5]. In this approach, the free volume distribution of a polyimide with preferably high intrinsic free volume can be altered by changing the content of azide [4]. The change in the polymer free volume by incorporating the azide network is anticipated to bring about a parallel change in the pore size distribution of the corresponding CMSM. In this study, pseudo-IPNs comprising of azide and poly(2,3,5,6-phenylene-2,2'-bis(3,4-carboxylphenyl) hexafluoropropane) diimide (6FDA-TMPDA) were used to fabricate CMSMs [6]. The effects of azide loading and heat treatment temperature on the CO_2/N_2 transport properties of the CMSMs were investigated [6].

Methodology

6FDA-TMPDA was synthesized by chemical imidization. Azide was used without further purification. Dichloromethane was the solvent for preparing 6FDA-TMPDA/azide pseudo-IPNs. The chemical structures of 6FDA-TMPDA and azide are shown in Figures 1(a) and 1(b), respectively.

Figure 1. Chemical structures of (a) 6FDA-TMPDA and (b) 2,6-Bis(4-azidobenzylidene)-4-methylcyclohexanone
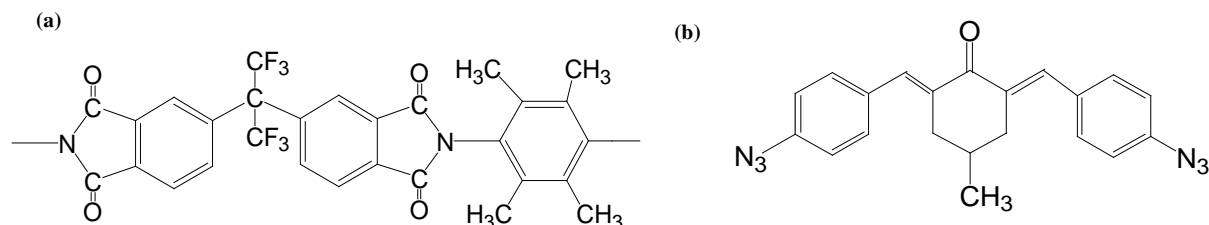
To prepare the film casting solution, the azide monomer was first dissolved in dichloromethane and stirred for 1 hr. Subsequently, 6FDA-TMPDA was added to the solution and stirred overnight. The polymer concentration in the solvent is 5 wt% while the azide loading in the polymer varied from 0 to 30 wt% [6]. The solution was filtered before ring casting onto a Si wafer plate at 25 ^{0}C. After solvent evaporation, the nascent film was annealed at 250 ^{0}C. Figures 2(a) and (b) illustrates the annealing and carbonization protocols, respectively.

Figure 2. (a) Heat treatment protocol for final annealing temperatures of 350 to 450 ^{0}C (b) Pyrolysis protocol for final carbonization temperatures of 550 to 800 ^{0}C

(a)

1: Hold at 50 ^{0}C for 30 min
2: Increase to T1 at 3 ^{0}C/min
3: Hold at T1 for 60 min
4: Natural cooling to 50 ^{0}C

T1 is in the range of 350 to 450 ^{0}C

Temperature (^{0}C)

Time (min)

(b)

1: Hold at 50 ^{0}C for 30 min
2: Increase to 400 ^{0}C at 3 ^{0}C/min
3: Increase to T2 at 1 ^{0}C/min
4: Hold at T2 for 60 min
5: Natural cooling to 50 ^{0}C

T2 is in the range of 550 to 800 ^{0}C

Temperature (^{0}C)

Time (min)
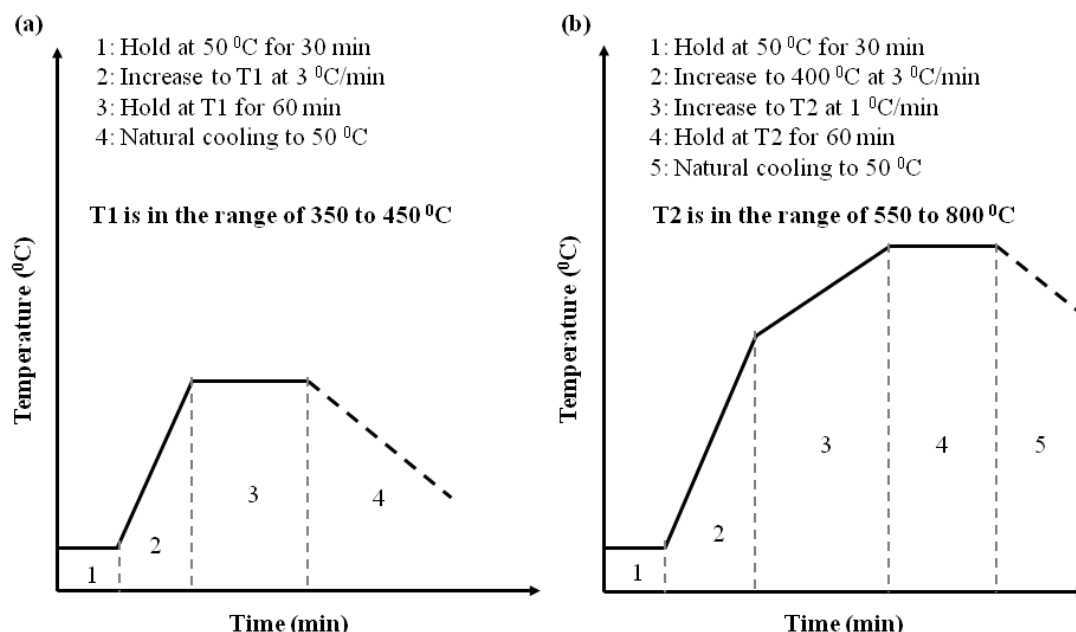
The membranes were characterized by thermal gravimetric analysis (TGA) and X-ray diffraction (XRD). The pure gas measurements were done using a variable-pressure constant-volume gas permeation cell at 10 atm and 35 ^{0}C.

Results and Discussion

The 6FDA-TMPDA polyimide starts to decompose at around 400 ^{0}C and the maximum rate of degradation occurs at 538 ^{0}C [6]. The initial weight loss at 400 ^{0}C up to 500 ^{0}C was due to the degradation of CF_3 groups and the subsequent decomposition beyond 500 ^{0}C was attributed to the imide groups [7]. The 6FDA-TMPDA polyimide shows a second decomposition peak at around 600 ^{0}C. The decomposition curves of 6FDA-TMPDA/azide pseudo-IPNs display the characteristics of the pristine polyimide. The incorporation of the azide network decreases the thermal stability of the polymeric films and the onset of decomposition occurs in the range of 200-300 ^{0}C [6]. The weight loss at 200-300 ^{0}C is possibly due to decomposition of thermally liable amine (N-H) groups.

For 6FDA-TMPDA/azide (90-10) annealed or pyrolyzed at a temperature in the range of 250 to 800 ^{0}C, the local maxima for CO_2 permeability occurs at 550 ^{0}C [6]. The highest N_2 permeability is obtained at 450 ^{0}C. With rising temperature, the CO_2/N_2 permselectivity decreases initially, reaches a minimum at 425 ^{0}C and elevates with further temperature increase [6]. The glass transition temperature of 6FDA-TMPDA/azide (90-10) is 411 ^{0}C [5]. Therefore, between 250 to 425 ^{0}C, the creation of pores from the evolved gases and the enhancement in polymer chain mobility (near the glass transition) are the governing processes which accounts for the higher permeability and lower permselectivity [6]. In the range of 450 to 650 ^{0}C, two competing effects of pore evolution from gas release and structural evolution from molecular rearrangement are present [6]. This can be inferred from the smaller changes in gas permeability and selectivity. As the temperature goes beyond 650 ^{0}C, the densification of the structure accounts for the drastic decline in gas permeability and the rapid elevation in permselectivity.

To understand the underlying structural properties of the CMSMs that account for the observed gas transport behaviors, the membranes were characterized using XRD. For the 6FDA-TMPDA/azide (90-10) that was carbonized at 550 ^{0}C, there is a broad peak over the

d-spacing range of 4.4 to 6.8 Å [6]. This broad distribution of approximated inter-segmental distance explains for the higher gas permeability and lower selectivity of the membrane. At a pyrolysis temperature of 800 ^{0}C, a bimodal profile with d-spacings of 4.0 and 2.0 Å is observed [6]. This corresponds to the better permselectivity and smaller permeability of the 6FDA-TMPDA/azide CMSM that is prepared at a pyrolysis temperature of 800 ^{0}C.

The pristine polyimide and 6FDA-TMPDA/azide pseudo IPNs with different azide contents were carbonized at 550 and 800 ^{0}C, and the gas transport properties are summarized in Tables 1 and 2 [6]. For the CMSMs prepared at 550 ^{0}C, the addition of 10 wt% azide leads to a higher gas permeability but further increase in the azide content to 30 wt% results in a lower permeability. The higher permeability and lower selectivity of 6FDA-TMPDA/azide (90-10) CMSM correspond to the broad peak of its XRD spectra. The disappearance of the broad peak for 6FDA-TMPDA/azide (70-30) indicates a shift and sharpening of the pore size distribution, which results in a lower gas permeability and higher selectivity.

Table 1. Pure gas permeability of 6FDA-TMPDA/azide pseudo-IPNs pyrolyzed at 550 ^{0}C

| Sample | Permeability (Barrer) | | CO_2/N_2 selectivity |
	CO_2	N_2	
6FDA-TMPDA	6810 ± 125	277 ± 0.6	24.6 ± 0.4
6FDA-TMPDA/azide (90-10)	9290 ± 170	358 ± 17	26.0 ± 0.8
6FDA-TMPDA/azide (70-30)	3640 ± 17	151 ± 0.2	24.2 ± 0.1

Table 2. Pure gas permeability of 6FDA-TMPDA/azide pseudo-IPNs pyrolyzed at 800 ^{0}C

| Sample | Permeability (Barrer) | | CO_2/N_2 selectivity |
	CO_2	N_2	
6FDA-TMPDA	1460 ± 17	46.6 ± 0.1	31.3 ± 0.3
6FDA-TMPDA/azide (90-10)	851 ± 9.1	25.6 ± 0.2	33.2 ± 0.1
6FDA-TMPDA/azide (70-30)	280 ± 7.0	8.85 ± 0.2	31.7 ± 0.1

At a temperature of 550 ^{0}C, two competing effects of pore evolution from gas release and structural evolution from molecular rearrangement are present. The 6FDA-TMPDA/azide pseudo-IPN is apparently homogenous as indicated by the presence of a single glass transition temperature [5]. However, the transition is broad especially for 6FDA-TMPDA/azide (70-30) [5]. This implies the existence of multiple nano-domains with varying compositions. The dimensions of these nano-domians for 6FDA-TMPDA/azide (70-30) CMSM are possibly larger and the distribution within the polyimide is more heterogeneous, as compared to the 6FDA-TMPDA/azide (90-10) CMSM. The variation in the homogeneity of the pseudo-IPN precursor creates CMSM with different pore connectivity. As the 6FDA-TMPDA/azide (90-10) CMSM prepared at 550 ^{0}C is more homogenous, it possibly exhibits better pore connectivity which accounts for the enhancement in gas permeability [6]. Conversely, for the 6FDA-TMPDA/azide (70-30) CMSM prepared at 550 ^{0}C, the pores are trapped within the denser and more impermeable azide-rich nano-domains [6]. Hence, the gas permeability decreases. At a carbonization temperature of 800 ^{0}C, the dominant process that is occurring is the transformation and rearrangement of molecular structure and a CMSM with denser morphology is obtained. Therefore, for the membranes pyrolyzed at 800 ^{0}C, the gas permeability decreases and permselectivity increases with higher azide content.

The CO_2/N_2 gas separation performance of the CMSMs is plotted against the Robeson's upper bound as depicted in Figure 3 [6,8]. As illustrated in Figure 3, the CMSMs that are pyrolyzed at 550 ^{0}C outperform conventional polymeric membranes and the CO_2/N_2 separation performance falls on or above the upper bound. It was highlighted by Merkel et al. that in the treatment of flue gas by membranes, the separation performance is limited by the difference in pressure ratio [1]. It is redundant to have membranes with exceptionally

high selectivity. In fact, membranes with high permeability and reasonable selectivity of about 20 to 40 are preferred for use in post-combustion CO_2 capture. Therefore, the 6FDA-TMPDA/azide (90-10) membrane that is carbonized at 550 ^{0}C exhibits CO_2/N_2 separation performance that meets the aforementioned criteria for flue gas purification.
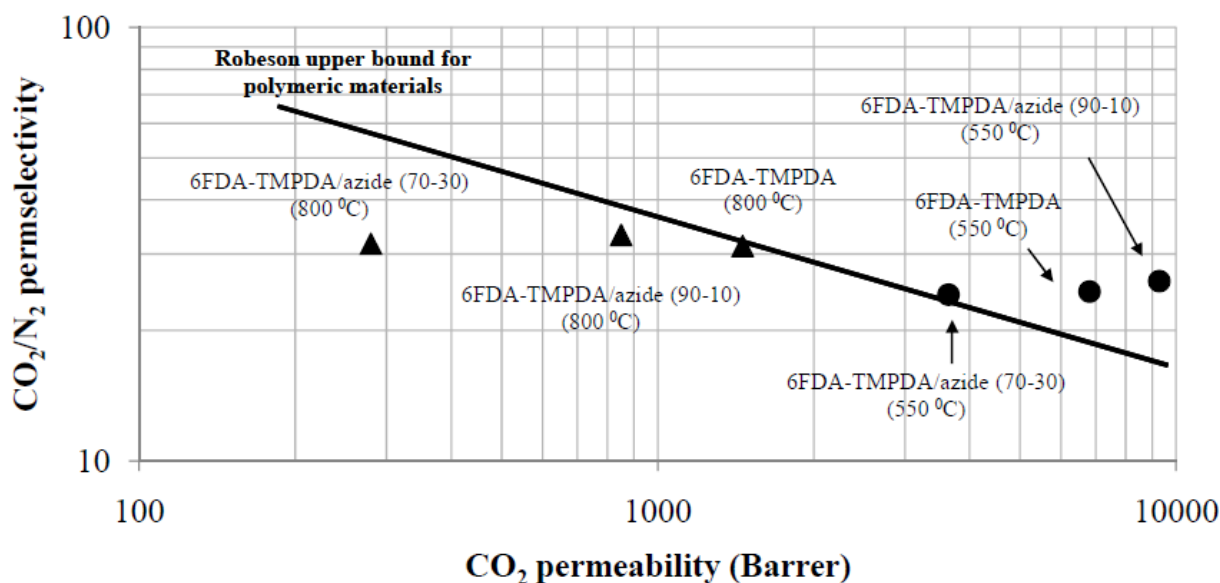
Conclusions

Carbon membranes that are derived from polyimide/azide pseudo-IPNs exhibit good CO_2/N_2 transport properties which are determined predominantly by the azide loading and pyrolysis temperature [6]. The 6FDA-TMPDA/azide (90-10) CMSM pyrolyzed at 550 ^{0}C has a CO_2 permeability of 9290 barrer and CO_2/N_2 selectivity of 26, which is suitable for use in CO_2 capture from flue gas [6].

References

[1] Merkel TC, Lin H, Wei X, Baker R. Power plant post-combustion carbon dioxide capture: An opportunity for membranes. J Membr Sci 2010;359:126–39.
[2] Kim YK, Park HB, Lee YM. Preparation and characterization of carbon molecular sieve membranes derived from BTDA–ODA polyimide and their gas separation properties. J Membr Sci 2005;255:265–73.
[3] Steel KM, Koros WJ. An investigation of the effects of pyrolysis parameters on gas separation properties of carbon materials. Carbon 2005;43:1843–56.
[4] Lie JA, Hägg MB. Carbon membranes from cellulose and metal loaded cellulose. Carbon 2005;43:2600–7.
[5] Low BT, Chung TS, Chen H, Jean YC, Pramoda KP. Tuning the free volume cavities of polyimide membranes via the construction of pseudo-interpenetrating networks for enhanced gas separation performance. Macromolecules 2009;42:7042–54.
[6] Low BT, Chung TS. Carbon molecular sieve membranes derived from pseudo-interpenetrating polymer networks for gas separation and carbon capture. Carbon 2011; 49: 2104-12.
[7] Shao L, Chung TS, Pramoda KP. The evolution of physicochemical and transport properties of 6FDA-durene toward carbon membranes; from polymer, intermediate to carbon. Microporous Mesoporous Mat 2005;84:59–68.
[8] Robeson LM. The upper bound revisited. J Membr Sci 2008;320:390–400.

Modeling and scale-up study of post combustion CO$_2$ absorption using new absorption solvents

Chinmay Kale, Andrzej Górak, Laboratory of Fluid Separations, TU Dortmund Dortmund, Germany;

Inga Tönnies, Hans Hasse, Laboratory of Engineering Thermodynamics, TU Kaiserslautern, Kaiserslautern, Germany.

Abstract

Post combustion capture of CO$_2$ via reactive absorption (RA) using amines is seen as one of the most attractive solutions to remove CO$_2$ from flue gases in large industrial plants such as refineries, power plants and petrochemical industry. The dimensions of the columns used in these industries will be much larger than those used for other industrial applications. Therefore for an efficient design of columns for such scales, a detailed scale-up study is necessary. This study should be based on a rigorous rate based model along with the detailed experimental research. In this work, a user defined rigorous rate-based model is validated initially and its role in a scale-up study and commercialization of the technology is explained consequently.

Key words: CO$_2$, amines, reactive absorption, rate-based model, scale-up

1. Rigorous rate-based model

The rigorous rate-based model used in this work considers a packed bed RA column which is axially discretised into smaller packing segments for detailed analysis. In the model, the mass transfer across the gas-liquid interface is described by the two-film theory. Multi-component diffusion in the film is calculated using the Maxwell-Stefan equation. It is assumed that phase equilibrium exists only at the phase interface. Because the chemical reaction takes place only in the liquid phase, the chemical kinetics is integrated into the balances on the liquid side. For instantaneous reaction, chemical equilibrium constants are used to calculate the equilibrium composition. Mass transfer coefficients are calculated from empirical correlations which are in turn dependent on physical properties, packing type and hydrodynamics. The

liquid film can be further discretised in radial direction into several segments to study composition profile across the film. The mole and heat balance equations for the multicomponent system are solved in each segment. To determine axial temperature profiles, differential energy balance equations are solved [1].

2. Process simulator

A wide variety of commercially available and in-house developed process simulators have been used to study reactive absorption processes. Aspen Plus® (RateSep), Aspen HYSYS®, ProTreat™, ProMax and gPROMS are commercially available simulators and Chemasim and CO2SIM are the examples of in-house process simulators [2]. Main advantages of these simulators are the availability of different chemical kinetics, different types of columns with variety of column internals, thermodynamic models and empirical mass transfer correlations as built-in functions. These in-built functionalities and the user friendly interface make these simulators easier to operate. However, often it is difficult to have an access to the governing model equations. The user cannot examine the influence of the model equations on simulation results. Furthermore, modifications and application of newer correlations becomes difficult. Many times the operating window of these simulators is limited. This is especially an important issue in scale-up studies where changing column dimensions can cause a complete different process behavior both in terms of hydrodynamics and chemical kinetics. Here it is necessary that the user has a complete access to the model equations for a better understanding of the model results. The model also offers user to study the process in depth by switching to different options with respect to various process phenomena, e.g. adiabatic or non-adiabatic process, Fick's or Nernst-Planck diffusion etc.[3]

The model presented here (see section 1) allows the user to formulate all the equations and correlations. The model is implemented in the simulation environment Aspen Custom Modeler® which uses an interface with Aspen Properties® to calculate the thermodynamic and physical properties. The Electrolyte NRTL model was chosen to describe the non-idealities in the reaction system.

3. Model validation results

To validate the above-described model, pilot plant experiments of CO_2 absorption in monoethanolamine (MEA) were carried out. The pilot-scale absorption column has an inner diameter of 0.125 m and a packing height of 4.2 m with Sulzer BX packing [4]. The reaction system includes two kinetically controlled reactions and four equilibrium reactions. The kinetic rate constants and equilibrium reaction constants are taken from literature [5]. Steady-state simulations were carried out using the inputs from experiments. The results of simulations are given in Table 1. The height of an individual packing segment was changed in order to get stable concentration and temperature profiles (Fig. 1, 2: for flow rate - 2.45mol/s). For the reaction between CO_2 and MEA, kinetics of Hikita et al. [6] was implemented. Mass transfer correlations of Rocha et al. [7] were used along with the correlation of Tsai et al. [8] for the calculation of the interfacial area.

Table 1: Comparison of experimental and model results: overall CO_2 removal

No.	L_flow (mol/s)	L_flow (mol/s)	x_CO$_2$ mol/mol	x_CO$_2$ mol/mol	Total CO$_2$ absorbed (mol/s)		Relative deviation (%)
	exp.	model	exp.	model	exp.	model	
1	1.584	1.450	0.050	0.051	0.079	0.074	6.227
2	1.898	1.739	0.049	0.051	0.093	0,089	4.132
3	2.452	2.322	0.047	0.051	0.115	0.119	-3.800
4	2.466	2.352	0.048	0.050	0.120	0.118	1.543
5	2.817	2.620	0.047	0.051	0.132	0.134	-1.346
6	3.311	3.258	0.044	0.047	0.146	0.153	-4.319
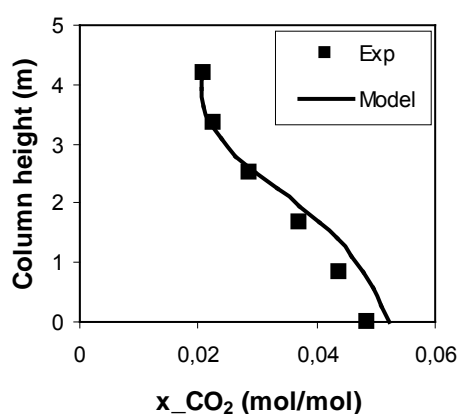
Fig. 1: Composition profile   Fig. 2: Temperature profile
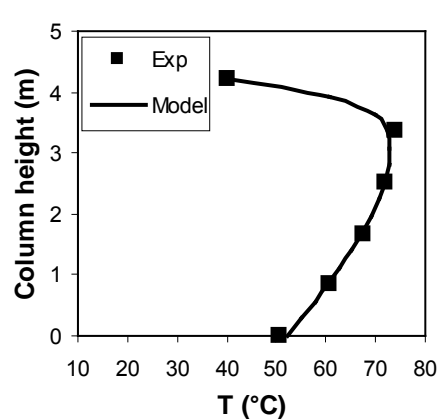
4. Conclusions

From the results it can be concluded that the user defined rigorous rate-based model of RA is validated (±7% accuracy). The validated model is an important analytical tool and can also be used for optimization study, sensitivity analysis and scale-up studies. The model has sub-models for the calculation of reaction kinetics, hydrodynamics and mass transfer parameters, which offers high flexibility. Unlike other commercially available simulation tools, the model gives the user complete access to governing equations, correlations and model structure which can be modified for a variety of column internals and new absorption solvents. This is very important in the scale-up study.

(Authors would like to thank Dr. Schoenmakers at TU Dortmund for his guidance)

5. References

1. E. Kenig, A.Górak, *"Reactive Absorption" in Integrated Chemical Processes (Ch. 9) edited by K. Sundmacher, A. Kienle, A. Seidel,* Wiley, Weinheim, 2005.
2. L. Öi, *CO2 removal by absorption: Challenges in modeling. Mathematical and Computer Modeling of Dynamical Systems*, 2010, 16 (6): p. 511-533.
3. C. Kale, I.Tönnies, H. Hasse, A. Górak, *"Simulation of Reactive Absorption: Model Validation for CO2-MEA system":* manuscript, ESCAPE-21, Greece, 2011.
4. H. Mangalapally, R.Notz, S. Hoch, N. Asprion, G. Sieder, H. Garcia, H Hasse, *Pilot plant experimental studies of post combustion CO2 capture by reactive absorption with MEA and new solvents.* En. Proc., 2009, (1): p. 963-970.
5. L. Kucka, *Modellierung und Simulation der reaktiven Absorption von Sauergasen mit Alkanolaminlösungen.* 2003, PhD Thesis.
6. H. Hikita, T. Murakami, T. Ishii, *The kinetics of reactions of carbon dioxide with monoisoporpanolamine, dyclycolamine & ethylenediamine by a rapid mixing method.* Chem. Eng. J., 1977, (14): p. 27–30.
7. J. Rocha, J. Bravo, J. Fair, *Distillation columns containing structured packings: A comprehensive Model for their performance. 2 Mass Transfer model.* Ind. Chem. Eng. Res., 1996, (35): p. 1660-1667.
8. R. Tsai, R. Eldridge, G. Rochelle, *Influence of viscosity and surface tension on the effective mass transfer area of structured packing.* En. Proc., 2009, 1(1): p. 1197-1204.

Variants of process heat extraction for post-combustion CO₂-capture plants in exergetic comparison

Presenting author: Dipl.-Ing. Norbert Pieper
Siemens AG - Energy Sector - Rheinstraße 100 - 45478 Mülheim / Ruhr

Co-author: Dipl.-Ing. Michael Wechsung
Siemens AG - Energy Sector - Rheinstraße 100 - 45478 Mülheim / Ruhr

The Post-Combustion Capture Process (PCC)

The post-combustion capture of CO_2 from the flue gases of fossil fired power plants by an absorption process represents one option to reduce the emissions of carbon dioxide.
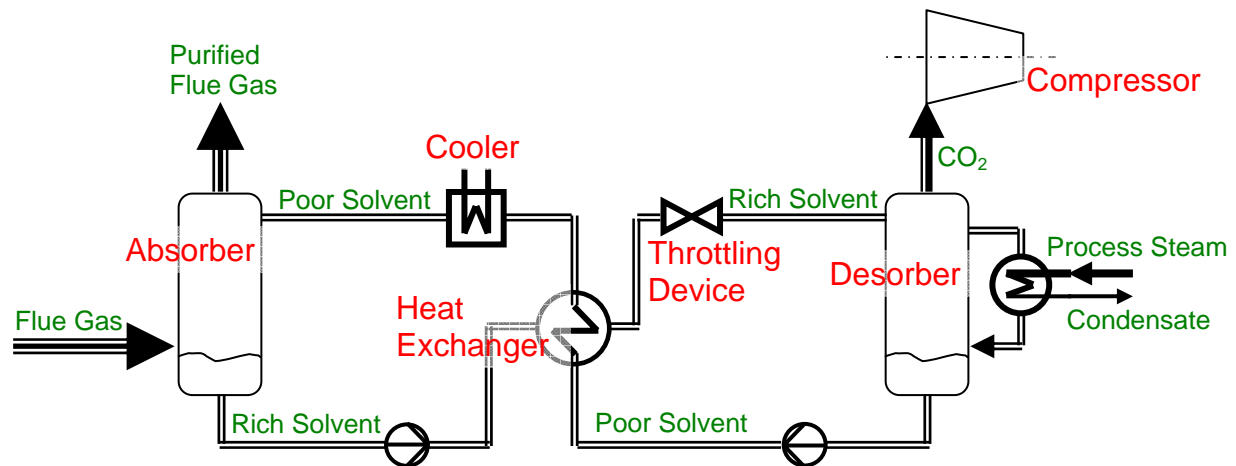
Figure 1: Schematic diagram of a post-combustion plant

The CO_2 in the flue gas is absorbed by a liquid solvent and desorbed under the addition of heat (ref. *Figure 1*). The separated CO_2 is finally sequentially compressed and cooled before it is directed to a permanent geological storage facility.

The main advantages of PCC are that it has only a relative small impact on the power plant process and therefore **standardized components** can be used, the **reliability** of the power plant is not reduced (since operation without capture is still possible), and existing plants can be **retrofitted**.

For a steam turbine the PCC process represents a thermal consumer. Similar to the extraction of hot steam for district heating, the heat is mainly transferred by condensation in a surface heat exchanger. The condensate remains in the water-steam-cycle and is admitted back into the feed water heating system at an appropriate posi-

tion. Therefore the requirements are very similar to other state-of-the-art process heat extractions (e.g. for district heating). The temperature level defined by the heat consumer is determined by the condensing pressure of the extracted steam and the terminal temperature difference of the heat exchanger.

Extraction of process steam from steam turbine

There are two principles applied to extract steam from the turbine (ref. *Figure 2*).
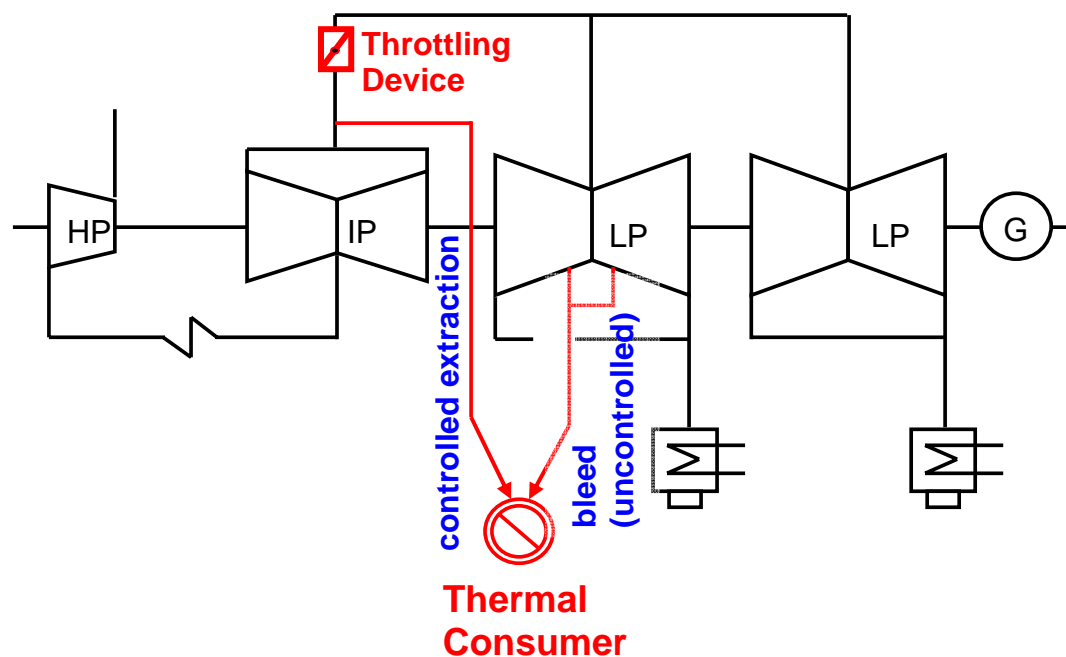
Figure 2: Variants of extracting steam from a steam turbine

Bleeds are typically used for regenerative feed water heating. A property of bleeds is that the pressure at the extraction point behaves proportional to the load of the following turbine section ("sliding pressure"). This means that the higher the extracted mass flow, the lower the pressure at the extraction point. On the other hand the pressure at the extraction point has to be higher than the pressure in the heat exchanger, so it can be the case that not enough steam is provided if an uncontrolled bleed is used.

In contrast to the uncontrolled bleed, a **controlled extraction** is capable of maintaining the pressure at the extraction point independently of the turbine load. The required mass flow can be adjusted indirectly by using the throttling device in the main flow path of the turbo-set (ref. *Figure 2*). The disadvantage is that throttling losses occur in the flow to the following turbine section.

While bleeds can be positioned anywhere in the flow path of the turbine, controlled extractions are typically arranged between two turbine casings since a throttling device can be easily installed there.

The process of absorption typically calls for a constant temperature of the transferred heat. This means that the pressure at the extraction must be kept constant, independent of the turbine load point. This can be achieved by throttling the flow downstream of the extraction. Conventionally the steam is extracted between the intermediate pressure turbine and the low pressure turbine since this is where a butterfly control valve can be positioned. If the saturated steam temperature at the corresponding extraction pressure is equal to the required process temperature, no throttling in the design case, e.g. at full load, is necessary.

For the controlled steam extraction to provide process heat at a low temperature level, the connecting pipe between the IP- and LP-turbines is suitable. The choice of the design pressure at this position, subsequently called separation pressure, is highly relevant for the occurring losses in the water steam cycle. With the goal of minimising these losses, calculations were carried out, analysed and discussed. The calculations are based on an 800 MW coal fired power plant. The variation parameters were the separation pressure (between the IP- and LP-turbines) and the pressure in the desorber of the downstream process.

Exergetic contemplation of losses

The calculations are carried out contemplating exergetic losses. E**xergy** represents the part of energy that can be transferred into any other kind of energy. Energy consists of exergy and **anergy**, which cannot be used in a process. To define exergy and anergy the ambient temperature is the decisive factor. For steam power plants the temperature of the steam in the condenser can be used instead.

Exergetic loss (Throttling) EV:

Exergetic loss (Desuperheating) EV:

$$EV = \dot{m} \cdot \left[\mathbf{T_u} \cdot (\mathbf{s_1} - \mathbf{s_2}) \right] \qquad EV = \sum \dot{m}_i \cdot \left[\mathbf{h_i} - \mathbf{T_u} \cdot \mathbf{s_i} \right]$$

$\dot{m}$: mass flow
s: entropy
h: enthalpy
T_u: ambient temperature (absolute)

Figure 3: Calculation of exergetic losses for isenthalpic throttling and desuperheating

Choice of separation pressure and desorber pressure
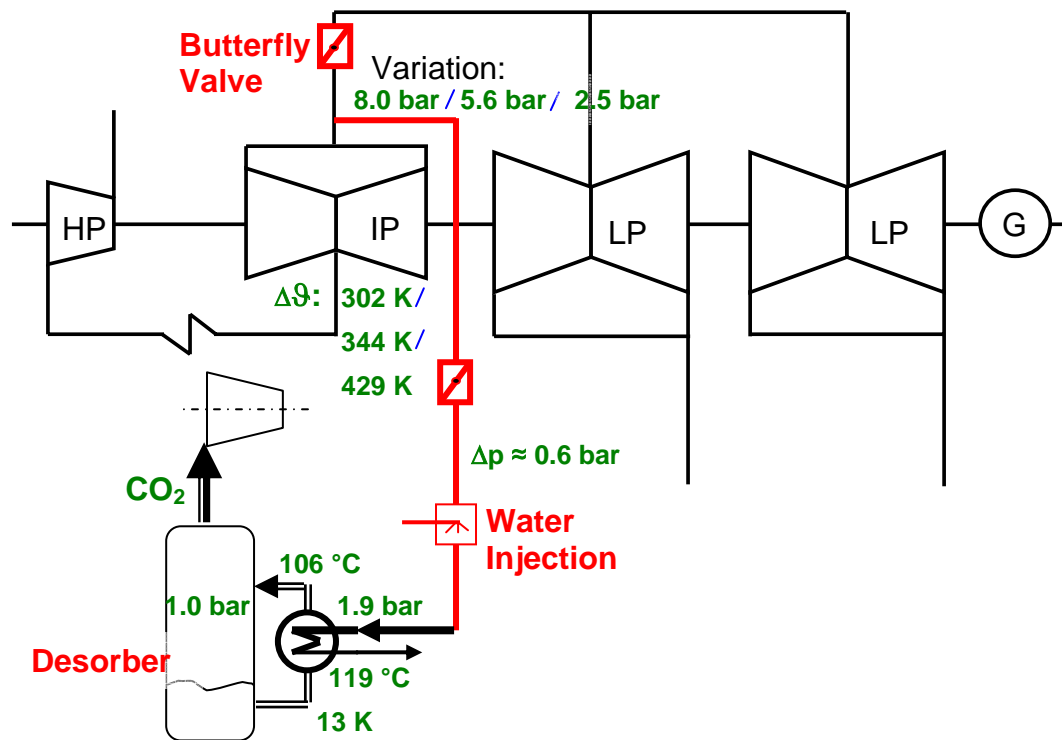
Figure 4: Variation of pressure at turbine extraction point for atmospheric operated desorber

For a high extraction pressure in combination with a low temperature level of the heat consumer large exergetic losses occur, either due to throttling (in the process steam line) or due to high terminal temperature differences in the heat exchanger.

For a low separation pressure, the high volumetric flows at the IP-exhaust call for large dimensions of the cross-over-pipe and the process steam pipe.

Depending on the design of the IP-turbine there might be additional restrictions for the choice of the separation pressure. For low separation pressures resulting in high temperature differences between inlet and exhaust steam, a modified design concept might be necessary.

For variants with an increased desorber pressure it is important to consider the auxiliary power of the capture plant as well, especially of the CO_2-compressor, since the compression also starts with the increased pressure. Another relevant aspect of increased desorber pressure could be the influence of the dimensions of the desorber depending on the volumetric flow of the captured CO_2.

Results and conclusions

After summarizing all relevant occurring losses, the variants can be compared.

Additional summarized exergetic losses of the variants:

Pressure at extraction point	Pressure at desorber		
	1.0 bar	1.6 bar	2.8 bar
2.5 bar	**Base (#)**		
3.6 bar		**1.5 MW (#)**	
5.6 bar	**24.5 MW**	**14.7 MW**	**6.2 MW (#)**
8.0 bar	**35.0 MW**	**25.1 MW**	**16.6 MW**

Table 1: Additional exergetic losses of analysed variants

#: no throttling in process steam line or increased terminal temperature difference in the heat exchanger

The throttling of the process steam, or the increased terminal temperature difference in the heat exchanger causes significant exergetic losses. By increasing the separation pressure together with the desorber pressure the total losses can be limited.

The main conclusions which can be derived are listed below:

- Low separation pressures are beneficial for the provision of process steam. Limitations may result from the design of the IP-turbine, or from high volumetric flows.

- To retrofit a power plant with post-carbon capture without modifying the steam turbine, exergetic losses can be avoided by increasing the desorber pressure. Most often this is more economical than to adapt the steam turbine to lower separation pressures.

- The pressure in the desorber represents an additional degree of freedom. However it can only be applied if the thermal stability of the solvent is sufficiently stable at increased temperatures.

- Siemens uses an amino acid salt as solvent, which is characterized by very high temperature stability. This has the advantage that the pressure in the desorber can be used as an additional degree of freedom.

- Siemens is in the position to evaluate all components along the process chain (from fossil fired boiler to water/steam cycle, including the steam turbine, up to the processes of capturing and compressing the CO_2) as well as their interaction, and to optimize the overall system.

- Siemens develops appropriate concepts with the aim of minimising the decrease in efficiency for the application of Carbon Dioxide Capture and Storage (CCS).

Nonlinear Model Predictive Control for operation of a post combustion absorption unit

J. Åkesson[a,b], G. Lavedan[a], K. Prölß[a], H. Tummescheit[a], S. Velut[a]

[a]Modelon AB, Ideon Science Park, Lund, Sweden

[b]Department of Automatic Control, Lund University, Sweden

Introduction

One of the most promising processes to separate carbon dioxide (CO_2) from flue gas in coal-fired power plants in order to reduce its emission to the environment is based on absorption with aqueous amine solutions. A schematic of the process is shown in Figure 1.
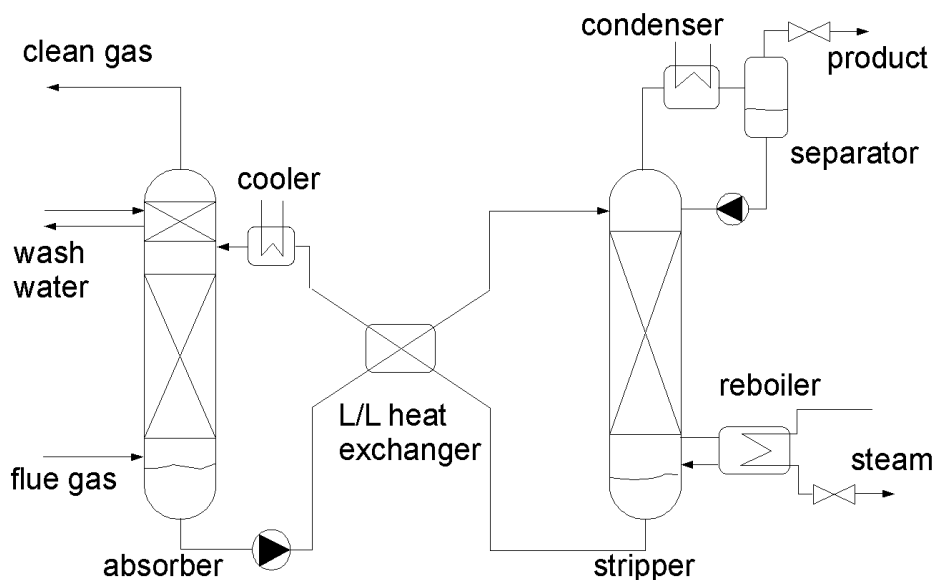
Figure 1: Schematic of an amine scrubbing process to remove CO_2 from flue gas.

The cleaned gas is released to the environment, while the rich solution is regenerated in the stripper at elevated temperatures driven by bled steam from the power generation process. After water condensation from the exiting gas phase the CO2 product stream is compressed and stored. This process drastically reduces overall power plant efficiency. Minimizing the amount of steam required in the reboiler is therefore the task with highest priority in the optimization of this process.

With an increasing demand on the plant's flexible operation in the face of frequent load, dynamic simulation and optimization are seen as important tools to ensure an efficient incorporation of the carbon capture into the power generation. This paper presents results achieved within a larger project aiming at developing an optimization technology for advanced model-based control of the separation plant.

Background

Modeling

The post-combustion separation unit was modeled with Modelica, an equation-based modeling language for dynamic simulation, which is supported by a number of different platforms. The focus was on the two column models, which describe the mass transfer-driven absorption of CO_2 from the flue gas by a MEA (mono-ethanolamine) -solution and the corresponding process in the stripper column. For this work only the stripper unit models including reboiler and condenser are considered in the following study. A description of the models, as well as validation with experimental data and physical model reduction to meet the requirements of an optimization routine are presented in [1].

Model Predictive Control

Model Predictive Control (MPC) is an advanced control method that relies on the online solution to optimal control problems. Every time new plant measurements are available, the MPC controller makes use of a model to predict the future plant behavior and to compute the control action that minimizes a cost function defined over a prediction horizon. The first part of the optimal control variable trajectories is then applied to the process and the controller waits for new measurements. This so called-receding horizon control strategy is an efficient feedback algorithm that can handle multi-input multi-output systems and constraints on any process variables.

JModelica.org

Solving optimal control problems may be computationally challenging, in particular for non-linear models. The software platform JModelica.org [2] is used to solve the dynamic optimization problems from the MPC formulation applying a direct

collocation method together with the open-source Nonlinear Programming solver IPOPT [3].

Application of nonlinear MPC to the stripper unit

Problem formulation

The control problem is formulated as in standard MPC using a quadratic cost function penalizing deviations of the controlled variable from a reference value, as well as variations in the control signal. The variable to be controlled is the removal rate defined as a CO_2 balance across the absorber. The chosen control signal is the heat flow rate to the reboiler. An upper bound on the reboiler pressure is imposed to avoid MEA degradation occurring at high temperatures. Both the control and the prediction horizons are set to 1000s. The sampling time is chosen to be 100s.

Results

The continuous-time optimization problem, containing 50 states, 1493 equations and 1493 variables, is transformed by JModelica.org into a large scale discrete-time Nonlinear Program with 29824 equations. Performance of MPC is now evaluated in a simulation where the desired removal efficiency is increased, see Figure 2. The heat flow rate to the reboiler is rapidly increased from its start value of 0.7 MW to 1.05 MW, leading to a removal efficiency of about 0.8 at time t=400s. At around 500s, the reboiler pressure reaches its maximal allowed value of 1.95 bar and the heat flow rate decreases slightly to avoid constraint violation. Because of the high condenser pressure, the target efficiency of 0.9 cannot be achieved in this optimization setup. In contrast to [1] the optimized trajectories are derived iteratively by solving a sequence of open-loop control problems. Solving a single problem takes about 60s, which is below the sampling-time of 100s required for real-time control. Future work includes the addition of the MEA circulation rate as second control signal and the implementation of an observer to estimate parts of the state that cannot be measured online.
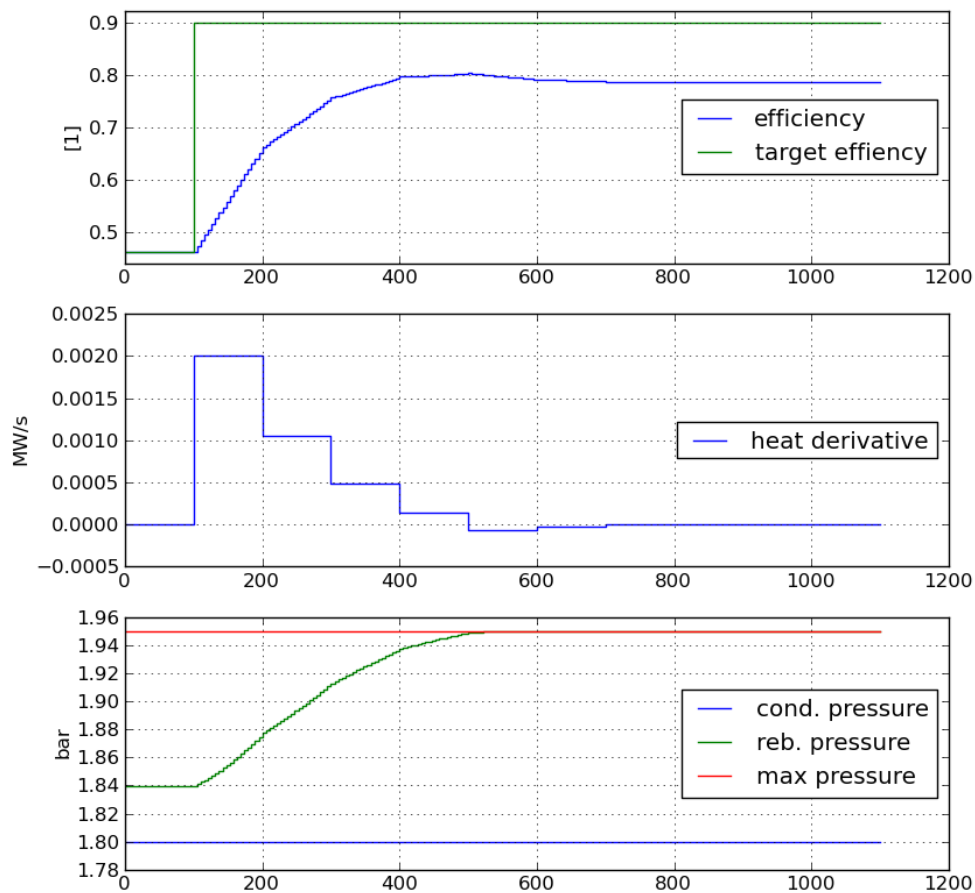
Figure 2 Optimized trajectories when the target efficiency is changed to 0.9 after 100 seconds. From top to bottom: removal efficiency, heat derivative, condenser pressure and reboiler pressure.

References

[1] Åkesson, J. et al. Models of a post-combustion absorption unit for simulation, optimization and non-linear model predictive control schemes. In *8th International Modelica Conference*, March 2011

[2] Åkesson, J. et al.Modeling and Optimization with Optimica and JModelica.org—Languages and Tools for Solving Large-Scale Dynamic Optimization Problem. Computers and Chemical Engineering, 2010.

[3] Wächter A, Biegler LT. On the implementation of an interior-point filter line-search algorithm for large-scale nonlinear programming. Mathematical Programming , 2006;106 (1); 25-58.

Absorption and Desorption Modelling United

Philip Loldrup Fosbøl, Kaj Thomsen, Center for Energy Resources Engineering(CERE), DTU Department of Chemical and Biochemical Engineering, Technical University of Denmark (DTU), DK-2800 Kongens Lyngby, Denmark

Solvent based CO_2 capture is performed using scrubbing. It is currently the state of art technology for cleaning flue gasses and similar carbon dioxide rich streams. The technology has only been proven for smaller bench scale and pilot test using amines. It is yet to be built full scale, for capturing CO_2 from coal fired power plants. On a long term basis new processes may substitute this equipment. In the mean time the amine units will be successful in reducing the emission of CO_2, especially from coal fired power plants. There is a huge potential to reduce the energy demand with the existing technology.

Principles and case studies

In this work a generic model will be presented for the simulation of both absorption and desorption. It involves a complete rate based equation scheme for the column tower, linked to models of the reboiler and condenser. The core modular parts are discussed and an overview of the thermodynamic modelling, transport relations, and physico-chemical properties will be presented.

New concepts, methods, tools, and ideas are given in order to explain the principles of solvent based CO_2 capture.

The calculations show the properties inside the column as function of column height, compared to experimental measurements. Result on energy consumption, simulation scenarios, and method evaluation will be presented, supported by case studies based on real life capture process parameters. A comparison towards recent experimental pilot studies is part of the results.

Title:

Development and Validation of a Process Simulator for Chilled Ammonia Process to Capture CO_2

Author(s):

Rameshwar Hiwale, Joseph Naumovitz, Ritesh Agarwal, Rasesh Kotdawala & Fred Kozak

Company: Alstom Power

Abstract

The Chilled Ammonia Process (CAP) is a post-combustion technology that captures CO_2 emitted from the power plants for sequestration and storage. Deployment of this technology requires a flexible process simulation tool for design that can evaluate various CAP configurations to achieve the lowest possible capital cost, energy demand and operating cost in the context of the power plant operating objectives. This paper is focused on incorporating the knowledge gained from CAP field pilots with plant capacities ranging from 1,000 to 100,000 metric tons of CO_2 captured per year into our modeling tools to ensure success for predicting full scale unit performance.

A robust process simulation tool using Aspen Plus is developed by Alstom to design CAP CO_2 Capture facilities. Underpinning this development, thermo–physical properties and chemistry were regressed using data from laboratory and literature. To validate the model, experimental steady state data from the lab-scale pilot plant in Sweden, field pilot plants in United States and Sweden, and a Process Validation Facility (PVF) in United States were compared with model results. This comparison validated the process simulation tool across a range of CAP operating conditions and flue gas sources.

The paper presents the methodology that Alstom utilized to:

- Ensure quality of field data from calibrated instruments

- Implement advanced data reconciliation techniques

- Characterize the accuracy of simulator predictions

- Analyze the developed simulation tool to ensure reproducibility of results independent of plant size

This validated model will be used to design and optimize future CAP scale-up facilities.

Commercial Scale Test Validation of Modern High Performance Structured and Random Packings for CO2-Capture Ranking

Michael Schultes, Raschig-Jaeger Technologies, Mundenheimerstrasse 100, 67061 Ludwigshafen, Germany; Simon Chambers, Brad Fleming
Raschig-Jaeger Technologies, 1611 Peachleaf St., Houston TX, USA 77039

Keywords: Destillation, CO2-Absorption, Raschig Super-Pak, Raschig Super-Ring

Energy and performance-efficient CO_2 capture in the field of gas absorption/stripping will become an increasingly important technology in various industrial and environmental applications for decades to come. To meet the goal of optimized CO_2 capture performance, high capacity/high mass transfer efficiency/low pressure drop modern packings are required. To support these requirements, a series of commercial/pilot scale tests have been conducted on high performance random and structured packings.

Capacity-efficiency-pressure drop-liquid hold-up examples from Commercial Test Columns will be described. Test results clearly demonstrate superior all round performance of modern high performance structured or random packings over the well-known standard metal packings.

Beside the distillation tests hydraulic air-water and mass transfer measurements from CO2 absorption into caustic solution performed will be presented. Again comparison data will be given for high performance random and structured packings.

All data presented will answer the question if distillation test data can be used for a ranking list of packings in CO2 absorption processes.

Step Change Adsorbents and Processes for CO_2 capture "STEPCAP"

T.C. Drage[1] A.I Cooper[3], R Dawson[3], J Jones[3], C Cazorla Silva[4], <u>C.E. Snape</u>[1], L. Stevens[1], X. Guo[4], J. Wood[2], J. Wang[2]

[1]Department of Chemical and Environmental Engineering, Faculty of Engineering, University of Nottingham, Nottingham, NG7 2RD, UK.
[2]Chemical Engineering, The University of Birmingham, Edgbaston, Birmingham, B15 2TT, UK.
[3]Department of Chemistry, Crown Street, The University of Liverpool, Liverpool, L69 7ZD, UK
[4]Department of Chemistry, University College London, London, WC1H 0AJ, UK.

Abstract

STEPCAP is a multipartner consortium project, the aim of which is to develop a targeted range of novel CO_2 adsorbents for carbon capture. This research into materials and process development is essential to achieve the potential cost and efficiency benefits offered by solid sorbents capture technologies over the current state of the art processes. Firstly, this paper will discuss the key materials and process challenges associated with developing solid sorbents. This will lead into a discussion of materials development in STEPCAP which is based on a fundamental understanding of adsorption processes to design and optimise material properties and form. The development and performance of the three classes of materials under development in this study, microporous polymers, surface modified hydrotalcites, and co-doped sorbents, which offer potential for a step change increase in adsorption capacity and performance over previously developed materials will be discussed. Modified hydrotalcites such as, amine modified layered double hydroxides (LDH's) have been synthesized via the exfoliation and grafting route. In addition, novel conjugated microporous polymers synthesized through Sonogashira-Hagihara coupling have also been investigated and have demonstrated similar capacities. Critically, due to the hydrophobic nature of some of these adsorbents, identical performance has been observed in the presence of moisture, an advantageous property for operation in the water saturated environment of flue gases. This presentation will also present data on the performance of these materials in simulated flue gases as well after simulated temperature swing regeneration cycles to assess the stability and lifetime of the sorbents.

Introduction

Recognising that fossil fuels will continue globally as part of a diverse energy mix for some time[1], targets and strategies have been developed to reduce greenhouse gas emissions, for example the European Unions Sustainable Energy Technology (SET) Plan[2]. Rapid development and implementation of these strategies will be required if the warnings of potentially damaging climate change reported by the Intergovernmental Panel on Climate Change (IPCC) are to be avoided[3], a task that is made more challenging when set against the significant global increase in energy demand[1]. Europe is committed to an 80% reduction in greenhouse gas emissions by 2050[4] and similar emissions reduction targets have been proposed and committed to on a global scale[5].

The current state of the art technologies for post-combustion capture, amine solvent scrubbing, uses aqueous solutions of alkanolamines to achieve CO_2 separation from flue gas[6-8]. Whilst this technology is the current state of the art and will be used in the first generation of carbon capture plant, the technology has a number of drawbacks in terms of complexity in operation, high pH solvents leading to corrosion of metal piping, and the energy-intensive regeneration of the solvents[6]. This high energy usage of this process has led to the proposal of a range of potentially more efficient and less energy intensive second and third generation capture technologies[9]. The development of a solid adsorbent capture technology is one of the most promising alternative capture technologies[9]. A key motivation for the development of solid adsorbents for carbon capture is the potential energy saving shown by theoretical studies. These studies suggest that an adsorbent system with a

cyclic capacity approaching or better than 3 mmol g^{-1} could significantly reduce the energy requirement of post-combustion capture by 30-50% compared with amine solvent systems[10]. A wide range of materials have been developed for this application[11] and include, supported amines and immobilized amines[12-16] activated carbons[17-19], Hydrotalcites[20], zeolites[21], inorganic-organic hybrid materials such as Metal Organic Frameworks (MOFs)[22]. Of all the materials developed and tested the challenge still remains to develop materials that achieve these performance targets and are fully stable under the conditions of post-combustion flue gases[23].

Experimental

Adsorbent materials have been characterised and tested using a range of techniques. Characterisation of materials has focussed on determining the physical and chemical properties of the solid sorbent materials. This has been conducted using a range of techniques, for example, elemental analysis, powder x-ray diffraction (XRD), diffuse reflectance infrared Fourier transform spectra (DRIFTS), textural properties have been determined by N_2 adsorption analysis . Thermogravimetric analysis (TGA) has been used to determine the thermal stability of the materials as well as measure CO_2 adsorption capacity and cyclic capacity[14].

Results and Discussion

To realise the potential of solid sorbent for carbon capture two developments are required, new porous materials and plant integration processes. The key challenges for materials development and requirements in terms of: operating conditions, gas composition, stability and lifetime required to make solid sorbents a viable large scale CO_2 capture process are described in this presentation[24].

To date a wide range of materials have been developed and tested as part of the STEPCAP project. The key materials under development are, microporous polymers, surface modified hydrotalcites, and co-doped sorbents. Performance of these materials has been assessed under a range of conditions and will be presented. Current key developments are summarised as follows:

Hydrotalcites and conjugated microporous polymers have been studied as potential adsorbents for CO_2 capture[25, 26]. Modified hydrotalcites such as, amine modified layered double hydroxides (LDH's) were synthesized via exfoliation and grafting route. The influence of primary and secondary amines on carbon dioxide adsorption was investigated. One hydrotalcite with 3-[2-(2-Aminoethylamino) ethylamino]propyl-trimethoxysilane, containing both a primary and secondary amine functional groups showed a steady increase in CO_2 adsorption capacity of 0.74 - 1.76 mmol g^{-1} from 25 - 80°C through the flue gas temperature range.

Synthetic microporous polymers possess some of the highest reported surface areas[27] and some preparative routes might in principle be applicable to CCS applications[28]. A key benefit of porous organic chemistries is the very diverse synthetic organic chemistry which is available, both in terms of the wide range of monomers that can be exploited either by direct incorporation[29-31] or by the possibility of post-synthetic modification of networks to include functional groups reactive to CO_2. These routes to materials synthesis are being explored as part of the STEPCAP project. Incorporation of functional monomers has been shown to be useful in tuning the isosteric heat of adsorption of CO_2 by these materials[32]. A further advantage of organic polymeric networks over other highly porous synthetic materials such as hybrid inorganic-organic materials is their high moisture stablility together with high thermal stability[27]. However, despite recent reports of uptakes of around 3 mmol g^{-1} at ambient temperatures[33] microporous organic polymers have yet to achieve high enough CO_2 loadings under the required conditions to be commercialised.

Conclusions

The development of solid sorbents for CO_2 capture is an area of significant academic and industrial interest. The composition of the flue gases in post-combustion capture and the

requirements for material performance to minimise the energy penalty of the capture process present a significant challenge for materials development. To date, a wide range of functional materials have been and will continue to be developed with potential to make breakthrough. Whilst at present the required cyclic capture capacities can be achieved, one of the main challenges still remains to develop materials that can operate reliably and over a large number of cycles in a flue gas environment, a challenge which will form the future focus of the STEPCAP project.

References
[1] World Energy Outlook 2008 Edition, International Energy Agency, 2009.
[2] P. Capros, L. Mantzos, N. Tasios, A. De Vita, N. Kouvaritakis, EU energy trends to 2030-Update 2009, 2010.
[3] E. Rubin, L. Meyer, H. de Coninck, IPCC Special Report: Carbon Dioxide Capture and Storage, 2005.
[4] Department of Trade and Industry. Meeting the Energy Challenge: A White Paper on Energy, 2007.
[5] United Nations Framework Convention on Climate Change (UNFCCC). Report of the Conference of the Parties on its sixteenth session, held in Cancun from 29 November to 10 December 2010. Part one: Proceedings., 2011.
[6] C.L. Leci, Financial implications on power generation costs resulting from the parasitic effect of CO_2 capture using liquid scrubbing technology from power station flue gases, Energ Convers Manage, 37 (1996) 915-921.
[7] H.J. Herzog, E.M. Drake, Greenhouse Gas R&D programme. IEA/93/oE6, (1993).
[8] R.M. Davidson, Post-combustion carbon capture from coal fired plants - solvent scrubbing. IEA Clean Coal Centre, 2007.
[9] J.D. Figueroa, T. Fout, S. Plasynski, H. McIlvried, R.D. Srivastava, Advancesn in CO_2 capture technology - The US Department of Energy's Carbon Sequestration Program, Int J Greenh Gas Con, 2 (2008) 9-20.
[10] M.L. Gray, K.J. Champagne, D. Fauth, J.P. Baltrus, H. Pennline, Performance of immobilized tertiary amine solid sorbents for the capture of carbon dioxide, Int J Greenh Gas Con, 2 (2008) 3-8.
[11] R. Davidson, Post-combustion carbon capture – solid sorbents and membranes. IEA CLean Coal Centre, 2009.
[12] X.C. Xu, C.S. Song, J.M. Andresen, B.G. Miller, A.W. Scaroni, Novel polyethylenimine-modified mesoporous molecular sieve of MCM-41 type as high-capacity adsorbent for CO_2 capture, Energ Fuel, 16 (2002) 1463-1469.
[13] X.C. Xu, C.S. Song, J.M. Andresen, B.G. Miller, A.W. Scaroni, Preparation and characterization of novel CO_2 "molecular basket" adsorbents based on polymer-modified mesoporous molecular sieve MCM-41, Micropor Mesopor Mat, 62 (2003) 29-45.
[14] T.C. Drage, A. Arenillas, K.M. Smith, C.E. Snape, Thermal stability of polyethylenimine based carbon dioxide adsorbents and its influence on selection of regeneration strategies, Micropor Mesopor Mat, 116 (2008) 504-512.
[15] P.J.E. Harlick, A. Sayari, Applications of pore-expanded mesoporous silicas. 3. Triamine silane grafting for enhanced CO_2 adsorption, Ind Eng Chem Res, 45 (2006) 3248-3255.
[16] R. Serna-Guerrero, E. Da'na, A. Sayari, New Insights into the Interactions of CO_2 with Amine-Functionalized Silica, Ind Eng Chem Res, 47 (2008) 9406-9412.
[17] C. Pevida, T.C. Drage, C.E. Snape, Silica-templated melamine-formaldehyde resin derived adsorbents for CO_2 capture, Carbon, 46 (2008) 1464-1474.
[18] A. Arenillas, K.M. Smith, T.C. Drage, C.E. Snape, CO_2 capture using some fly ash-derived carbon materials, Fuel, 84 (2005) 2204-2210.

[19] T.C. Drage, A. Arenillas, K.M. Smith, C. Pevida, S. Piippo, C.E. Snape, Preparation of carbon dioxide adsorbents from the chemical activation of urea-formaldehyde and melamine-formaldehyde resins, Fuel, 86 (2007) 22-31.

[20] S. Walspurger, L. Boels, P.D. Cobden, G.D. Elzinga, W.G. Haije, R.W. van den Brink, The Crucial Role of the K+-Aluminium Oxide Interaction in K+-Promoted Alumina- and Hydrotalcite-Based Materials for CO_2 Sorption at High Temperatures, Chemsuschem, 1 (2008) 643-650.

[21] P. Xiao, J. Zhang, P. Webley, G. Li, R. Singh, R. Todd, Capture of CO_2 from flue gas streams with zeolite 13X by vacuum-pressure swing adsorption, Adsorption, 14 (2008) 575-582.

[22] A. Torrisi, R.G. Bell, C. Mellot-Draznieks, Functionalized MOFs for Enhanced CO_2 Capture, Cryst Growth Des, 10 (2010) 2839-2841.

[23] S. Sjostrom, H. Krutka, Evaluation of solid sorbents as a retrofit technology for CO_2 capture, Fuel, 89 (2010) 1298-1306.

[24] T. Drage, C. Snape, L. Stevens, J. Wood, J. Wang, A. Cooper, R. Dawson, G. Guo, C. Satterley, R. Irons, Materials challenges for the development of solid sorbents for post-combustion carbon capture, Journal of Materials Chemistry, (In Prep).

[25] J. Wang, L. Stevens, T. Drage, J. Wood, Preparation and CO_2 adsorption of amine modified Mg-Al LDH via exfoliation route, Chem Eng Sci, (In Press).

[26] J. Wang, L. Stevens, T. Drage, J. Wood, Preparation and CO_2 adsorption of amine modified layered double hydroxide via anionic surfactant-mediated route (In Prep).

[27] H. Ren, T. Ben, E.S. Wang, X.F. Jing, M. Xue, B.B. Liu, Y. Cui, S.L. Qiu, G.S. Zhu, Targeted synthesis of a 3D porous aromatic framework for selective sorption of benzene, Chem. Commun., 46 (2010) 291-293.

[28] C.D. Wood, B. Tan, A. Trewin, H.J. Niu, D. Bradshaw, M.J. Rosseinsky, Y.Z. Khimyak, N.L. Campbell, R. Kirk, E. Stockel, A.I. Cooper, Hydrogen storage in microporous hypercrosslinked organic polymer networks, Chem Mater, 19 (2007) 2034-2048.

[29] R. Dawson, A. Laybourn, R. Clowes, Y.Z. Khimyak, D.J. Adams, A.I. Cooper, Functionalized Conjugated Microporous Polymers, Macromolecules, 42 (2009) 8809-8816.

[30] R. Dawson, A. Laybourn, Y.Z. Khimyak, D.J. Adams, A.I. Cooper, High Surface Area Conjugated Microporous Polymers: The Importance of Reaction Solvent Choice, Macromolecules, 43 (2010) 8524-8530.

[31] J.-X. Jiang, A.I. Cooper, Microporous organic polymers: design, synthesis and function, Topics Curr. Chem., 293 (2009) 1-33.

[32] R. Dawson, D.J. Adams, A.I. Cooper, Chemical tuning of CO_2 sorption in robust nanoporous organic polymers, Chemical Science, (2011).

[33] M.G. Rabbani, H.M. El-Kaderi, Template-Free Synthesis of a Highly Porous Benzimidazole-Linked Polymer for CO_2 Capture and H_2 Storage, Chemistry of Materials, 23 (2011) 1650-1653.

Ionic Liquids for carbon dioxide capture: Process selection

J. Albo, J.Cristóbal and A. Irabien, Departamento de Ingeniería Química y Química Inorgánica. E.T.S. de Ingenieros Industriales y Telecomunicación. Universidad de Cantabria, 39005 Santander, Spain. e-mail: alboj@unican.es

Abstract

Experimental values for the solubility of carbon dioxide in a number of ionic liquids have been included in a database for properties estimation. The highest CO_2 experimental absorption was found in a poly(ionic liquid) $_P$[[VBTMA][PF$_6$]], however the solubility can be enhanced by including tris(heptafluoroethy) trifluorophosphate [FEP] in the anion. An analysis of cation/anion structure in terms of the process separation performance is carried out.

Introduction

The main disadvantages of the well-known process of CO_2 capture from flue gas using monoethanolamine (MEA) are the high solvent losses due to their evaporation and energy requirements; therefore process intensification must be applied. The properties of Ionic liquids (ILs) make them strong competitors of conventional solvents [1]. The most widely used ionic liquids are those based on alkyl imidazolium (1-alkyl-3-methylimidazolium) [2,3] as it is believed that these ionic liquids provide good solubility at low pressures. Among the anions, those that arouse more attention are the fluorides such as hexafluorophosphate ($[PF_6]$) or bis (trifluoromethylsulfonyl) imide ($[Tf_2N]$) [4]. In this work, the solubility data reported in literature at a range of temperatures and pressures is discussed. Absorption process perform at high pressures may be of interest because the resulting CO_2 product must be compressed before transport to the final storage.

Methodology

It has been developed a database composed of CO_2 solubility experimental values reported in literature ranging from 0.014 to 70.242 wt% on a range of operating conditions from 0.09 to 946 bars and temperature from 5 to 300ºC. The number of different cations and anions in the database are 35 and 29 respectively, which leads to 1015 ionic liquid combinations. As there are potentially over one million simple ILs,

a group estimation method from the database permits evaluate which ILs reports higher solubility in terms of Henry´s law constant. To this end, data are subjected to linear regression in MATLAB. Descriptors are used as a function of the presence of different cation/anions and the result is normalized between -1 and 1 as showed in Figure 1. Cation (p-vinybenzyl)trimethylammonium [p-VBTMA] and fluorinated anions such as tris(heptafluoroethy)trifluorophosphate [FEP], (Tf$_2$N) and (PF$_6$
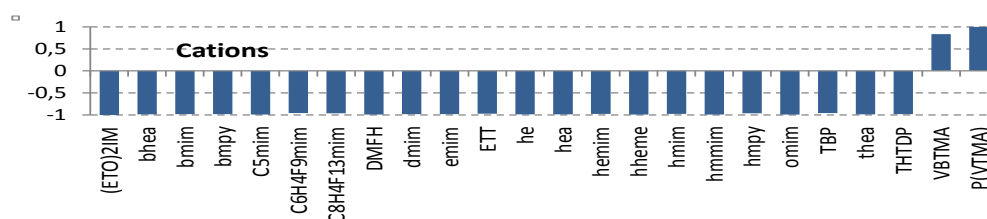
As can be seen, the CO_2 is less soluble in non-fluorinated anion [NO$_3$] and [DCA]. The highest solubility is reported with anions containing fluoroalkyl groups such as, [TFO] and [Tf$_2$N]. This effect is explained by favorable interactions fluoroalkyl-CO_2 and the increased size of the anion [5].

The effect of the cation selection on CO_2 solubility is less significant than the anion effect as it is shown in Figure 2b, in agreement with literature results [6]. It is observed that fluorinated cations produce a slight increase in the solubility value and the higher the number of fluorine groups, the higher its value, i.e: 1-methyl-3-(3,3,4,4,5,5,6,6,6-nonafluorohexyl)imidazolium ([C6H4F9mim]) and 1-(3,3,4,4,5,5,6,6,7,7,8,8,8-tridecafluorooctyl)-3-methylimidazolium ([C$_8$H$_4$F13mim]) case [7].

Temperature influence on solubility: Anion/Cation effect

CO_2 solubility decreases with increasing temperature. Again the cation selection is less significant in comparison to the anion selection. Solubility for some ILs i.e. [hmim][Tf$_2$N] and [bmim][BF$_4$] decreases approximately 35 % for a range of temperature of 65ºC when pressure is 1 bar. Besides, this negative influence is more evident at higher mole fractions of CO_2.

Process operating conditions

The exhausted gas in a coal-fired power plant exits the burner at approximately 370ºC and cooled to approximately 40ºC through the wet flue gas desulfuration device or a direct contact cooler (DCC) in order to avoid the negative effect of temperature in the absorber. CO_2 product at the end of the capture process must be compressed to approximately 130 bars before being transported [8]. Since absorption increases with pressure, is interesting to analyze solubility at this high operating pressure. Table 1 show the database values of two combinations of ILs with cation 1-butyl-3-methylimidazolium ([bmim]) and anions ([Tf$_2$N] and [PF$_6$]) in comparison to MEA at real operating conditions for absorption of CO_2 capture plants and in carbon dioxide transport to final storage [9].

Table1: CO_2 solubility at 40ºC and real process pressures

Solvent	Pressure	Solubility (wt%)	Ratio
MEA (22.7 wt%)		0.63[1]	
[bmim][PF$_6$]	1.2	0.11	5.72
[bmim][Tf$_2$N]		0.19	3.32
MEA (22.7 wt%)		1.15[1]	
[bmim][PF6]	130	0.89	1.29
[bmim][Tf2N]		1	1.15

[1] From Vrachnos et al., 2006 [10].

Conclusion

A database containing 1015 ionic liquid combinations has been developed for solubility estimation trough a group contribution method. The selection of the cation has result of less significance when designing a task-specific ionic liquid for CO_2 absorption. The inclusion of fluorinated groups such as [Tf$_2$N] and [PF$_6$] in the structure increase the solubility, although there are disadvantages associated with their use, such as high price and poor biodegradability.

A comparison of the use of MEA - ILs at real operating conditions has been carried out. CO_2 solubility at 130 bars pressure for selected ILs is very close to that value reported for MEA (1.15wt%), which means a similar circulation rate. Therefore ILs could become strong competitors of conventional solvents at high pressures. Further works will include a high number of ionic liquids combinations for a more robust database analysis.

References

[1] S. Supasitmongkol and P. Styrring, Energy Environ. Sci. 3, 1961-1972, 2010.

[2] S. Keskin, MS Thesis, Boğaziçi University, 2006.

[3] L.M. Galán Sánchez et al., Chem. Eng. Res. Des. DOI: 10.1205/cherd06124.

[4] A. Jalili et al., J. Chem. Thermodyn., 42, 1298–1303, 2010.

[5] C. Cadena et al., J. Am. Chem. Soc, CHEM. 126, 5300-5308, 2004.

[6] S. N. V. K. Aki et al., J. Phys. Chem. B, 108, 20355-20365, 2004.

[7] M. J. Muldoon et al., J. Phys. Chem. B, 111, 9001-9009, 2007.

[8] A.B. Rao and E.S. Rubin, Environ. Sci. Technol., 36, 4467-4475, 2006.

[9] D. Singh et al., Energ. Convers. Manage., 44, 3703-3091, 2003.

[10] A. Vranchos et al., Ind. Eng. Chem. Res. 45(14), 5148-5154, 2006.

Solubility of CO_2 in Functionalized Ionic Liquid

Subham Paul[a], Saravanamurugan Shunmugavel[b], Anders Riisager[b], Rasmus Fehrmann[b] Erling H. Stenby[a], and Kaj Thomsen[a]

[a]Center for Energy Resources Engineering, Department of Chemical and Biochemical Engineering, Technical University of Denmark, 2800 Kgs. Lyngby, Denmark

[b]Centre for Catalysis and Sustainable Chemistry, Department of Chemistry, Technical University of Denmark, 2800 Kgs. Lyngby, Denmark

Abstract

Ionic liquids can be promising candidates as absorbents in CO_2 removal, as some are quite stable even at temperatures greater than 573 K with negligible vapor pressure. There are many reports on CO_2 capture using common ionic liquids - typically referred to as first-generation ILs. The CO_2 capture ability for these ionic liquids is, however, limited due to relatively weak physi-sorption and absence of chemical absorption. Owing to this, task-specific ionic liquids have been developed which are able to make a chemical bond between CO_2 and functionalized ionic liquids at ambient conditions. It appears, however, that this type of bonding is too strong to make reversible absorption/desorption economic in technical scale.

In this work, the solubility of CO_2 in new functionalized ionic liquid is measured using a Rubotherm magnetic suspension balance (Rubotherm Präzisionsmesstechnik GmbH, Germany). Experimental results are presented for the total pressure above liquid mixtures of carbon dioxide and the ionic liquid for a temperature range from (298.15 to 323.15) K.

Pretreatment of synthetic sorbent for sequentially carbon dioxide capture

Stendardo S[1], Herce C[1,2], Calabrò A[1]

[1] ENEA, Italian National Agency for New Technologies,
Energy, and the Sustainable Development
Via Anguillarese, 301, S. Maria di Galeria, 00123, Rome, Italy

[2] Chemical Engineering Department, University of L'Aquila
Monteluco di Roio 67040 L'Aquila, Italy

Keywords: solid sorbent, carbon capture, carbonate chemical looping, pretreatment

In this study pre-treatment of synthetic solid sorbent for sequentially CO_2 capture has been analysed. The sorbents were synthesized by means of a CaO hydrolysis technique to generate sorbents with 75 and 85% of active phase CaO. The sorbents also contain a calcium aluminate phase acting as a binder of the active phase (CaO). Pretreatment was accomplished in a thermo-gravimetric analyser (TGA) exposed in an atmosphere of 86% N_2 and 14% CO_2 under 600 °C. The as-synthesised sorbent and the pretreated sorbent have been characterised by scanning electron microscope, nitrogen physisorption tests, and multi-cycling carbonation-calciation test in TGA (100 cycles). Here, the CO_2 uptake took place at programmed temperature (600 °C) in an atmosphere of 25/75 % CO_2/N_2 with two different conditions tested: a) severe condition: regeneration under 1000 °C, and b) mild condition: regeneration under 900 °C. In both cases the calcination atmosphere was composed of 86% N_2 and 14% CO_2 and 100 °C/min heating rate. The experimental results show significant improvement in the stability of the CO_2 uptake capacity over multiple cycles when comparing the synthetic sorbents to natural dolomite. Pretreated sorbents show a further increase in CO_2 uptake. For instance, for the 85% CaO synthetic sorbent an increase of 91% for the CO2 uptake has been found during the first cycle in the sequentially CO2 capture. After that the uptake decreases but still remains 64% above the uptake found for the as-synthesised sorbent up to the 50th cycle.

ADVANCED MEMBRANE DESIGN FOR OXYGEN SEPARATION

R. Kriegel, M. Schulz, K. Ritter, L. Kiesel, U. Pippardt, M. Stahn, I. Voigt

Fraunhofer Institute for Ceramic Technologies and Systems IKTS, Hermsdorf, Germany

Keywords: *membrane technology, oxygen separation, mixed ionic electronic conductors*

1   Introduction

High temperature O_2 separation using MIEC (Mixed Ionic Electronic Conductor) membranes is an energy-efficient alternative to cryogenic air separation, but the different level of development complicates a reliable assessment of this preindustrial technology regarding energy demand, capital and operation costs. A competitive oxygen production using high temperature membrane separation is proposed for a minimal flux of 10 ml_STP/(cm$^2 \cdot$ min) [1, 2]. The oxygen permeation of MIEC membranes depends on the membrane thickness but also on operation conditions, e. g. on temperature, gas velocities, overpressure of feed air and vacuum pressure [3] used for O_2 extraction. A minimal oxygen production rate per volume unit seems to be much more meaningful for economic assessment, because of the direct correlation to the investment costs for an industrial plant. Besides, different membrane designs are entailed by special drawbacks, e. g. fragile construction, high local stresses, big joining areas and the risk of leakages, high pressure drops entailed with energy losses and so forth.

2   Oxygen permeation of different membrane designs

Three different membrane designs based on BSCF were manufactured and characterized regarding oxygen permeation, The geometric dimensions of a monolithic tube, an asymmetric membrane tube and a thin-walled capillary are summarized in Table 1. Fig. 1 showing a SEM picture of the asymmetric BSCF membrane and a capillary bunch joined with machined BSCF pellets. The total leakage of the asymmetric membrane tube was measured to be $1.7 \cdot 10^{-1}$ mbar $\cdot$ l/s.

Oxygen permeation measurements were carried out with a special experimental setup designed for a fast comparison of the performance of different oxygen membranes. Com-

Table 1: Dimensions [mm] of BSCF ($Ba_{0.5}Sr_{0.5}Co_{0.8}Fe_{0.2}O_{3-\delta}$) membranes used for O_2 permeation tests

membrane type	outer diameter	wall thickness	length
monolithic tube	14.2	1.5	250
asymmetric tube	14.4	1.4	250
capillary	3.20	0.25	250

mercially available cable glands were used to seal the open cold ends of the sample tubes outside the furnace. The internal space of each membrane was evacuated by a vacuum pump and heated up to the measuring temperature. The vacuum level and the associated driving force was changed stepwise at high temperature using a pressure regulating valve. The isothermal zone at the closed end of the membrane was approximately 15 cm long. The total O_2 flux was determined after the vacuum pump using a mass flow meter and oxygen sensors. Air was used as feed gas at environmental conditions. Normalization to the hot working membrane area was realized using a comprehensive data set for BSCF flat

membranes determined with another test rig, as was recently described [4].

Total and normalized O_2 fluxes of the three different membranes depending on the driving force are depicted in Fig. 2. Obviously, the asymmetric membrane possess the highest O_2 flux 4.3 times higher in comparison to the monolithic tube. Although the total O_2 flux of the capillary is the smallest because of their limited dimension, the normalized O_2 flux is located relatively close to the asymmetric membrane, especially at a low driving force. The apparent loss at higher driving forces is caused by the pressure drop inside the narrow capillary afar from the pressure sensor. It has to be noticed that an energy efficient vacuum operation is limited to vacuum pressures above 50 mbar [5] and low driving forces below 1.4.
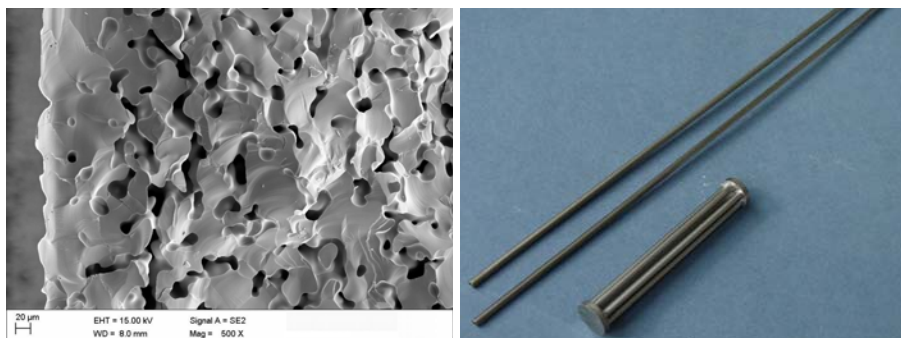
Fig. 1: Left: SEM picture of the cross section of an asymmetric BSCF membrane; Right: Capillaries and a RAB joined capillary bunch (10 cm length)
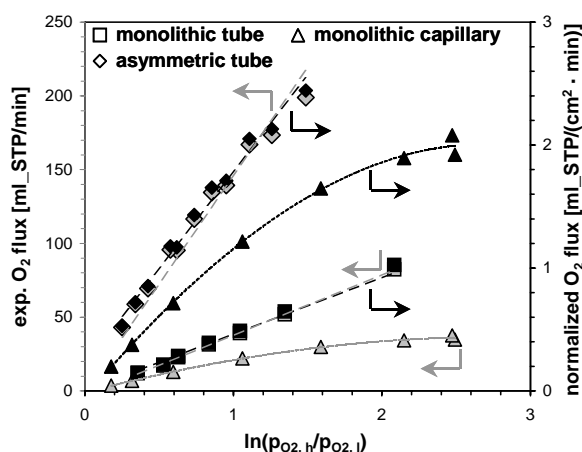
Fig. 2: Oxygen flux through different types of BSCF membranes at 850 °C, environmental air outside, vacuum inside

3 Advanced membrane design

Oxygen production in pilot scale using monolithic tubes [5] and hollow fibers [6] was already proven. However, an energy efficient oxygen production requires high membrane areas per volume unit, but also low pressure drops. This results in gas velocities below 10 m/s in contrast to 25 m/s postulated in [2].

Two advanced membrane designs with a high membrane area per volume are depicted in

Fig. 3: CAD drawings of a capillary bunch and a stack of planar cells supported by O_2 withdrawal tube

Fig. 3. It has to be noticed that a decreasing inner diameter of a capillary or hollow fiber is entailed by a growing pressure drop, especially at low pressures. This is also true for planar cell stacks developed by Air Products & Chemicals aimed at a production rate of 1 ton per day [7]. A promising alternative to the concepts shown in Fig. 3 is the development of multi-channel honeycombs, but up to now feasibility in pilot scale was not shown.

4 Mechanical stress depending on membrane design

Production of pure O_2 using MIEC membranes always needs an oxygen partial pressure gradient usually accompanied by a absolute pressure difference. Therefore, mechanical stress

inside a working membrane could be critical for its mechanical integrity, especially for filigree membrane designs. Moreover, remarkable creeping at high temperatures was described by different authors for BSCF [8, 9] seems to be critical for application due to the narrowing of small channels with time.

Table 2: Geometry [mm] of BSCF membranes used for simulation of mechanical stress for 0.05 bar O_2 to 1, 5, 20 bar air at 850 °C

membrane type	outer dimensions	wall thickness	comments
monolithic tube	10.0 outer Ø	1.0	5 %, 10 % out of round
Capillary	3.5 outer Ø	0.25	
planar cell	100 x 100	0.5	2 mm prop with 10 and 3 mm distance

Therefore, mechanical stress was calculated using the software COMSOL for membranes and conditions summarized in Table 2. The maximal tensile stress depending on outer pressure is depicted in Fig. 4. As expected, the highest values were observed for planar membranes, especially at the higher prop distance located above the upper limit of the diagram. The stress of the thin-walled capillary is a little bit higher compared to the monolithic tube.

Apart from mechanical loads stress can be induced by crystal lattice expansion caused by different local oxygen stoichiometry [10, 11]. Fig. 5 contains the oxygen stoichiometry at the membrane surfaces calculated by a semi-empirical defect model [12]. Although the oxygen stoichiometry increases with air overpressure, the difference to the permeate side is always low, independent on the membrane geometry. However, the chemically induced tensile stress is high compared to the mechanical stress shown in Fig. 4 with the exception of the disadvantageous planar membrane. According to the works mentioned chemically induced stress dominates the whole stress situation even for the mild conditions of oxygen production from air. All together, total stress is much higher for planar membranes compared to tubular ones and is in the range of fracture stress [13]. Besides, tensile stress

Fig. 4: Maximal first principle mechanical stress at 850 °C depending on outside pressure (50 mbar inside) for tubes, capillaries with different out of roundness and planar membranes with different distance of supplying props
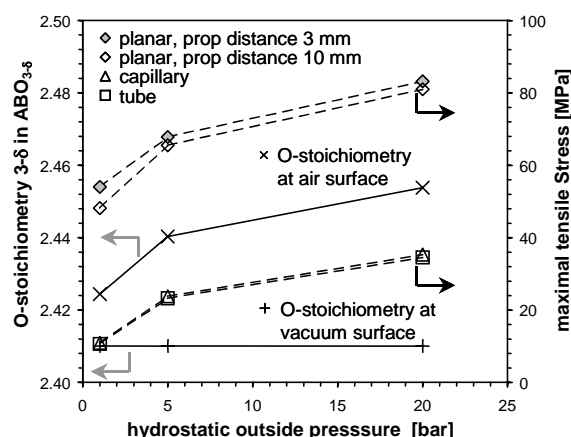
Fig. 5: Oxygen stoichiometry of BSCF and chemical induced stress at 850 °C for tube, capillary and planar membranes with different distance of supplying props

of tubular membranes working with overpressure from the outside can be minimized close to zero by perfection of roundness.

5 Economic aspects of membrane production

An estimation of material requirements, oxygen flux and production costs for different membrane designs based on BSCF is summarized in Table 3

	archetype	unit	tube	19 capillary bunch	stack with 100 cells
Table 3 Material requirement, oxygen flux and production costs of different membrane designs					
components and material	dimensions	[mm]	10 x 8	3.5 x 3[1]	100 x 100 x 1.5[2]
	component active length [mm]	[mm]	1000	500	600
	membrane area [cm^2]	[cm^2]	283	970	16000
	material solid volume	[cm^3]	28,3	25	1280
	component mass	[kg]	0.150	0.133	6.784
	number of membrane components		353.357	103.093	6.250
	total mass	*[kg]*	*53.000*	*13.660*	*42.400*
O$_2$ flux	per component[4]	[ml_STP/min]	194	2000	20180
	total oxygen flux	*[10^{3}kg/day]*	*141*	*424*	*259*
reactor	distance between components	[mm]	6	6	20
	reactor volume	*[m^3]*	*13.5*	*6.7*	*8.0*
costs	raw material[4]	k€	10.600	2.730	8.480
	capital, depreciation[5]	k€	1.000	1.360	950
	production, personnel	k€	1.300	1.310	4.570
	total[5] sum for 10.000 m^2	k€	12.900	5.400	14.000
	membrane costs[6] per ton O$_2$	**[€/10^{3}kg O$_2$]**	**50 €**	**7 €**	**30 €**

[1]capillary distance 1.5 mm; [2]membrane thickness 0.5 mm, cell height 1.5 mm, prop width 2 mm, prop distance 3 mm, vertical cell distance 4 mm, [3]at ln(p$_{O2}$) = 1, 850 °C; [4]150 €/kg and 25 % rejection rate; [5]5 years, [6]per year

Obviously, the total O$_2$ flux of capillary bunches is the highest one compared to the other membrane designs because of the lowest self-supporting membrane thickness reached for this design. The high package density results also in a minimized reactor volume. According to the high cost fraction of the raw material BSCF dominating the total production costs, thin-walled capillary bunches seems to be the most economic choice. All together, the membrane production cost per ton O$_2$ seems to be competitive regarding an averaged price of 23 to 30 € per ton O$_2$ produced by an industrial cryogenic air separation plant. Besides, it has to be noticed that the oxygen production rate could be significantly enhanced using higher pressure differences.

Capillary bunches will be much more stable than planar cell stacks comparable regarding volume density and oxygen flux. Further flux enhancement could be realized by asymmetric membranes together with advanced membrane designs but an economic assessment is questionable because of the coating effort presently uncertain.

References

[1]   Bredesen, R., Sogge, J., Seminar on the Ecological Applications of Innovative Membrane Technology in the Chemical Industry, 1996
[2]   Vente, J., Haije, W.G., IJpelaan, R., Rusting, F.T., J. of Membr. Sc., 278 (2006) 66-71
[3]   Kriegel, R., Burckhardt, W., Voigt, I., Schulz, M., Sommer, E., Proc. 10. ICIM, 18.-22.08.2008, Tokyo, Japan, ISBN 978-4904353-01-1
[4]   Schulz, M., Kriegel, R., Kämpfer, A., J. Membr. Sc., in press
[5]   Kriegel, R., in: J. Kriegesmann (Ed.), DKG Handbuch, 119. Delivery complement, 11/2010, Chapter 8.10.1.1, pp. 1-46
[6]   Tan, X., Wang, Z., Meng, B., Meng, X., Li, K., J. Membr. Sc. 352 (2010), 189–196
[7]   Carolan, M.F., van Stein, E.E., Armstrong, P.A., Jülicher Werkstoff-Kolloquium, Jülich 2009
[8]   Yi, J., Bouwmeester, H.J.M., Lein, H.L., Grande, T., Proc. 10. Intern. Conf. Inorg. Membr., Tokyo 2008
[9]   Rutkowski, B., Malzbender, J., Beck, T., Steinbrech, R.W., Singheiser, L., J. Europ. Cer. Soc. 31 (2011) 493–499
[10]   Schulz, M., Kriegel, R., Kaps, Ch., 1St Intern. Conf. on Ceramics, Toronto, Kanada 2006
[11]   Schulz, M., PhD thesis, Bauhaus University, Weimar 2010
[12]   Kriegel, R., Kircheisen, R., Töpfer, J., Sol. St. Ionics 181 (2010), S. 64 – 70
[13]   Huang, B.X., Malzbender, J., Steinbrech, R.W., Singheiser, L., J. Membr. Sc. 359 (2010) 1-2, 80-85

Testing of nanostructured gas separation membranes in the flue gas of a post-combustion power plant

M. Bram, K. Brands, W.A. Meulenberg, H.P. Buchkremer, D. Stöver

Forschungszentrum Jülich GmbH, D-52425 Jülich, Germany;

G. Göttlicher, EnBW Energie Baden-Württemberg AG, D-76131 Karlsruhe, Germany;

J. Pauls, Helmholtzzentrum Geesthacht, D-21502 Geesthacht, Germany

Nanostructured gas separation membranes are promising candidates for the separation of CO_2 from the flue gas of fossil power plants. Well-defined atomic structures in the range of a few Angstrom are required to separate CO_2 from N_2 in existing post-combustion power plants and H_2 from CO_2 in prospective integrated gasification combined cycle (IGCC) power plants. Today, CO_2/N_2 and H_2/CO_2 gas separation with membranes has been demonstrated mainly on a laboratory scale, while less is known about membrane performance and stability under real conditions. To extend the state of knowledge, a test bed was put into operation in the flue gas stream of a hard-coal-fired power plant (EnBW Rheinhafendampfkraftwerk, Karlsruhe), which enabled the long-term functional test of ceramic as well as polymer gas separation membranes for up to 1100 hours. For the first time, a CO_2 enrichment from 12 Vol. % in the flue gas to 57 vol. % in the permeate of a polymer membrane was demonstrated. Due to operating this membrane in direct contact with flue gas, the flow rate was reduced from 0.86 $m^3/m^2 \cdot h \cdot bar$ to 0.07 $m^3/m^2 \cdot h \cdot bar$ within the first 400 hours. This reduction was mainly caused by the deposition of ash particles and gypsum suggesting the need of developing effective membrane protection strategies. In addition, ceramic membranes were tested under the same conditions. Even if demonstration of CO_2 gas separation with ceramic membranes requires further modifications of the membrane materials, the long-term exposure in the power plant led to first results regarding adherence of functional layers and chemical stability.

Polymer Membranes for Separation of CO_2 - An Overview

Volker Abetz, Torsten Brinkmann, Sergey Shishatskiy, Jan Wind
Institute of Polymer Research, Helmholtz-Zentrum Geesthacht
Max-Planck-Str. 1, 21502 Geesthacht, Germany

History

The possibility for small molecules to pass through a wall made of solid material is known since middle of the 19th century when Graham has formulated his law of diffusion. The first implementation and consideration of use such membranes in real life were done already in the middle of 20th century when van Amerongen and Barrer carried out systematic investigations of gas transport through polymers. The next breakthrough was achieved by Loeb and Sourirajan in 1961 by development of the anisotropic membrane formation process suitable for continuous membrane production in industrial scale.

Since then many big players in the field of industrial chemistry have developed a number of membranes and membrane separation units suitable for various separation tasks. The interest to membrane separation increased with the development of the "resistance model" for the multicomponent membranes which opened efficient methods to cure defects of the thin separation layer.

The era of the industrial membrane gas separation have been started when Monsanto installed (1977) the Prism membrane system in a commercial-size plant for the H_2/CO separation and in 1980 have announced its commercial availability.

But the first patent related to membrane gas or vapour separation was filed as early as in 1936 on the topic of concentration of desired organic compounds from mixtures of gases by separation through the film or diaphragm such as a thin sheet of rubber.[1]

Background

Polymeric membranes utilize the ability of the gas molecule to be dissolved in the polymer and diffuse through the polymer bulk. All membrane processes of gas or vapour separation use partial pressure difference on the feed and permeate side of the membrane. Due to the difference in the ability of polymer matrix to dissolve gas and vapour molecules and ability of dissolved molecules to diffuse by jumping from one free volume void to another the separation of gas and vapour mixtures occurs. Diffusion primarily depends on the size of the penetrant and is generally independent on pressure applied to the membrane. The solubility of gas in polymer on the contrary strongly depends on the pressure and changes according to the gas condensability.

Polymers can be roughly divided into two major groups by their state under separation conditions: glassy polymers with the glass transition temperature T_g higher than the temperature under separation conditions, and rubbery polymers with T_g lower than the temperature of the media under separation. Glassy polymers with the "frozen" free volume separate small molecules mostly according to their kinetic diameter and rubbery polymers according to gas or vapour condensability.

Polymeric membranes in industrial applications

Over the last 60 years, since the pioneering work of Barrer, thousands of polymers were tested for their gas and vapour separation properties. However, just a few of them have found their way to industrial production.[2] Table 1 summarizes polymers and their applications as membranes.

CO_2 separation from natural gas was one of the first applications of a gas separation membrane (1981, CO_2, H_2S separation form natural gas by Delta Engineering Corp.) and still is the most developed membrane based gas separation technology. Large plants for natural gas sweetening were installed by UOP (Separex), Cynara, Kvaerner, US Air products, Ube utilizing membranes made of glassy polymers: cellulose acetate, polyimides, polyaramide, polysulfone packed in spiral wound (CA) and hollow fiber modules.

Until 2004 there was no information on the interest to separate CO_2 from its mixtures with nitrogen except from one case: reduction of the CO_2 emission on the off-shore platforms in Norway. Kvaerner in cooperation with GORE has pilot tested a membrane contactor system based on the GORE-TEX membrane and reported it to public as early as 1998 [3]. But since the Kyoto protocol the problem of carbon sequestration and storage (CSS) became very sound and

research in this area is well funded. As a result at least two new membranes have been developed and pilot scale tests started.

MTR developed a thin film composite membrane (TFCM) based on a Pebax® polymer which is commercialized under the trade name Polaris®. The membrane is packed into spiral wound modules and has been tested for the treatment of off-gases of Redhawk natural gas power plant providing production/capture of 1 ton CO_2 per day.

HZG (previously GKSS) took part in the Helmholtz-Allianz MEMBRAIN "Gas separation membranes for zero-emission fossil power plants" and has developed the TFCM based on Polyactive®. As Pebax®, Polyactive® is a poly(ethylene glycol) containing multiblock copolymer. The membrane is produced in pilot scale and samples were tested under off-gas conditions in the coal powered Rheinhafen-power station (Karlsruhe).

Sweetening and conditioning of biogas to the pipeline standards can be done by either rubbery of glassy polymer based membranes depending on the raw material composition. In many cases the selectivity of the existing membranes is not high enough for an energy efficient separation and therefore the development of new membrane materials continues for this purpose.

Future

There seems to be a natural border for the CO_2/N_2 selectivity (Figure 1). During the last 10 years development of new polymeric and hybrid organic/inorganic materials allowed to push up the CO_2 permeability while the selectivity does not exceed 90. Research groups around the globe study ways to solve the problem by incorporation various materials into the polymer matrix.

Mixed matrix membranes comprising two separation materials: inorganic porous particles embedded into a selective polymer matrix were suggested [4] as a possible way to combine the good mechanical but poor separation properties of polymers and excellent selectivity provided by porous inorganic materials. During the last 10 years this approach was widely acknowledged by the scientific community. Various porous materials were tested including zeolites, carbon molecular sieves (CMS), metallo-organic frameworks (MOF), zeolitic imidazolate frameworks (ZIF). To our knowledge, unfortunately none of these approaches led to reliable and processable membranes to date.

Carbon molecular sieves in the form of flat sheet membranes or hollow fibers can be mentioned here as well as an emerging membrane type since polymers are used as a precursor. A number of groups have demonstrated outstanding properties of CMS membranes for CO_2 separation (e.g. M.B.Hägg [5]) but the application of these membranes is hindered due to the brittleness of the material.

Active transport of sour gases and CO_2 in particular has been intensively studied for at least 20 years.[6] Various active groups as $-NH_2$, $-NH_3^+X^-$, or polyacids were incorporated into polymers chemically or by blending. Some of these systems have shown very encouraging results but experienced problems like loss of activity or desalting. If these problems will be overcome, it can be expected that for applications with a low pressure difference such as treatment of the off-gas active transport membranes will find the way to the market.

References:

1. F. E. Frey "Process for concentrating hydrocarbons", U.S. Patent 2,159,434 filed June 27, **1936**
2. P. Bernardo, E. Drioli, G. Golemme "Membrane Gas Separation: A review/State of the Art", *Ind. Eng. Chem. Res.* **2009**, *48*, 4638-4663
3. O. Falk Pederson, H. Dannstrom, M. Gronvold, D. Stuksrud, O. Ronning, "Gas Treatment Using Membrane Gas/Liquid Contactors" 5th International Conference on Greenhouse Gas Control Technologies, Cairns, Australia, August 13-16 (2000)
4. S. Kulprathipanja, R. W. Neuzil, N. N. Li, "Separation of Fluids by Means of Mixed Matrix Membranes," U.S. Patent No. 4 740 219 (1988)
5. X. He,M.-B.Hägg, "Hollow fiber carbon membranes: Investigations for CO_2 capture", *J. Membr. Sci.,* in press, available online 9 November **2010**
6. A. Hussain, M.-B. Hägg, "A feasibility study of CO_2 capture from flue gas by a facilitated transport membrane", *J. Membr. Sci.* **2010**, *359*, 140–148

Table 1. Polymers used for industrial membrane production to this date

Polymer	Membrane type	Applications	Company
Poly(phenylene oxide)	As [*)	O_2/N_2	Aquillo, Parker-Hannifin UBE
Polysulphone	As	H_2/N_2 (H_2/CH_4, H_2/CO) CO_2/CH_4	Permea (Air Products)
Polyaramid	As	O_2/N_2	MEDAL (Air Liquide)
Polyimide	As	O_2/N_2 H_2O/Air $H_2/(N2, CO, C_{1+})$	MEDAL (Air Liquide) IMS (Praxair) UBE
Poly(4-methylpentene-1)	As	O_2/N_2	Dow
Cellulose Acetate	As, TFCM [*)	CO_2/CH_4	Separex (UOP) Dow Envirogenics GASEP
Ethyl Cellulose	As, TFCM	CO_2/CH_4	GKSS/HZG
Poly(dimethyl siloxane)	TFCM	VOC/Air O_2/N_2	GKSS/HZG MTR Permea UOP General Electric
Poly(vinyl trimethyl silane)	As	O_2/N_2	USSR
Polycarbonate	As	O_2/N_2, H_2/N_2, H_2/CH_4	Generon
Tetra bromo polycarbonate	As	O_2/N_2	Generon (MG) DOW
Teflon AF	TFCM	VOC/perm. Gas O_2/N_2	MTR, CMS
PEBAX	TFCM	CO_2/N_2, CO_2/CH_4	MTR GKSS/HZG
Polyactive	TFCM	CO_2/N_2, $CO_2/Biogas$	GKSS/HZG

AS – Asymmetric membrane; TFCM – Thin film composite membrane
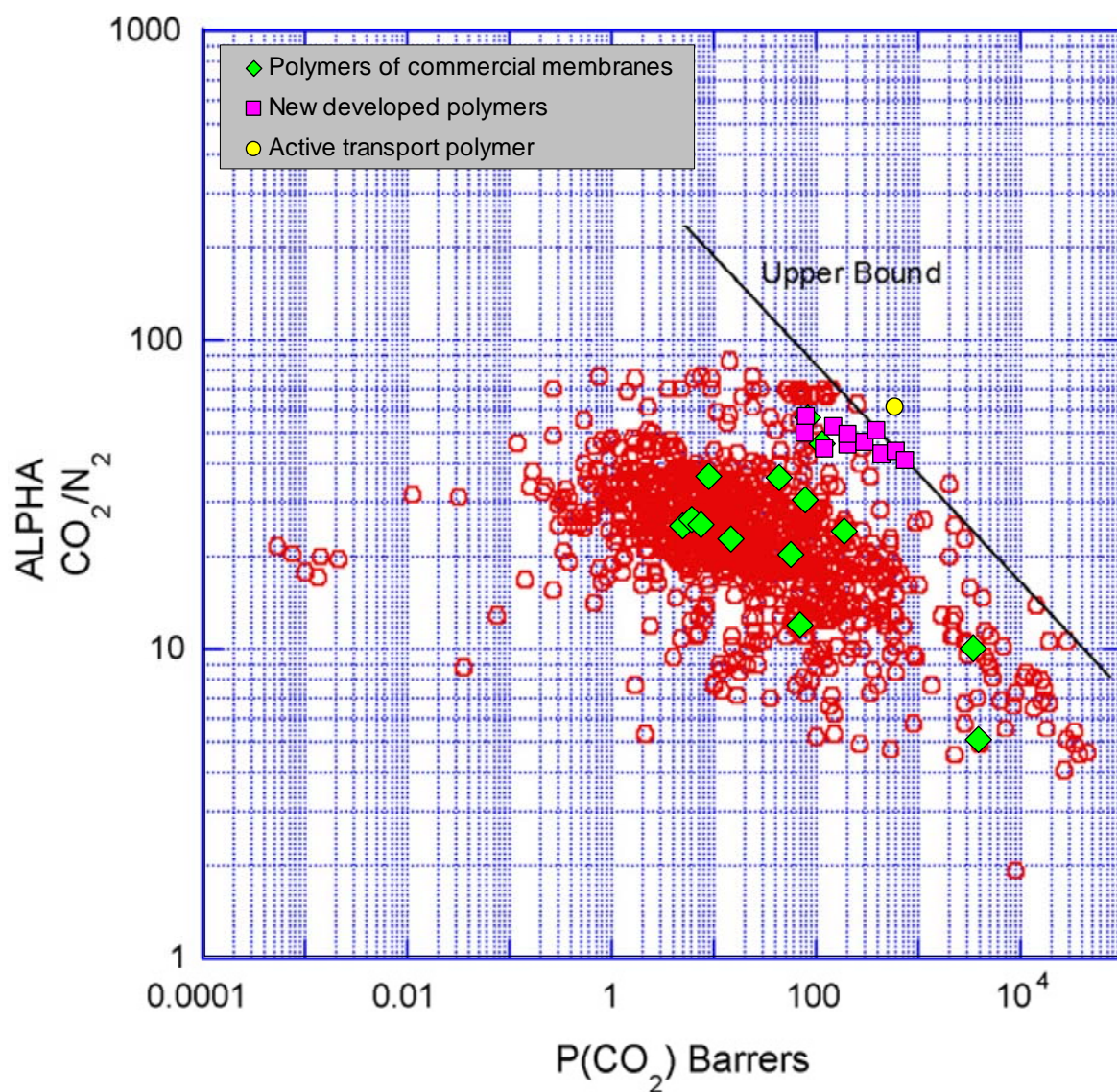
Figure 1. Robeson (2008) plot of CO_2/N_2 selectivity vs CO_2 permeability coefficients with polymers of commercial membranes marked green. New polymeric materials developed in frames of MEMBRAIN project are shown in pink and yellow.

IONIC LIQUID COATED ZEOLITE –PDMS MIXED MATRIX MEMBRANE FOR GAS SEPERATION

Muhammad Hussain, Chair of Separation Science and Technology Uni-Erlangen, Erlangen, Germany, Prof. Dr. Axel König , Chair of separation Science and Technology Uni- Erlangen, Erlangen, Germany

1. INTRODUCTION:

It is well known that both high permeability and selectivity are desirable in membrane processes. For example high selectivity leads to more purity in the product gas and high permeability requires a smaller membrane area, which leads to lower costs for membrane units. However, the achievement of both benefits at a time has turned out to be a difficult challenge.

In order to overcome this limitation, the idea of mixed-matrix membranes (MMMs) came up by combining both the polymer and the filler that have properties above the upper bound line of the Robeson Plot [1]. These fillers are molecular sieves, such as carbon molecular sieves (CMS) or zeolites. Especially the latter one can provide higher permeability and selectivity, due to their specific sorption and shape selective properties. Kulprathipanja et al. [2] were pioneers in the study of zeolite-polymer mixed-matrix membranes in 1980s.

Although MMMs offer advantageous opportunities compared to pure polymer or molecular sieve membranes although there have been obstacles concerning modeling of MMMs. As in many publications reported, the observed permeabilities are higher than the ones predicted by the Maxwell model. Moreover, that difference rises with increasing filler fraction. Mahajan R. and Koros W. [3] explained that this phenomenon occurs due to the poor contact between the zeolite and polymer phase, which leads to de-wetting of the polymer chains. As a result, that non-binding interface forms a gap, where the gas could easily pass through instead of penetrating through the zeolite phase. This could explain the higher apparent permeabilites and sometimes leads to the same selectivity as of the pure polymer. Mahajan et al. has determined the size of the gap by using modeling studies. The value was around 260nm.

Ionic Liquids (ILs) are defined as a diverse group of salts, which are in molten (liquid) state under 100°C [4]. Several advantageous properties of ILs as for example their thermal and chemical stability, beneficial viscosities, negligible vapor pressure and high solubility's for various substances makes them attractive for supported Ionic Liquid membranes (SILMs) in gas separation processes [5].

In this work, [EMIM]Tf2N and [EMIM]TfO (which will often be abbreviated in this work as Tf2N and TfO for convenience), are applied primarily as zeolite-coatings in order to reduce or

even fill the interfacial inorganic-organic void.

2. Experimental:

2.1 Membrane synthesis Procedure:

Primarily the synthesis process can be classified into zeolite coating, polymer filling and membrane casting. The main component of each membrane is PDMS next to IL-coated ZSM-5 serving as the Filler. The mass fractions of these ILs on Zeolite are 10 wt%, 20 wt% and 30 wt%. Afterwards the coated filler was blended in different mass fractions 17 wt%, 38 wt% and 57 wt% into PDMS. Following labeling system has been adopted to explain the coating and filling process: [IL-ω_{Coat}-ω_{Fill}-gas]. For example, the Nitrogen experiment on a 17 wt% filled membrane with 10 wt% [EMIM] [Tf$_2$N] coated zeolite is described as: [Tf$_2$N -10wt%-17wt%-N$_2$].

2.2 Gas permeation measurements:

The pure gas permeability has been measured using a constant volume variable pressure apparatus. The gas permeability was measured by the following (Eq.(1)):

$$P_o = \frac{\delta_M}{A_M(p_{iF} - p_{ip})} * \frac{V}{RT} * \frac{dp_{iF}}{dt} \tag{1}$$

The permeability P_o is reported in „Barrer"(10^{-10}cm^3 (STP) cm cm^{-2} s^{-1} cmHg^{-1}).

$\frac{dp_{iF}}{dt}$ feed pressure change (bar) of component i with time (t), **T** is the operational temperature (K), **R** is the universal Gas constant, **V** is the volume of the autoclave (1.4 litre), A_M is the active permeation area of membrane(51.5 cm^2), δ_M is the thickness of the membrane, and $(p_{iF} - p_{ip})$ is the partial pressure difference between feed side and the permeate side of component i.

$$\alpha_{A/B} = \frac{P_A}{P_B} = \frac{D_A}{D_B} * \frac{S_A}{S_B} \tag{2}$$

The ideal selectiviy $\alpha_{A/B}$ is the ratio of permeability coefficient of component A and B. While **D$_A$, S$_A$** and **D$_B$, S$_B$** are the solubility and diffusivity coefficients of individual components.

For mixture of gases permeate and retantate flow rates were measured by using bubble flow meters. Gas chromatogram (G-1530A) was used to measure permeate and feed side compositions.

2.3 Polymer - IL penetration Model:

It has been presumed that the gas permeates alternately through the polymer and IL-phase, without any interaction with the zeolite phase. Due to this binary path, the Maxwell model can

be applied, considering the permeability of IL as the particle or filler permeability (P_{Fil}) and the polymer permeability (P_{pol}) as the continuous phase permeability. Still zeolite component must not be neglected; its volume (V_{Zeo}) contributes to the overall filler volume fraction ϕ_{Fil} in equation (3).

Overall coated filler volume (V_{Fil}) is the sum of volume of zeolite (V_{Zeo}) and volume of IL (V_{IL}) whereas overall volume of the MMM (V_{MMM}) is the sum of volume of polymer(V_{Pol}), volume of zeolite (V_{Zeo}) and volume of IL (V_{IL}).

$$\phi_{Fil} = \frac{V_{Fil}}{V_{MMM}} = \frac{V_{Zeo} + V_{IL}}{V_{Pol} + V_{Zeo} + V_{IL}} \tag{3}$$

$$P_{Membrane} = P_{Pol} \cdot \frac{P_{Fil} + 2P_{Pol} + 2\phi_{Fil}(P_{Fil} - P_{Pol})}{P_{Fil} + 2P_{Pol} - \phi_{Fil}(P_{Fil} - P_{Pol})} \tag{4}$$

3. Results and Discussion:

3.1 Thermogravemetric Analysis (TGA):

The TGA has been applied to detect the quality of IL-coating on zeolite. The system is stable till ~240 °C .Optimal coating means no IL decomposition or evaporation during the coating process. This would lead to respective weight loss of IL from IL coated zeolite. Fig. 1 shows the weight-loss curves for Tf_2N coated zeolites, containing each coating level i.e. 10% ,20% and 30% respectively. It can be seen, that the overall weight losses are a bit higher than the corresponding coating levels. This can be explained by the strong solubility property of IL, especially for diverse components like water from the atmosphere and also presence of acetonitrile (coating solvent) cannot be neglected.
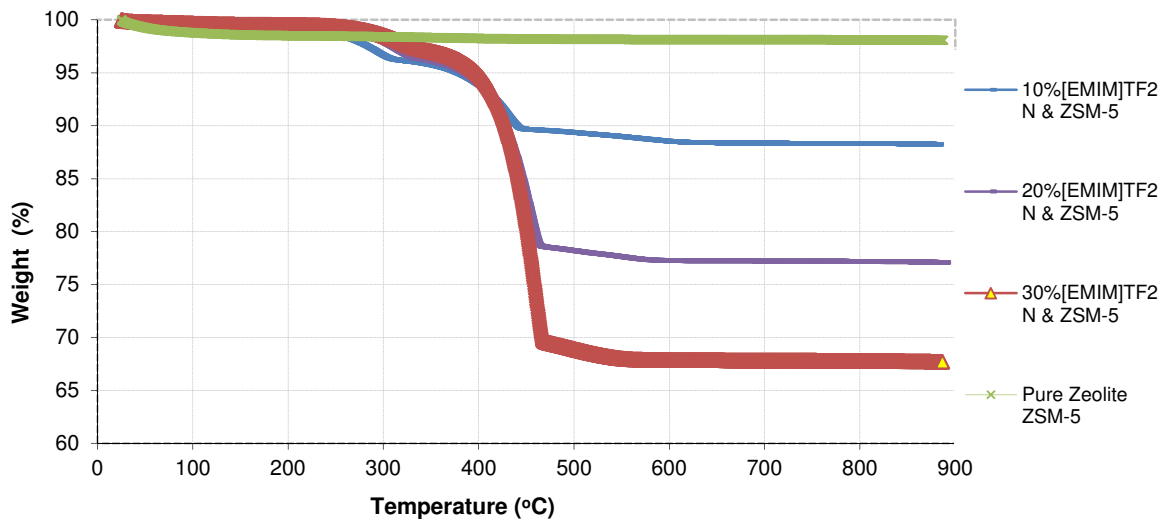
Fig. 1: **Weight-loss curve of [EMIM]Tf2N coated ZSM-5 zeolite**

3.2 Permeability and Selectivity Results and Discussion:

An overall decrease in permeability for each gas has been observed with increasing coating or filling level. The trend is shown in Fig. 2 for the experiments [Tf$_2$N-allwt%-56wt%] (allwt% stands for every variation of IL coating weight fractions). In case of [Tf2N-30wt%-38wt%] membranes, there is hardly a decrease in permeability compared to the 20 wt% IL-coated equivalents. Therefore, no more investigation in less filled membranes of those coating-sets occurred.
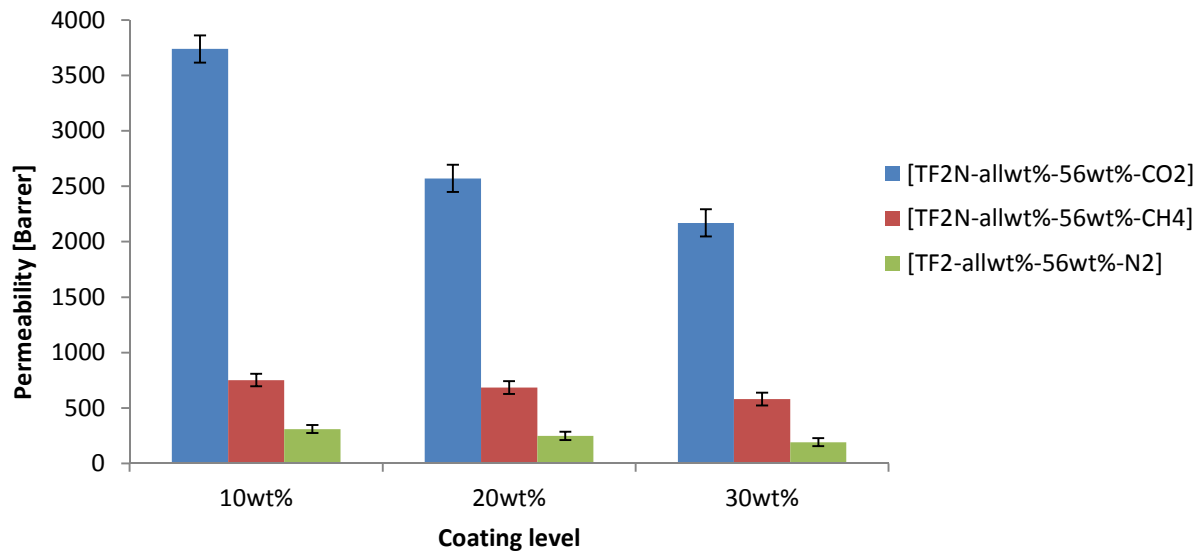
Fig. 2: **Permeability decrease with increasing coating level in [TF2N-allwt%-56wt%-all gases]**

No remarkable trend in selectivity with increasing coating or filling level for all gas pairs has been observed. Thus, the average selectivity factors for all gas pair combinations are summarized in the following table 1:

Table 1: Averaged selectivity factors for all gas pairs

	α_{CO_2/N_2}	α_{CO_2/CH_4}	α_{CH_4/N_2}
TfO-membranes	8,8	3,4	2,7
Tf$_2$N-membranes	10,7	4,0	2,7

3.3 Modeling results:

Equations (3) and (4) have been used to determine the modeling results. Fig 3 shows modeling and experimental permeability values as a function of filling level. The importance of the appropriate coating level has been demonstrated with [Tf$_2$N-10wt%-allω_{Fill}-N$_2$] and [Tf$_2$N-20wt%-allω_{Fill}-N$_2$] for instance. Due to approximately equal model results for 10 wt%

and 20 wt% coating, they have been averaged in Fig. 3.
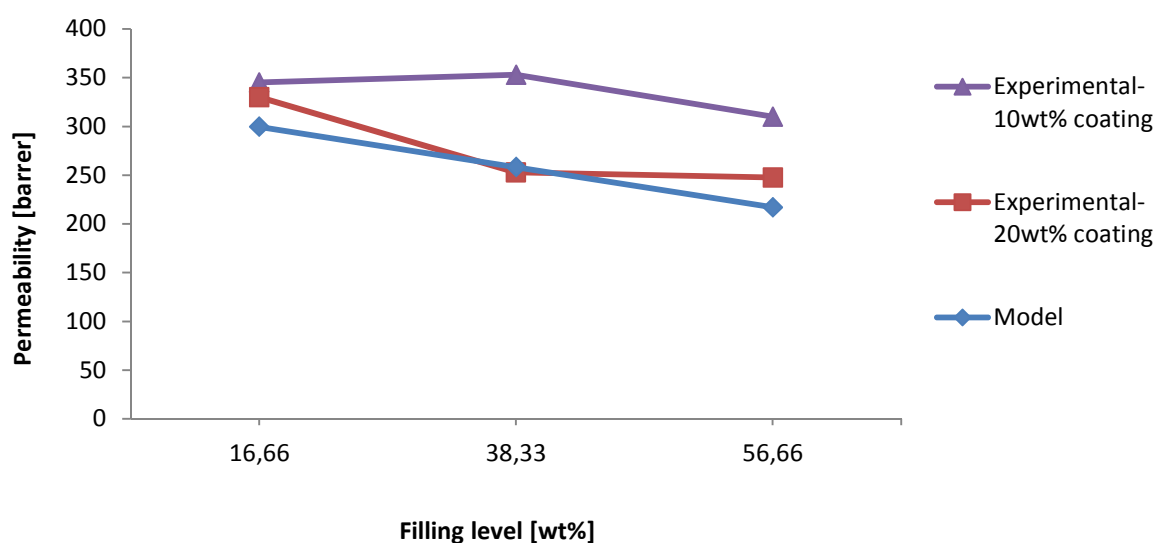
Fig. 3: **Comparison of [Tf$_2$N-10wt%-allω$_{Fil}$-N$_2$] and [Tf$_2$N-20wt%-allω$_{Fil}$-N$_2$]**

Best model fitting has been observed for methane in case of both ILs, where both $\Delta P_{20wt\% \text{ TFO}}$ and $\Delta P_{20wt\% \text{ Tf2N}}$ reach 4,8%, as shown in Fig. 4 for 20wt% TfO-coated filler in PDMS.
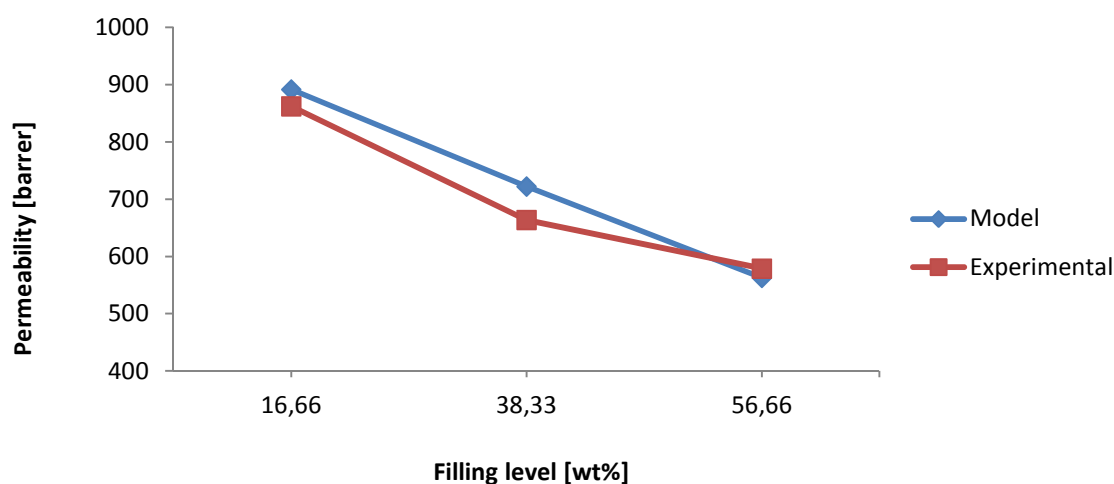
Fig. 4: **Best model fitting with [TFO-20wt%-allω$_{Fil}$-CH$_4$] membrane**

4. CONCLUSIONS:

In this work the inorganic-organic void interface has been closed using ILs. The quality of IL coating on zeolite surface has been evaluated using TGA results that show the ILs are well distributed during the coating process.

A decrease in permeability has been observed with both; by increase in coating of IL on zeolite surface and by increase in filling levels of the coated zeolite in PDMS. Moreover, no appreciable change in selectivity has been observed.

The Polymer-IL penetration model may provide reliable permeability predictions. The modeling results were mostly close to the experimental values at 20wt% coating. Moreover, that agreement occurred especially for all results for methane with deviation values up to $\Delta P20wt\%=4,8\%$ for [EMIM]Tf$_2$N coated fillers.

References:

1. Robeson, L.M., *Polymer membranes for gas separation.* Current Opinion in Solid State and Materials Science, 1999. **4**(6): p. 549-552.

2. Kulprathipanja, S., et al., Separation of a monosaccharide with mixed matrix membranes 1988: U.S.

3. Mahajan, R. and W.J. Koros, *Mixed Matrix Membrane Materials With Glassy Polymers Part 1.* Polymer Engineering & Science, 2004. **42**(7): p. 1421.

4. Kirchner, B., Ionic Liquids: 290 (Topics in Current Chemistry). 2009: Springer Verlag.

5. Freemantle, M., *An Introduction to Ionic Liquids*. 1st ed. 2009, Cambridge: Royal Society of Chemistry.

Functional materials for separation of carbon dioxide from flue gas, natural and biogas streams

Claudia Staudt

Heinrich-Heine University Duesseldorf, Institute for Organic and Macromolecular Chemistry, Universitätsstr. 1, 40225 Duesseldorf, staudt@uni-duesseldorf.de

Introduction

For the separation of gases but also vaporous and liquid mixtures, membrane-based processes are gaining increasing attention although this technology is quite young compared to conventional separation technologies like distillation, absorption or extraction. Many membrane-based processes have been established in an industrial scale, e. g., oxygen/nitrogen separation, natural gas purification, dehydration of solvents, as well as the removal of hydrogen from ammonia production or low molecular weight components from equilibrium reactions. Membrane technology offers many advantages like little maintenance, simplicity of operation and the units are small and compatible. Furthermore the processes are low energy consumptive. However, nowadays discussions on environmental as well as energy issues are playing an important role, whereas membrane processes are predestinated for the reduction of emissions from air (vapor recovery units) from water, e.g. treatment of waste water from large hospital complexes or recycling of valuable starting materials, like recycling of ethylene and propylene from vent streams in polyethylene or polypropylene production units.

Natural gas treatment

The removal of carbon dioxide from natural gas streams using membranes has been extensively studied by researchers all over the world since decades [1] and many companies like UBE, DuPont, VaPerma, MTR etc. are offering commercial solutions. The treatment of natural gas streams includes the removal of water, carbon dioxide and hydrogen sulfide in order to prevent corrosion and to meet pipeline specifications ($\leq$ 2 mol% carbon dioxide and $\leq$ 4 ppm hydrogen sulfide) [2]. But as the worldwide energy demand increases, new gas fields have to be developed, many with high levels of carbon dioxide and even high hydrogen sulfide content. And although natural gas treatment with membranes is commercialized, it cannot be used in these cases since plasticization effects or degradation of the membrane material is observed which lead to irreversible loss of separation performance [3]. Therefore new approaches must be developed to reach more stable materials for the treatment of natural gas streams [4,5].

Biogas treatment

In the last couple of years a large number of biogas production plants have been installed. For example, in Germany 1.14 billion m^3 /year of biogas is currently produced and new, easy operating systems with low energy consumption are necessary to upgrade biogas to pipeline

quality. But, depending on the raw material which is used for the gasification process, the efficiency shows significant variations, e.g. 973 m^3 biogas per ton of biomass is obtained if fat and grease components as raw materials are used and less than 30 m^3/ton if pig or cow manure is used. Also the carbon dioxide concentration and hydrogen sulfide concentration is varying depending on the biomass. Typically up to 50% carbon dioxide and up to 3 % of hydrogen sulfide are occurring in biogas streams. Although it has been calculated that membranes would offer a major advantage because of its low energy consumption and simplicity of operation compared to glycol and alkanole amine treatment followed by conversion of hydrogen sulfide to sulfur using the Claus process, only a few papers have been published so far investigating different membrane materials for biogas treatment [6-9].

Flue gas streams

The recovery of CO_2 from flue gases of power plants has been examined for the first time in 1992 [10,11]. The streams obtained in post combustion process, is mainly a low pressure, wet carbon dioxide/nitrogen mixture. Various studies showed that the present state of the art polymer membranes are less expensive and energy demanding than alkanol amine absorption or cryogenic processes. On the other hand, the membranes are less competitive to absorption processes in terms of selectivity and final CO_2 purity [12]. However, membrane technology has significant environmental benefits, since its application does not result in by-products causing emissions or requiring further treatment and disposal [13]. Since the flue gas streams are currently cooled down to 40-60°C and the carbon dioxide/nitrogen separation factors are quite similar or even higher for the separation of carbon dioxide and nitrogen compared to carbon dioxide to methane, several membrane materials which are able to overcome the so-called Robeson upper bond limit are of high interest [14].

Robeson Upper bond for carbon dioxide/methane

In Fig. 1 the so-called Robeson Upper bond from 1991 and 2008 [15] is shown for carbon dioxide/methane separation, which is relevant for the biogas as well as natural gas treatment. Thereby selectivity of a membrane material is plotted versus the permeability of carbon dioxide. It is obvious that rubbery polymeric materials are showing high permeabiltity combined with low selectivity whereas for the glassy polymers it is vice versa. So far all commercial polymers are found beyond the Robeson upper bond limit of 2008, most of them are even lying under the 1991 limit. Interesting materials with very high permeability as well as high selectivity are polymers with specific side groups which are able to rearrange during thermal treatment [16]. Other interesting approaches which lead to significantly improved separation characteristics are carbonized cross-linked polymer blends. Thereby cross-linking is induced with diamines as additives in a mixture of different polyimides. With this approach selectivities for carbon dioxide and methane between 100 and 200 can be reached [17]. Polymeric materials with extremely high carbon dioxide permeability are PIMs which might be especially of interest for post combustion carbon dioxide capture since the flow rates are rather high [18-20].
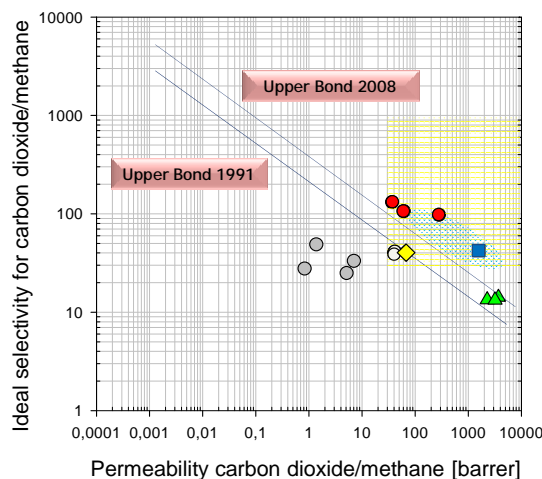
Fig. 1 Upper bond diagram for CO_2/CH_4 separation, commercial polymers,(○), polymeric materials after thermal rearrangements (■) and green area, PIMs (▲)polymer blends crosslinked and carbonized(●), mixed matrix membranen (◇), area postulated with crosslinked mixed matrix membranes (yellow area)

Finally mixed matrix membrane materials as well as crosslinked mixed matrix materials or hybrid materials combining the high permeation rates of inorganic materials and the superior mechanical properties of polymeric materials are extremely promising candidates [21] governing the direction for implementing membrane based processes in order to reduce the carbon dioxide emissions set free in natural gas and biogas streams but also in flue gases from coal-burning power plants.

[1] Richard W. Baker, Future Directions of Membrane Gas Separation Technology, Membrane Technology and Research, Ind. Eng. Chem. Res., 2002, 41 (6), pp 1393.

[2] J. Hao, P.A. Rice, S.A. Stern, Upgrading low-quality natural gas with H_2S- and CO_2-selective polymer membranes, Part II. Process design, economics, and sensitivity study of membrane stages with recycle streams, Journal of Membrane Science 320 (2008) 108.

[3] John D. Wind, Claudia Staudt-Bickel, Donald R. Paul, and William J. Koros, Solid-State Covalent Cross-Linking of Polyimide Membranes for Carbon Dioxide Plasticization Reduction, *Macromolecules* 2003, *36,* 1882.

[4] David W. Wallace, Jason Williams, Claudia Staudt-Bickel, William J. Koros, Characterization of crosslinked hollow fiber membranes, Polymer 47 (2006) 1207.

[5] Rajeev Satish Prabhakar, B.Tech.(Hons), M.S., Low Hydrocarbon Solubility Polymers: Plasticization-resistant Membranes for Carbon Dioxide Removal from Natural Gas, Dissertation, The University of Texas at Austin, 2004

[6] T.C. Merkel and L.G. Toy, Comparison of Hydrogen Sulfide Transport Properties in Fluorinated and Nonfluorinated Polymers, Macromolecules, 2006, 39,7591-7600

[7] Masoud Kayhanian & David J. Hills, Membrane Purification of Anaerobic Digester Gas, Biological Wastes 23 (1988) 1.

[8] S. Sridhar, T. M. Aminabhavi, S. J. Mayor, and M. Ramakrishna, Permeation of Carbon Dioxide and Methane Gases through Novel Silver-Incorporated Thin Film Composite Pebax Membranes, *Ind. Eng. Chem. Res.* 2007, *46,* 8144.

[9] Christopher J. Orme, Frederick F. Stewart, Mixed gas hydrogen sulfide permeability and separation using supported polyphosphazene membranes, Journal of Membrane Science 253 (2005) 243.

[10] J. Van Der Sluijs, C. Hendriks, K. Blok, Energy Convers. Manag. 33 (1992) 429.

[11] P. Feron, A. Jansen, R. Klaassen, Energy Convers. Manag. 33 (1992) 421.

[12] M. Czypereka, P. Zappa, H.J.M. Bouwmeesterb, M. Modigellc, K. Ebertd, I. Voigte, W.A. Meulenberga, L. Singheisera, D. Stovera, Gas separation membranes for zero-emission fossil power plants: MEM-BRAIN, Journal of Membrane Science 359 (2010) 149.

[13] Marius Sandru, Siv Hustad Haukebø, May-Britt Hägg, Composite hollow fiber membranes for CO_2 capture, Journal of Membrane Science 346 (2010) 172.

[14] Eric Favrea , Membrane processes and post combustion carbondioxide capture: Challenges and prospects, Chemical Engineering Journal, 2011, in print

[15] Lloyd M. Robeson, The upper bound revisted, *J. Membr. Sci.*, 320, 2008, 390.

[16] Ho Bum Park, Chul Ho Jung, Young Moo Lee, Anita J. Hill, Steven J. Pas, Steven T. Mudie, Elizabeth, Van Wagner, Benny D. Freeman, David J. Cookson, Polymers with Cavities Tuned for Fast Selective Transport of Small Molecules and Ions, *Science,* 318, 2007, 254

[17] Seyed Saeid Hosseini, Tai Shung Chung, Carbon membranes from blends of PBI and polyimides for N_2/CH_4 and CO_2/CH_4 separation and hydrogen purification, *J. Membr. Sci.,* 328, 2009,174.

[18] Bader S. Ghanem, Neil B. McKeown, Peter M. Budd, Nasser M. Al-Harbi, Detlev Fritsch, Kathleen Heinrich, Ludmila Starannikova, Andrei Tokarev and Yuri Yampolskii, Synthesis, Characterization and Gas Permeation Properties of a Novel Group of Polymers with Intrinsic Microporosity: PIMPolyimides, *Macromolecules,* 42, 2009, 7881

[19] Neil B. McKeown and Peter M. Budd, Polymers of intrinsic microporosity (PIMs): organic materials for membranes separations, heterogeneous catalysis and hydrogen storage, Chem. Soc. Rev., 35, 2006, 675

[20] Peter M. Budd, Neil B. McKeown and Detlev Fritsch, Free volume and intrinsic microporosity in polymers, *J. Mater. Chem.,* 2005, 15, 1977-1986

[21] A.M.W. Hillock, S.J. Miller, W.J. Koros, Crosslinked mixed matrix membranes for the purification of natural gas: Effects of sieve surface modification, *J. Membr. Sci.,* 314 (1-2), 2008, 193.

Heat exchanger design for an oxyfuel-process utilizing oxygen from an O_2-transport membrane

V. Verbaere, M. Förster, R. Kneer, Institute of Heat and Mass Transfer,
RWTH Aachen University

1. Introduction

As the capture of CO_2 from conventional fuel combustion with air is inherently energy intensive, oxyfuel combustion, where pure O_2 obtained from an air separation unit (ASU) is used, is considered a worthwhile alternative. However, for flame temperature control, the pure O_2 stream needs to be diluted with recycled flue gas. The major efficiency drawback in oxyfuel combustion is caused by the ASU. For example, processes using the well-established cryogenic technique for O_2 production are typically associated with a penalty of 10%-points [1]. Therefore, using high temperature membranes as ASU, known also as ion transport membranes (ITM), may be more efficient. The membrane technology is expected, from an economic and environmental perspective, to have a major role to play in the mitigation of CO_2 resulting from fossil fuel combustion [2].

At RWTH Aachen University OXYCOAL-AC, a joint project between industry and university researchers, has investigated the potential for ITM usage with pulverised coal combustion since 2004. At RWTH Aachen University six institutes working on the field of energy, process engineering and material technology have provided the scientific part, supported by 6 industrial companies[1]. Using process simulations, Stadler et al. [3] determined a minimum achievable penalty of 5.2%-points for the OXYCOAL-AC process.

Elevated temperatures, typically 800-900°C, together with an enlarged differential pressure across the membrane, are required to obtain an appropriate O_2 flux. For industrial size power plants it follows, that a heat flow rate, which amounts to 10-30% of the plant thermal capacity, has to be transferred to the feed air. Therefore, heat exchangers advantageously positioned either in the boiler or in the recycled flue gas pipe will have to be used.

Due to severe process constraints (temperature, pressure and flue gas composition), the design of such heat exchangers has to be addressed. Full consideration must be given to the design of the feed air heater (FAH, see figure 1) to guarantee an effective process integration of the ITM. This work investigates the impact of FAH design characteristics on process efficiency and membrane area requirement. Two variants of the OXYCOAL-AC process have been considered.

---

[1] RWE Power AG, E.On AG, Hitachi Power Europe, Linde AG, MAN Turbo, and WS-Wärmeprozesstechnik

2. Process description

2.1. Reference process

The processes investigated are based on the Reference Power Plant North Rhine-Westphalia [4], which is characterised by a net efficiency of 45.9% and steam parameters of 600/620°C and 285/60 bar. All processes investigated relate to a gross electric power output of 600 MW. The simulations have been carried out using a *Matlab* based code.

2.2. OXYCOAL-AC 4-end concept

A central feature of the 4-end concept, shown in Fig.1a, is a membrane integrated in the recycled flue gas pipe. Hot recycled flue gas (875°C) and preheated feed air (757°C) are thereby intended to heat the membrane to the required operation temperature. On the membrane feed surface, O_2 is absorbed and transported by diffusion to the permeate surface, where it is swept by recycled flue gas. This method provides a high O_2 partial pressure difference and a high O_2 flux across the membrane. In standard conditions, the average O_2 partial pressure ratio attains a value of $\Delta p_{O2\_av} = 24.5$. The exit N_2-rich stream from the membrane releases mechanical energy in a turbine and ultimately provides additional heating to the feedwater (not represented in the sketch). As the major components located in the recirculation path are vulnerable to dust and sulphurs, a hot-gas cleaning device, made of ceramic candle filters, cleans the flue gas.
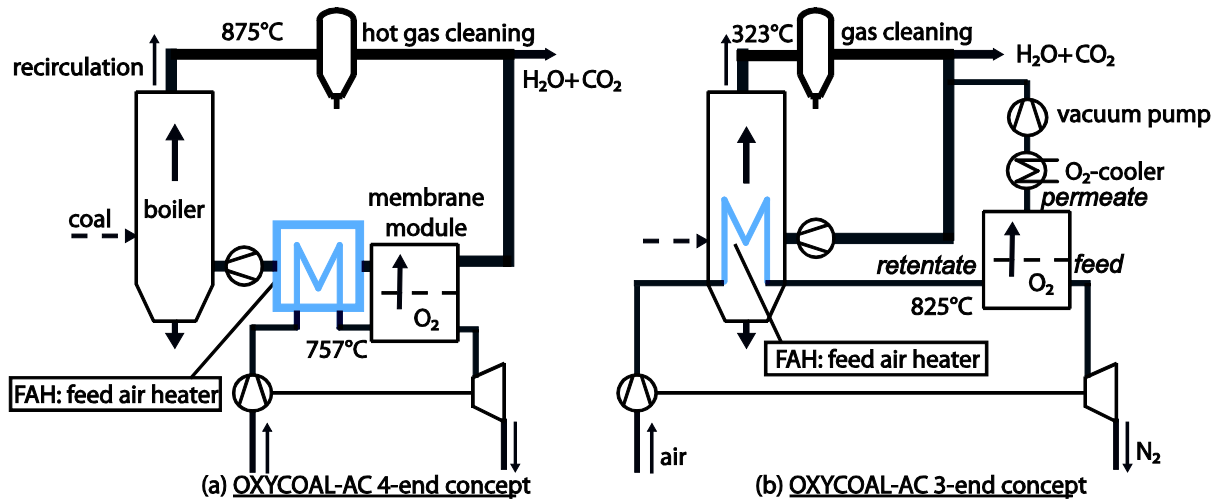
Figure 1: OXYCOAL-AC processes with a four-end and a three-end membrane module

A large part of the cleaned flue gas goes through the membrane where it is enriched with O_2. Eventually, it is cooled by the FAH and transported by a hot gas blower to the burners. O_2 concentration at the burners attains 17 %-vol. The low O_2 concentration, still enables an efficient combustion [5]. The not-recirculated flue gas releases subsequently heat to the economizer and to the feedwater.

The analysis has been carried out for a CO_2 capture rate of 90% with 5% remaining impurities. This adds an energy penalty of 130 kWh$_{el}$ per tonne of CO_2 sequestrated [6]. In contrast with air fired processes, process variants developed within the OXYCOAL-AC

project are based, to a greater extent, on turbo machinery, which puts a heavy strain on process efficiency. In this respect, Stadler et al. [7] proposed realistic lower and upper limits for polytropic efficiencies. The conservative values are used in the present simulations. Finally, ingress air has been restricted to 1% of flue gas mass flow. Non condensable gases actually increase significantly the compression work and the condensation duty of the CO2 separation process [8]. Under standard conditions, a net plant efficiency of 38.5% and a adiabatic flame temperature of 1648°C have been determinated.

2.3. OXYCOAL-AC 3-end concept

Currently available membrane materials (perovskite) suffer performance deterioration under action of CO_2 [9]. An alternative referred to as 3-end concept, shown in Fig.1b, keeps membrane and flue gas separated. A significant O_2 partial pressure difference throughout the membrane is then attained through pressurizing feed air and simultaneously applying vacuum on the permeate surface. Since recycled flue gas exhibits a significant lower temperature (323°C), it is inadequate to heat entirely the feed air. Hence feed air heating takes place within the combustion chamber (up to 825°C). To apply vacuum on the permeate surface and convey pure O_2 into gas recirculation, Beggel [10] suggests the use of a non-lubricated liquid pump, since O_2 represents a potential risk. O_2 concentration at the burner has been set to 17 Vol.-%.

Changing the membrane integration from the 4-end version to 3-end requires an increased membrane surface area for similar process efficiencies. This is due to a significant lower average O_2 partial pressure ratio across the membrane. The O_2 partial pressure ratio at the end of the membrane has been set to $\Delta p_{O2\_end} = 2$. The average O_2 partial pressure ratio between feed and permeate surfaces then attains $\Delta p_{O2\_av} = 5.5$.

3. Results

Oxyfuel combustion including O_2-transport membranes has been studied by many investigators, with most of the simulations performed on process efficiency [3,6,7,10] and membrane area [11]. The new results reported here include:

- a sensitivity analysis of characteristic parameters of the membrane (O_2 separation ratio in the feed stream and pressure ratio between feed and permeate sides) on net plant efficiency, membrane area and FAH design parameters (heat transfer rate, effectiveness and heat capacity rate ratio),
- the effect of O_2 concentration in recycled flue gas,
- the effect of FAH internal pressure drop on plant efficiency.

Effectiveness is defined as the ratio between actual heat transferred and maximal heat transferable in a counter-flow heat exchanger.

3.1. OXYCOAL-AC 4-end concept

a. Sensitivity analysis of characteristic parameters of the membrane

The net plant efficiency (Fig.2a) and the membrane specific area (Fig.2b) increase with increasing membrane O_2 separation ratio and decreasing pressure ratio β. Low O_2 separation ratios increase the air flow rate, which in turn increases the power deficit between the turbine and the air compressor and also decreases the flue gas temperature at the burners. In exactly the same way, high pressure ratios increase the power deficit between the turbine and the air compressor: as the air compressor discharge temperature increases, less heat is required from the recycled flue gas, which would result in a lesser drop in flue gas temperature. An undesirable consequence of decreasing O_2 separation ratio is a rise in heat flow rate (Fig.2c), effectiveness ε and heat capacity rate ratio C* (Fig.2d) for the FAH. All of this is in line with increasing the heat transfer area.
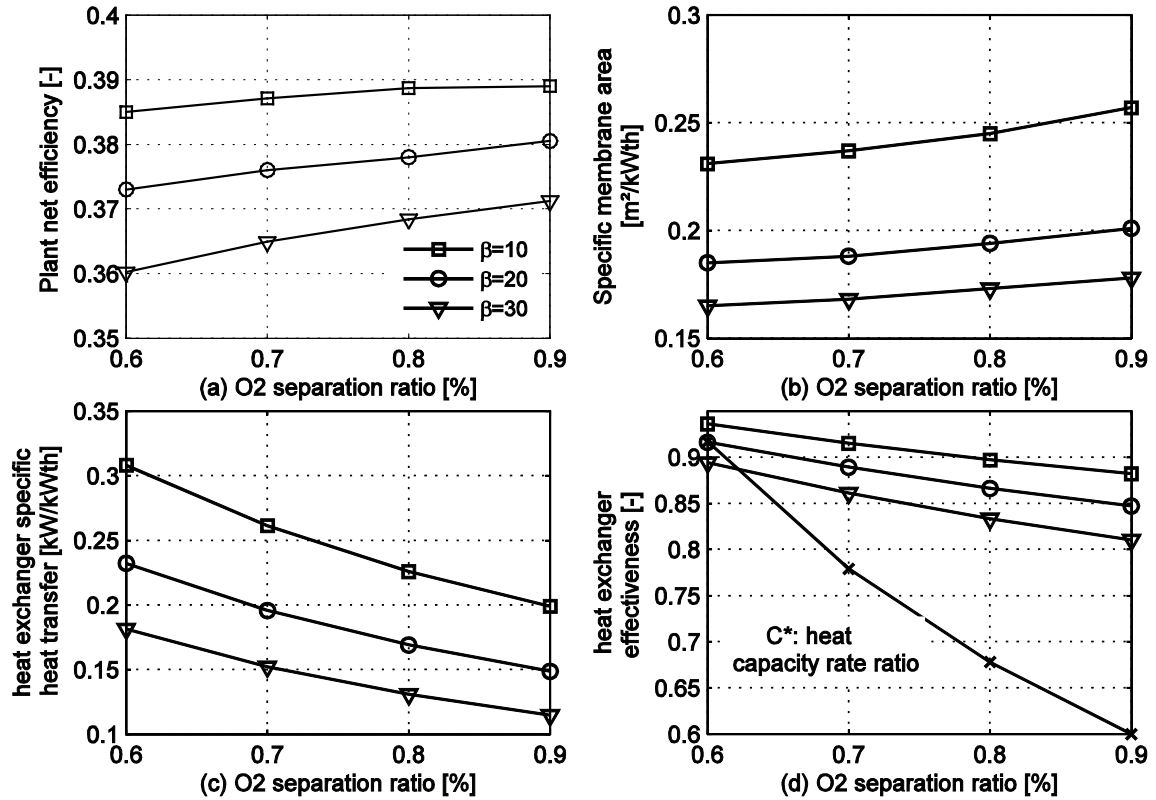
Figure 2: Sensitivity analysis of the OXYCOAL-AC 4-end concept for variable membrane pressure ratio β and O_2 separation ratio: (a) plant net efficiency, (b) specific membrane area, (c) FAH: specific heat transfer (d) FAH: effectiveness and heat capacity rate ratio.

b. Effect of O_2 concentration in recycled flue gas

Increasing O_2 concentration increases adiabatic flame temperature and also brings hot gas blower power expenditure down. Hence, a substantial gain in net plant efficiency (0.5 %-points for an O_2 increase of 6 Vol.-%) is obtained. It also acts in a manner that the O_2 flux across the membrane slightly decreases. No significant difference in terms of heat transfer

rate in FAH is observed. However, as the flue gas flow rate decreases, the temperature difference in the heat exchanger decreases, i.e. the exchanger effectiveness increases.

c. Effect of FAH internal pressure drop

The net plant efficiency decrease has been determined in relation with FAH pressure drop: at equal pressure drop, the net plant efficiency is lowered by the flue gas stream 31 times more, than by the pressurized air stream.

3.2. OXYCOAL-AC 3-end concept

a. Sensitivity analysis of characteristic membrane parameters

The net plant efficiency (Fig.3a) reaches a peak in the region between 70 and 80% of O_2 separation ratio. This is due to two competing effects. At low O_2 separation ratio, the net plant efficiency is predominantly impeded by the high air flow rate and the resulting high energy consumption of air compressor. In contrast, at high O_2 separation ratios, low O_2 partial pressure in the feed needs to be counterbalanced by a higher vacuum on the permeate side. The fact that the air pressure decrease on the membrane feed side coincides with a decrease of the net plant efficiency has been discussed before. Please note that net plant efficiencies attained by the 3-end and 4-end concepts are very similar to each other.
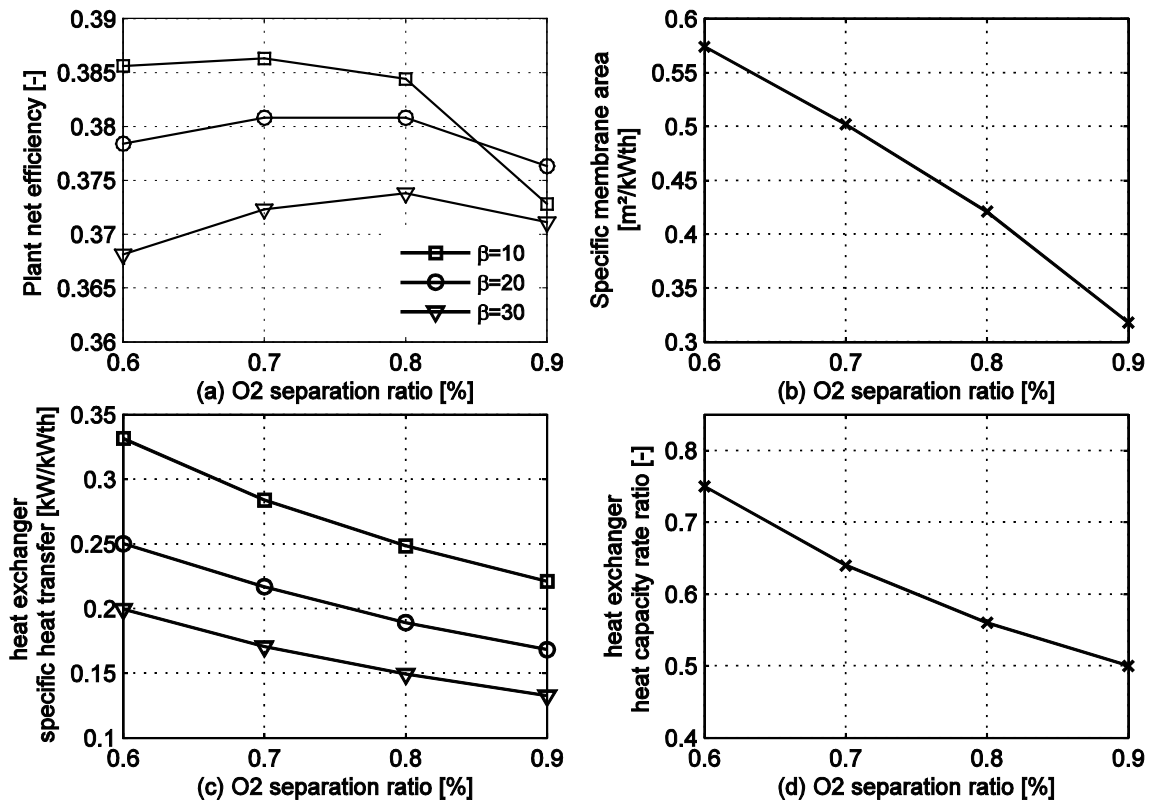
Figure 3: Sensitivity analysis of the OXYCOAL-AC 3-end concept for variable membrane pressure ratio β and O_2 separation ratio (a) plant net efficiency, (b) specific membrane area, (c) FAH: specific heat transfer (d) FAH: heat capacity rate ratio.

Unlike the 4-end concept, the O_2 transport across the membrane of the 3-end concept decreases with increasing O_2 separation ratio (Fig.3b). One must keep in mind that for a constant Δp_{O2_end}, O_2 partial pressure ratio imbalance along the length of the membrane

increases with increasing O_2 separation ratio. Regarding the heat transfer rate (Fig.3c) and the heat capacity rate ratio (Fig.3d) in FAH, 3-end and 4-end concepts exhibits the same qualitative behaviour.

b. Effect of O_2 concentration in recycled flue gas

The simulations have shown that the efficiency gain through higher flue gas O_2 is insignificant.

c. Effect of pressure drops in FAH

With respect to the 4-end concept, the dependence of net plant efficiency on FAH pressure drop has decreased: the impact of the flue gas stream on the net plant efficiency is 22 times higher than that of the feed air stream. This is attributable to a decrease in recirculation temperature, which in turn leads to a reduced hot gas blower power expenditure.

4. **Conclusion**:

In the context of CCS power plants based on oxyfuel combustion with O_2-transport membrane the main factors exerting an influence on the membrane feed air heater have been analysed. In order to provide a comprehensive approach, this development has been put into perspective with the impact on the net plant efficiency and the membrane area.

5. **Acknowledgement**:

6. **References**:

[1] Davison J.; *Performance and costs of power plants with capture and storage of CO₂*; Energy 32 (2007) 1163-1176

[2] Dyer P., Richards R., Russek S., Taylor D.; *Ion transport membrane technology for oxygen separation and syngas production*; Solid State Ionics 134 (2000) 21-33

[3] Stadler H., Beggel F., Habermehl M., Persigehl B., Kneer R., Modigell M., Jeschke P.; Oxyfuel coal combustion by efficient integration of oxygen transport membranes, International Journal of Greenhouse Gas Control 5 (2011) 7-15

[4] VGB PowerTech e.V., editor; *Konzeptstudie Referenzkrafwerk NRW*; VGB PowerTech e.V., Essen, 2004

[5] Toporov D., Bocian P., Heil P., Kellermann A., Stadler H., Tschunko S., Förster M., Kneer R.; *Detailed investigation of a pulverized fuel swirl flame in CO₂/O₂ atmosphere*, Combust. Flame 155 (2008) 605-618

[6] Pfaff I., Kather A.; *Comparative thermodynamic analysis and integration issues of CCS steam power plants based on oxy-combustion with cryogenic or membrane based air separation*; Energy Procedia 1 (2009) 495-502

[7] Stadler H., Beggel F., Persigehl B. Kneer R., Modigell M., Jeschke P.; The *OXYCOAL-AC process: Component behaviour and thermodynamic efficiency*; 4th Int. Conf. Clean Coal Tech. for our Future (2009), R. Davidson ed.

[8] Li H., Yan J., Yan J., Anheden M.; *Impurity impacts on the purification process in oxyfuel combustion based CO2 capture and storage system*; Applied Energy 85 (2009) 202-213

[9] Kneer R.; *Developing components for an integrated coal-firing power plant process with membrane-based oxygen supply*, 42nd IUPAC Congress Chemistry Solutions, 02.-07.08.2009, Glasgow, UK

[10] Beggel F., Engels S., Modigell, M., Nauels N.; Oxyfuel combustion by means of high temperature membranes for air separation; 4th Int. Conf. Clean Coal Tech. for our Future (2009), in Robert Davidson Ed.

[11] Castillo R.; Thermodynamic analysis of a hard coal oxyfuel power plant with high temperature three-end membrane for air separation; Applied Energy 88 (2011) 1480-1493

Oxygen Supply for Oxyfuel Power Plants by Oxy-Vac-Jül Process

J. Nazarko, M. Weber, E. Riensche, D. Stolten, Juelich Research Center, Germany

1 Introduction

Oxy-fuel processes are based on the elimination of nitrogen from the oxidizer flow entering the combustion chamber in order to get a flue gas that consists almost exclusively of CO_2 - after application of common flue gas cleaning steps and vapor condensation. Oxygen can be supplied by various processes. Cryogenic air separation on medium scale is state of the art, but it requires an energy of 0.245 kWh_{el}/kg_{O2}[1] to supply oxygen with a common purity [1, p. 20]. Energetic optimization allows to reduce the energy consumption to 0.175 kWh_{el}/kg_{O2}, but it results in an impurity content of up to 5 vol% [1, p. 21]. Substitution by a membrane based oxygen supply will be successful only, if the CO_2 avoidance cost can be reduced.

2 Oxygen supply using Perovskite membranes

Perovskite is gas-tight ceramic material allowing mixed ionic-electronic oxygen permeation with a perfect selectivity [2, p. 239], which enables single-stage separation. It´s ABO_3 structure consists of a cubic close packing of large A cations (e.g. La^{3+} or Sr^{2+}) and oxygen ions, while the smaller B cations (e.g. Co^{3+}, Co^{4+}, Fe^{3+}, Fe^{4+}) occupy the octahedral cavities furthest from A ions. Transport occurs via oxygen vacancies. Thermal activation sufficient for technically relevant transport is reached only at temperatures above 700°C [3, p. 6]. The flux is given by the Wagner equation [4, p. 3]:

$$j_{O_2} = -\frac{1}{L \times \left(1 + 2L_C / L\right)} \times \frac{RT}{16F^2} \times \frac{\sigma_{ion} \times \sigma_{el}}{\sigma_{ion} + \sigma_{el}} \times \ln\left(\frac{p(O_2^{Feed})}{p(O_2^{Permeat})}\right)$$

Here, R is the gas constant, F is the Faraday-constant, σ are the conductivities, L is the membrane thickness an L_C a critical thickness, below which surface kinetics prevail [4, p. 3].

3 Classification of the membrane based Oxyfuel concepts

Membrane based oxyfuel-concepts for coal power plants (Table 1) can be distinguished by the methods for air or membrane heat-up and for generation of driving force for the oxygen transport. Following heating methods are known and partially combined:
- Air compression
- Regeneration
- External heating (e.g. inside of the boiler)
- Use of hot flue gas (either membrane heating by use as sweep gas or air heating).

Driving force is generated by
- Compression of the feed gas (followed by expansion of the retentate)
- Vacuum on the permeate side
- Sweeping on the permeate side at atmospheric pressure.

From the three measures for generation of the driving force for the oxygen transport and their possible four combinations in principle seven different oxyfuel classes come out. Four promising concepts are listed in Table 1, which are subject of evaluation.

---

[1] Ambient conditions: 20°C, 1.01325 bar, 60% humidity, product temperature 15°C.

Table 1: Classification of the membrane based oxyfuel concepts

		OXYCOAL-AC	OXY-CLEAN	OXY-VAC-JÜL	OXY-SWEEP-JÜL
Driving force generation	Feed side	Compressor and turbine	Compressor and turbine	------	------
	Perm. side	Sweep with flue gas	---- / vacuum suction	vacuum suction	Sweep with flue gas
Total pressure	Feed side	10-20 bar	10-20 bar	1 bar	1 bar
	Perm. side	1 bar	1 bar / < 1 bar	< 0.2 bar	1 bar
Heating of membrane feed gas		Compressor / flue gas	Compressor / flue gas	Recuperator / flue gas	Recuperator / flue gas
Reference power plant (without CCS)		Externally Fired CC	Externally Fired CC	Steam power plant	Steam power plant
Flue gas recycling (temp. level)		hot	cold	cold	hot-cold-hot
Flue gas recycling (flow rate)		large	small	small	very large

4 OXY-VAC-JÜL concept

In the OXY-VAC-JÜL concept air compression and sweeping with flue gas is avoided. Sufficient driving force results from the generation of a strong vacuum at the permeate side of the membrane (Fig. 1).

An air blower compensates the pressure losses in the membrane module and the heat exchangers. The recuperative air preheating is designed with parallel fresh air streams and the corresponding two hot streams of the depleted air and the produced oxygen. Final air heating up to 850°C takes place in the boiler. A certain air excess is needed, because membrane modules can separate only a part of the oxygen contained in the air. The degree of separation is limited by the oxygen content in the retentate: its partial pressure is always higher than the vacuum pressure on the permeate side.

This concept offers several advantages:
- Elimination of compression and expansion of the fresh air
- Cold flue gas recycling, and thus with low flow rate and with recycle blower and flue gas cleaning similar to the cryogenic process
- Flue gas, consisting of CO_2, H_2O and impurities, is not contacting the membrane material.

The disadvantages are:
- Special requirements on heat exchangers and tubing resulting from vacuum.
- Large peripheral components compared to the concepts with feed compression.
- oxygen handling at high temperatures needed.

Fig. 1: Flowsheet of the simulated OXY-VAC-JÜL concept

5   Thermodynamic boundary conditions

For the thermodynamic analysis of the OXY-VAC-JÜL concept the hard coal-fired "Reference power plant NRW" [5, p.] is chosen as reference and orientation for the power plant components including the water steam cycle.

The air data are calculated on the basis of
   -   the air composition given in Landolt-Börnstein
   -   the Magnus equation for the saturation vapor pressure and
   -   the correction factor for water vapor in air compared to steam

These data as well as the composition of the coal "Klein Kopje" are input parameters for the simulation. A pressure of 1.01325 bar and a temperature of 11°C for the environment is fixed, the relative humidity of the air amounts to 60%.

The thermodynamic calculations are carried out using the commercial programmes
   -   PRO II, version 8.3.3, for air and coal path, combustion and flue gas path
   -   Ebsilon Professional, version 9.00, for the water steam cycle (IAPWS-IF97 water steam table).

The oxygen demand of 70.9 Nm³/s results from
   -   the thermal heat input of 1210.3 MW_{th}
   -   the coal type Klein Kopje
   -   oxydant ration of 1.15 for oxyfuel combustion
   -   the simulated flue gas recirculation ratio of 68.7%, which adjusts the caloric combustion temperature to 2124°C [6, p. 161] and
   -   the oxygen content in the recycled flue gas, which amounts to 3.61 Vol.-%.

From safety reasons the temperature of the hot oxygen should not exceed 200°C outside the membrane module. Therefore, two vacuum compression steps with intercooling are foreseen. The waste heat of the compression is used in the water steam cycle for preheating of the condensate. An adiabatic efficiency of 75% is assumed for the vacuum compressors. The oxygen partial pressure in the retentate is 10% higher in relation to the oxygen partial pressure in the permeate.

For the feed/retentate side of the membrane and for the air- respectively flue gas sides of the heat exchangers a pressure loss of 2% of the absolute pressure value is assumed. Therefore, the air blower has to compensate a pressure loss of 80 mbar in total.

The boundary conditions of the waste heat use of the flue gas, the coal drying and the flue gas recycling are published in [6, p. 160-161]. Table 2 gives an overview of the parameters and characteristic data of the simulated OXY-VAC-JÜL concept.

Table 2: Parameters of the simulated membrane based OXY-VAC-JÜL concept

parameter	data	unit
caloric combustion temperature	2124	°C
operating temperature of membrane	850	°C
flue gas temperature after steam generator	370	°C
Recirculated flue gas in front of combuster	350	°C
coal mass flow	48,429	kg/s
excess oxygen	1,15	------
leak air fraction	0,00	------
Vacuum compressor, adiabatic efficiency	75	%
blower, efficiency	75	%
oxygen partial pressure ratio retentate / permeate	1,1	------
gas/gas heat exchanger, terminal temperature difference	50	K
gas/coolant water heat exchanger, terminal temperature difference	12	K
pressure loss per apparate passage	20	mbar

6   Results

The net plant efficiency of the OXY-VAC-JÜL concept (including CO_2 compression) is shown in Fig. 2 as a function of the O_2 separation degree. A maximum can be observed at a separation degree of 60%. At lower separation degrees, high flow rates of fresh air and depleted air lead to higher energy demand of the air blower and larger amounts of waste heat in the depleted air, leaving the plant at 69.3°C. At higher separation degrees, the electric energy demand of the vacuum compressor increases, since lower vacuum pressure levels are required, as shown by the red curve in Fig. 3.

Whether the optimum design point can be realized, depends on the availability of suitable vacuum compressors; with the assumptions on pressure loss made, the suction pressure of the vacuum compressor is 20 mbar lower than the pressure values given in Fig. 3.
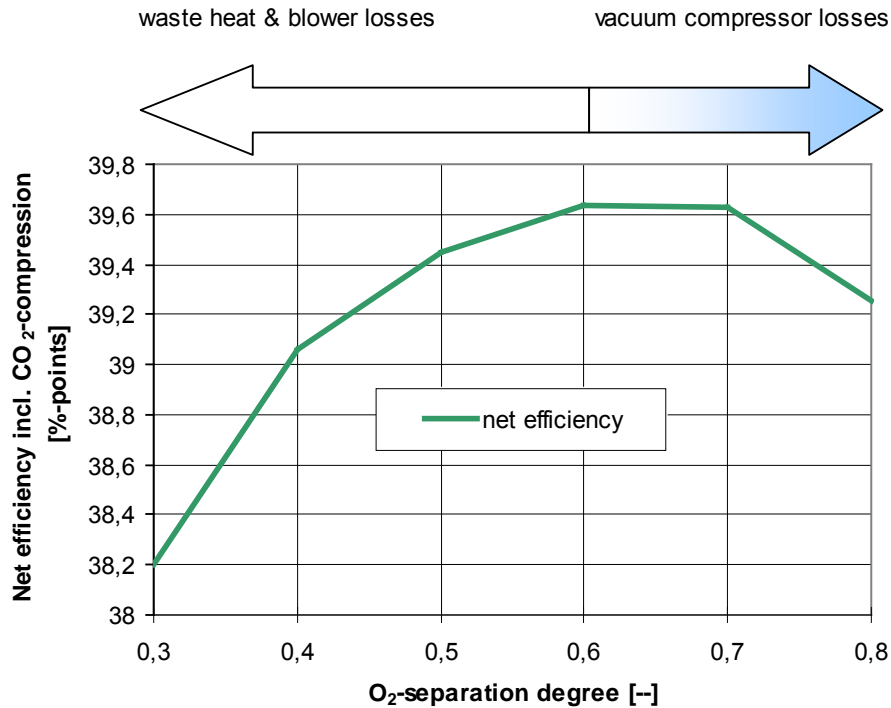
Fig. 2: Net plant efficiency of the OXY-VAC-JÜL concept as a function of the O_2 separation degree (net efficiency of the reference plat is 45.6 %)
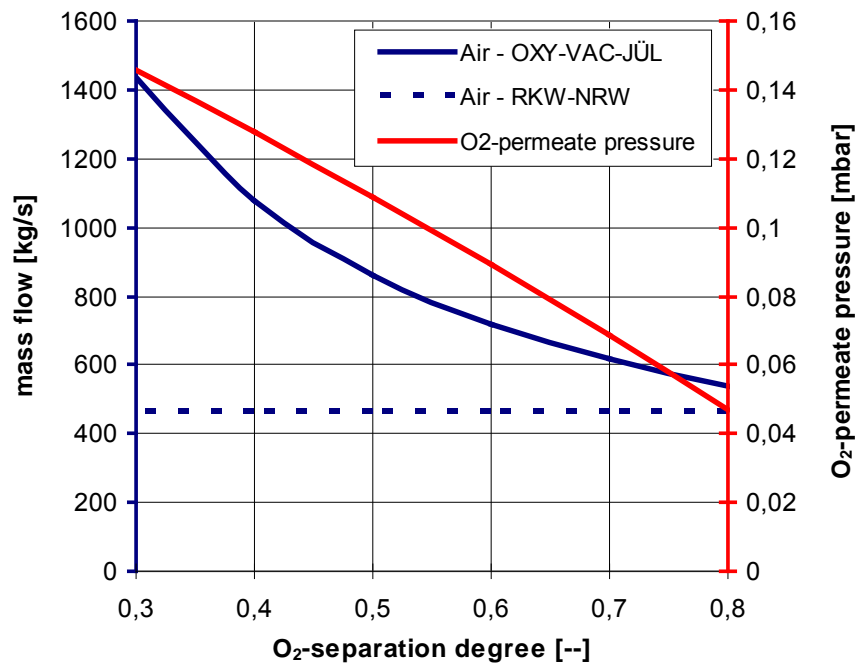
Fig. 3: Air mass flowrates and O_2 permeate partial pressure as a function of the O_2 separation degree

A low O_2 separation degree leads to a high air demand (Fig. 3, blue curve). The air flow of the reference power plant NRW (air ratio 1.15) amounts to 470 kg/s (Fig. 3, dashed line). The air demand of OXY-VAC-JÜL ranges from 540 to 1440 kg/s. The membrane unit supplies 99.2 kg/s of oxygen. Compared to stoichiometric oxygen supply, this value is by a factor of 1.047 higher.

The energy need for oxygen supply by OXY-VAC-JÜL concept is composed of the consumptions of the two vacuum compressors and of the air blower as well as the heat supplied in the boiler multiplied by the steam process gross efficiency (Fig. 4).

Positive effects of membrane based oxygen supply on the plant efficency (hot oxydant supply to the boiler, waste heat use in the steam cycle) are not shown here but included.
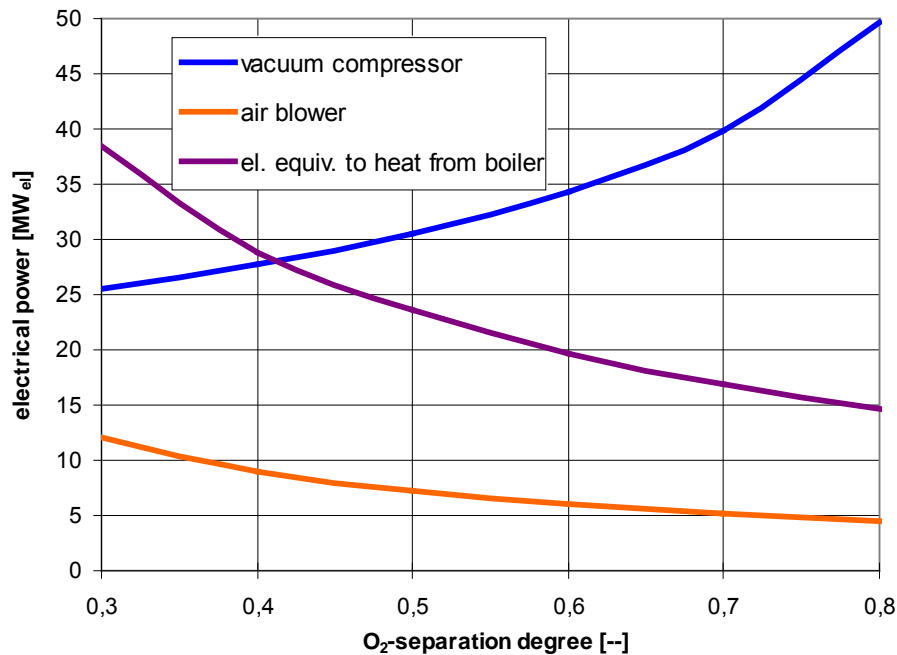
Fig. 4: Energy demand for oxygen supply

7   Summary

Applying OXY-VAC-JÜL concept to the "Reference power plant NRW" results in net plant efficiencies ranging from 39.4 to 39.6 %-points (including CO_2 compression) for a wide range of oxygen separation degrees (50 to 75%). In the frame of the assumptions made and at an optimal degree of O_2 separation of 60%, the oxygen supply by OXY-VAC-JÜL concept requires a net electric energy of 0.098 kWh_{el}/kg_{O2} – including all negative and positive effects of integration into the power plant. The corresponding values for the cryogenic air separation technology are 0.245 kWh_{el}/kg_{O2} (today, high O_2 purity) and 0.175 kWh_{el}/kg_{O2} (optimized for oxyfuel, lower O_2 purity). This results in lower efficiency penalties for the OXY-VAC-JÜL concept: the difference is 4.3 respectively 2.3 %-points. The values are obtained assuming realistic component data: 50 K terminal temperature difference in heat exchangers, 20 mbar pressure loss for each apparatus passage and 75% adiabatic efficiency of the vacuum compressors.

8   Literature

[1]   G. BEYSEL, Enhanced Cryogenic Air Separation. A proven Process applied to Oxyfuel, 1st Oxyfuel Combustion Conference, Cottbus, 2009.
[2]   N. ITOH, T. KATO, K. UCHIDA, K. HARAYA: Preparation of pore-free disk of $La_{(1-x)}Sr_xCoO_3$ mixed conductor and its oxygen permeability. In: *Journal of Membrane Science* 92 (1994), p. 239.
[3]   S. BAUMANN, M. BETZ, L. BLUM, J. MALZBENDER, T. MARKUS, A. MÖBIUS, J. NAZARKO, E. RIENSCHE, R.W. STEINBRECH, R. TREBBELS, W.A. MEULENBERG, OXYMEM - Mischleitende, keramische Membranen zur Sauerstoffbereitstellung für fossil gefeuerte Kraftwerksprozesse (Oxygen Transport Membrane), - Forschungsbericht. BMWi-Förderkennzeichen: 0327739B, Jülich : Forschungszentrum Jülich GmbH, 2009.
[4]   M. BETZ, S. BAUMANN, W.A. MEULENBERG, D. STÖVER, Dünnschichtmembranstrukturen im System (A,Sr)(Fe,Co)O3-d, - Abschlusskolloquium OXYMEM, 17.02.2010, Jülich : Forschungszentrum Jülich GmbH, 2010.
[5]   VGB POWERTECH E.V. (Hrsg.) *Konzeptstudie Referenzkraftwerk Nordrhein-Westfallen (RKW NRW).* VGB PowerTech Service GmbH, Verlag technisch-wissenschaftlicher Schriften: Essen, 2004.
[6]   J. NAZARKO, E. RIENSCHE, L. BLUM, D. STOLTEN, Optimierung der Oxyfuel-Kraftwerkskonzepte mit der Sauerstoffbereitstellung durch Hochtemperaturmembranen, in: M. Beckmann, A. Hurtado (Eds.), 42. Kraftwerktechnisches Kolloquium 2010: Sichere und nachhaltige Energieversorgung, Technische Universität Dresden, Dresden, 2010, pp. 147-168.

Pilot Module for oxygen separation with BSCF membranes

A. Kaletsch, Aachen University/ IWM, Aachen/ Germany; E.M. Pfaff, Aachen University/ IWM, Aachen/ Germany; C. Broeckmann, Aachen University/ IWM, Aachen/ Germany; N. Nauels, Aachen University/ AVT, Aachen/ Germany; M. Modigell, Aachen University/ AVT, Aachen/ Germany

Abstract

The CCS-Technology seems to be a promising technology for reducing CO_2-emissions of coal-fired power plants. To capture and store CO_2, the exhaust gas needs a high purity grade. This can be realized by firing in an atmosphere of pure oxygen and re-circulated CO_2. Providing the required oxygen by liquid air separation, results in a significant net efficiency loss of the power plant process. An alternative is to supply pure oxygen by Oxygen Transport Membranes (OTM). Regarding the membrane material, perovskite type ceramics like BSCF ($Ba_{0.5}Sr_{0.5}Co_{0.8}Fe_{0.2}O_{3-\delta}$) with mixed ionic and electronics conductivity (MIEC) at high temperatures can be used.

Within the OXYCOAL-AC Project a 15 m² membrane area Pilot Module equipped with BSCF-tubes for oxygen separation has been developed. The module aims to produce more than 300 000 liters pure oxygen per day.

1. Introduction

About 75% of anthropogenic CO_2-emissions are produced by fossil fired power plants [1]. To improve coal fired power plants in relation to their environmental acceptability the carbon capturing and storage (CCS) technology is an important measure. One of three main approaches for CO_2 capture is the oxyfuel combustion, where the fossil fuel is combusted with pure oxygen instead of air. This leads to a flue gas mainly consisting of CO_2 and water which can be readily captured. State of the art to provide the pure oxygen is by cryogenic air separation. The critical disadvantage regarding this process is an efficiency drop of the power plant process of 8% - 12% [2, 3].

Another possibility to provide the oxygen is the use of ceramic oxygen transport membranes (OTM) [4, 5, 6]. At high temperatures, these membranes are able to separate oxygen from air with an infinite selectivity.

There are currently several research projects investigating the characteristics and the use of OTM membranes for a power plant process, but still most OTM-reactor concepts are bench-scale-modules. In the OXYCOAL-AC Project a Pilot Module is developed, which works as a standalone equipment for oxygen supply.

2. Principles of oxygen transport across MIEC-Membranes

As membrane material for OTM-reactors, perovskite type ceramics like BSCF with mixed ionic and electronic conductivity (MIEC) are suitable. Due to oxygen vacancies in the lattice, which become highly mobile at elevated temperature (>700°C), those materials show a good conductivity for oxygen ions. The parameters affecting the oxygen transport J_{O2} can be expressed by the simplified Wagner´s equation (Eq.1), as it is mainly the temperature, the membrane thickness and material properties. The driving force for oxygen ions through the membrane is provided by a difference in oxygen partial pressure on its feed (p_{O2air}) and permeate (p_{O2flue}) side.

$$J^{''}_{O_2} = C_{(T)} \frac{1}{s_m} \ln \frac{p_{O_2 air}}{p_{O_2 flue}} \qquad \text{(Eq.1)}$$

$C_{(T)}$=constant, which depends on material and temperature; s_m=thickness of membrane

By applying high temperatures and high differences in oxygen partial pressure, the oxygen flux across the membrane is increased, but at the same time those operating conditions cause mechanical loading of the membrane. Consequently, not only functional properties like oxygen permeation have to be considered but also mechanical, thermo-physical and chemical properties.

The integration of the membrane into the power plant process can be done in two different ways: the three-end and the four-end operation [7]. In the 4 end integration, re-circulated exhaust gas is used as a sweep gas to achieve a low oxygen partial pressure on the permeate side while on the feed side pressurized air is used. By increasing feed air pressure, oxygen flux across the membrane is increased as well (Fig.1).
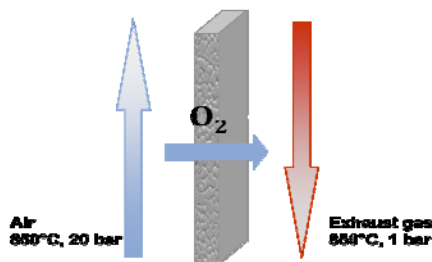
Fig.1: Oxygen assimilation over the membrane by using overflowing sweep gas

In the three-end concept no sweep gas is used. The oxygen partial pressure difference is provided by applying pressurized air on the feed side of the membrane and vacuum on the permeate side. Stadler et al. determined the net efficiency loss for a coal fired power plant to 5.8-%-points, assuming an average partial pressure ratio ($p_{O2,feed}/p_{O2,permeate}$) of 5 [8].

There is also the option to increase the oxygen flux by reducing the membrane thickness. To realize very thin membranes there is the possibility to coat a porous structure with a thin membrane layer. But increasing permeation by reducing membrane thickness is limited due to oxygen surface exchange kinetics [9]. Betz et al. found out, that the oxygen permeability of a supported dense membrane with a thickness of 70 µm on a porous layer is only 30% higher than of a 1 mm monolithic membrane [10]. Furthermore, investigations from Q. Jiang et al. show, that the values of oxygen permeation of a composite membrane are lower than the theoretically values calculated by Wagner`s equation [11]. A problem in case of composite membranes is that the substrate has to be very porous otherwise the permeation of oxygen gets suppressed. In addition, the survey of Q. Jiang et al. expresses, that by increasing the porosity of the substrate, the oxygen flux reaches higher values. But a high porosity means a low mechanical stability.

3. Membrane design

3.1 Membrane material

Concerning the membrane material, a lot of influencing factors have to be considered. A compromise between particular needs for the process and solutions that can be realized by available production technology has to be found. The most attractive material for OTM-applications is the perovskite type ceramic BSCF. This material shows a high oxygen flux at temperatures from 800 °C - 900 °C and an acceptable mechanical strength.

The disadvantage of BSCF is the poor chemical stability in CO_2 and SO_2 enriched atmospheres. Investigations from Engels et al. [12] show a decrease of oxygen permeation about 80% in case of increasing the CO_2 concentration in the sweep gas from 0% up to 15%. By using a pure CO_2-atmosphere a decomposition of the BSCF structure can be observed. That makes it impossible to use in the 4-end mode, where the sweep gas mainly consists of CO_2 and water. Other possible materials like $Sr_{0,5}Ca_{0,5}Mn_{0,9}Fe_{0,1}O_{3-\delta}$ (SCMF), $Sr(Co_{0,8}Fe_{0,2})_{1-y}Ti_yO_{3-\delta}$ (SCFT) or $La_{0,6}Ca_{0,4}Fe_{0,75}Co_{0,25}O_{3-\delta}$ (LCFC) have better chemical stabilities, but show a smaller oxygen flux in the order of one magnitude [13, 14]. For BSCF

different permeation ratios are released in literature [15-19]. However, comparing different investigations is difficult, because oxygen flux depends on sample geometry, sample surface, operation conditions and also on the microstructure of the material [20].

3.2 Membrane manufacturing

To equip the OXYCOAL-AC Pilot Module tubular membrane geometry was chosen. Compared to planar BSCF membranes, tubular membranes have several advantages. By using tubes, high packing fractions are possible and in case of a defect, only the defective tube has to be changed, not the whole stack.

For tubular structures there are a few manufacturing possibilities, for example extrusion or cold isostatic pressing. Better results were archived by isostatic pressing what made it the favourable manufacturing technique for the equipment of the Pilot Module. The tubes have a length of 500 mm, a diameter of 15.5 mm and a wall thickness of 0.8 mm. To press the ceramic material to tubes, a special pressing mold is required. Also the ceramic powder has to be granulated, that means the powder get mixed with specific additives. This is beneficial for filling the pressing molds and the pressing process. After compacting the ceramic granulate with pressures up to 180 MPa, the green compacts were cut to their final dimension plus a shrinking allowance, because the tubes shrink during the sintering about 14%. Sintering temperature amounts to 1100 °C with a holding time of 5 hours. Those parameters have been identified during last years research activities. Especially the microstructure of the BSCF was optimized relating to the membrane performance.

After sintering the tubes are joined to metal parts. Before assembling the membranes in the Pilot Module all tubes get checked in a burst test bench. That kind of proof test guarantees the gas tightness of the membranes as well as the resistance against external pressure of up to 20 bar at a temperature of 850 °C. Investigations regarding the mechanical strength of BSCF show, that the strength of the material at 850 °C is only 60% of the stability at room temperature. Therefore the tubes get tested in the burst test bench with 35 bar external pressure at ambient temperature.

3.3 Joining techniques

In the OXYCOAL-AC module concept, the tubular ceramic membranes have to be joint gas tight on metal parts to assemble them in the pilot module. One possibility is to braze with glass or metal solders. Brazing metal on ceramic is a difficult process. But it is the only alternative to get a high temperature resistant sealing. One typical problem of metal-ceramic-bonds is the difference in thermal expansion. But in this case, the coefficient of thermal expansion from BSCF has nearly the same high value as the heat resistance steel X15CrNiSi25-20. Therefore glass solders are not qualified, because they have usually low expansion coefficients. Wang et al. [18] and Shao et al. [21] used glass ceramic sealants to join BSCF in their oxygen permeation testing device and after measuring and cooling down to room temperature the mismatch of thermal expansion has damaged sealant and membrane.

For brazing with metal solder it has to be taken into account, that the OTM works in oxidizing atmosphere, so only noble-metals can be used as solder material. A common active metal material for ceramic/metal brazing is a Silver-Copper-Titanium solder. But active brazing needs vacuum for processing and this condition decompose OTM-Materials.

Weil et al. [22-24] introduced a technology called Reactive Air Brazing (RAB) which works with a Silver-Copper-oxide solder, which can be brazed in air atmosphere. Investigations carried out at IWM show, that it is possible to reach reactive brazed BSCF-metal-bonds, which have gas tightness up to temperatures of 850 °C. This technology seems to be the most promising technology in this case but there are still no tests concerning its long term stability. Therefore currently the creep behavior of reactive air brazed high temperature membranes are going to be investigated.

In the OXYCOAL-AC Pilot Module the joint patch of the membranes is cooled down to 200 °C. So alternatively to brazed tubes also tubes which are joined with special epoxy glues can be used.

4. Module design

By designing a module concept the first aim is to reach a permeation area which is as high as possible. Also, thin wall thicknesses of the membranes are needed. There are few design concepts for membrane modules with tubular and also planar structures worldwide. The second generation of modules developed within the OXYCOAL-AC-project, which actually is going to be finished, will be equipped with monolithic BSCF tubes.
The ceramic tubes are joined on metal housing. With those housings, the tubes were inserted into a cooled metal flange. This flange is able to hold 300 tubes with a length of 500 mm on both sides, since the module consists of a symmetric assembly, of two separated pressure vessels, see Figure 2.
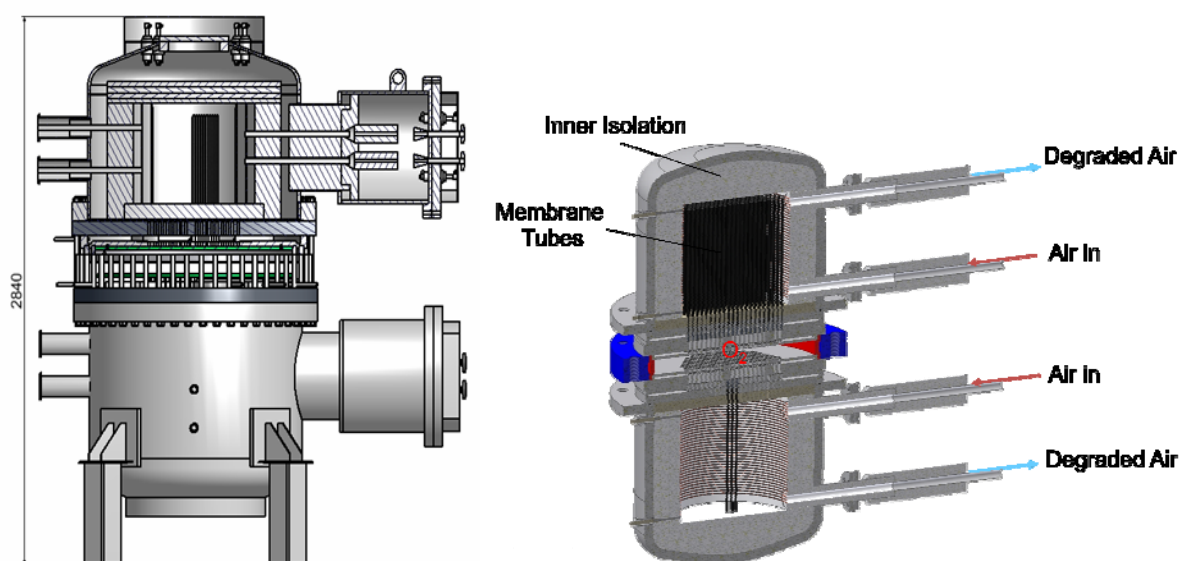
Fig.2: Principle assembly of the OXYCOAL-AC Pilot Module with 15 m² membrane area

Every tube has al membrane area of 246 cm², which results in a total membrane area of about 15 m² for the Pilot Module. According to a permeation rate of 2 Nml/cm²min, the Module is able to supply 0.6 t oxygen per day.
The Module works in three-end operation with a possible gauge pressure of 20 bar on the feed side and a vacuum of 0.3 bar at the permeate side. These conditions seem to be suitable for power plant integration as shown in [8].
The pre-heated pressurized air streams into the vessel, where it passes the tubes. The oxygen that permeates through the membrane tubes is collected within the flange, where it is additionally cooled down to temperatures below 200 °C and conveyed to the vacuum pump. The required temperature is reached by electric preheating of the air stream and an additional heating inside the module.

5. Permeation results

Figure 3 shows the experimental results of a 1m² Lab-scale Membrane Module, that uses the same principle for the cooled flange as the pilot module under construction.
In different experiments the module was equipped with 250 mm and 500 mm one-sided closed tubular BSCF membranes with a wall thickness of 0.8 mm, as described in section 3.2. The experiments were performed at temperatures of 800 °C and 850 °C. The difference in oxygen partial pressure was realised by applying pressurized air up to 15 bar on the feed

side of the membrane and by applying a moderate vacuum down to 0.3 bar on the permeate inner side of the tubes.

Figure 3 shows a linear dependence of the permeation ratio and the logarithmic partial pressure ratio as described by the Wagner equation (Eq.1) for all sets of experiments.
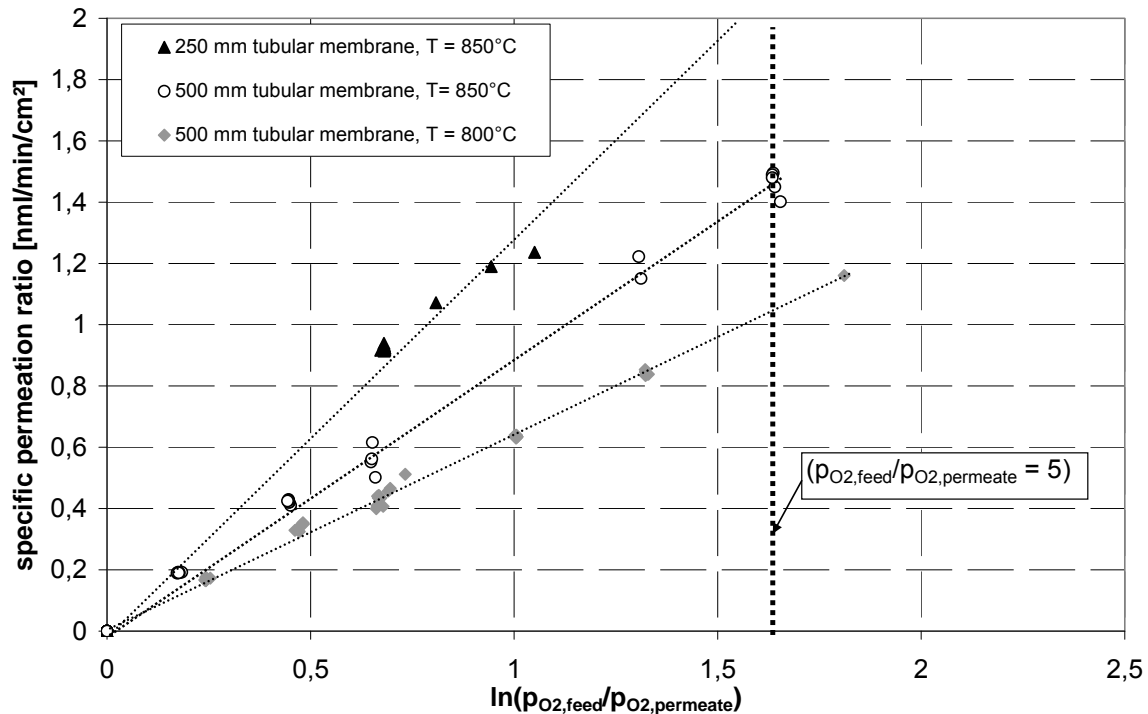
Fig.3: Permeation results of the 1m² -Membrane Module

As also can be seen, the shorter membrane tubes show a higher specific permeation ratio than the ones with a length of 500 mm. It was found out that the reason for this difference lies in insufficiently preheated feed air. Since the top of the longer tubes is adjusted closer to the feed air inlet, the temperature reaches only 730 °C, 680 °C respectively. Therefore, a part of the 500 mm tubes shows far lower permeation ratio compared to the 250 mm tubes, where the desired temperature is reached all along the membrane length.

Applying a partial pressure ratio of $(p_{O2,feed}/p_{O2,permeate}) = 5$, which is assumed to be suitable for power plant integration [8], the 500 mm tubes reach a permeation ratio of 1.46 Nml/cm²/min. Extrapolating the experimental results for the short membrane tubes, a permeation ratio of more than 2 Nml/cm²/min can be reached under these conditions.

Conclusion and Outlook

Within the OXYCOAL-AC Project a Pilot Module for oxygen separation by ceramic OTM with a membrane area of 15 m² has been developed. In the Module monolithic BSCF tubes are used under three-end conditions. This Pilot Module will start running in July of 2011 at Aachen University. The feasibility of this membrane concept was demonstrated at a 1 m² lab-scale Module.

A production technology for membrane tubes has been developed. About 700 membrane tubes have been successfully produced and quality tested in a particular developed proof test.

An important future task is the proof of long term stability of the entire membrane plant under service conditions, regarding functional properties like permeation rate and mechanical properties like strength and creep behaviour.

Acknowledgements

References

[1] B.Metz, O.Davidson, H.de Coninck, M.Loos, L.Meyer (Eds.), Carbon Dioxide Capture and Storage, IPCC (2005), Cambridge University Press, UK. pp 431

[2] A.Kather and S.Gunter, the Oxycoal process with cryogenic oxygen supply, Naturwissenschaften (2009); 69(9):1-18

[3] I.Pfaff, A.Kather, comparative thermodynamic analysis and integration issues of CCS steam power plants based on oxy-combustion with cryogenic or membrane based air separation, Energy Procedia 1 (2009) 495-502

[4] E.M.Pfaff, M.Zwick, Oxyfuel Combustion using Perovskite Membranes, mechanical properties and performance of engineering ceramics and composites III, ceramic engineering and science proceedings, 28-2,(2007)

[5] R.Kneer, D.Toporow, M.Förster, D.Christ, C.Broeckmann. E.Pfaff, M.Zwick, S.Engels, M.Modigell, OXYCOAL-AC: towards an integrated coal-fired power plant process with ion transport membrane based oxygen supply, Energy Environ.Sci. (2009)

[6] Broeckmann, C.; Dabbarh, S.; Pfaff, E.; Zwick, M.: Membranen für die Luftzerlegung aus gemischt leitenden keramischen Werkstoffen; in: Kolaska, H. (Hrsg.): Energie- und ressourceneffizienz durch Pulvermetallurgie; Tagungsband zum 28. Hagener Symposium, Hagen, 26.-27.11.2009, S. 69-88

[7] E.M.Pfaff, M.Zwick, S.Dabbarh, C.Broeckmann; Module Design for MIEC Membranes in OXYCOAL-AC, CCT, Dresden, May2009

[8] H.Stadler, F.Beggel, M.Habermehl, B.Persigehl, R.Kneer, M.Modigell, P.Jeschke; Oxyfuel coal combustion by efficient integration of oxygen transport membranes; International Journal of Greenhouse Gas Control 5 (2011) 7-15

[9] H.M. Bouwmeester, A.J. Burggraaf, dense ceramic membranes for oxygen separation, fundamentals of inorganic membrane science and technology, Amsterdam,1996

[10] M.Betz, S.Baumann, W.A. Meulenberg, ceramic membranes for Oxyfuel power plants, int. conference on clean Coal Technologies CCT2009, Dresden, 2009

[11] Q. Jiang, K.J. Nordheden; Oxygen permeation study and improvement of $Ba_{0.5}Sr_{0.5}Co_{0.8}Fe_{0.2}O_X$ perovskite ceramic membranes; Journal of Membrane Science 369 (2011) 174-181

[12] S. Engels, T.Markus, M.Modigell; Oxygen permeation and stability investigations on MIEC membrane materials under operating conditions for power plan processes, Journal of Membrane Science 370 (2011) 58-69

[13] J.F Vente, S. McIntosh, W.G. Haije and H.J.M. Bouwmeester, Properties and performance of $Ba_xSr_{1-x}Co_{0.8}Fe_{0.2}O_{3-\delta}$ materials for oxygen transport membranes, J. Solid State Electrochem. (2006), 10: 581–588.

[14] M.Schultz, et al., Assessment of Co2 stability and oxygen flux of oxygen permeable membranes, J. Membr. Sci. (2011)

[15] S.Liu, G.R.Gavalas, Oxygen selective ceramic hollow fiber membranes, J. Membr. Sci. (2005), pp. 103–108.

[16] H. Lu, J. Tong, Y. Cong, W. Yang, Partial oxidation of methane in $Ba_{0.5}Sr_{0.5}Co_{0.8}Fe_{0.2}O_{3-\delta}$ membrane reactor at high pressures, Catal. Today 104 (2005), pp. 154–159.

[17] J.F. Vente, W.G. Haije, Z.S. Rak, Performance of functional perovskite membranes for oxygen production, J. Membr. Sci. 276 (2006), pp. 178–184.

[18] H. Wang, Y. Cong, W. Yang, Oxygen permeation study in a tubular $Ba_{0.5}Sr_{0.5}Co_{0.8}Fe_{0.2}O_{3-\delta}$ oxygen permeable membrane, J. Membr. Sci. 210 (2002), pp. 259–271.

[19] W. Zhu, W. Han, G. Xiong and W. Yang, Mixed reforming of heptane to syngas in the $Ba_{0.5}Sr_{0.5}Co_{0.8}Fe_{0.2}O_{3-\delta}$ membrane reactor, Catal. Today 104 (2005), pp. 149–153.

[20] Baumann, Schulze-Küppers et al., Influence of sintering conditions on microstructure and oxygen permeation of $Ba_{0.5}Sr_{0.5}Co_{0.8}Fe_{0.2}O_{3-\delta}$ (BSCF) oxygen transport membranes, Journal of Membrane Science, 2010

[21] Z. Shao, W. Yang, Y. Cong, H. Dong, J. Tong, G. Xiong, Investigation of the permeation behavior of a BSCF oxygen membrane, J. Membr. Sci. 172 (2000) 177-188

[22] K.S. Weil, J.S. Hardy, J.P. Rice, J.Y. Kim, Brazing as a means of sealing ceramic membranes for use in advanced coal gasification process; Fuel85 (2006) 156-162

[23] J.Y. Kim, J.S. Hardy, K.S. Weil; Effects of CuO Content on the wetting behavior and mechanical properties of a Ag-CuO Braze for ceramic joining; J.Am.Soc. 88 (2005) 2521-2527

[24] K.S. Weil, C.A. Coyle, J.T. Darsell, G.G. Xia, J.S. Hardy; Effects of thermal cycling and thermal aging on the hermeticity and strength of silver- copper-oxide air brazed seals; J. of Pow.Sou. 152 (2005) 437-447

THE ALBERTA SALINE AQUIFER PROJECT (ABSTRACT)

James A. M. Thomson[1] and Stephan Broek[2]

[1] Norwest Corporation, 950 S. Cherry St., Suite 800, Denver, CO 80246, USA, [2] Hatch Ltd., 700, 840-7th Avenue S.W., Calgary, Alberta, T2P 3G2, Canada

ABSTRACT

Canada's oil and gas industry is centered in the province of Alberta. The Western Canadian Sedimentary Basin, which comprises most of the province, contains significant oil, gas, coal-bed methane, shale gas, and coal resources. The industrial heartland area, near Edmonton, contains large CO_2 emitters, including tar sands upgrading plants and coal fired power stations. The provincial and federal governments have created multiple initiatives to encourage research into, and practical application of geological carbon sequestration. Alberta is fortunate in having multiple large opportunities for enhanced oil recovery, CO_2 storage in depleted oil and gas reservoirs, and sequestration in saline aquifers. Potential sequestration sites may be near emission centers, or aligned along strategic pipeline corridors.

There is little experience to-date with CO2 injection into saline aquifers. The Alberta Saline Aquifer Project (ASAP), an initiative by Enbridge Inc., brought together multiple industry partners to prepare and execute a demonstration program for sequestration of CO_2 in a saline aquifer. This paper presents the high-level conclusions of Phase 1 of this study. The authors hope that other developers can learn from the framework of the ASAP project.

Coupled Processes during CO_2 Storage - Example of the Ketzin Pilot Site

Sonja Martens, Fabian Möller, Axel Liebscher, Stefan Lüth, Thomas Kempka, Andrea Förster, Michael Kühn; GFZ German Research Centre for Geosciences, Telegrafenberg, 14473 Potsdam, Germany

At Ketzin, near Berlin, the GFZ German Research Centre for Geosciences operates Europe's longest-running on-shore CO_2 storage site with the aim of increasing the understanding of geological storage of CO_2 in saline aquifers. The Ketzin field laboratory is Germany's first CO_2 storage site and fully in use since the injection started in June 2008. After 34 months of operation, about 48,500 tons of CO_2 have been injected. Monitoring at Ketzin integrates geological, geophysical, geochemical and microbiological investigations for a comprehensive characterization of the reservoir and the CO_2 migration at various scales. Integrating field and lab data, both static geological and dynamic flow modelling are conducted in different stages. Our presentation summarizes the key results.

CO_2 injection and monitoring

Research at Ketzin, funded by the EU project CO_2SINK and further national projects (e.g. CO_2MAN), began in April 2004 (Förster et al., 2006, Martens et al. 2011, Würdemann et al. 2010). Until 2004, natural gas was seasonally stored at about 280 m depth at Ketzin (Figure 1). The Ketzin anticline is therefore well studied. Based on these existing data as well as new exploration research from recent projects, three additional wells have been drilled in 2007 to depths of about 800 m for the CO_2 storage operation. One of these wells (CO_2 Ktzi 201/2007; abbrev. Ktzi) serves as an injection and observation well, while the other two (CO_2 Ktzi 200/2007, CO_2 Ktzi 202/2007; abbrev. Ktzi 200 and Ktzi 202) serve solely as observation wells for monitoring the injection and the subsurface migration of the CO_2 (Figure 2).
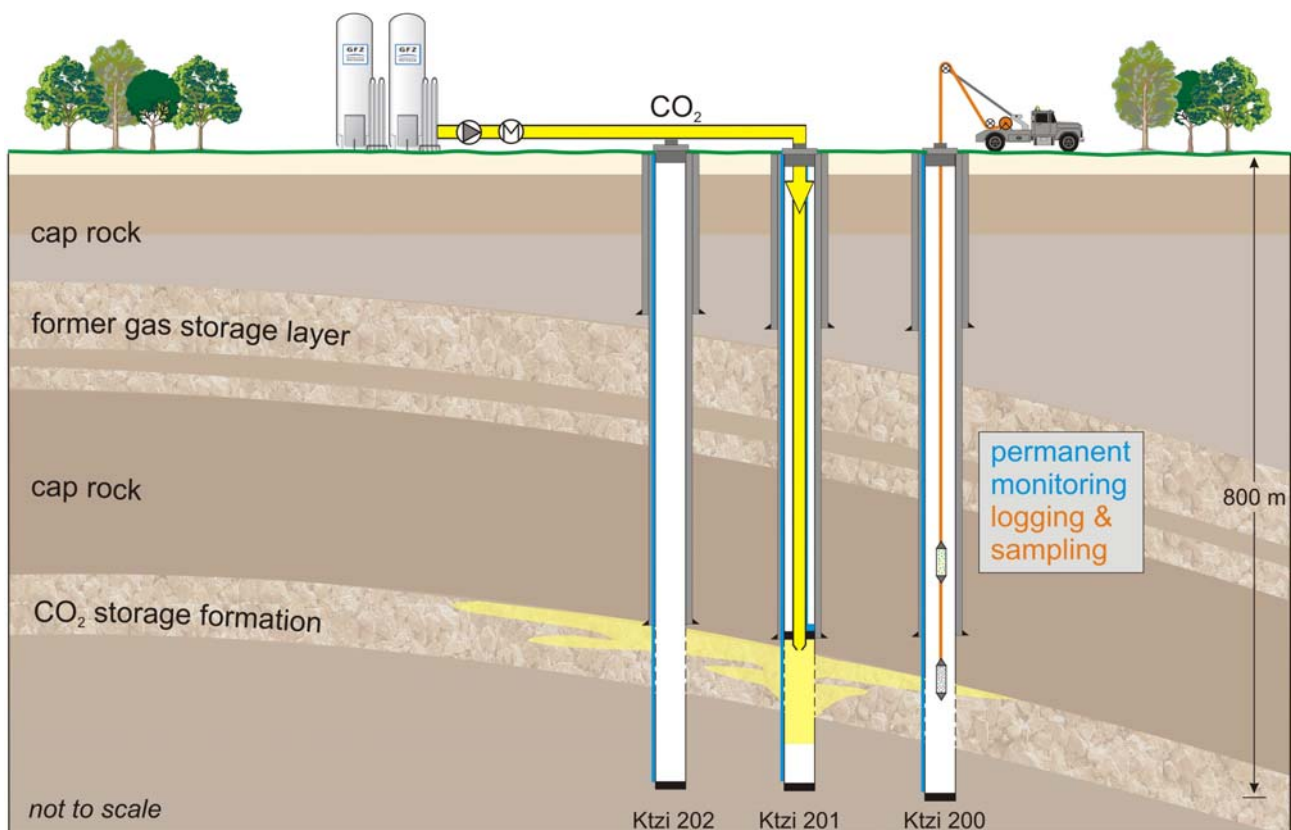
Figure 1: Schematic of the Ketzin anticline (dome structure) with three wells. Migration of CO_2 is indicated (yellow) within the reservoir beneath the cap rock.
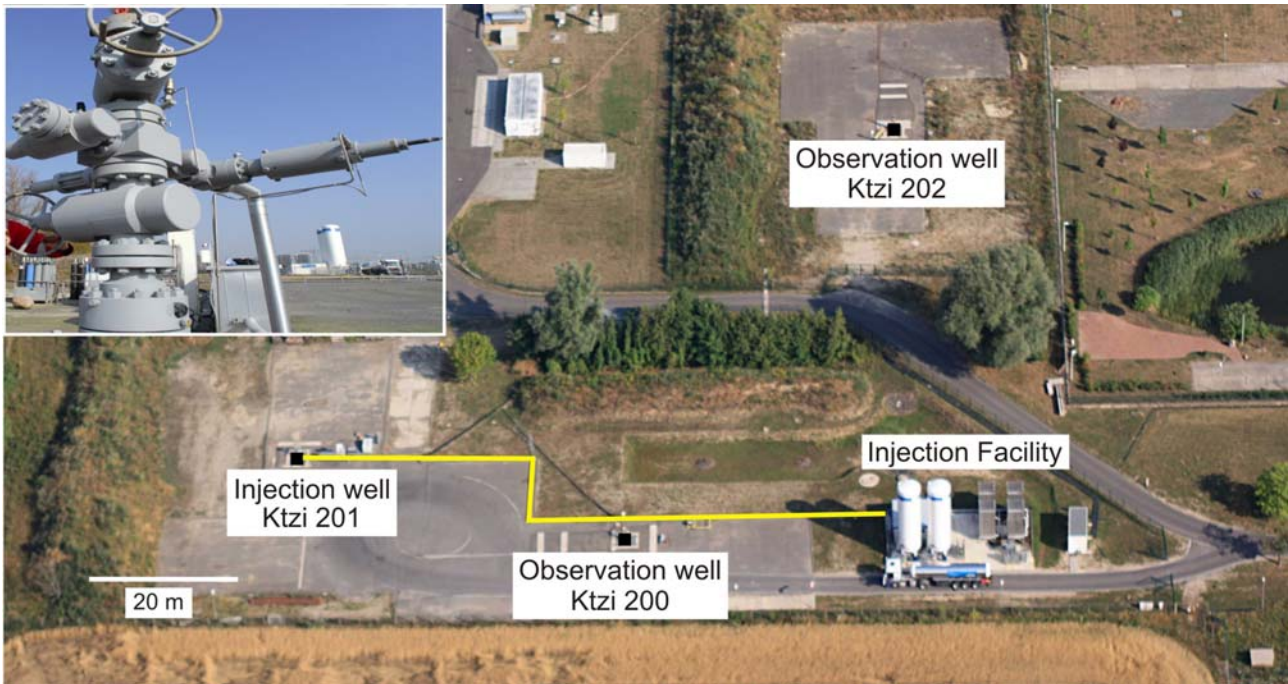
Figure 2: Aerial view of the Ketzin pilot site displaying the injection facility, the pipeline (yellow) from the storage tanks to the injection well (Ktzi 201) and both observations wells (Ktzi 200, 50 m away from injection; Ktzi 202, 112 m away from injection).

Since start of the CO_2 injection on June 30, 2008, the injection facility operates reliably and safely. By the end of April 2011 about 48,500 tons of CO_2 have been injected via the well Ktzi 201 into the target reservoir, a sandstone section of the Stuttgart Formation (Upper Triassic) at a depth of about 630 to 650 m. The Stuttgart Formation is lithologically heterogeneous consisting of fluvial sandstones and siltstones alternating with mudstones (Förster et al. 2010).

An interdisciplinary monitoring concept integrates geophysical, geochemical and microbial investigations at Ketzin (Giese et al. 2009). Following baseline measurements prior to the injection (Förster et al. 2006) repeat measurements are carried out for joint interpretations and a comprehensive characterization of the reservoir and the CO_2 migration process.

- Surface and down-hole geophysical measurements are applied to test and optimize the resolution of different methods and to visualize the CO_2 plume. Active seismic is spearheaded by time-lapse 3D monitoring, carried out in 2005 (baseline) and 2009. The CO_2 signature could be detected by an increased reflectivity at the top of the target reservoir, by a change in the attenuation behaviour and by a reduced propagation velocity within the reservoir (Lüth et al. 2011). After ~15 months of injection, the CO_2 plume was concentrated around the injection well with a lateral extent of ~ 300 to 400 m and a thickness of ~ 5 to 20 m. Quantifying the CO_2 imaged by the 3D seismic data is still challenging due to the relatively small CO_2 amount, the heterogeneous reservoir and the limited information on CO_2 saturation.

- Electric Resistivity Tomography (ERT) is another essential part of the monitoring concept. ERT is shown to be sensitive to saturation changes caused by the migration of the supercritical CO_2 within the originally brine-filled reservoir (Schmidt-Hattenberger et al. 2011). A time-lapse sequence from a permanently installed vertical electric resistivity array (VERA) in all three Ketzin wells shows a significant resistivity increase at the reservoir level since the beginning of the CO_2 injection.

- Temperature conditions in all wells are monitored using distributed temperature sensing. The temperature evolution within the injection interval, the CO_2 arrival and the evolution of two-phase P/T conditions in both observations wells are detected with high temporal and spatial resolution (Henninges et al. 2011).

Static and dynamic modelling of the Ketzin pilot site

All data available from the Ketzin wells and the different monitoring techniques are compiled in a geological model of the site. Geological modelling (Norden et al. 2010) and dynamic flow modelling (Kempka et al. 2010) are conducted in different stages, e.g. incorporating pre-existing data and information from drilling, monitoring and laboratory experiments. Integrating field and lab data, numerical modelling is currently conducted in order to investigate coupled processes in the Stuttgart Formation and its caprock taking into account hydrodynamics, thermodynamics, geochemistry and geomechanics.

Detailed static geological models were developed in the post-drilling phase already before start of the injection. This was in advance to the numerical models conducted (Kempka et al. 2010). The models were developed taking into account the heterogeneous lithological conditions in the Stuttgart formation. Here, the challenge was geological modelling of the alternating sequences of sandy string-facies and muddy floodplain-facies rocks. For that purpose, a diversity of information from local and regional origin was incorporated and combined in a geological model. The facies modelling, yielding the distribution of high permeable sand-channels throughout the floodplain-facies rocks were produced using stochastic modelling. The geometry of the fluvial channel belts was modelled using an object modelling code. Subsequent to the facies modelling process, the petrophysical modelling of permeability and porosity within each facies was carried out, including lateral variability in properties.

These models were applied for dynamic flow simulations. The arrival time of CO_2 at the first observation well (Ktzi 200) was successfully matched. The calculated results for the arrival of the gaseous CO_2 varied between 8 and 17% for the simulators applied compared to measured 21 days which is in fairly good agreement. However, the arrival time at the second observation well (Ktzi 202) was predicted much earlier, after 60 - 80 days, compared to the observation of 271 days. Question then was what the reason is for the unpredicted observation.

Due to the fact that efficient history matching requires an integrated iterative modelling framework, the Ketzin model was set up anew. Operational as well as monitoring data were integrated: (1) We used literature data of fluvial systems for characterisation. (2) The attribute analysis based on 3D seismic for the Stuttgart formation was taken into account as well. (3) 4D seismic results were used to involve the CO_2 distribution into the interpretation. (4) Measurements with the permanently installed electrodes provide resistivity data and information about the state of saturation. (5) Pulse neutron gamma tests in the wells provide additional information about the state of saturation.

All the revised data lead to an updated facies model of the Stuttgart formation. Regional trends and information about channel geometry were taken from the literature. Based on the logs the sand and clay content of the formations were revised. Seismics provide information about the structure of the Stuttgart formation and the channels around the wells. Next step was to update the petrophysical data and to integrate all the knowledge from the observation.

At first, the static geological model is validated by dynamic simulations of the pressure development. Result is that the simulated and observed pressure data coincide very well. Second, the model is as well in very good agreement with observed arrival times of the CO_2 in both the observation wells. Current modelling activities involve the investigation of coupled processes at Ketzin by geochemical and geomechanical modelling.

Conclusion and outlook

The Ketzin project is thus far the only active CO_2 storage site in Germany and demonstrates successful CO_2 storage and interdisciplinary monitoring in a saline aquifer on a research scale. The gained results underline the necessity for further storage projects on a demonstration scale.

The CO_2SINK project ended in March 2010. CO_2 injection, complementary monitoring and modelling with a particular focus on abandonment continue at Ketzin. Two projects CO_2MAN (CO_2 Reservoir Management, funded by the Federal Ministry of Education and Research) and CO_2CARE (CO_2 Site Closure Assessment Research, funded by the EU) succeed CO_2SINK.

References

Förster, A., Norden, B., Zinck-Jørgensen, K., Frykman, P., Kulenkampff, J., Spangenberg, E., Erzinger, J., Zimmer, M., Kopp, J., Borm, G., Juhlin, C., Cosma, C., Hurter, S. (2006): Baseline characterization of the CO_2SINK geological storage site at Ketzin, Germany: Environmental Geosciences, 13 (3), 145-161. doi:10.1306/eg.02080605016.

Förster A., Schöner R., Förster H.-J., Norden B., Blaschke A.-W., Luckert J., Beutler G., Gaupp R., Rhede D. (2010): Reservoir characterization of a CO_2 storage aquifer: The Upper Triassic Stuttgart Formation in the Northeast German Basin Marine and Petroleum Geology, 27 (10), 2156-2172, doi:10.1016/j.marpetgeo.2010.07.010.

Giese, R., Henninges, J., Lüth, S., Morozova, D., Schmidt-Hattenberger, C., Würdemann, H., Zimmer, M., Cosma, C., Juhlin., C. and CO_2SINK Group (2009): Monitoring at the CO_2SINK Site: A Concept Integrating Geophysics, Geochemistry and Microbiology. Energy Procedia 1, 2251-2259.

Henninges J., Liebscher A., Bannach A., Brandt W., Hurter S., Köhler S., Möller, F., CO_2SINK Group (2011): P-T-ρ and two-phase fluid conditions with inverted density profile in observation wells at the CO_2 storage site at Ketzin (Germany). Energy Procedia, 4, 6085-6090, doi:10.1016/j.egypro.2011.02.614.

Kempka T., Kühn M., Class H., Frykman P., Kopp A., Nielsen C.M., Probst P. (2010): Modeling of CO_2 arrival time at Ketzin – Part I., Int. J. Greenhouse Gas Control, 4 (6), 1007-1015, doi:10.1016/j.ijggc.2010.07.005.

Lüth S., Bergmann P., Giese R., Götz J., Ivanova A., Juhlin C., Cosma C. (2011): Time-Lapse Seismic Surface and Down-Hole Measurements for Monitoring CO_2 Storage in the CO_2SINK Project (Ketzin, Germany). Energy Procedia, 4, 3435-3442, doi:10.1016/j.egypro.2011.02.268.

Martens S., Liebscher A., Möller F., Würdemann H., Schilling F., Kühn M., Ketzin Group (2011): Progress Report on the First European on-shore CO_2 Storage Site at Ketzin (Germany) - Second Year of Injection. Energy Procedia, 4, 3246-3253, doi:10.1016/j.egypro.2011.02.243.

Norden B., Förster A., Vu-Hoang D., Marcelis F., Springer N., Le Ni I. (2010): Lithological and petrophysical core-log interpretation in CO_2SINK, the European CO_2 onshore research storage and verification project, SPE Reservoir Evaluation & Engineering, 13 (2), 179-192.

Schmidt-Hattenberger C., Bergmann P., Kiessling D., Krueger K., Rücker C., Schuett H., Ketzin Group (2011): Application of a Vertical Electrical Resistivity Array (VERA) for Monitoring CO_2 Migration at the Ketzin Test Site: First Performance Evaluation. Energy Procedia, 4, 3363-3370, doi:10.1016/j.egypro.2011.02.258.

Würdemann H., Möller F., Kühn M., Heidug W., Christensen N.P., Borm G., Schilling F.R., the CO_2SINK Group (2010): CO_2SINK - From site characterisation and risk assessment to monitoring and verification: One year of operational experience with the field laboratory for CO_2 storage at Ketzin, Germany. Int. J. Greenhouse Gas Control, 4 (6), 938-951, doi:10.1016/j.ijggc.2010.08.010.

Wednesday, June 22, 2011

Technology development for IGCC with CCS

Mark Prins, Rob van den Berg, Evert van Holthoon (Gasification Technology)

Eva van Dorst, Frank Geuzebroek (Gas Separation &Treating)

Shell Projects and Technology, Amsterdam, Netherlands

1. Introduction

Legislation will soon require more efficient plants and significant carbon capture & sequestration (CCS) capabilities. Pre-combustion CCS has a natural fit with Shell's technology portfolio, in view of the strong position of its entrained flow gasification technology. The first application of the Shell Coal Gasification Process (SCGP) has been in the 250 MW power plant in Buggenum, the Netherlands; details may be found in Appendix A. IGCC schemes based on SCGP have desirable environmental characteristics [1]: very low sulphur and NO_x emissions, and smaller cooling water requirements than coal boilers with steam cycle. Produced syngas has high partial pressure of carbon monoxide; after shifting to carbon dioxide, CCS is relatively easy.

The purpose of this paper is to show how the high coal-to-power efficiencies of IGCC can be further improved, and the efficiency penalty incurred for pre-combustion removal of CO_2 minimized. This requires improved technologies; the steps needed to develop such technologies, by Shell and by others, are explained in detail.

2. IGCC with and without CCS

Figure 1 shows a typical IGCC process scheme. An IGCC plant requires additional units for CCS (coloured orange). Firstly, the syngas is shifted with steam:
$CO + H_2O = CO_2 + H_2$

CO_2 is removed/compressed, and the gas turbine is fired with hydrogen-rich syngas. An in-house feasibility study has been carried out, based on commercial and near-commercial technologies (see next section). Methodology: modelling of the gasifier using in-house design tools; modelling of the Water Gas Shift and gas treatment units in flowsheeters; configuring the Combined Cycle Power Plant (CCPP) in GT Pro. ISO conditions were applied with condenser pressure of 40 mbar (a). Generator losses of 0.2% were taken into account; the gas turbine was fully loaded. The steam cycle was optimized by low-level heat integration (low stack temperatures).

2nd Int. Conference on Energy Process Engineering Efficient Carbon Capture for Coal Power Plants
June 20 - 22, 2011 in Frankfurt/Main, Germany

150

Table 1: IGCC power plant with and without CCS; based on 2 gasification strings

	IGCC	IGCC + 90% CCS
Total plant fuel input (MWth, LHV)	2166.3	2610.0
Gas Turbines power output (MW)	720.6	816.6
Steam Turbines power output (MW)	475.2	525.6
Plant power output, gross (MW)	1195.8	1342.2
Auxiliary Power (MW)	145.1	259.9
Plant power output, net (MW)	1050.7	1082.3
Gross Efficiency (%)	55.20	51.42
Net Efficiency (%)	48.50	41.47

The results are summarized in Table 1. Without capture, today's efficiency in Buggenum of 43% can be improved by more than 5% (points). With long-term technology improvements (e.g. in gas turbines; using construction materials that are already available), over 50% is expected to be possible. For a plant with 90% CO2 capture, the 40% efficiency barrier can be surpassed, and the penalty of carbon capture limited to 7%. This presents a significant improvement over other studies with a penalty in the range of 9-11%, based on conventional capture technologies. E.g. the Electric Power Research Institute reported a drop of 9% [3]. For comparison: post-combustion capture has a higher penalty of 11-13%, depending on technology, partial pressure of carbon dioxide, and conditions for amine regeneration.
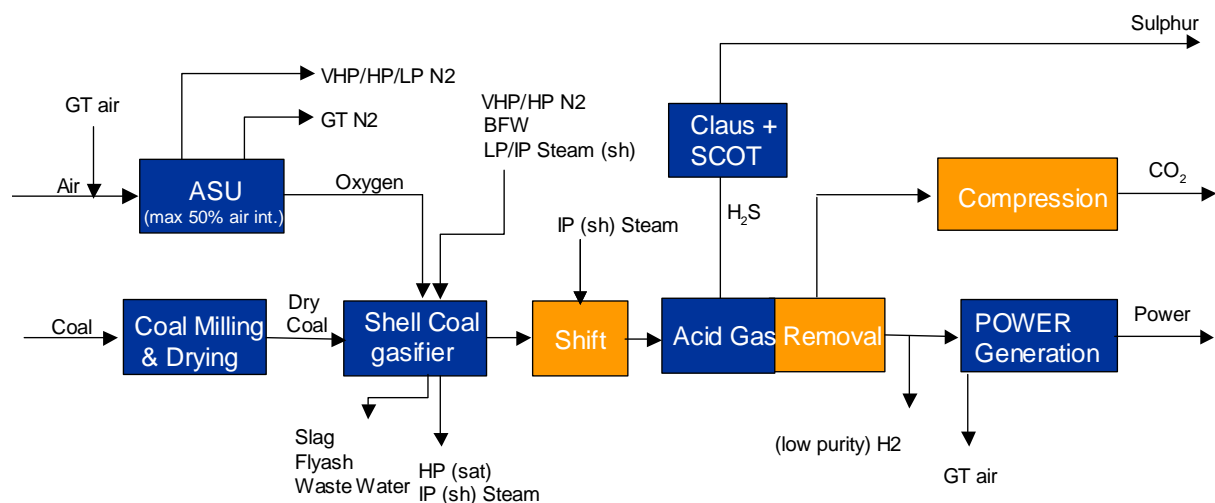
Figure 1: IGCC process scheme with carbon dioxide separation and compression

2nd Int. Conference on Energy Process Engineering Efficient Carbon Capture for Coal Power Plants
June 20 - 22, 2011 in Frankfurt/Main, Germany

151

3. Technology development

3.1 SCGP gasifier

The IGCC study is based on an SCGP employing 6 coal burners. This results in a significant capacity increase since the 1993 Buggenum SCGP, with 4 burners. The operating pressure is higher and matches with novel gas turbines. The syngas cooler is designed for maximum production of high-pressure, saturated steam; superheating in the HRSG of the CCPP.

3.2 Water Gas Shift

A novel low-steam CO sour WGS process is introduced in this study. It is based on the principle of using steam as the limiting reactant. A process using a sulphur-tolerant water-gas shift catalyst (that suppresses methanation) has been installed and commercially proven at several SCGP licensee sites.

The unit is conveniently located immediately after the SCGP, which includes a low-temperature water scrubber that moisturizes the syngas. In a conventional High Temperature Shift / Low Temperature Shift design, a large amount of steam is added for temperature control. This negatively impacts IGCC efficiency and leads to a large amount of water in the product gas, that has to be knocked out.

3.3 Sulphur removal

The THIOPAQ^{TM} biological desulphurization process is selected for removing H_2S from the shifted syngas. It enables direct production of elemental sulphur, replacing Shell's Sulfinol process & Claus/SCOT unit applied at the Buggenum plant. The process combines a high-pressure absorber and a low-pressure bioreactor.

In the absorber, H_2S and part of CO_2 are removed from the sour gas by an alkaline solvent. High H_2S removal efficiency can be achieved, as the solvent entering the absorber is lean in H_2S. The absorption proceeds according to these reactions:

$$H_2S + CO_3^{2-} \Rightarrow HS^- + HCO_3^-$$

$$CO_2 + CO_3^{2-} \Leftrightarrow 2HCO_3^-$$
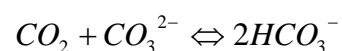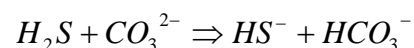
In the above reaction, alkalinity is consumed. This alkalinity consumption is compensated by the oxidation of H_2S to elemental sulphur in the bioreactor. It proceeds under oxygen controlled conditions according to the following reactions:

2nd Int. Conference on Energy Process Engineering Efficient Carbon Capture for Coal Power Plants
June 20 - 22, 2011 in Frankfurt/Main, Germany

152

$$HS^- + \tfrac{1}{2}O_2 + HCO_3^- \Rightarrow S^O + CO_3^{2-} + H_2O$$

$$2HCO_3^- \Leftrightarrow CO_3^{2-} + H_2O + CO_2$$
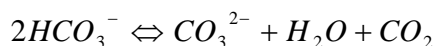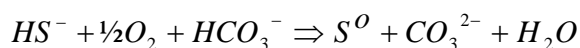
The THIOPAQ^{TM} process has been licensed many times for natural gas; we expect to demonstrate its suitability for industrial syngas soon.

3.4 Carbon dioxide removal and compression

ADIP-X was selected as the solvent because of the good CO_2 removal kinetics in the absorber, the high CO_2 carrying capacity and the low viscosity. It combines the benefits of a chemical solvent (high purity of absorbed CO_2) and physical solvent (low amount of heat for regeneration). ADIP-X is a mixture of the tertiary amine N-methyl di-ethanol amine (MDEA), the secondary diethylene di-ethanol amine (piperazine) and water. Staged flash regeneration is applied with pre-heating of the fat solvent at relatively low temperature (<100°C). This allows low value heat sources to be utilized (e.g. from the hot syngas ex WGS and the CO_2 compressor intercoolers), and maximises the amount of CO_2 flashed-off at around 5 bar. The latter stream bypasses the first compression stage(s), minimising required compression power. CO_2 is conditioned and compressed to 120 bar, for sequestration. The CO_2 compressor is multi-stage with intercooling, and has a polytropic efficiency of 80% (in line with [2]).

3.5 Gas turbine

A modern G-class gas turbine, already available for syngas in the US 60 Hz market, is selected for this study. It achieves a combined cycle efficiency of over 59%, a significant improvement over the E-class gas turbine used in the Buggenum IGCC and today's F-class gas turbines [4]. The trend continues in the future: increasing Turbine Inlet Temperatures, enabled by improved materials of construction, in combination with higher compression ratios. More gas turbines shall be modified for hydrogen firing, as vendors know how to handle the high burning velocity of hydrogen (e.g. by modified burners, blade cooling and/or exhaust gas recirculation).

Air side integration with ASU was not considered, to keep the IGCC flexible. Fuel gas humidification and nitrogen dilution was applied in order to achieve NOx emissions below 25 ppm. For stricter emission targets, it is recommended to use a catalytic de-NOx unit incorporated into the HRSG.

2nd Int. Conference on Energy Process Engineering Efficient Carbon Capture for Coal Power Plants
June 20 - 22, 2011 in Frankfurt/Main, Germany

153

4. Conclusions and recommendations

For IGCC applications, the Shell Coal Gasification Process offers high thermal efficiency and feedstock flexibility. The process has been fully proven and its development continues, together with the development of larger, more efficient gas turbines. Near-commercial technology can push IGCC coal-to-power efficiency above 48%. The penalty for pre-combustion CO_2 removal can be minimized to only 7%, which widens the efficiency gap with post combustion CCS solutions.

These results stress the importance of R&D (both on a medium and long term) and commercialisation pathways needed to realise the required improvements. Shell's commitment to Clean Coal Energy and combined expertise in coal gasification, gas treating, syngas conversion, carbon capture and storage as well as enhanced oil/gas recovery contribute to make zero emission power a reality.

References

1. H.J. van der Ploeg, T. Chhoa, P.L Zuideveld. The Shell Coal Gasification Process for the US industry. Gasification Technology Conference, Washington DC, October 2004.
2. C. Chen, E.S. Rubin. CO_2 control technology effects on IGCC plant performance and cost. Energy Policy 37 (2009) 915-924.
3. G. Booras, N. Holt, R. Schoff. EPRI IGCC Study Cost and Performance Results. Gasification Technology Conference, Washington DC, October 2008.
4. Single train IGCC of 400 MWe and 46%+ efficiency. Public study by Shell Internationale Petroleum Maatschappij, General Electric Company, GEC Alsthom, Air Liquide, 1996.

2nd Int. Conference on Energy Process Engineering Efficient Carbon Capture for Coal Power Plants
June 20 - 22, 2011 in Frankfurt/Main, Germany

154

APPENDIX A: Shell Coal Gasification Process

The Shell Coal Gasification Process (SCGP) is an entrained flow type of a gasifier, which uses a dry feed system. Coal is pulverized and dried to 2% moisture before being pressurized with nitrogen or CO_2 in lock hoppers. The gasification pressure is commercially proven up to around 45 bar and the operating temperature may well exceed 1500°C. To control the inner gasifier wall temperature, water is circulated in a membrane wall to generate steam for utilization in the power cycle. The ash is converted to slag, of which the majority leaves the gasifier in a liquid flow via the bottom and is solidified in a water bath, whereas the rest is entrained in the hot gas flow. In the standard SCGP line-up, this gas is cooled to 800-900°C by adding cold recycled quench gas into the hot gas stream, which allows molten slag particles to solidify and prevents these from hitting the quench pipe wall. After the quench, the sensible heat of the raw syngas is recovered in a syngas cooler (SGC), which cools the gas down to 340-360°C. In this syngas cooler, HP/MP steam is raised which may be used in a combined cycle for electricity generation. A dry solids removal system with candle filters separates out the flyash. Finally, a wet scrubbing system removes any remaining particles down to a very low level and also other impurities such as halides. Figure A.1 shows the overall SCGP process scheme.
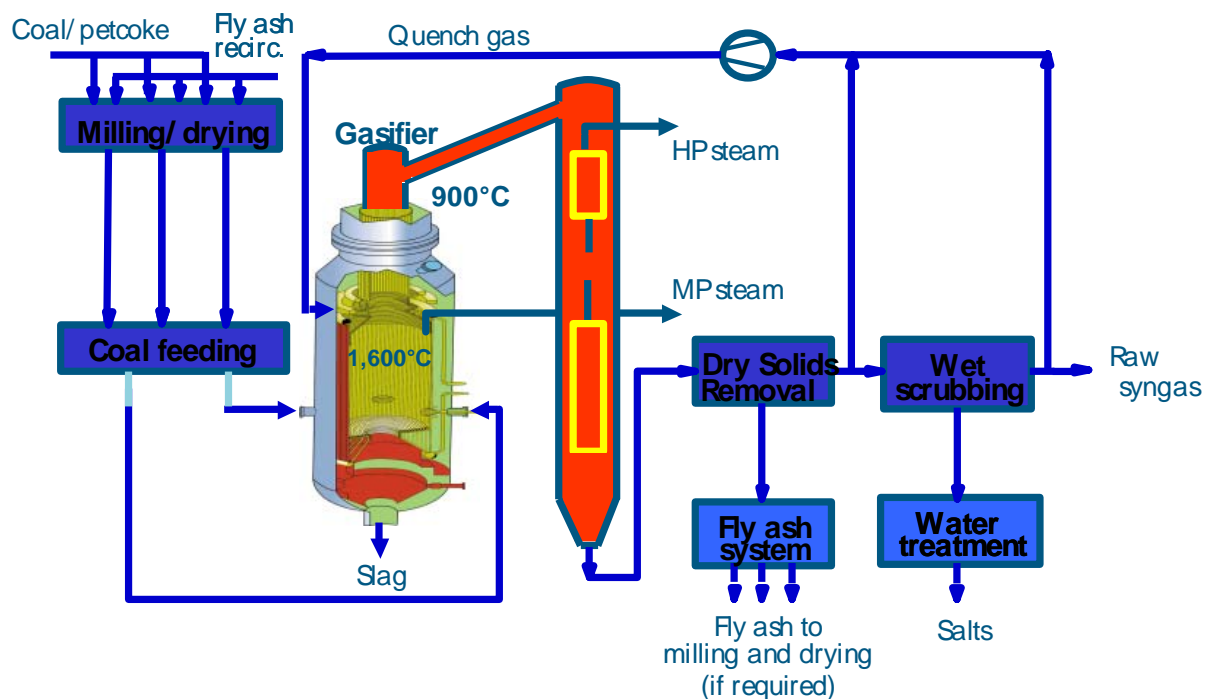
Figure A.1: Overview of Shell Coal Gasification Process

2nd Int. Conference on Energy Process Engineering Efficient Carbon Capture for Coal Power Plants June 20 - 22, 2011 in Frankfurt/Main, Germany

155

The SCGP has several key features, which are essential for successful IGCC application:

- Dry feeding system: coal is transferred with carrier gas (usually nitrogen, although carbon dioxide may also be used) to the gasifier. A high gasification efficiency is thus achieved, typically 4-5% higher than gasification of water slurries. This is essential for the economics of IGCC, in which every percentage point counts. It is also of great importance for Carbon Capture and Sequestration, as the minimum amount of CO_2 per kWh is produced and needs to be sequestered.

- Multiple burners: whereas other gasifiers use only a single burner, the SCGP has multiple side-fired burners. This allows scale-up to large gasifiers that can fuel the world's largest gas turbines, even under cold environmental conditions.

- Membrane wall: whereas other gasifiers use a refractory lined vessel, the SCGP has a water-cooled membrane wall. This allows firing at higher temperatures, which means that virtually any type of fuel has been successfully gasified, offering maximum fuel flexibility. The SCGP also has high operating flexibility with respect to short-term coal quality changes. Furthermore, the conversion of coal/coke is almost complete (carbon conversion >99%), so that fuel costs are low.

- Heat recovery from the hot syngas: a typical energy balance is shown in Figure 2. As noted, the cold gas efficiency is very high (82%); the rest of the energy contained in the solid fuel is converted into heat, but the largest part of this is recovered as useful steam. This steam may be routed to the Combined Cycle Power Plant (CCPP), to ensure optimal coal-to-power efficiency.

- Dry solids removal: flyash is removed in candle filters. Compared to other gasification processes, in which flyash is removed as a water slurry, this limits water usage and optimizes environmental performance.

- High availability and low maintenance cost owing to the robustness of the membrane wall gasifier (designed for 25-year life time) and the long lifetime of

2nd Int. Conference on Energy Process Engineering Efficient Carbon Capture for Coal Power Plants
June 20 - 22, 2011 in Frankfurt/Main, Germany

156

coal burners (every two years, the burners get a complete overhaul and are ready for the next operating period).

The first demonstration of the SCGP has been in the Integrated Gasification Combined-Cycle (IGCC) power plant, located in Buggenum, the Netherlands. The power plant was built by Demkolec BV and started up in 1993. It has been in commercial operation since 1998, gasifying 2,000 ton/day coal producing $4.0 \ 10^6$ Nm^3 syngas. Thermal input of coal intake amounts to 585 MW, with gross output of 284 MW (156 MW from gas turbine, 128 MW from steam turbine) and net output of 253 MW. This corresponds to 43% LHV efficiency.

This IGCC demonstration was the first large-scale project in Europe, a major milestone for combining a chemical plant (gasification) with a power plant (CCPP). It employs a Siemens V94.2 gas turbine with a maximum integrated Air Separation Unit (ASU) from Air Products. The gas turbine, steam turbine and generator have been designed as single shaft. Gas treating is accomplished with Shell Sulfinol-M (MDEA based solvent) for >99% sulphur removal. Coals can be switched ''on-the-fly'' and co-feed of biomass and bio sludge have been run successfully. Gasification pressures and temperatures are 25-28 bar and 1500^{0}C. Solidified molten slag, flyash and sulphur are recovered as saleable by-products. The plant is presently owned and operated by NUON. Many lessons have been learned to improve its operation, fuel flexibility, and availability, to the benefit of future power plants.

2nd Int. Conference on Energy Process Engineering Efficient Carbon Capture for Coal Power Plants June 20 - 22, 2011 in Frankfurt/Main, Germany

157

An Improved SELEXOL™ Processing Scheme Reduces CO$_2$ Capture and Compression Costs

Robin Matton
UOP NV (A Honeywell Company), Antwerpen, Belgium
Raj Palla
UOP LLC (A Honeywell Company), Des Plaines, USA

Abstract

Gasification industry is starting to require more and more stringent specifications on the CO2 stream impurities. In a typical gasification Selexol design for segregated H2S and CO2 removal into their respective purified streams, the CO2 produced is at a reasonable pressures but still requires large amount of compression for geologic sequestration or enhanced oil recovery (EOR) applications. The captured CO2 stream may contain up to five percent of impurities that can be recovered. Some of the components in the CO2 streams currently considered as a regulated HAP pollutants. This CO2 compression has been found to be single most energy sink compared to all other elements in the gasification complex. Meeting the CO2 purity requirements with conventional systems is cost-prohibitive.

UOP is working on few innovative schemes that will reduce capture and compression costs compared to the conventional designs. The new processing not only reduces the capture and compression costs but also meets continuous CO2 venting requirements in case of emergency. This paper will describes some of the characteristics of the applied flow schemes and provide details on the acid gas removal and CO2 capture economics.

CO$_2$ Absorption Pilot Plant – Design, Commissioning, Operational Experience, and Applications

Agnes von Garnier, Dr. Andreas Orth, and Tobias Stefan; Outotec GmbH, 61440 Oberursel, Germany; Dr. Volker Giese and Raquel Fernández Rodiles, BASF SE, 67056 Ludwigshafen, Germany

Introduction

Outotec has recently commissioned its new CO$_2$ absorption pilot plant at its R&D center in Frankfurt am Main, Germany. The pilot plant applies BASF's licensed aMDEA^{TM} technology for acid gas removal to remove CO$_2$ and H$_2$S from metallurgical process gas. It complements Outotec's circulating fluidized bed (CFB) pilot plant allowing for the treatment of process gas from coal and biomass gasification as well as from iron ore direct reduction.

The CO$_2$ absorption plant was planned to demonstrate Outotec's proprietary Circofer$^®$ process for the direct reduction of iron ore fines based on coal. The fluidized bed based Circofer process offers the opportunity of using raw materials such as iron ore fines and coal, avoiding capital-intensive agglomeration processes and coke making. Coal is partly combusted with oxygen to provide the required heat, and it also serves as reduction agent. The gas leaving the CFB reactor is dedusted and washed to remove CO$_2$ to below 1%. The remaining carbon monoxide and hydrogen are recycled as reduction gas to the CFB.

Integration into the 700 mm CFB pilot plant

The CFB pilot plant at Outotec's R&D Center in Frankfurt is suited for gasification and combustion of any kind of feedstock, as well as for direct reduction of iron ore fines. Its core is a CFB reactor with 700 mm inner diameter. Both, a wet and a dry gas cleaning allow a very flexible operation of the plant in. Fig. 1 shows the setup under reducing conditions for the Circofer process. Fine grained iron ore is fed to the CFB reactor together with fine coal and oxygen and the solids are fluidized with a hydrogen- nitrogen-gas mixture. In order to maintain the CFB at the desired temperature of about 950°C, char particles are recycled via cyclone 1 into a heat generator, mixed with fresh coal and partly combusted with oxygen. The mixture serves as heat carrier to the CFB and the solid carbon is used as reduction agent. In a second cyclone dust is separated and recycled directly to the CFB. The remaining offgas is cooled in the evaporation cooler and dedusted in the radial flow scrubber.

Previously, the off gases were burnt in the after burning chamber and hydrogen from a trailer was used to simulate the process gas recycle. The new CO_2 absorption plant allows now to recycle the process gas, mainly H_2 and CO, in a closed loop into to CFB reactor, thus eliminating the need for hydrogen from external sources.
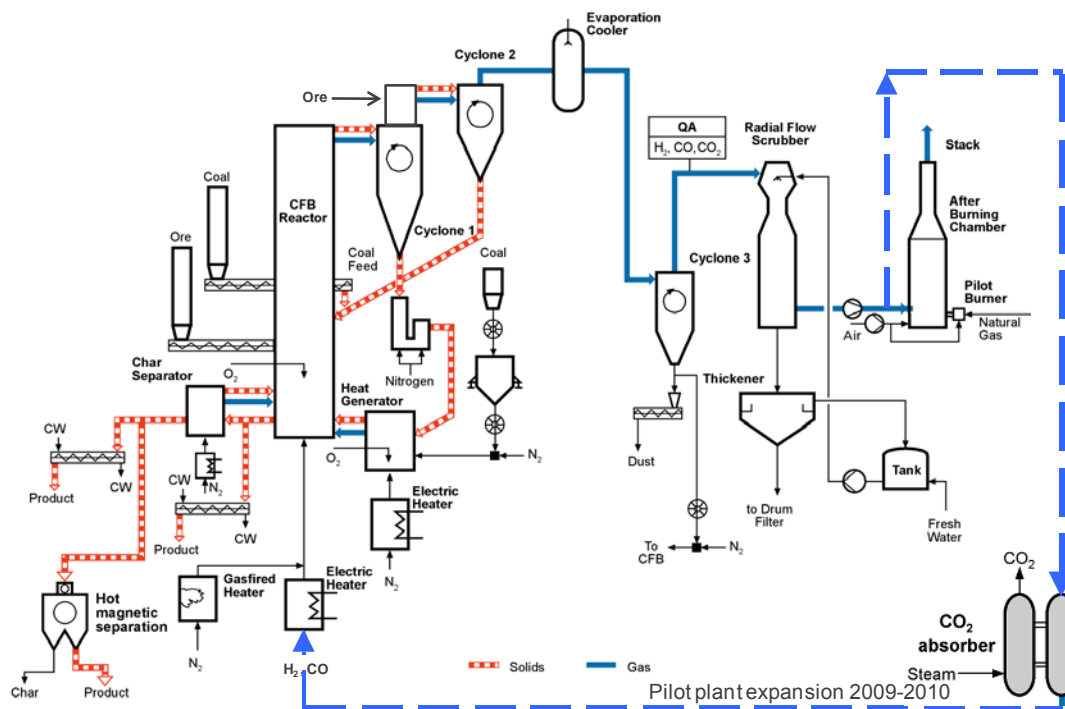
Fig. 1: The 700 mm CFB pilot plant modified for Circofer operation mode including the new CO_2 absorption plant.

Design of the CO_2 absorption pilot plant

For a close reproduction of the industrial scale Circofer® process, the gas leaving the 700 mm CFB pilot plant after the Radial Flow Scrubber and the ID fan at atmospheric pressure is compressed to approximately 500 kPag. A liquid ring compressor was chosen as it is not very sensitive to remaining dust and tar particles in the cleaned gas. Subsequently, the gas is additionally scrubbed and cooled before entering the two-stage absorber in which CO_2 and H_2S are absorbed by an aqueous aMDEA^{TM} solution. Process gas leaving the absorber, mainly consisting of CO, H_2 and N_2, is recycled to the CFB plant via a droplet separator. The washing solution is depressurized to partly degas the CO_2 before entering the regenerator column. The main regeneration is achieved by heating the solution in the kettle-type reboiler which is designed as a bypass of the regenerator. As no steam network is available on site an electrically heated reboiler is used. The washing solution circulates between the

two absorbers and the regenerator passing an internal heat exchanger. A part of the recycled solution is led through a series of mechanical and activated carbon filters to remove tar and remaining dust particles. The removed CO_2 rich gas leaves the desorber unit to an after burning chamber after condensation of the water vapor.

Fig. 2: Flowsheet of the CO_2 absorption plant.

Commissioning and first operational experience

The pilot plant was successfully tested on up to 750 Nm³/h tar and dust loaded process gas from the gasification of coal achieving a CO_2 removal efficiency of over 80%. The content of CO_2 in the dry incoming gas was significantly higher than the design case. The high tar load of the gasification gas led to a significant dark coloration of the aMDEA solution and to solid residues during the initial phases of the tests. The mechanical filter and the activated carbon filter removed the dissolved impurities so that the recycled solution was observably clear again.

During Circofer operation the recycled process gas contained less than 0.5% CO_2 after scrubbing, corresponding to a CO_2 removal rate of over 95%. 100 Nm³/h of recycle gas were introduced in the CFB via an electric gas heater while additional N_2 was provided to achieve sufficient fluidization.

Tab. 1: Typical operational data during operation with Circofer.

Gas		after Liqid Ring Compr.	after CO_2 Absorp. Unit
Temperature	°C	50	35
Pressure	kPag	450	440
Volume Flow	Nm³/h	400	300
Gas Composition (dry)			
CO_2	%-vol.	13.5	0.3
CO	%-vol.	12.1	13.0
H_2	%-vol.	12.2	15.0
CH_4	%-vol.	1.0	0.8
O_2	%-vol.	0.1	0.5
N_2	%-vol.	Balance	Balance
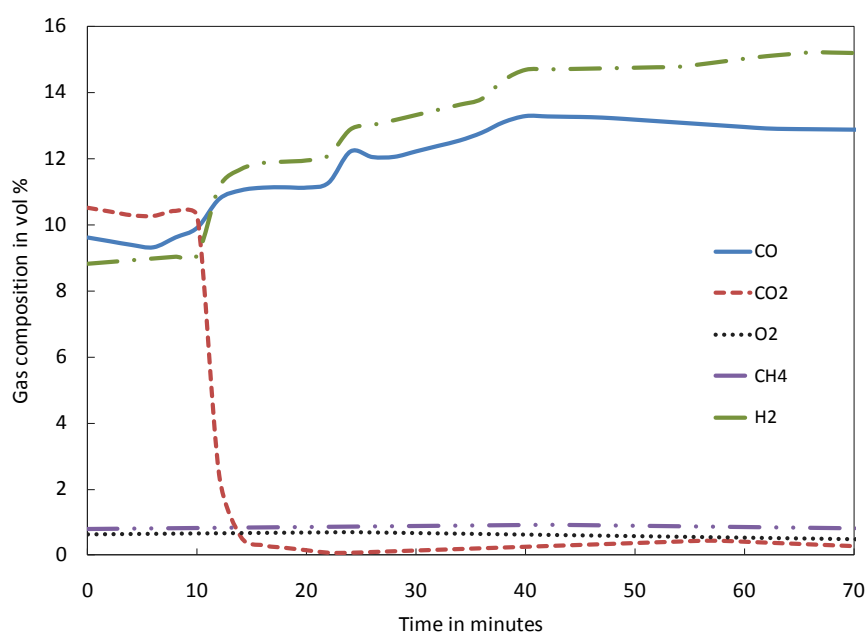
Fig. 3: Typical transient behavior of gas composition when bringing CO_2 scrubbing plant online.

Conclusion and further applications

The CO_2 absorption plant complements the CFB pilot plant allowing for the cleaning of process gas from iron ore direct reduction as well as from coal and biomass gasification. The facility also features integrated gas cleaning steps allowing for the treatment of pressurized gases rich in dust and tars. This makes it a unique facility for testing CO_2 absorption under real process conditions similar to an industrial plant. The removed gases can be used in other processes or for underground storage as envisaged in carbon capture and storage (CCS) approaches. The new pilot plant also plays an important role in the development of the company's sustainable technologies for the growing energy industry providing the testing facilities to reduce the carbon footprint of coal and biomass based energy production as well as of the oil winning from oil shale according to the new Enefit280 process.

CO$_2$-Capture in Combined
Solid Oxide Fuel Cell (SOFC)-Gasification-Cycles
by Water Vapour Condensation

Prof. Dr. techn. Reinhard Leithner, Dipl.-Ing. Christian Schlitzberger
Institut für Wärme und Brennstofftechnik, Technische Universität Braunschweig,
Germany (www.wbt.ing.tu-bs.de, E-Mail: r.leithner@tu-bs.de)

Abstract

Increasing energy demands, limited resources, pollutants- and CO$_2$-emissions caused by the use of fossil fuels require a more efficient and sustainable energy production. Due to their high electrical efficiencies as well as fuel and application flexibility, Solid Oxide Fuel Cells (SOFC) offer a great potential to meet future energy demands. The fuel gases hydrogen and carbon monoxide, which are electrochemically convertible in SOFCs have to be generated by reforming or gasification of hydrocarbons. The combination of an allothermal gasifier with a SOFC represents an innovative concept for high efficient hydrocarbon based power generation.

In this combination, the gasifier, using recycled anode off gas or steam at least during start up as gasification agent, is heated by the waste heat of the SOFC, transferred e.g. via heat pipes. The produced H$_2$- and CO-rich syngas is passed through the fuel cell, generating electrical energy. This mass flow and thermal coupling of the SOFC and the endothermic steam gasification process is called chemical heat pump. Depending on the fuels used, system efficiencies of about 60 % can be achieved, even though the SOFC itself reaches only an electrical efficiency of approximately 50 %. Additionally, due to an innovative cascaded SOFC-design, resulting in high fuel utilization of 90 % and higher, a post-combustion of the off gases is not longer necessary. Because of the SOFC membrane allowing only an oxygen-ion flow and the SOFC design without the mixing of anode and cathode exhaust gas flows, an effective CO$_2$-separation without efficiency loss can be realized by simply condensing the water vapor in the anode off gas. Applying a combined water-gas-shift-membrane-reactor in front of the condenser the CO remaining in the anode off gas is converted into H$_2$, which is separated from the anode off gas using a palladium-membrane. The water vapor which is needed as gasification agent or the fuel flow through the other side of the membrane-reactor and recycle the H2 into the gasification process.

The aim of the presented work was to show a first dimensioning of such a combined cycle and its energetic analysis concerning operation and feasibility. With the program ENBIPRO developed at the IWBT of TU Braunschweig for general cycle simulation purposes, the theoretical feasibility of the concept and a high electrical efficiency of about 60 % including CO$_2$-separation were proven.

Introduction

The need/wish to sequestrate CO$_2$ is based on the assumption put forward by the International Panel of Climate Change (IPCC) that CO$_2$ may be the major driving force in climatic changes, which means that especially the anthropogenic CO$_2$ emissions resulting from the combustion of fossil fuels like coal, oil and natural gas will increase the atmospheric CO$_2$-content, which in turn will lead to higher temperatures in the atmosphere. The 0.03% CO$_2$ in the atmosphere has a 22% share of the natural greenhouse effect of 33 K necessary for life on earth. Water vapour has the main share of 62% of the natural greenhouse effect [Leithner2005]. CO$_2$-emissions can be reduced by less power consumption, increasing efficiency, increasing CO$_2$ free power like nuclear or renewable power or finally by carbon

capture and sequestration (CCS). Lower CO_2 emissions simultaneously result in less fossil fuel consumption, offering the possibility to use fossil fuels for longer time, and in lower emissions of other pollutants like SO_x, NO_x or particulate matter except when applying most of the CCS methods. The reason is that most of the CCS methods cost a lot of additional energy. There are only a few methods, which lead to an intrinsic CO_2-separation, especially two groups of methods [Leithner2005]:

a) Metal Oxid Cycles
   Oxygen is transported to the fuel by metal oxides which are reduced to pure metals by the fuel. The metals are separated and transported into the air, where the metals re-oxidize and the cycle starts again. Applicable metals are: nickel, copper, iron, zinc or cadmium [Knoche1967], [Knoche1968].

b) Oxygen Ions Transporting Membrane Cycles. There are two possibilities again:
   a. the electrons flow back in the membrane itself or
   b. the electrons flow from one membrane surface (anode) to the other (cathode) via an external electricity cycle. The latter is the case in Solid Oxide Fuel Cells – SOFC

Combined SOFC-Gasification/Reformer Process Concept

Combining an SOFC with an allothermal reforming or gasification process offers the opportunity to realize high electrical system-efficiencies. In such a process the SOFC-waste heat is transferred to the gasifier or reformer e.g. by conduction or by heat pipes allowing also to use less excess air, because the air is not used so much for cooling any more, and the hot anode off-gas consisting of water vapor, CO_2 and unused fuel gas (mainly CO) is partly recycled as gasification medium to the endothermic water steam and CO_2 gasification or reforming process increasing simultaneously the fuel utilization. Applying a cascaded stack design an additional increase in fuel utilization and efficiency can be achieved. Those combined processes are capable to convert all sorts of accordingly conditioned hydrocarbons, i.e. fossil fuels or renewable fuels. The combination of a SOFC with an allothermal gasification or reforming reactor can be described by the term "chemical heat pump", as the waste heat of the fuel cell is used to provide energy for the endothermic gasification or reforming reactions. In the gas generation reactor, the waste heat is partially converted into chemical energy of the produced gas. Figure 1 shows the simplified working principle of such a chemical heat pump [Schlitzberger2006]. E.g. the fuel flow entering the gasifier or reformer with a certain lower heating value LHV is considered as being 100 % energy flow, to which approximately 40 % heat flow are added, representing the waste heat from the SOFC that is recycled into the gasifier/reformer via recycled anode off-gas and heat transfer. Without losses the produced gas flow represents 140 % energy flow related to the fuel flow entering the gasifier or reformer with an increased LHV. Due to the SOFC's electrical efficiency of about 50 %, half of the chemical energy of the produced gas is converted into electrical energy, which leads to a cycle efficiency of up to 70 %, neglecting various losses. The other part is converted into heat, which is recycled into the
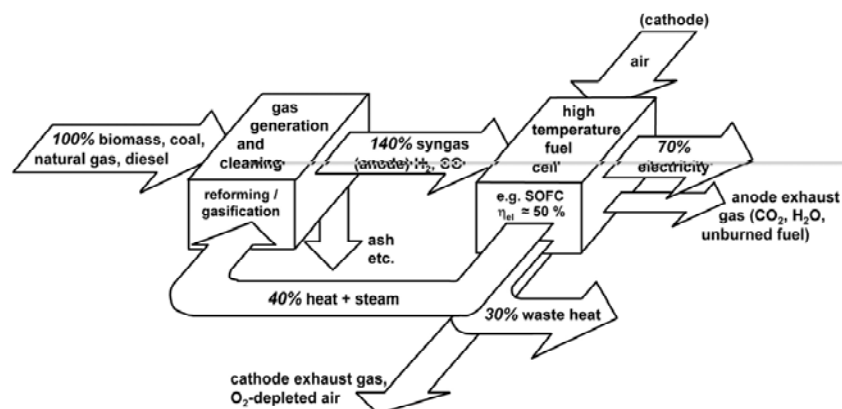

Figure 1. Principle of a chemical heat pump [Schlitzberger2006]

gas generation reactor or leaves the SOFC as waste heat within the cathode and anode off-gases together with unburned fuel [Schlitzberger2006].

Today still autothermal reforming ATR or partial oxidation POx are often used together with high amounts of excess air for cooling to limit the temperature increase and also mixing of anode and cathode exhaust gases to burn the unused fuel of the anode exhaust gas. Consequently microturbines etc. are proposed to use the high amount of waste heat. But such a process cannot lead to high efficiency and in addition has not a simple design and the possibility to separate CO_2 simply by condensing the water vapor is abolished. Only a few SOFC systems possess a mass and thermal coupling between fuel processing and fuel cell. Examples for such SOFC systems are those developed by Siemens-Westinghouse (tubular stack design) [Winkler2002], Rolls Royce (integrated planar flat tube stack design) [Travis2007], Forschungszentrum Jülich (planar stack design) [Steinberger-Wilckens2004] and FuelCell Energy, Inc. (planar stack design) [Katikaneni2002]. In the Siemens-Westinghouse and the Rolls Royce systems the fuel processing is divided into pre-reforming and indirect internal reforming (IIR) with partially recycled hot anode off-gas (using an injector or alternatively a hot gas blower) and direct internal reforming (DIR) of the remaining unconverted higher hydrocarbons entering the SOFC-section using in-situ the generated waste heat and steam. In the Forschungszentrum Jülich design the thermal coupling is realized by stacking the planar SOFC and IIR-reformer sections, whereas in the FuelCell Energy stack the fuel processing is mainly realized by direct internal reforming. Examples for parallel and serial electrical interconnection of the single SOFC-cells represent the Siemens-Westinghouse stack and the stack design developed by Rolls Royce respectively. Nearly all system-concepts include an afterburning of the SOFC off-gases.

Stack-Design

Figure 2 shows an innovative cascaded, planar SOFC-stack design without use of bipolar plates, developed at the Institute for Heat- and Fuel-Technology of the Technische Universität Braunschweig. The internal stack electrical interconnection represents a combination of serial and parallel connections. The voltage increases in fuel flow direction because of the cascaded connection of the equipotential surfaces and the current increases with the number of stack levels [Leithner2004a,b].
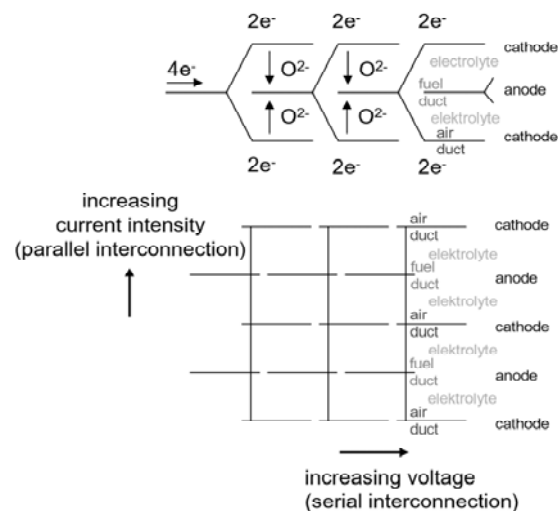

Figure 2. Internal interconnect structure [Leithner2004a,b]

Cycle-Design

The basic cycle (more sophisticated cycles see [Leithner2007b]) shown in Figure 3, can be divided into four parts: Gasification with gas cleaning, cascaded SOFC, heat transfer system between SOFC and gasifier and CO_2-separation with heat recovery. The gas produced by the allothermal steam gasifier, which consists mainly of H_2, CO, CH_4, CO_2, H_2O, is cleaned from ash, tar and gaseous pollutants like sulphur-and chlorine compounds. To minimize heat losses, hot gas cleaning technologies like ceramic filter candles, desulphurisation on lime-absorbers and catalytic tar reduction are particularly suitable. To overcome the pressure losses on the fuel-gas side, a high-temperature fan is used. In the SOFC the chemical energy of the combustible gases is converted into electrical energy and heat. Air and fuel flows are heated by the exhaust gases. After being used to preheat air and fuel flows, the

anode exhaust gas flows through a CO-shift reactor, where the residual CO is converted into H_2 and CO_2 using catalysts. In the following steam-washed counter-current membrane the H_2 is separated from the exhaust gas and re-enters the cycle together with the steam as gasification agent. After passing an expander and a condenser, the anode exhaust gas consists mainly of CO_2, which is compressed and supplied to further use or storage.
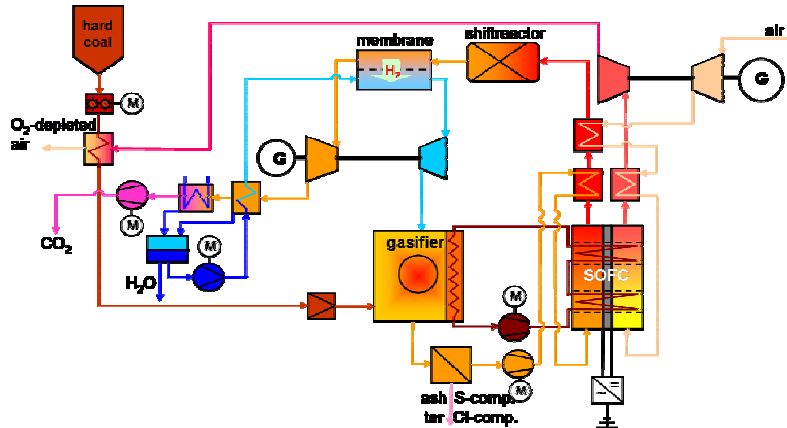

Figure 3: Basic cycle configuration for hard coal as fuel

Energetic Analyses

The energetic analysis of the concept was performed with the cycle simulation program ENBIPRO developed at the Institute for Heat- and Fuel Technology. With the simulation program the theoretical feasibility of the concept and a high electrical efficiency were proven. For the first draft of a hard coal fuelled cycle shown in Figure 3, an electrical system efficiency of 58.5 % including CO_2 compression (62.1 % without) were calculated. However, the obtained results have to be considered a first estimation, due to the made simplifications and assumptions.

References

[Katikaneni2002] Katikaneni, S., Yuh, C., Abens, S., and Farooque, M., 2002, „The Direct Carbonate Fuel Cell Technology: Advances in Multi-Fuel Processing and Internal Reforming," Catalysis Today, Volume 77, Issues 1-2, 1 December 2002, Pages 99-106.

[Knoche1967] Knoche K.F.: Das Enthalpie-Entropie Diagramm zur exergetischen Beurteilung von Verbrennungsvorgängen, Brennstoff-Wärme-Kraft BWK 19, Nr.1 January 1967

[Knoche1968] Knoche K.F. and Richter H.: "Verbesserung der Reversibilität von Verbrennungsprozessen," Brennstoff-Wärme-Kraft, Vol. 20, No. 5, May 1968, pp. 205-210.

[Leithner2004a] Leithner, R., 2004, „Patentanmeldung DE 102 00 401 566 0A1 (Struktur eines SOFC-Stapels)" (German Patent Application).

[Leithner2004b] Leithner, R.: „Patentanmeldung DE 103 00 466.1 (Brennstoffzellen mit integrierter Vergasung) und DE 103 05 806.0 (Brennstoffzelle mit integrierter Vergasung oder Reformierung)" (German Patent Application)

[Leithner2005] Leithner R.: Energy Conversion Processes with Intrinsic CO2 Separation, Transactions of the Society for Mining, Metallurgy and Exploration Volume 318, 2005, pages 161-165

[Leithner2007a] Leithner, R.: "Combined cycles for CO2-capture with high efficiency", International Journal of Energy Technology and Policy Volume 5, No. 3, 2007, ISSN: 1472-8923.

[Leithner2007b] Leithner, R. and Schlitzberger, C., 2007, "Patenanmeldung DE 10 2007 015 079.4 (Verfahren zum Betrieb und Konstruktion einer SOFC mit integrierten Wärmetauschern, integrierter Reformierung oder Vergasung, integrierter Anodenabgasrückführung und integrierter Wärmeauskopplung)" (German Patent Application).

[Schlitzberger2006] Schlitzberger C., Leithner R.: High Temperature Fuel Cells with Integrated Biomass Gasification and CO2-Separation, 19th International Conference on Efficiency, Cost, Optimization, Simulation and Environmental Impact of Energy Systems – ECOS, Crete, 12-14 July 2006

[Steinberger-Wilckens2004] Steinberger-Wilckens, R., et. al., 2004, „Progress in SOFC Stack Development at Forschungszentrum Jülich," European SOFC Forum, Luzern 2004 (in German).

[Travis2007] Travis, R. and Bernardi, D., 2007, "Towards a 1 MW Pressurized Fuel Cell System", 5th International ASME Fuel Cell Science, Engineering & Technology Conference New York, USA 18/20.06.2007.

[Winkler2002] Winkler, W., 2002, „Brennstoffzellenanlagen," Springer Verlag (in German).

ELCOGAS pre-combustion 14 MWt carbon capture pilot plant

Dr. Pilar Coca, ELCOGAS, S.A., Puertollano, Spain; Mr. Pedro Casero, ELCOGAS, S.A., Puertollano, Spain; Mr. Francisco García-Peña, ELCOGAS, S.A., Puertollano, Spain

Introduction

ELCOGAS S.A. is a Spanish company established in 1992 and shared by European electrical companies and equipment suppliers. It operates the Puertollano 335 MWe_{ISO} IGCC demonstration power plant. This IGCC plant is the largest IGCC plant in the world using solid fuel in a single pressurised entrained flow gasifier, being in commercial operation since 1998 with synthetic gas. Its design fuel is a mixture 50:50 of coal (high content of ash) and pet-coke (high content of sulphur). The total power production up to Dec 2010 is 21,052GWh (mainly using syngas).

As a demonstration plant, ELCOGAS has obtained important achievements showing the potential of IGCC technology, including its advantages and disadvantage and identifying its main improvement and optimisation lines. Regarding this point, the ELCOGAS IGCC R&D activities are based on the opportunity that the IGCC technology offers related with fuel flexibility (test with different coals, pet-coke, biomass, wastes, …), multi-production (electricity, hydrogen, synthetic gasoline, biodiesel, …) and zero emissions production (reduction of emissions, CO_2 capture …).

Carbon Capture Pilot Plant description

Currently, the ELCOGAS largest investment in R&D is focused on carbon capture topic, covered by the National Singular and Strategic Projects Initiative, called $PSE-CO_2$. The main milestone of the $PSE-CO_2$ project has been the **construction of a 14 MWth pilot plant** fed by a 2% slip-stream of the Puertollano IGCC power plant and able to capture 100 t/d of CO_2, while producing 2 t/d of high purity H_2 and using proven and commercial technology. This pilot plant aims are to demonstrate the feasibility of CO_2 capture and H_2 production in an IGCC that uses solid fossil fuels and wastes as main feedstock as well as to obtain economic data enough to scale it to the full Puertollano IGCC capacity in synthetic gas production

The underlined participants in the project are ELCOGAS (coordinator), University of Castilla-La Mancha (UCLM), CIEMAT (Spanish research centre) and INCAR (coal Spanish research centre) being the original budget 18.5 M€, currently is €14.7 million.

Both Spanish Government (Spanish Science & Research Minister) and Regional Government are funding the project through the Strategic and Singular Project Programme (PSE), being their contribution approximately 50% of the total budget.

The following figure shows a general view of the IGCC plant and the pilot plant.
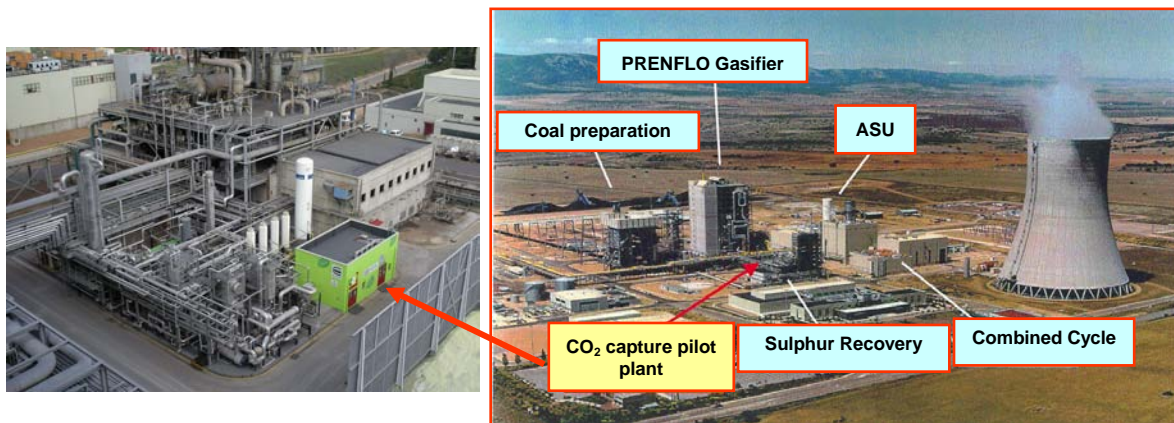

Figure 1. **CO_2 capture & H_2 co-production pilot plant: location**

The pilot plant is fed with syngas –approximately 3,600 Nm^3/h, dry base- from the IGCC power plant that can be desulphusired, i.e., it comes downstream the IGCC desulphurisation unit (called sweet gas) or the syngas can be fed sulphurised, i.e. upstream the desulphurisation unit (called sour gas).

The process of the 14 MW_{th} pilot plant (see the figure below) consists on a two step shifting unit to convert CO into CO_2, a CO_2 separation unit -based on absorption processes with amines (sweet/sour) as catalysts- and a H_2 purification unit (PSA), being all of them commercial processes. Auxiliary systems and full control have been integrated in the existing IGCC. All processes used in the pilot plant are being utilised at this moment by the chemical industry, so its innovation is their integration and use in the power industry.
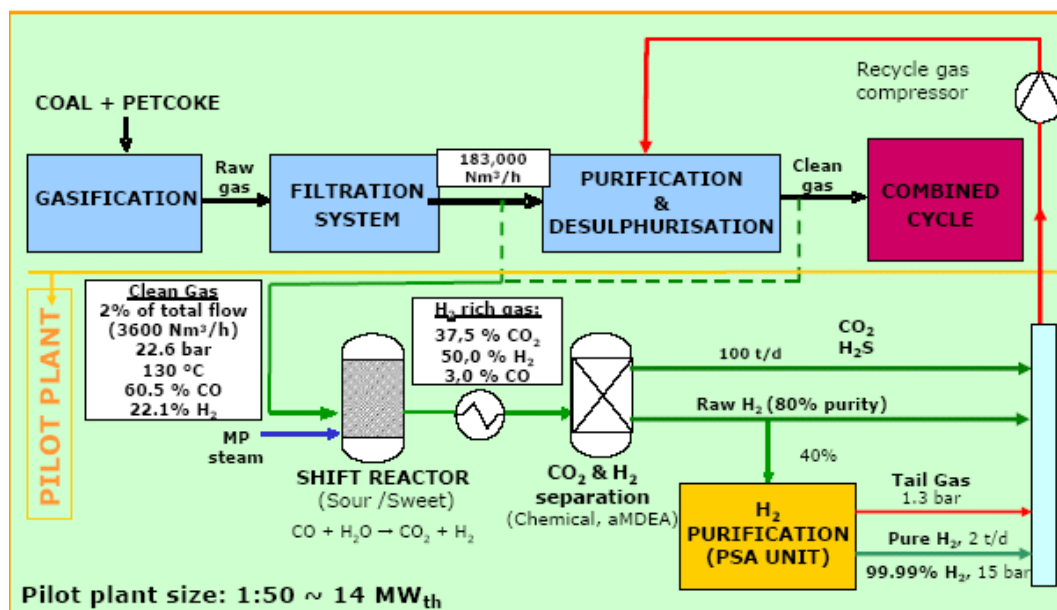
Figure 2. Flow diagram of the CO_2 capture & H_2 production pilot plant

The **first tonne of CO_2 was captured on 13th September 2010** (thus becoming the first installation of this kind in the world) and the commissioning was accomplished by October 2010. Characterization tests are being carried out since November 2010 until June 2011, covering the two different feeding syngas conditions as well as two different configurations, with and without H_2 co-production.

As a brief description of the main **learning** in **project phase** can be mentioned: the finance delay due to funding calls, delay in the main equipment supply -more than 12-14 months-, the detailed engineering was conditioned by suppliers and the pilot plant construction was also delayed due to safety permits since it is installed in an operating plant, finally lack of experimented personnel implied a delay on the commissioning.

The first battery tests using the sweet catalyst were undertaken from Oct 2010 to Feb 2011. The table below shows the composition of the main streams:

	Shifted gas		CO_2		H_2 rich gas		Pure H_2	
	Expected	Lab Analysis	Expected	Lab Analysis	Expected	Lab Analysis	Expected	Lab Analysis
H_2	50.05	51.88	0.19	0.314 - 1.31	79.75	82.3 – 83.14	99.99	99.959- 99.995
CO	2.92	1.85	0	0.053 - 0.07	4.65	2.86 - 3.78	4 ppm	N/A
CO_2	37.56	37.36	99.78	98.2 - 99.622	0.5	0.02 - 0.82	1 ppm	N/A
N_2	8.76	8.30	0.01	0.05 - 0.28	13.97	12.2 - 13.6	15 ppm	4 - 17 ppm
Ar	0.71	0.60	0.02	0.01 - 0.09	1.13	0.89 - 0.97	80 ppm	3 - 14 ppm

Table 1. Main results obtained from pilot plant in sweet operation (dry base)

Main **learning in the sweet characterisation tests** has been an unexpected reactivity in first step of shifting unit since in design CO conversion into CO_2 was estimated to be of 85% and 15% in the second step. However, in operation, the CO conversion was of 95% in first step and 5% in the second step, what would make possible to consider a shifting process with only one step using the sweet catalyst.

Auxiliary consumption was lower than estimated in design, being the integration of O&M in the existing IGCC very easy, the rate of CO_2 captured is 91.7% and the cold gas efficiency is 89.5%. The first estimation cost of avoided CO_2 is approximately 25-30 €/t for the existing IGCC, which has been obtained from the pilot plant data.

For the second battery tests, which will take place from May to June 2011, the sour catalyst will be tested, expecting to get final results by the end of July 2011. These final results will include comparison of the pilot plant's behaviour under the two different operation conditions, optimization of steam/gas ratio at shifting unit for the correct operation of the plant, optimization of energy balance and real costs obtaining of CO_2 capture and H_2 co-production.

Future activities

Once the PSE project is finished, ELCOGAS proposal is to use the pilot plant as an R&D platform in order to develop new projects related to these research areas: optimisation of catalysts for shift reaction (including tests on a variety of different catalysts), development and demonstration of new processes for CO_2-H_2 separation, demonstration of processes for CO_2 treatment and the improvement of integration between the CO_2 capture facility and the IGCC power plant to increase efficiency.

With the aforementioned and taking into account the results to be obtained from the pilot plant, ELCOGAS has the opportunity to contribute to the optimisation of IGCC technology subsequently to optimisation of the clean coal technologies. So, improvements and processes, which are being set out for the design of new plants, can be tested and developed even at commercial scale, leading to ultra-efficient and zero-emissions energy plants based on gasification of low cost fuels.

Process Development for Integrated Coal Gasification SOFC Hybrid Power Plants

Dipl.-Ing. Michael Krüger, DLR (German Aerospace Centre), Institute of Technical Thermodynamics, Pfaffenwaldring 38-40, 70569 Stuttgart, Germany

Introduction

On the path towards sustainable electric power generation, an increase in efficiency of fossil-fuel power plants and a reduction of CO_2-emissions are both necessary. Improvements in energy efficiency and an introduction of carbon capture and storage (CCS) demand optimization and retrofitting of existing power plant processes as well as a development of advanced power plant concepts that have mid- to long-term economic viability. This is of extraordinary importance, especially considering the already perceptible significant need for new and replacement electricity generation capacity in Germany, Europe and around the world.

In addition to the already well analyzed integrated gasification combined cycles (IGCC), hybrid power plants with fuel cells and integrated coal gasification promise to have the potential to achieve a high power plant efficiency, as well as to provide an opportunity for carbon dioxide capture.

Hybrid power plants incorporating high temperature fuel cells and coal gasifiers are currently at the development and simulation stage. So far, only a few investigated concepts have been described in literature; these assume a time frame for realisation in the distant future. Because of this, these concepts include subsystems and components that do not represent the current state-of-the-art.

Objective and approach

The main goal of the project is to find the most efficient low-carbon power plant configuration, by integrating high temperature fuel cells (SOFC – solid oxide fuel cells) in IGCC using state-of-the-art power plant components.

In the case of coal-based power generation, IGCC can be considered the reference standard regarding efficiency and emissions; it has been widely implemented on an industrial scale. An optional implementation of CCS in IGCC coal power plants also

has significant advantages over other coal fired power plant technologies. The development of this technology is highly advanced and moreover, the integration of a SOFC as a stage before the combined cycle power block is feasible without substantial changes to the IGCC system.

Development and modelling of suitable concepts for hybrid power plants

Various concepts of integrated coal gasification SOFC hybrid power plants have been considered and simulated with Aspen Plus^{TM} software, extended by several user implemented models, such as a coal gasifier, SOFC and air separation unit. The figure below presents the developed base case of a hybrid power plant with possible options for CO_2-capture.
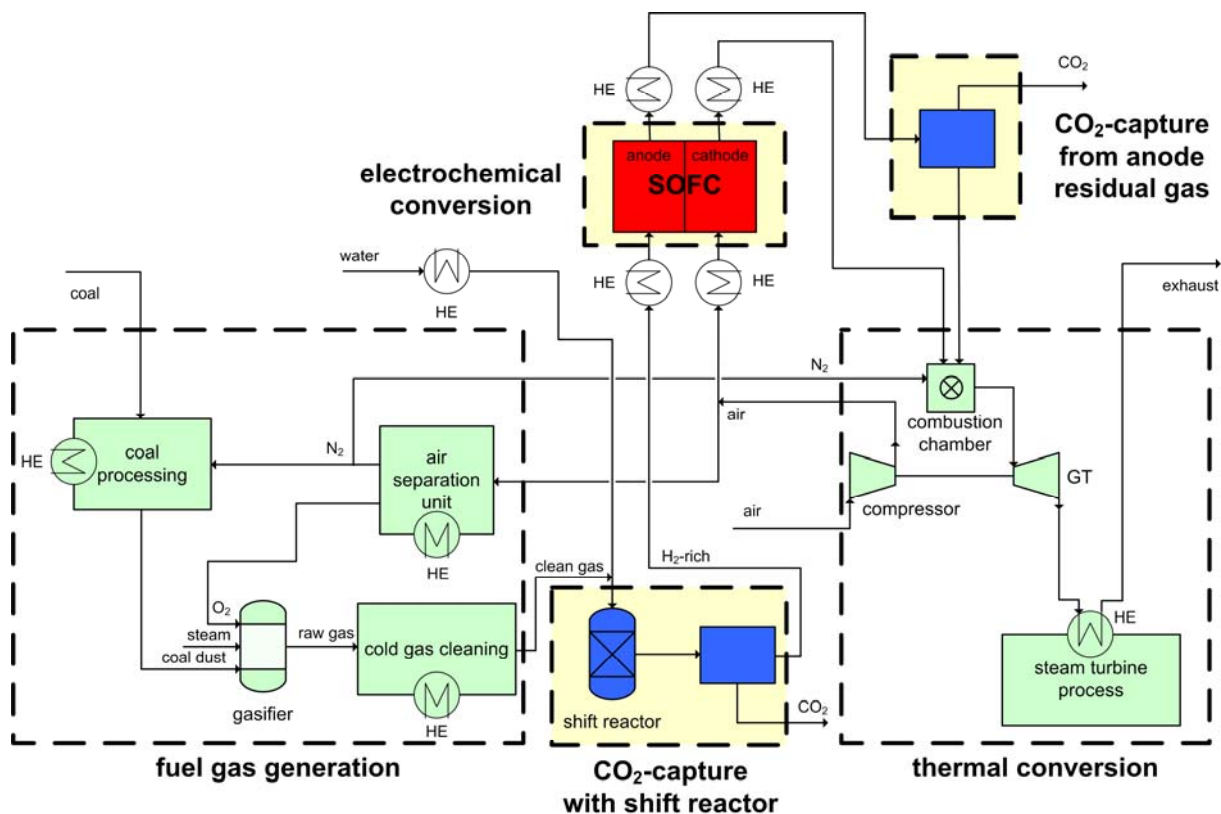
It is clear that integrated coal gasification SOFC hybrid power plants consist of many components and subsystems that coincide with those of the IGCC power plants. In addition, there are SOFC and optional process technologies, such as water gas shift reactor and technologies for carbon dioxide capture.

Before simulations of the overall systems could are possible, all subsystems and components have to be modelled at a similar depth of detail. Only the main energetic components, i.e. SOFC, were modelled in greater detail. Furthermore, the usage in complex systems and the flexibility under various conditions has been taken into consideration. Created models have been verified by measured or operating data found in literature. The last step of the component modelling consisted of appropriate sensitivity analysis in order to test the models under conditions present in developed overall systems.

This was followed by modelling and simulation of reference power plants, in particular the IGCC of Puertollano and an IGCC with CCS based on the Puertollano IGCC.

Simulation of the developed integrated coal gasification SOFC hybrid power plants has been divided into two steps. The first step is the basic analysis of the systems, by means of simulation of simplified sub-processes without a coal gasifier, gas cleaning or air separation plant. This allows for an overcoming of the high complexity of the overall systems and thereby facilitates parameter studies to indicate general tendencies. As a result of this first step, a preliminary assessment of the various concepts has been reached. In the second step, the overall systems were simulated with optimal parameters gained from step one. A comparative assessment and a definition of guidelines have been carried out via these steps.

Results

The essential energetic and ecological criteria to evaluate concepts for power plants are the net efficiency and specific CO_2-emissions.

The effectiveness of the straightforward solution, i.e. removing CO_2 from SOFC anode residual gas, is low, caused by limited fuel utilization of the fuel cell. The most effective case is the combination of a water-gas-shift-reactor and a physical absorption process before the SOFC-anode. This is due to the high partial pressure of CO_2 and the supply of SOFC with a rich hydrogen gas. This results in a three percentage points higher efficiency than the most investigated IGCC with CO_2-capture.

Investigations of Reduction Behavior of Manganese Oxide as Oxygen Carrier Material for Chemical Looping Combustion

Maciej Wrobel, Outotec GmbH, Frankfurt am Main, *M. Buchmann*, TUBAF, Freiberg, Germany; *Dr -Ing. habil. A. Saatci*, Outotec GmbH, Frankfurt am Main
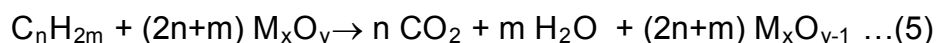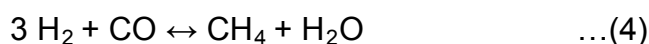
Introduction

Chemical looping combustion (CLC) represents a novel combustion technology, where two discrete reactors are used to separate reduction from oxidation reaction. The main objective of this combustion process is to generate energy and pure carbon dioxide (CO_2) stream that can be captured and stored. The oxygen-carrier materials which are circulated between these separate reactors, are then oxidized in the circulating fluidized bed (first reactor) with the generation of energy. While in the second reactor, the oxygen carrier material is reduced and then finally recycled to the first reactor.

The reaction in the first reactor can be represented as the following:

$$MnO_n + xO_2 = MnO_{n+x/2} \qquad \ldots(1)$$
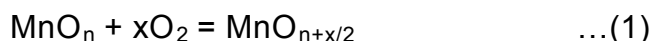
The CLC of coal is more complex than the combustion of methane or natural gas. A direct usage of solid fuel requires a major overhaul of entire fuel reactor due to gasification reactions (*equations 2 to 4*). In addition, it requires fluidization medium to be high pressurized steam (energy intensive) or CO_2 (product of CLC).

The conversion process during CLC of solid fuel is a function of gasification reactions kinetic (*equations 2 to 4*) and reaction kinetic reduction of metal oxide(s) (*equation 5*):

$$C + H_2O \leftrightarrow CO + H_2 \qquad \ldots(2)$$
$$C + CO_2 \leftrightarrow 2CO \qquad \ldots(3)$$
$$3 H_2 + CO \leftrightarrow CH_4 + H_2O \qquad \ldots(4)$$
$$C_nH_{2m} + (2n+m) M_xO_y \rightarrow n\ CO_2 + m\ H_2O + (2n+m)\ M_xO_{y-1} \ldots(5)$$

Theoretically, the kinetics of metal oxide(s) reduction (*equation 5*) is much faster than the kinetics of gasification reactions (*equations 2 to 4*). In other case, the content of CO in the off-gas stream from the fuel reactor (and the specific consumption of solid fuel) will increase.

Experimental

In the performed study, manganese oxide sintered material was used as oxygen carrier material in the fluidized bed reactor. Two different types of cokes were utilized: brown coal chars (BRCC) and black coal char (BLCC). Thermogravimetry (TG) measurements were performed with Netzsch Jupiter F1. The TG experiments were conducted with different morphology and surface area of manganese oxide in the form of sintered and fine powder MnO_2 (purity of 99.99 %, <20 μm in particle size). The TG procedure was performed in three steps: (1)-preheating to 850°C with 20K/min in nitrogen flow, (2)-temperature stabilization for 15 min and finally (3)-reduction with a CO/CO_2 gas mixture for the duration of 60 min.

The fluidization experiments were conducted in a laboratory fluidized bed reactor with internal diameter of 50 mm. The fluidizing atmosphere was made of nitrogen and carbon dioxide gas mixtures with total flow rate of 700 L/h of 30%N_2-70%CO_2. The gasification of coal and direct reduction of manganese sinter were investigated at two different temperatures (850 °C and 950 °C) and with retention time of 30 min. An infrared off gas analyzer was used to analyze continuously the amount of CO concentration in the course of gasification of coal and the reduction of manganese.

Results

Kinetics of coal gasification (reactivity of coal)

Kinetically, the gasification process is the slowest reaction in the fuel reactor and therefore the kinetics of this reaction governs the size of the fuel reactor. The gasification reaction process was described in equation 3. The reaction rate of this reaction is a function of the available amount of carbon (C_a) and the difference between the present carbon dioxide partial pressure ($p_{CO2}{}^{ex}$) and its partial pressure in equilibrium ($p_{CO2}{}^{eq.}$) [1]:

$$dC/dt = -k_C \cdot C_a \cdot (p_{CO2}{}^{ex} \cdot p_{CO2}{}^{eq}) \qquad \dots(6).$$

By the use of equation 6 and the results from the reactivity experiments (CO content in off-gas), the reaction constant k_C for the brown coal char could be calculated

Kinetics of the reduction

In the first stage Mn_2O_3 is reduced to Mn_3O_4; while in the second stage Mn_3O_4 is reduced to MnO. The first stage of reduction process is very fast in oxygen lean atmosphere at 850 °C, enabling quick decomposition of Mn_2O_3 to Mn_3O_4.

The slowest stage is the reduction from Mn_3O_4 to MnO. Thus, the kinetics determining step is the second stage with reaction as follows:

$$Mn_3O_4 + CO \rightarrow MnO + CO_2 \quad …(7)$$

The reduction of Mn_3O_4 is the reaction of first order with a driving force (partial pressure of CO):

$$dO/dt = -k_O \cdot O_a \cdot (p_{CO}^{ex} \cdot p_{CO}^{eq}) \quad …(8)$$

Where O_a is the available amount of oxygen, p^{ex}_{CO} is partial pressure of CO, p^{eq}_{CO} is the partial pressure of CO in equilibrium (calculated with HSC 7.0)

The kinetics of reduction was investigated in thermogravimetric unit. The materials were heated at 850°C with gases in different proportions of CO/CO_2. The maximum registered weight loss ratio (dO/dt) with corresponding O_a (available amount of oxygen in the sample) were plotted as a function of CO partial pressure. The slope of the lines is equivalent to the reaction rate constant k_O. Table 1 summarized the reaction rate constants for different materials.

Table 1. Reaction rate constants for the different materials

k_O / k_C	Mn -sinter (coarse, 850°C)	Mn -sinter (ground, 850°C)	pure Mn_3O_4 (ground, 850°C)	BRCC (coarse, 850°C)	BLCC (coarse, 850°C)	BRCC (coarse, 950°C)	BLCC (coarse, 950°C)
$(s \times bar)^{-1}$	0.0391	0.106	0.2035	0.001	~$2 \cdot 10^{-5}$	0.003	~$1.3 \cdot 10^{-4}$

Estimation of CO-content in off-gas from fuel reactor:

The simplified reaction of reduction with coal is as follows:

$$2Mn_3O_4 + C \rightarrow 6MnO + CO_{2(g)} \quad …(9)$$

The CO concentration in steady state (p_{CO}^{ex}) is also a function of k_O/k_C and can be approximated as [1]:

$$p_{CO}^{ex} = \frac{k_c + k_o.p_{CO}^{eq} - k_c.p_{CO_2}^{eq}}{k_c + k_o} \quad …(10)$$

The results of calculation for different (k_o/k_c) rates for sinter coarse/ground manganese, and pure Mn_3O_4 were plotted in Figure 1.
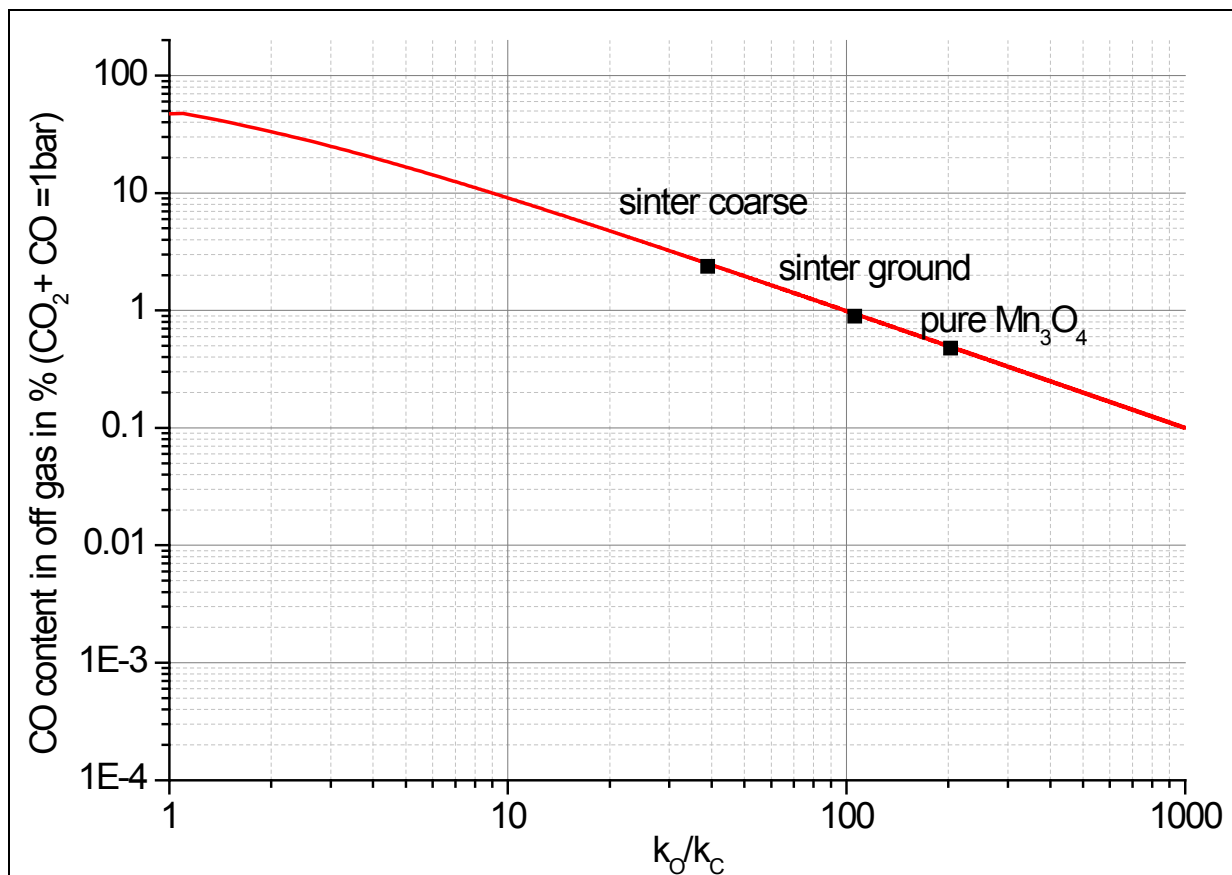
Figure 1. Calculated CO content at 850°C as function of k_O/k_C (k_C for BRCC)

Direct reduction of manganese sinter in stationary fluid bed

The results indicate that the reduction between 5 to 15 min was insufficient at temperature of 850°C. The maximum evolution of CO in the off-gas was recorded to be 1% and after 30 minutes of reduction, the CO concentration was dropped to 450 ppm. The reduction of manganese sinter at 950°C occurs much faster than that at temperature of 850°C. After 12 min of reduction, the concentration of CO in the off gas reached 450 ppm with maximum CO evolution of 4%.

The experimental results suggest that the CO content in the off-gas could be reduced significantly by increasing the amount of sintered material, that is a hyperstoichiometric ratio of oxide material to the coal. High CO concentration reading in the off-gas indicates that the reduction was incomplete. The highest degree of reduction (R) was achieved by reduction with BRCC at 950°C (R=36.4%). At 850°C, the degree of reduction with BRCC was reduced to merely 26.5% due to low reactivity of coal at the range of 850-950°C.

Table 2 show the summary of calculated parameters from the experimental data. The estimated reaction rate constants were simulated and calculated using AspenPlus 7.0 for 20-MW CLC unit.

Table 2. Summary of AspenPlus calculations

Coal conversion - 90%	Retention time [min]	Sinter material / coal in [t/t]	CO in off-gas [%]	Required amount of CO_2 [kNm³/h]
Equilibrium reached after 5 min	5	49	0.09	78.3
Measured kinetics	5	710938	0.00003	1127547
	30	3383	0.00007	32191
	60	417	0.001	7932

Conclusions

The evaluation reaction kinetics of reduction and gasification process allows estimation of CO concentration in the off-gas during steady-state reduction. The minimum theoretical amount of CO concentration in the off-gas with grounded Mn_3O_4 and brown coal char is 0.45%, while for coarse sinter is 2.37%. The char particles was significantly decreased in their size during coal gasification and considerable part of the particles floats above the sinter material, hindering it from further reaction. As a result, the outcomes of direct reduction of manganese sintered in stationary fluidized bed reactor are not well within our expectation. This can be avoided by using CFB technology although it would require much higher gas velocities in the reactor. The simple reactor design for chemical-looping combustor for natural gas might not be suitable for effective combustion of solid fuel at 850°C [2] as it required major modifications such as: (1) external gasification unit, (2) ash or oxygen carrier separator, (3) gas scrubbing unit for CO gas stream, and (4) CFB fuel reactor. This major modification makes CLC technology for solid fuels much more sophisticated and less applicable to industrial scale.

References

[1] A. Saatci, „*Die Reaktionen der Auf- und Entschwefelung bei der Direktreduktion von Eisenerzen mittels Kohle*", Ph.D Thesis, TU Berlin (1973)

[2] N. Berguerand, A.Llyngfelt „*Batch testing of solid fuels with ilmenite in a 10 kWth chemical looping combustor*" Fuel 89, p1749 – 1762 (2010)

Separation of CO_2 in Coal Fired Power Plants without Efficiency Losses?!

Reinhard Leithner; Martin Strelow; Silvia Magda; Fridolin Röder; Christian Schlitzberger; Institut für Wärme und Brennstofftechnik, Technische Universität Braunschweig, Germany (www.wbt.ing.tu-bs.de, E-Mail: r.leithner@tu-bs.de)

Motivation

Due to the growing world energy demand, an increased annual consumption of fossil fuels is to be expected and thus also a rise in the carbon dioxide emissions into the atmosphere, with their impact on the global climate. Substantial efforts are therefore needed in developing new power plant technologies for CO_2 separation from exhaust gases. Three main methods are envisaged for the CO_2 capture: pre-combustion, post-combustion and oxyfuel-combustion [1,2. The current work presents a post-combustion CO_2 capture solution feasable for new power plant construction and in principle also for retrofit [3].

Concept of the Carbonate Looping Process

The principle of carbonate looping follows the scheme of Figure 1. The CO_2 rich flue gas is fed to a fluidized bed reactor operating at temperatures of 600°C. In the presence of reactive lime and under heat release the CO_2 is carbonated [4]. The backward endothermic reaction takes place at about 900°C in a twin fluidized bed reactor, with water vapor resulted from the calcination to be fed as fluidization gas. The necessary heat input for the
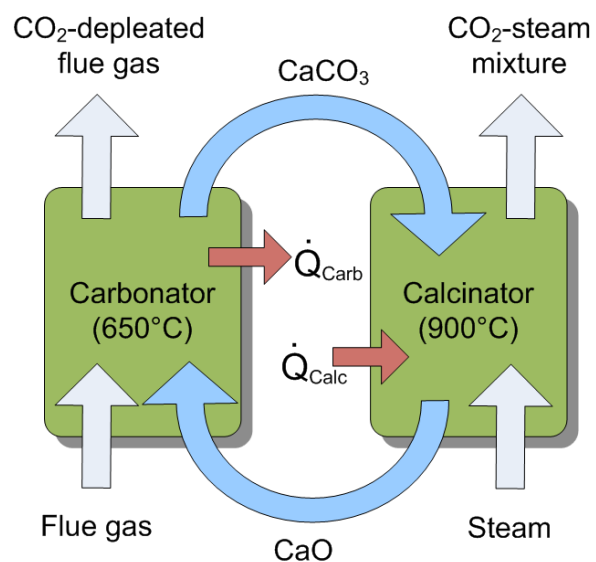

Figure 1: Carbonat-Looping-Process

reaction is provided by radiation in the combustion chamber with the tubes of the calcinator or high temperature heat pipes in a fluidized bed calcinator. Evaporation of the water-steam cycle will be dislocated to the carbonator. This layout ensures an CO_2-seperation of up to 90 % [6] and is not to be used after the flue gas cleaning

system, but part of the flue gas path and the water-steam cycle. The use of a pressurized carbonation reactor and of a downstream water-steam-CO_2-turbine enables additional energy generation (Figure 2).
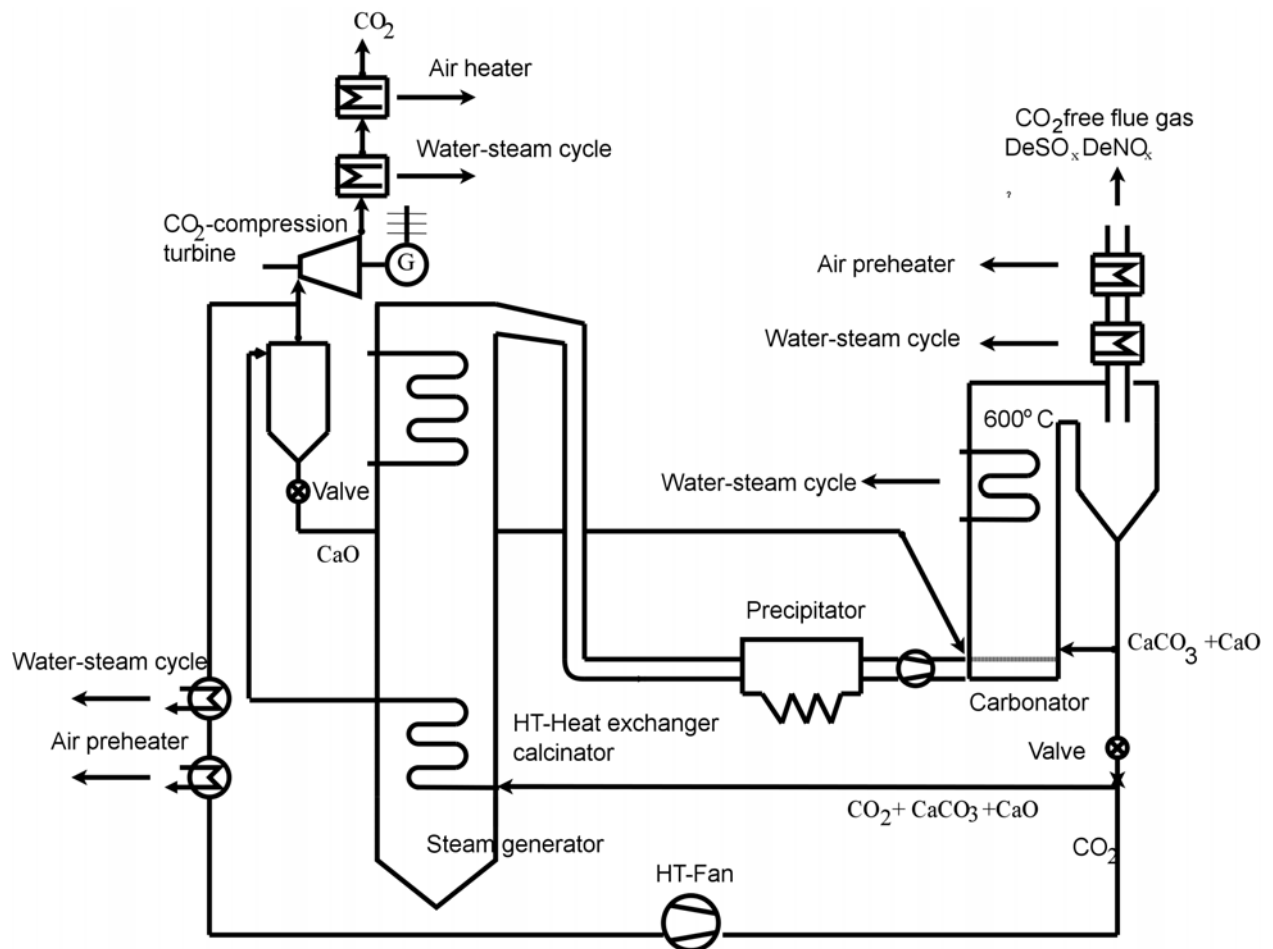

Figure 2: Simplified flow scheme of a power plant with carbonate looping and water-steam-CO_2-turbine

Power plant and carbonate looping modelling

By means of the simulation program EnBiPro (Energie-Bilanz-Programm, engl.: energy-balance-programm) [7, 8] devloped at the Institut für Wärme und Brennstofftechnik the modelling of a 1052 MW coal-fired power plant was undertaken as reference case. Carbonate looping components were modeled also and implemented in EnBiPro. The thermodynamic equilibrium was used to model the calcination and carbonation reactions [9]. In order to ensure that the steam parameters upstream the turbine inlet are kept constant the reference power plant had to be modified. Furthermore along the evaporator, additional heat surfaces were integrated (e.g. air pre-heater and superheater heating surfaces). The simulations

were performed for full load operation. Figure 3 shows the flow chart of the simulated power plant (simplified scheme of the water-steam-cycle).
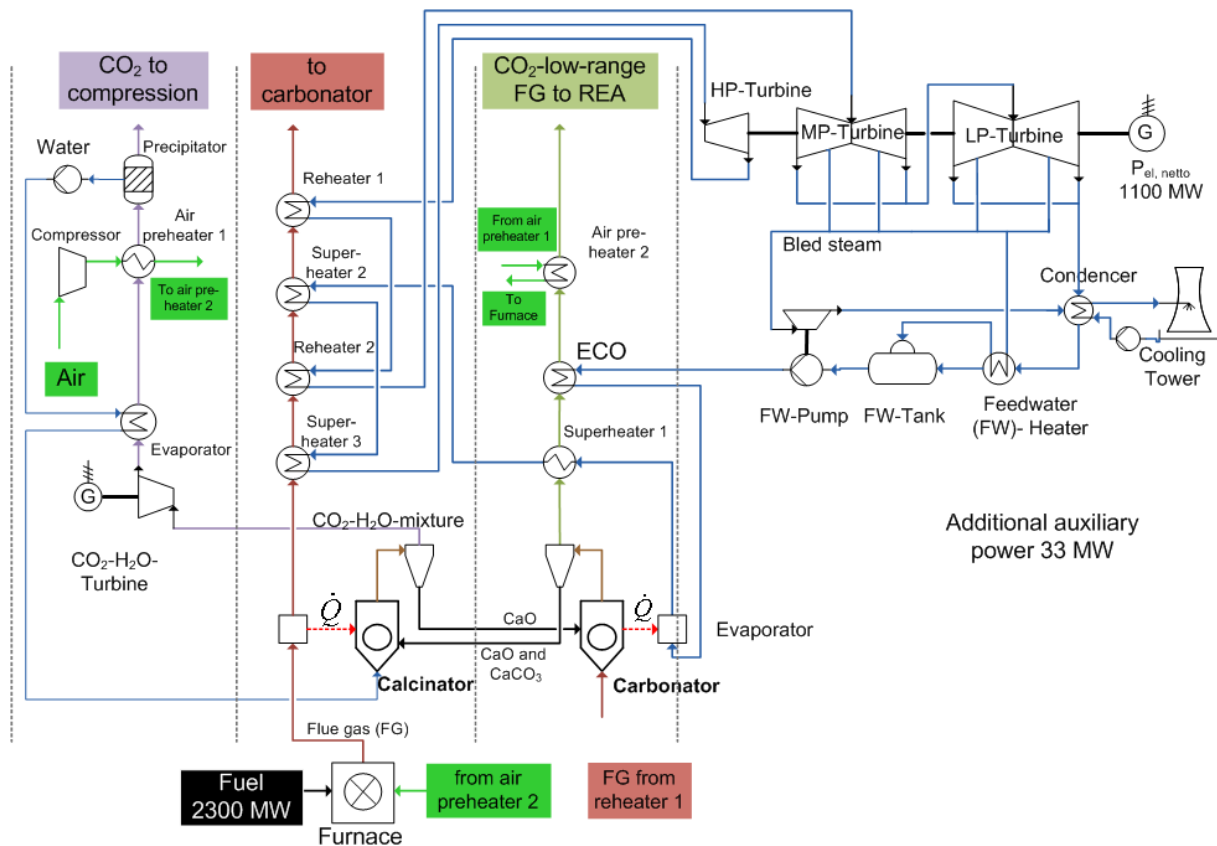

Figure 3: Flow chart of a coal fired power plant using carbonate looping

Simulation results

The use of the carbonate looping process results in a reduction of 3 % of the mass flow in the water-steam cycle. By using a retrofit concept and the water-steam turbine a net electrical capacity of 1050 MW was achieved (the reference plant has a capacity of 1055 MW). This is due to a higher compressor power which is needed for the carbonation reactor. With 45.3 % no significant difference exists between the carbonate looping plant and the reference power plant (efficiency of the reference plant: 45.4 %). If the additional energy required for the CO_2-compression is accounted for then the electrical net efficiency decreases to 41.7 %, i.e. the efficiency decreases by 0.1 % or 3.7 % without respectively with CO_2 compression, which is well below the power losses of other CO_2 removal concepts, e.g. chemical looping, absorption and adsorption associated with losses of 10-20% of the power plant efficiency [10].

	Reference power plant	Power plant with CO_2-separation	Power plant with CO_2-separation and compression
Steam turbine inlet: mass flow	824.3 kg/s	793.0 kg/s	793.0 kg/s
Steam turbine inlet: temperature	869 K	869 K	869 K
Fuel heat input	2322 MW	2322 MW	2322 MW
Steam turbine: electrical output	1103 MW	1062 MW	1062 MW
CO2-H2O-Turbine: electrical output	-	39 MW	39 MW
Ausxilliary power	33 MW	33 MW	33 MW
Air compression power	14 MW	17 MW	17 MW
CO2-compression power	-	-	81 MW
Power plant capacity	1055 MW	1051 MW	970 MW
Gross efficiency	47.5 %	47.4 %	47.4 %
Net efficiency	45.4 %	45.3 %	41.7 %

Table 1: Simulation results for the reference and carbonate looping power plant

References

[1]   Leithner, R.: Energy Conversion Processes with Intrinsic CO_2 Separation, Transactions of the Society for Mining, Metallurgy, and Exploration, Volume 318/2005, Littleton, USA, 2005.

[2]   Clarke, D. et al.: CO_2 Capture and Storage – A VGB Report on the State of the Art, Verlag technisch-wissenschaftlicher Schriften, Essen, 2004

[3]   Leithner, R., Scheffknecht, G.: CO_2-Abscheidung mit Energiegewinnung und andere Kreisläufe mit Adsorption und Absorption von Gasen, Deutsches Patent- und Markenamt, DE 10 2008 020 414.5, Bundesrepublik Deutschland, 2008

[4]   Leithner, R. et al.:Carbon capture from fossil fuels fired power plants without effciency loss, ECM 2009 4th European Combustion Meeting, Wien, 2009

[5]   Epple, B., Ströhle, J.: CO_2 Capture Based on Chemical and Carbonatee Looping, VGB PowerTech, 11 (2008) S. 85-89

[6]   Florin, N.; Harris, A.: Enhanced hydrogen production from biomass with in situ carbon dioxide capture using calcium oxide sorbents, Chemical Engineering Science, Volume 63, Issue 2, January 2008, Pages 287-316

[7]   Zindler, H.: Dynamische Kraftwerkssimulation, PhD Thesis, Der andere Verlag, Braunschweig; 2007

[8]   Epple, B., Leithner, R. et al. : Simulation von Kraftwerken und wärmetechnischen Anlagen, Springer Verlag, Wien, 2009

[9]   Orsini, C.: CO_2-Abscheidung aus Kraftwerksabgasen mit Hochtemperatur- wärmetauschern und Energieerzeugung, Diploma thesis at IWBT, Braunschweig, 2009

[10] Radgen, P. et al.: Verfahren zur CO_2-Abscheidung und Deponierung, Abschlussbericht, Fraunhofer-Institut für Systemtechnik und Innovationsforschung, Karlsruhe, 2005

Posterprogramme

NUMERICAL SIMULATION OF OXI-FUEL COMBUSTION IN A CEMENT KILN

D. Granados[1], J. Mejía[1], F. Chejne[1], C. Gómez[1], A. Berrío[2], W. Jurado[2]

[1]Universidad Nacional de Colombia, Escuela de Procesos y Energía, Medellín, Colombia;
[2]Cementos ARGOS, Medellín, Colombia

Abstract

In order to evaluate the heat transfer mechanism in a cement kiln driven by oxy-fuel combustion, two mathematical models of the process were developed. The first model accounts for global process transformation by solving macroscopic mass and energy balance equations. The second model is based on the 3D mass, energy, species, momentum, turbulence and radiation transport equation, coupled to a chemical kinetic model of the pyrolisis and gas-solid and gas-gas reactions. The discrete phase (coal) was simulated following a Lagrangian approach. The impact of the flue gas recirculation on the oxy-fuel combustion process was parametrically studied. The 3D model was solved by using a commercial computational fluid dynamics (CFD) solver. The global model and the CFD simulation showed good similarities in the results. The simulation results of both models predicted similar values of the maximum flame temperature (9%) and 2% difference for the convective energy flux. In addition, the flame length and convection and radiation energy contribution to the clinker was compared. The models can be used for the evaluation of different energy scenarios in cement kilns in order to increase the energy efficiency and clinker production.

Keywords: CFD, rotary kilns, heat transfer, oxygen combustion, carbon dioxide

1. INTRODUCTION

The coal combustion process with air is used in the cement industry for the clinker chemical transformations. The combustion process has a significant impact on the environment, particularly on greenhouse gases emissions (NOx, CO_2, and other). The cement industry is one of the largest industrial sources of CO_2, accounting for 1.8 Gt/y of emissions worldwide in 2005 [1].It representing 5-6% of global emissions of CO_2 [2]. Emissions of CO_2 can be reduced by carbon capture and storage processes (CCS), but few studies have been done on CCS in the cement industry [1]. In the oxy-fuel combustion process, high concentration of oxygen is fed to the kiln, which is diluted with recirculated CO_2 from the flue gas in order to keep a suited flame temperature. Carbon dioxide is the main component of the flue gases along with small quantities of nitrogen, carbon monoxide, water and other [3].

The oxy-fuel combustion does not generate (or little quantities) NOx because there is few nitrogen in the oxidizing stream. In the other hand, as the CO_2 partial pressure is high it may be easy captured and subsequently stored, increasing the efficiency of the capture process. This will generate an alternative to reduce CO_2 emissions to the environment [3].

Some authors and research institutes have worked in the oxy-combustion topics in order to assess the technology and improve the CO2 capture. The international Energy Agency (IEA) studied the oxy-fuel combustion in a cement plant was studied without taking into account the kiln temperature and reactions. F. Zeman and K. Lackner [4] studied the reduction of pollutants emissions on a cement kiln with oxy-fuel combustion. The European Cement Research Institute [5]. Studied the limitations and requirements technological, energy balances impacts, clinker quality, plant operation and identification of gas components of oxy-fuel cement kilns.

2. GLOBAL PROCESS ANALYSIS

A thermodynamic analysis of the oxy-fuel combustion in the kiln was done using a global model to the process shown in the Figure 1.
In Figure 1, air enters to the Air Separation Unit (ASU) which is separated into nitrogen and oxygen. The oxygen is mixed whit the flue gases, previously cooled in the heat exchanger

1. This mixture is the oxidizing gas stream or "artificial air" which is divided into primary (APG) and secondary (SG) streams. The primary stream is injected in the burner together with the coal. The secondary stream retrieves heat energy with the product in heat interchanger 2.
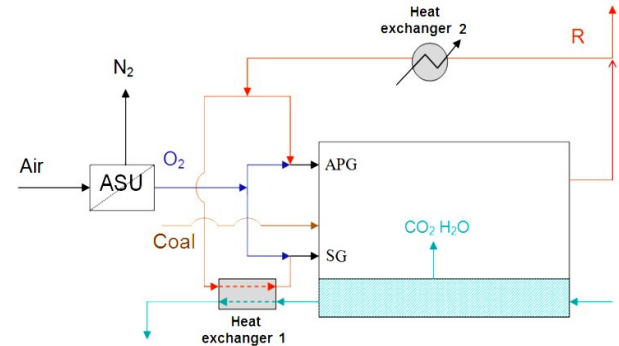

Figure 1. Oxy-fuel process scheme

It is considered that coal was previously dried (70%), and only CO_2 is produced in the combustion of coal. It is assumed that the kiln is adiabatic. The kiln operating conditions are presented in Table 1.

Table 1. Operating conditions considered by the global model simulations.

C_E (GJ/Ton)	E (%)	O_P (w/w)	T_R (K)	T_S (K)	T_C (K)
4	10	0.995	367	300	300

T_O (K)	T_{GS} (K)	R (w/w)	RPM	FVS	P (bar)
300	1073	0.4 - 0.9	1.5	0.1	1

In Table 1, C_E, E and O_P are the specific energy consumption of the process, oxygen excess and oxygen purity in the ASU output respectively. T_R, T_S, T_C, T_O and T_{GS} are the temperature of the recirculation stream, solids, coal, oxygen and oxidizing secondary stream respectively. R, RPM, FVS and P are the range of flue gas recirculation, kiln's angular velocity, volumetric fraction of solids and pressure respectively.

3. CFD SIMULATION

A kiln with 2.5m internal diameter and 40m in length [7] was chosen for this study (see Figure 2). The mesh used in this study was developed in a previous work [7] and was later incorporated to the FLUENT 6.3 software. Mesh independence test was done in order to select a computational mesh that gives a low computational cost with similar accuracy of finer meshes [7].
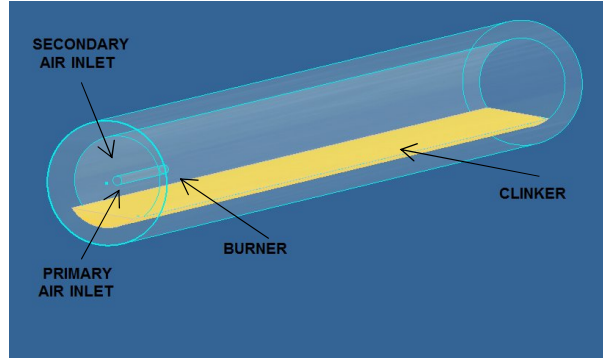

Figure 2. Scheme of the kiln

The model solves steady - mass, momentum and energy conservation equations [8] coupled to turbulence [8], radiation [9], non-premixed combustion [9], dispersion devolatilization models.

The oxy-fuel combustion simulations were done for pulverized coal combustion by changing the mass flow rate and composition of the oxidizing gas streams. The flue gas recirculation was changed between the 0.3 and 0.85. In addition a simulation using air as oxidant was also carried out in order to compare the simulation results.

The boundary conditions are shown in Table 2. An additional consideration in the simulation was that the oxidizing gas in the inlet (resulting to combine oxygen from de ASU and flue gas recirculation) is only formed by oxygen and carbon dioxide. The composition and mass flow rate of the primary and secondary oxidizing steams were calculated using the global model, and they are presented in Table 4 respectively. The inlet temperature was constant (300 K).

Table 2. Boundary conditions in FLUENT

Boundary in the kiln geometry	Numerical boundary conditions
Primary gas-fuel input	MASS FLOW INLET
Secondary gas input	MASS FLOW INLET
Flu gas output	OUTFLOW
Internal and external wall	WALL
load of lime and limestone	SOLID (inert)
Internal gas	FLUID

Table 3. Molar fraction for O_2 and CO_2 for all recirculation cases

Recirculation	O_2	CO_2
30%	68%	32%
40%	65%	35%
55%	51%	49%
60%	47%	53%
65%	42%	58%
70%	37%	63%
80%	28%	72%
85%	23%	77%

Table 4. Oxidizing gas mass flow

Recirculation	Primary gas (kg/h)	Secondary gas (kg/h)
30%	0.858	0.050
40%	0.828	0.117
55%	0.790	0.618
60%	0.778	0.861
65%	0.768	1.169
70%	0.757	1.576
80%	0.738	2.984
85%	0.729	4.381

The mathematical model was solved using FLUENT 6.3. Simulations finished with differences of 1×10^{-6} in the mass balances and between 1% ant 10% of differences for energy inputs and outputs for the different simulated cases.

4. RESULTS

4.1. Global Model

In the oxy-fuel combustion process, the partial pressure of carbon dioxide is higher than in the air combustion process. It will expect that, at constant temperature, the radiation will be more effective because carbon dioxide emissivity is higher than that of nitrogen. The adiabatic process temperature, for different recirculation ratios, is presented in Figure 3.
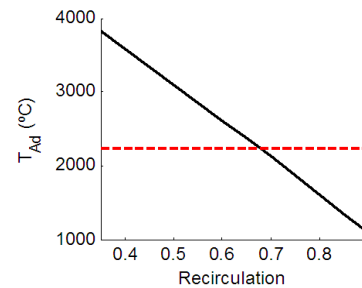

Figure 3. Adiabatic process temperature for different recirculation ratios.

The horizontal red line in the Figure 3, show the value of adiabatic temperature of the air-fuel process. It observes that the process temperature can be controlled with the recirculation fraction of the flue gases. To obtain the same adiabatic temperature when it use air as an oxidant (T=2230°C, see the horizontal line in the Figure 3) it's necessary to recirculate 67.8% of the output stream of the flue gases. This adiabatic temperature is very sensitive to small changes in the recirculated fraction. Close to R=67.8% the process temperature changed at a rate of 49.72°C per each percentage of unit recirculation.

On the other hand, it is necessary to evaluate the convective energy transfer between the solid and gas phases. The rate of heat transfer will depend of hydrodynamic parameters and transport and thermodynamic properties of the species. Nusselt number is evaluated through the correlation from Tscheng & Watkinson [11], that was developed for rotary kilns.

In order to achieve a similar Nusselt number for that in air combustion, the recirculation ratio is close to 68.2%. This recirculation is higher than that required to conserve the adiabatic process temperature. However, the thermal conductivity of the flue gases produced in the oxy-fuel combustion process is higher so the convective heat transfer

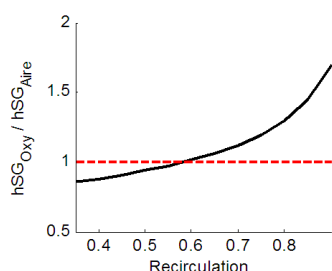coefficient will be higher for oxy-fuel combustion (see Figure 4).

Figure 4. Nusselt number for different recirculation ratios.

From Figure 5, it can be observed that the oxy-fuel combustion process gives a convection heat transfer coefficient higher to the air for recirculation ratios higher than 58.2%. Nevertheless, this limit increases to 60.4% when heat transfer to the solid phase and its endothermicity are considered.
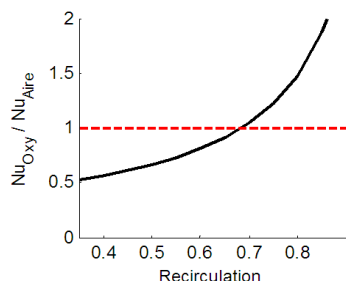

Figure 5. Convective heat transfer coefficient for different recirculation ratios.

Based on previous results, a recirculation range between 60.4%-67.8% can be used in order to achieve similar heat transfer characteristics for those obtained when the combustion takes place with air.

4.2. 3D Model

The convective and radiative energy transfer mechanisms to the solid bed is presented in Figure 6 for different recirculation ratios, and compared to the simulations when air is used in the kiln. As noted previously, the energetic contributions by radiation are higher when air is replaced by oxygen. In the ranges simulated by the 3D model, the oxy-fuel radiation to the bed is superior. On the other hand, the energy contribution to the bed by convection mechanism is higher than that for an air-based kiln when the recirculation ratio is higher than 60%. This result is similar to that obtained by the global model.
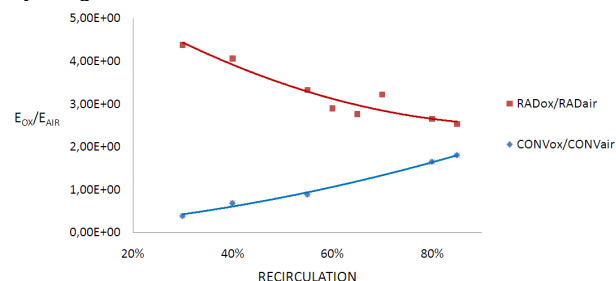

Figure 6. Energy transfer by convection and radiation for different recirculation ratios.

In the Figure 7 is presented the total energy flux to the bed for oxy-fuel (symbols) and air combustion (red line). An important feature presented In Figure 7 is that, independently from the recirculation ratio, the oxy-fuel kiln provides more energy to the solid bed, given the operating conditions and kiln configuration analyzed in this work. It might increase the clinker production or the decrease the specific fuel consumption per ton of clinker.
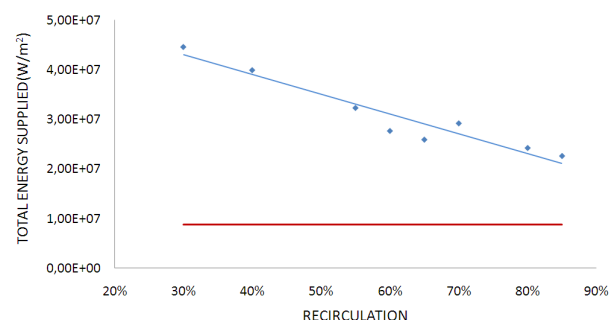

Figure 7. Total energy supplied to the solid phase for different recirculation ratios .

The influence of the recirculation ratio on the maximum flame temperature is presented in Figure 8. The model predicts that recirculation ratios lower than 77% provides higher temperatures than the air-based combustion. Comparison of the 3D model results with the global ones presented in Figure 3 reveal that the later model provides the shape of the temperature distribution.
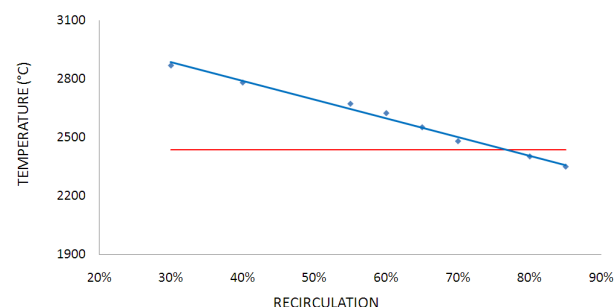

Figure 8. Maximum temperature of the process for different recirculation ratios.

.

The flame length of the oxy-fuel combustion (see Figures 9 and 10) is short for low recirculation ratios, because a higher partial pressures of oxygen is available for the oxidation reactions. As the recirculation increases, the flame length becomes larger, and becomes equal to that of the air-based combustion when the recirculation ratio is 68% (red line). From this recirculation ratio, the flame length increases up to two times the length of the air flame for a recirculation of 85%.
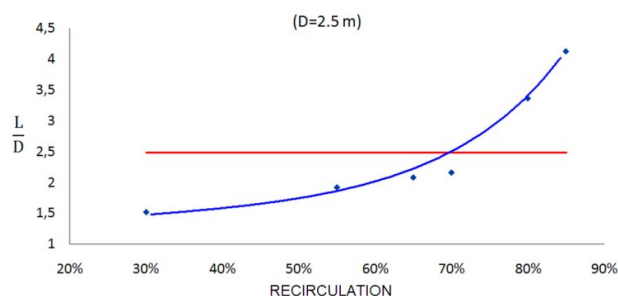

Figure 9. Recirculation effect in the length flame for different recirculation ratios

Qualitatively, Figure 10 shows that at high recirculation ratios the flame becomes thinner and larger than that obtained with air.
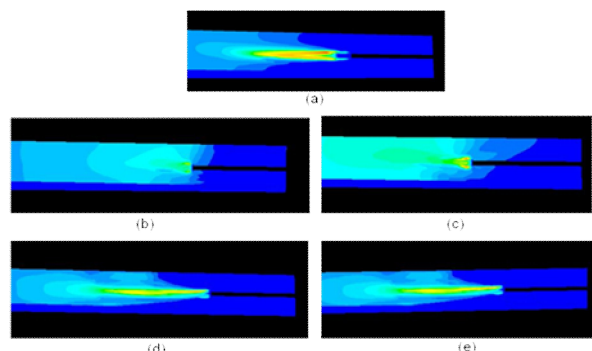

Figure 10. Flame lengths: a) Air, b) 30%, c) 55%, d) 65% and e) 80%.

An important aspect in relation to the oxy-fuel combustion in the kiln is that short flames and high temperatures can be achieved, which are good characteristics for the cement production process.

5. SUMMARY AND CONSLUSIONS

Two mathematical phenomenological models of the oxy-fuel combustion process in a cement kiln were developed: a global model and a local three-dimensional model. The flue gas recirculation effect on the heat transfer by convection and radiation mechanisms was presented. The models can predict for flame temperature, the energy transfer to the bed, the flame length and other important aspects of the process. The results of the global model showed good similarity with the three-dimensional model results at a much lower computational time. The models can be used for the evaluation of operating conditions in order to increase the kiln energy efficiency and clinker production rates.

6. ACKNOWLEDGMENTS

7. REFERENCES

[1] International Energy Agency. "CO2 Capture in the Cement Industry", Greenhouse Gas R&D programme, Gloucestershire, Final Report, 2008.

[2] ECRA (European Cement Research Academy) "ECRA CCS Project - Report about phase II", Duesseldorf, Technical Report, 2009.

[3] F. Zeman, "Oxygen combustion in cement production," *Energy Procedia,* vol. 1, pp. 187-194, 2009.

[4] F. Zeman and K. Lackner, "The Redusced Emission Oxygen Kiln," The Earth Institute at Columbia University, New york. 2008.

[5] "Carbon capture technology - Options and potentials for the Cement Industry," ECRA (European Cement Research Academy), Duesseldorf, Technical Report, 2007.

[6] A. H. Al-Abbas*, et al.*, "CFD modelling of air-fired and oxy-fuel combustion of lignite in a 100 KW furnace," *Fuel,* vol. 90, pp. 1778-1795, 2011.

[7] C. Parra, "Evaluación de la sustitución de carbón de síntesis en un horno de calcinación de la industria cementera," Maestría en Ingeniería Química, Facultad de minas, Universidad Nacional de Colombia, Medellín, 2009.

[8] H. K. Versteeg and W. Malalasekera, *An Introduction to Computational Fluid Dynamics, the Finite Volume Method.* London, 1996.

[9] "User's Guide," Fluent Inc.2006.

[10] V. V. Ranade, *Computational Flow Modeling for Chemical Reactor Engineering*. San Diego, 2002.

[11] S. H. Tscheng and A. P. Watkinson, "Convective heat transfer in a rotary kiln," *The Canadian Journal of Chemical Engineering,* vol. 57, pp. 433-443, 1979.

Aspen Plus Simulation for CO$_2$-flue gas separation of a coal-fired power plant

Udara Sampath P. R. Arachchige, Telemark University College, Porsgrunn, Norway;

Morten Christian Melaaen, Telemark University College, Porsgrunn, Norway

The CO$_2$ is one of the main pollutants for global warming and climate change effect. In order to carry on power generation by fossil fuel, CCS technologies are required to reduce the environmental impact by CO$_2$ emissions. The post combustion CO$_2$ capture via chemical absorption is the most effective and widely used technology in the CO$_2$ recovery process. This paper presents the detailed description of the chemical absorption process using MEA as a solvent and sensitivity analysis to improve the process performance. The model was developed in 'Aspen Plus' and possible chemical reactions were introduced using an electrolyte wizard. The 500MW coal power plant flue gas with 85% of CO$_2$ removal was considered. The process flow diagram of the removal process is given in Figure 1.
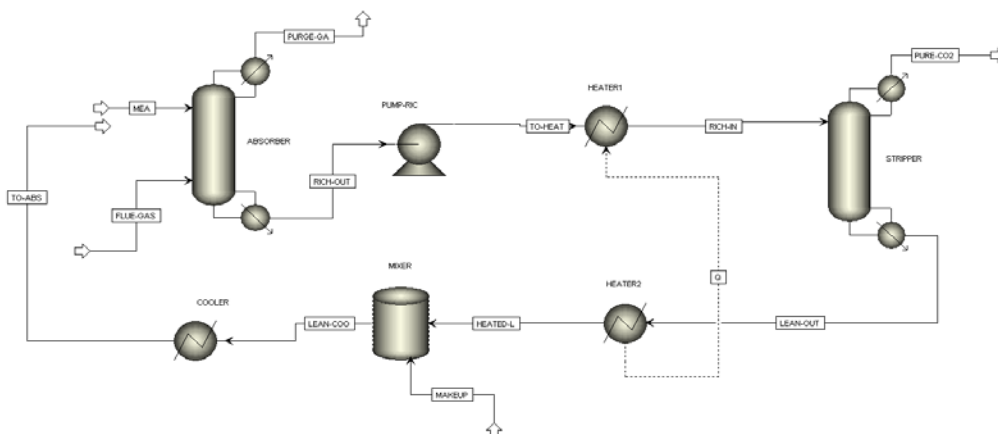

Figure 1: Process Flow Sheet

The sensitivity analysis was performed to check the effect of absorber pressure and packing height along with solvent temperature on re-boiler duty, re-boiler temperature and pump work. According to the total work requirement equation, the required work for CO$_2$ removal process was calculated for every single simulation step. The work for complete CO$_2$ recovery process decreases as the packing height and pressure of the absorber increases. Similarly, the work requirement decreases with increasing solvent temperature. The absorber pressure, packing height and solvent temperature are most important factors to reduce the work load for removal process. Future works have to be carried out to check the effect of other parameters, such as, stripper and absorber packing type and solvent flow rate effect etc.

Implications of the Part–Load Behaviour of an Integrated Post-Combustion CO_2 Capture Process for Hard-Coal-Fired Power Plants

Sebastian Linnenberg[1], Alfons Kather

Institute of Energy Systems, Hamburg University of Technology, Denickestr. 15, D-21073 Hamburg, Germany

1. Introduction

Due to the increasing amount of installed fluctuating energy sources, such as wind energy, the requirements on the operation of coal-fired power plants change. To maintain a stable energy supply, the fluctuating energy production of wind turbines needs to be compensated by increased flexibility, i.e. an enhanced part-load operation of coal-fired power plants. These requirements also remain valid for power plants with an integrated CO_2 capture process.

If the power plant is operated in part-load, flue gas parameters (i.e. composition, volume flow, temperature) change and the operation of the CO_2 capture unit and the CO_2 compressor deviates from their design point. Therefore, appropriate part-load capable models of an integrated overall process need to be developed.

2. Modelling

The influence of the CO_2 capture unit and the CO_2 compression on the net output of the power plant is examined by the combination of three independent models for the power plant, the CO_2 capture unit and the CO_2 compressor.

Power plant: The power plant model used in this work is based on a state-of-the-art hard-coal-fired power plant with high steam parameters. The main boundary conditions of the power plant at its design point are given in Table 1. To account for the part-load behaviour of the power plant and its effect on the overall process, several components (i.e. steam generator, steam turbines, heat exchangers and auxiliary power of the blowers and pumps) need to be modelled by using physical expressions or characteristic lines, which are derived from existing components. For a comprehensive overview of the complete modelling assumptions it is referred to [1, 2].

Table 1: Boundary conditions of the power plant at full-load

Gross (output) capacity (MW)	1100	Live steam conditions (°C, bar)	600, 285
Net (output) capacity (MW)	1017[*]	Reheated steam conditions (°C, bar)	620, 60
Net efficiency (%)	45.60	Flue gas mass flow (kg/s)	1020
Condenser vacuum (mbar)	39/49	Flue gas CO_2 concentration (vol.-%)	13.9
Pressure in the IP/LP crossover (bar)	3.9	Flue gas O_2 concentration (vol.-%)	3.3

[*]High aux. power of the power plant, due to electric driven feed water pump

Integration: The post-combustion CO_2 capture process (PCC) is integrated as a retrofit option to the existing hard-coal-fired power plant. The heat for the regeneration of the solvent is provided by extracting steam from the water-steam-cycle of the power plant at the IP/LP crossover. As the pressure in the IP/LP crossover is reduced if an additional steam extraction is foreseen, a pressure maintaining valve (PMV) is placed downstream the branch to the reboiler,

[1] Corresponding and presenting author. Tel.: +49-40-42878-2772; fax: +49-40-42878-2841

E-mail address: linnenberg@tuhh.de

upstream the LP turbine, to maintain a constant steam pressure and thus the temperature level in the reboiler required by the capture process. The condensate from the reboiler is forwarded to the feed water tank in the water-steam-cycle. For additional information, it is referred to [2,3,4].

CO_2 compressor: It is assumed, that a pipeline pressure of 110 bar is necessary to transport the separated CO_2 to the injection well. To realise the pressure increase of the CO_2 leaving the desorber an integrally-geared (radial) compressor with six stages, three intercoolers and an aftercooler is considered. As the working range (i.e. the variation of the CO_2 flow) of such compressors is commonly limited, three additional measures are considered to allow a reasonable working range at a constant discharge pressure of 110 bar:

First, adjustable inlet guide vanes are considered, which can enlarge the working range for the related volume flow to 72 % - 103 % [5]. Secondly, to increase the inlet volume flow, a part of the volume flow leaving the compressor is recycled (bypass operation). Using this measure, limitations of the working range can be avoided at the expense of a strongly increased power duty of the compressor. Thirdly, to reduce the high power duty of the compressor if bypass operation is used, four identical compressors, which can be separately switched off are considered [2,5].

Figure 1: Part-load behaviour of four CO_2 compressors at a constant pressure ratio of 55

By combining all three measures, the CO_2 compression can be realised for a reasonable working range. In Figure 1 the minimal specific power duty of the CO_2 compressor system is shown for different CO_2 volume flows.
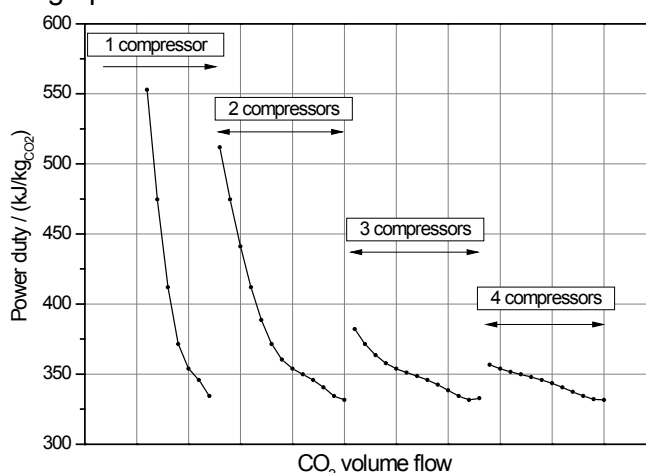
CO_2 capture unit: To allow a realistic simulation of the capture unit, the geometry of absorber and desorber must be taken into account. Therefore, it becomes necessary to calculate the mass and heat transfer as well as the kinetics of the chemical reactions of the capture process. In this work, the post-combustion CO_2 capture process is modelled by a rigorous rate-based model. The flowsheet of the CO_2 capture unit is based on a conventional CO_2 capture process using 30 wt.-% MEA. A detailed explanation of the capture process can be found in [1,2].

3. Overall process at full-load

As explained above, the heat for the reboiler is commonly provided by extracting low-pressure steam from the IP/LP crossover of the water-steam-cycle of the power plant. The effect of the steam extraction on the overall process (power plant, CO_2 capture unit and CO_2 compressor) is not only determined by the reboiler duty and the corresponding amount of extracted steam (quantity) but also by the temperature and pressure of the extracted steam (quality). The process parameters affecting the quantity and the quality of the extracted steam are the solvent circulation rate and the desorber pressure of the capture unit. For this reason, these process parameters need to be optimised with respect to the overall process [3,4]. As the solvent circulation and the desorber pressure also affect the design of the absorber and the desorber

column, the diameters of the columns need to be adjusted[2] to allow a fair comparison between the varied variables.

In Figure 2 the net efficiency penalty of the integrated overall process is shown for different solvent circulation rates (L/G) and different desorber pressures. Besides the effect of steam extraction, the auxiliary power of the capture unit (blower and solvent pumps) and the CO_2 compressor, and the auxiliary power of the cooling pumps are considered. To avoid an excessive degradation of the solvent, the desorber pressure is reduced to a maximum pressure of 2 bar. From Figure 2 it can be seen that the minimal net efficiency penalty occurs at
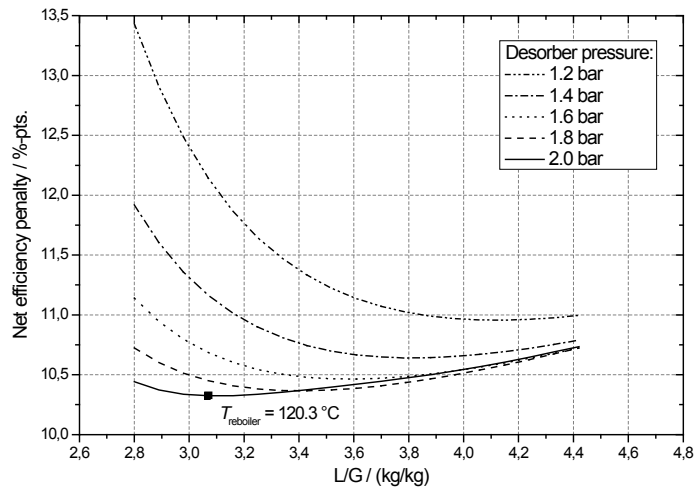

Figure 2: Net efficiency penalty of a hard-coal-fired power plant with PCC for different L/G and different desorber pressures

a desorber pressure of 2 bar and a L/G of 3.1. For the full-load operation of the power plant the minimal net efficiency corresponds to the minimal heat duty of the capture unit.

4. Overall process at part-load

If the power plant and thus the overall process is operated at part-load conditions, the interface quantities between the three sub-processes power plant, CO_2 capture unit and CO_2 compressor change. For instance, the flue gas parameters (i.e. CO_2- and O_2-concentration and flow), which strongly influences the CO_2 capture unit and the CO_2 compressor. Although the heat and the power duty of the CO_2 capture unit decrease with a decreasing flue gas flow [2], the net efficiency penalty increases at part-load conditions (see Figure 3). The higher efficiency penalty[3] at part-load conditions can be mainly attributed to the influence of the extracted steam on the steam turbine performance. If the power plant is operated at part-load conditions, the pressure level in the IP/LP crossover decreases. To maintain the pressure level in the IP/LP crossover at the pressure required by the CO_2 capture unit, the losses due to steam conditioning increase compared to full-load operation. The effect of the different interface quantities on the net efficiency penalty at different load conditions is shown in Figure 4.

As the pressure level in the IP/LP crossover change, the L/G and desorber pressure need to be adjusted in order to find the minimal net efficiency penalty. In Figure 3 it can be seen that the reduction of the steam quality (i.e. the reboiler temperature decrease with decreasing desorber pressure) overcompensates the higher heat duty of the reboiler (i.e. the reduction of the desorber pressure results in a higher reboiler duty) resulting in a decreased net efficiency penalty at part-load conditions. Due to the fact that the compressor is designed for the minimum efficiency penalty of the overall process at full-load (p_{des}=2 bar), the reduction in desorber pressure is restricted by the surge line of the CO_2 compressor [2].

---

[2] Including a security factor of 85 %, a maximum approach to flooding of 70 % is assumed.

[3] The efficiency penalty refers to the net efficiency penalty of the conventional power plant at the corresponding load (i.e. 45.0 at 70% and 42.5 at 40% load).
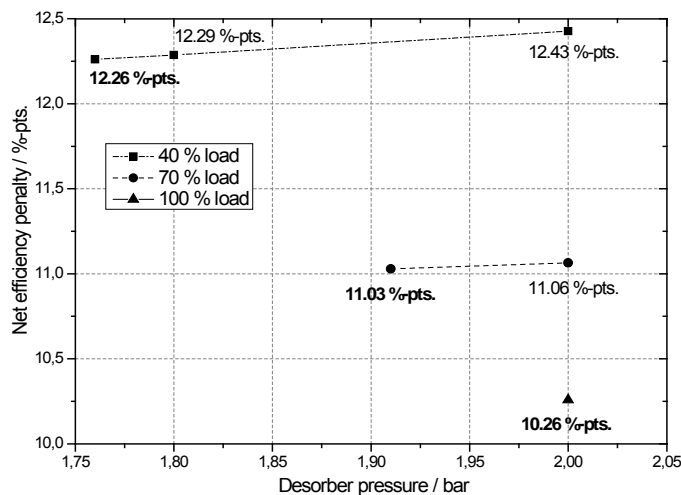
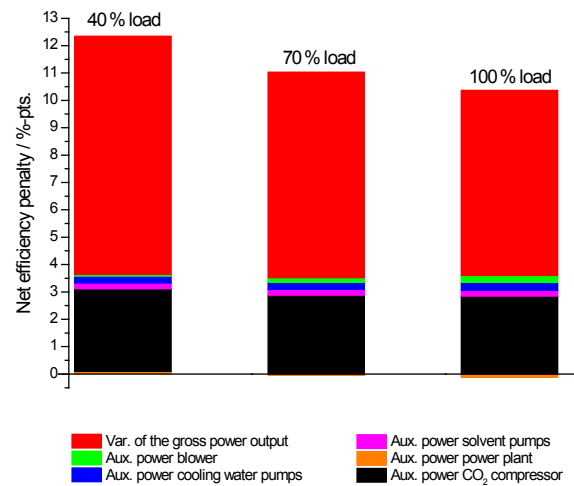**Figure 3**: Net efficiency penalty of a hard-coal-fired power plant in part-load

Figure 4: Net efficiency penalty of a hard-coal-fired power plant in part-load

5. Conclusions

The impact of the interface quantities (heat duty, cooling duty, power duty and reboiler temperature) was calculated for full-load and part-load conditions. It was shown that the net efficiency penalty of the overall process increases from 10.26 % at full load to 12.43 % at 40 % load due to the changed pressure levels in the different turbine sections of the power plant[4]. Furthermore, it was pointed out, that an optimisation of the process parameters (i.e. desorber pressure and solvent circulation rate) of the capture plant at a part-load of 40 % leads to an increase of the net efficiency from 12.43 % to 12.26 %.

Acknowledgements

Literature

[1]   LINNENBERG, S.; KATHER, A.: Evaluation of an Integrated Post-Combustion CO_2 Capture Process for Varying Loads in a Coal-Fired Power Plant using Monoethanolamine. In: *4th International Conference on Clean Coal Technologies*. Dresden, Germany, May 2009

[2]   KATHER, A.; LINNENBERG, S.; OEXMANN, J.: POSEIDON - Post-Combustion CO_2-Abtrennung: Evaluierung der Integration, Dynamik und Optimierung nachgeschalteter Rauchgaswäschen PTJ/0327785 / COORETEC (submitted for publication), 2011

[3]   LINNENBERG, S.; LIEBENTHAL, U.; OEXMANN, J.; KATHER, A.: Derivation of Power Loss Factors to evaluate the Impact of Post-Combustion CO_2 Capture Processes on Steam Power Plant Performance. In: *Energy Procedia* 1, September 2011

[4]   OEXMANN, J.: *Post-Combustion CO_2 Capture: Energetic Evaluation of Chemical Absorption Processes in Coal-Fired Steam Power Plants*. Hamburg University of Technology, Institut für Energietechnik, Phd thesis, January 2011.

[5]   LIEBENTHAL, U.; KATHER, A.: Design and Off-Design Behaviour of a CO_2 Compressor for a Post-Combustion CO_2 Capture Process. In: *5th International Conference on Clean Coal Technologies*. Saragozza, Spain, May 2011

---

[4] A detailed explanation is given in [2].

CO$_2$-stable and Co-free dual phase membrane for oxygen separation

Huixia Luo, Konstantin Efimov, Heqing Jiang, Armin Feldhoff and Jürgen Caro,

Institute of Physical Chemistry and Electrochemistry, Leibniz University Hannover,Callinstr. 3-3A D-30179 Hannover, Germany;

Haihui Wang,School of Chemistry & Chemical Engineering, South China University of Technology, No. 381 Wushan Road, Guangzhou 510640, China

1. Introduction

The increase of carbon dioxide emissions is considered as the main contribution to the global warming. Therefore, there is an urgent need to reduce the emissions of CO_2 into the atmosphere. Recently, CO_2 capture and storage technologies to reduce the CO_2 emissions from coal fired power plants have gained great attentions of decision makers in governments, industry and academia. There are three major concepts for CO_2 sequestration: post-combustion capture, pre-combustion separation and oxyfuel techniques [1]. Mixed oxygen ionic-electronic conducting ceramic membranes (MIECMs) have gained increasing attention due to their potential applications in oxygen supply to power stations for CO_2 capture according to the oxyfuel concept [2]. Such oxygen permeable membranes are demanding not only high oxygen permeability but also long-term stability. However, the perovskite-type membranes usually contain alkaline earth metals on the A site, which tend to react with CO_2 and form carbonates [3]. Dual phase membranes which consist of an oxygen ionic conducting (OIC) phase and an electronic conducting (EC) phase in a micro-scale phase mixture are considered to be promising substitutes for the single phase MIEC materials, since their compositions can be tailored according to practical requirements. However, due to the use of noble metals as electronic conductor and reactions between OIC and EC phases at high operation temperature, most of these composite membranes are too expensive or unstable [4]. Therefore, the development of new oxygen-permeable membranes with high CO_2 stability is highly desired. Herein, a novel earth alkaline-free CO_2-stable and cobalt-free composite dual phase membrane, 40 wt.% $NiFe_2O_4$ - 60 wt.% $Ce_{0.9}Gd_{0.1}O_{2-\delta}$ (abbreviated as 40NFO - 60CGO) is prepared and evaluated.

2. Experimental

The 40NFO-60CGO powder was prepared via a one-pot method. [5] The powders were calcined at 1000 °C for 10 h then pressed to disk membranes under a pressure of 10 MPa in a stainless steel module with a diameter of 18 mm. Green disks were pressure-less sintered at 1350 °C for 10 h. The dense disks were polished with 1200 mesh sandpaper from both sides to achieve a 0.5 mm membrane thickness. To improve the oxygen surface exchange rate on the air side, the membranes were coated with a $La_{0.6}Sr_{0.4}CoO_{3-\delta}$ (LSC) porous layer on one side with a paste made of 40 wt.% LSC powder and 60 wt.% terpineol.

The phase composition of the composite membrane was determined by powder X-ray diffraction (PXRD) using a PHILIPS-PW1710. The disc membranes were studied by scanning electron microscopy (SEM) and back scattered SEM (BSEM) using a JEOL JSM-6700F. The element distribution was studied on the same electron microscope by energy dispersive X-ray spectroscopy (EDXS) at 15 keV.

The oxygen permeation was studied in a self-made high-temperature oxygen permeation cell. A gold paste was used to seal the disk onto a quartz tube at 950 °C for 5 hours. Air was the feed; He and CO_2 have been used as sweep gases (29 ml/min, 99.995 % + 1 ml Ne/min as the internal standard gas). A gas chromatograph (Agilent 6890) was on line connected to the permeation apparatus. The leakage of oxygen was subtracted when the oxygen permeation flux was calculated. The total flow rate of the effluents was calculated from the change in the Ne concentrations before and after the permeator. The oxygen permeation flux calculation was shown in detail in [6].

3. Results and discussion

The dual phase membrane was synthesized using powder mixing and the one-pot method. X-ray diffraction (XRD) (Fig. 1) clearly confirmed that both 40NFO-60CGO membranes consist of only the two phases NFO and CGO. The unit cell parameter of the pure phases NFO (0.83455 nm) and CGO (0.54209 nm) are almost the same as in the 40NFO-60CGO dual phase material (NFO: 0.83350 nm, CGO: 0.54186 nm). The phase composition turned out to be stable with time. As an example, Fig. 1c shows the XRD of the spent 40NFO-60CGO membrane after the long-time oxygen separation with CO_2 as sweep gas as shown in Fig. 3.
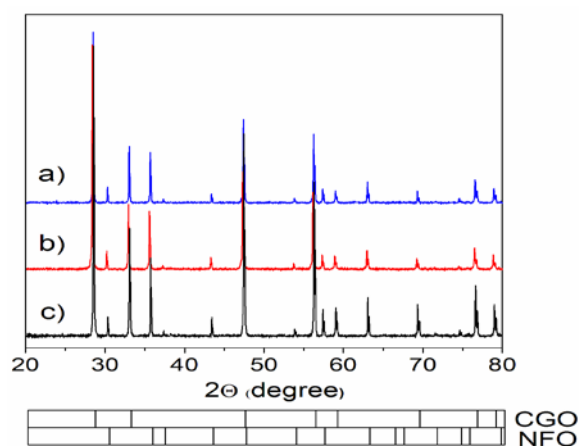
Fig.1 XRD patterns of the 40NFO-60CGO composite membrane prepared by powder mixing method (a), one-pot method (b) and one-pot membrane after CO_2 stability test (c).

Fig. 2 shows the results of SEM, BSEM, and EDXS of both membranes. For the membrane prepared by powder mixing (Fig. 2a, c, e), the grain size of CGO in these composite membranes is smaller (2 ~ 4 μm) than that of NFO (3 ~ 7 μm). Especially BSEM (Fig. 2c) shows that there is clustering of grains of one and the same type, i.e. NFO-NFO and CGO-CGO aggregation. In comparison to the powder mixing, the membrane prepared by the direct one-pot method shows much smaller grains and a higher homogenization of the NFO and CGO phases (Fig. 2b, d, f). By BSEM and EDXS, the NFO and CGO grains could be distinguished. The dark grains in BSEM are NFO and the light ones CGO since the contribution of the backscattered electrons to the SEM signal intensity is proportional to the atomic number. The same information is provided by EDXS. The green color (dark in the black-and-white version) is an overlap of the Fe and Ni signals, whereas the yellow color (light) stems from an average of the Ce and Gd signals.
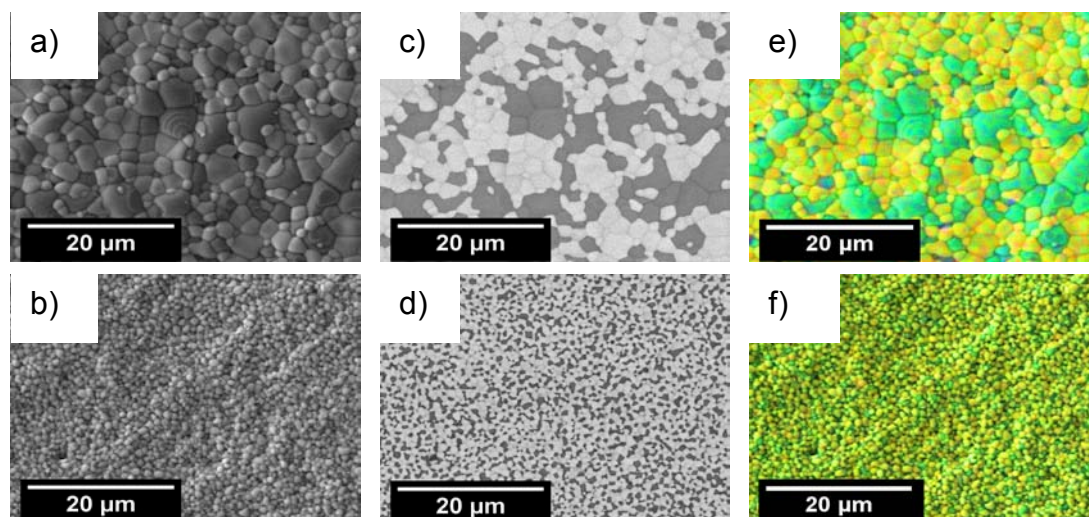
Fig. 2. Grain structure of the surface (top view) of the 40NFO-60CGO composite membrane after sintering at 1350 °C for 10h prepared by different methods: (i) powder mixing in a mortar by hand (up line, a), c), e), and (ii) direct one-pot method (down line, b), d), f): SEM (a and b), BSEM (c and d), and EDXS (e and f).

Fig. 3 shows the long-time behaviour of oxygen permeation flux through 40NFO-60CGO composite membrane at 1000 ^{o}C. During this oxygen permeation test, an

Fig. 3. Time dependence of oxygen permeation flux through 40NFO-60CGO membrane at 1000 ^{o}C using pure CO_2 as sweep.

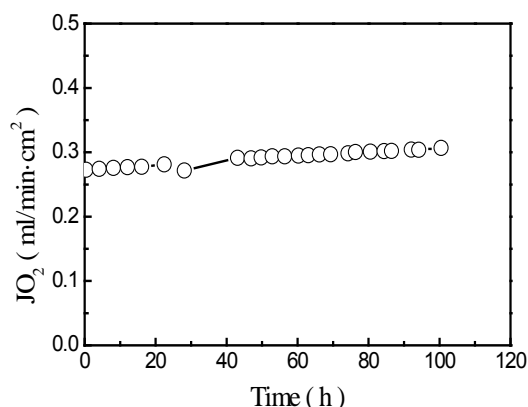oxygen permeation flux of about 0.30 ml/min·cm^2 was obtained at 1000 ^{o}C and no decrease of the oxygen permeation flux was found during the permeation test. After the oxygen permeation test, the sample was characterized by XRD, as shown in Fig. 1c. It can be seen that the dual phase structure was kept, which indicates that the 40NFO-60CGO exhibits an excellent structure stability under CO_2 atmosphere.

4. Conclusions

In conclusion, a novel CO_2-stable and Co-free dual phase membrane of the composition 40 wt.% $NiFe_2O_4$-60 wt.% $Ce_{0.9}Gd_{0.1}O_{2-\delta}$ (40NFO-60CGO) is successfully synthesized via a direct one-pot method and for comparison by powder mixing in a mortar. In a 100 h oxygen permeation using CO_2 as the sweep gas, no decline of the oxygen permeation flux was found indicating that our dual phase membrane is CO_2-stable.

5. Acknowledgements

References

[1] R. Kneer, D. Toporov, M. Förster, D. Christ, C. Broeckmann, E. Pfaff, M. Zwick, S. Engels M. Modigell, *Energy Environ. Sci.* **2010**,*3*,198.

[2] H.H. Wang, S. Werth, T. Schiestel, J. Caro, *Angew. Chem. Int. Ed.* **2005**,*44*,6906.

[3] J.X. Yi, S.J. Feng, Y.B. Zuo, Y.B Liu, C.S. Chen, *Chem. Mater.* **2005**,*17*,5856.

[4] K. Kobayashi, T. Tsunoda, Solid State Ionics **2004**,*175*,405.

[5] H.X. Luo, K. Efimov, H.Q. Jiang, A. Feldhoff, H.H. Wang, J. Caro, *Angew. Chem. Int. Ed.* **2011**,*50*,759.

[6] H.X. Luo, H.Q. Jiang, K. Efimov, H.H. Wang, J. Caro, AClhE J. DOI 10.1002/aic.12488.

Investigation of thermal and pO$_2$ stability of Ba$_{0.5}$Sr$_{0.5}$Co$_{0.8}$Fe$_{0.2}$O$_{3-\delta}$ for oxygen-transport membranes

C. Niedrig[1], S. Taufall[1], S. F. Wagner[1], W. Menesklou[1], E. Ivers-Tiffée[1,2]

[1] Institut für Werkstoffe der Elektrotechnik (IWE), Karlsruhe Institute of Technology (KIT), 76131 Karlsruhe, Germany

[2] DFG Center for Functional Nanostructures, Karlsruhe Institute of Technology (KIT), 76131 Karlsruhe/Germany

Ba$_{0.5}$Sr$_{0.5}$Co$_{0.8}$Fe$_{0.2}$O$_{3-\delta}$ (BSCF) has previously been identified as a composition with excellent oxygen-ionic and electronic transport properties reported by many research groups. In its cubic phase, this mixed-conducting perovskite is a promising candidate for oxygen,transport membranes (OTM) operated in the absence of carbon dioxide.

As the transport properties are very sensitive to changes in material composition and the occurrence of secondary phases, the long-term stability of BSCF under operating conditions is of crucial importance. This contribution is therefore focused on the stability of the BSCF cubic phase in the targeted temperature range for OTM applications (T = 700...900 °C) and in atmospheres with low oxygen contents. Previous studies in literature report a reversible phase transition from cubic to hexagonal at temperatures below 900 °C and suggest limited chemical stability below oxygen partial pressures pO$_2$ of around 10^{-6} bar.

Single-phase cubic BSCF powders were annealed in air and several pO$_2$ at different temperatures over varying periods of time. Phase composition was subsequently analyzed by means of X-ray diffractometry (XRD). Electrical conductivity of corresponding ceramic bulk samples was monitored between 700 and 900 °C over several hundreds of hours. From these combined data, an assessment of the thermal as well as the pO$_2$ stability of BSCF is facilitated.

Separation of CO_2/N_2 by a Carbon Membrane

Yuliya Wall, _Gerd Braun, Cologne University of Applied Sciences, Cologne, Germany;_
Nadine Kaltenborn, Ingolf Voigt, Fraunhofer Institute for Ceramic Technologies and Systems,
IKTS, Hermsdorf branch of the institute, Hermsdorf, Germany;
Gerd Brunner, Hamburg University of Technology (TUHH), Hamburg, Germany

Introduction

The membrane separation of gas mixtures has met with rising interest because of the great significance for industrial applications. Inorganic membranes, especially the carbon membranes have been identified as promising candidates for CO_2 separation from flue gas streams. In comparison to other gas separation membranes like polymeric materials, carbon membranes show better selectivity, heat resistance and chemical stability.

The first step of this study was to evaluate the use of carbon membranes, which were provided by Fraunhofer Institute for Ceramic Technologies and Systems IKTS (Hermsdorf branch of the institute), for the CO_2/N_2 separation in laboratory scale.

Experimental Set-up

Amorphous carbon or graphite-like carbon is plane structured with a defined lattice plane distance of 0.34 nm. Because of their brittleness, carbon membranes were synthesized on porous alumina tubes by dipcoating the tubes in a polymeric precursor solution and pyrolysis at temperatures above 873 K in an inert atmosphere. The tubes had an inner diameter of 7 mm, an outer diameter of 10 mm and a length of 250 mm.

A schematic illustration of the set-up is shown in Fig. 1. The feed gas mixtures with defined composition were supplied from the gas bottle (Praxair). The composition of the permeate stream was analysed by on-line gas chromatography equipped with a mass spectrometry detector.

The permeation and separation properties of the membranes were examined by means of the steady-state measurement method with pure gases and a CO_2/N_2 gas mixture (20/80 Mol %) in a temperature range from 293 K to 363 K and at feed pressures up to 1.4 MPa and atmospheric pressure on the permeate side.
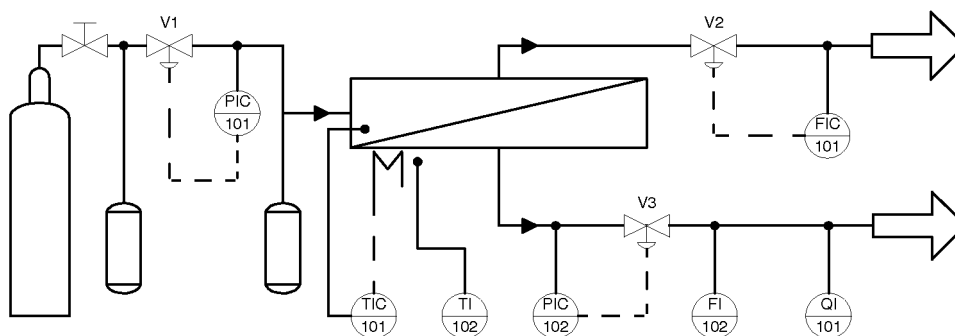

Figure 1. Schematic illustration of set-up.

Oxygen permeation performance of $La_{0.7}Sr_{0.3}Co_{0.5}Fe_{0.5}O_{3-\delta}$ membrane in different atmospheres with carbon dioxide

Jong pyo Kim[1], Department of Chemical Engineering, Chungnam National University[1], Daejeon[1], Republic of Korea[1]; Edoardo Magnone[2], Greenhouse Gas Research Center, Korea Institute of Energy Research[2], Daejeon[2], Republic of Korea[2]; <u>Jung Hoon Park</u>[3] Greenhouse Gas Research Center, Korea Institute of Energy Research[3], Daejeon[3], Republic of Korea[3]

$La_{0.7}Sr_{0.3}Co_{0.5}Fe_{0.5}O_{3-\delta}$ powders were prepared through thermal decomposition of amorphous citrate precursors by calcinations at 1300 ^{o}C. The material properties were characterized by thermogravimetric-differential thermal analysis, X-ray diffraction, and four probe method. The results show that the membrane sintered at 1300 ^{o}C possesses a rhombohedral distorted symmetry structure with space group of *R3c* (space-group number = 167). We have studied the variation in lattice parameters with temperature and have observed a linear decrease in lattice parameters with synthesis temperature. It was also observed that the particle size increased with increasing temperature in the range from 800 to 1300 ^{o}C. Electrical conductivity of sintered $La_{0.7}Sr_{0.3}Co_{0.5}Fe_{0.5}O_{3-\delta}$ ceramics increases with temperature through a maximum, then decreases at relatively higher temperatures, due to oxygen vacancy formation. Oxygen permeation was performed between 700 and 950 ^{o}C under different oxygen partial pressures (0.21, 0.42, and 0.63 atm) and carbon dioxide concentrations (300, 500, and 700 ppm). As the oxygen partial pressure increases from 0.21 to 0.63 atm, the oxygen permeation flux correspondingly increases from 0.23 to 0.33 mL/min•cm^2 at 950 ^{o}C. Long-term permeation at high temperature in carbon dioxide conditions (700 ppm) over $La_{0.7}Sr_{0.3}Co_{0.5}Fe_{0.5}O_{3-\delta}$ membranes gives rise to the change of rhombohedral crystal structure distortion and morphologic of surface membrane.

Hydrogen separation and stability of V-Y alloy membrane for pre-combustion capture

Sung Il Jeon[1], Department of Chemical Engineering, Chungnam National University[1], Daejeon[1], Republic of Korea[1]; Soo Hyun Choi[2], Greenhouse Gas Research Center, Korea Institute of Energy Research[2], Daejeon[2], Republic of Korea[2]; Jung Hoon Park[3] Greenhouse Gas Research Center, Korea Institute of Energy Research[3], Daejeon[3], Republic of Korea[3]; Sung Chan Nam[4], Greenhouse Gas Research Center, Korea Institute of Energy Research[4], Daejeon[4], Republic of Korea[4]

Hydrogen production is an important technical issue, which is related to future energy and environmental problems. Recently many studies on hydrogen membrane have been conducted for applying to pre-combustion capture process. Also hydrogen may be separated using membrane technology from the reformer and water-gas shift reaction mixture.

In this work, $V_{99}Y_1$ membranes of 12 mm diameter and 1.0 mm thickness were machined by wire cutting from about 25 g cast ingot prepared using vacuum arc melting machine. In order to eliminate the effect of the contamination layer, after polishing both sides of the membrane, reactive ion etching (RIE) was treated (~500nm) on both sides of the dissociation and recombination of the retentate and permeate sides. Using dc magnetron sputtering system, a thin layer of about 150 nm thick of pure palladium (purity=99.99%) was deposited on the etched surface of membrane. The crystal structure of the selected alloy membrane was characterized with an X-ray diffractometer. The morphology of the $V_{99}Y_1$ membrane and the thickness of the Pd-layer were analyzed with a scanning electron. The high temperature/pressure permeation cell in a flat geometry was constructed for studies of hydrogen permeation under the condition of pre-combustion process. Hydrogen permeation study was performed within the temperature range of 300-450 $^{\circ}$C at the pressure of 1-2 atm. The hydrogen flux was increased with temperature, showing the maximum of about 22.9 ml/cm^2 min under 100% hydrogen as feed at 450 $^{\circ}$C using Ar sweep gas.

A ZEOLITE (ZSM-5) PDMS (POLYDIMETHLYSILOXANE) MIXED MATRIX MEMBRANE FOR CO$_2$ SEPARATION

Muhammad Hussain, Chair of Separation Science and Technology Uni-Erlangen, Erlangen, Germany, Prof. Dr. Axel König , Chair of separation Science and Technology Uni- Erlangen, Erlangen, Germany

1. Introduction:

Membrane based gas separation occur due to the difference in the permeability of the species flowing through the membrane [1, 2]. Generally, the permeability of a gas through the membrane can be thought of as the product of diffusivity and solubility. Therefore, gas separation through membranes can be broadly categorized into diffusivity- based and solubility-based separation.

Solubility difference is inherently caused by differences in the molecular-level energetic interactions of the membrane material with the permeating species. The exploitation of "chemically specific" energetic interaction, such as hydrogen bonding, may lead to greatly enhanced selectivity; however even simple van der Waals dispersion forces, which tend to be stronger for larger molecules, may lead to significant selectivity. This can lead to a situation in which it is possible to have the preferential permeation of one of the component as compared to other. The solubility-selective mode is especially advantageous in applications where a dilute heavy molecular weight species contaminates a light gas feed stream [3].

Gas separation may be achieved with both inorganic and polymeric membranes and also by mixing former and later to take the best characteristics of both known as mixed matrix membranes.

Filling zeolite (silicalite-1) in polymer membranes especially in silicone rubber membranes have great advantage in separation of alcohol from water due to molecular sieve effects from zeolites and hydrophobic nature of silicalite-1**.** Furthermore, good permeation for gases are also been observed with silicalite-1 filled polymer membranes. Experimental results show that the separation factor $\alpha CO_2/N_2$ is increased from 11.6 to 17.1 with increasing of silicalite from zero to 70 wt% [4]**.**

In the present study the Mixed Matrix Membranes (MMMs) were prepared by incorporation of zeolite (ZSM-5) filler in PDMS matrix to separate CO_2 from CO_2-N_2 gas mixtures. The membranes were tested for single gas permeability of CO_2 and N_2 at different filler loadings.

1

Furthermore, prepared MMMs were evaluated for CO_2-N_2 gas mixtures to exploit the selective sorption property of zeolite for CO_2 at elevated pressures. It was presumed that the adsorption of CO_2 in pure zeolite filler is proportional to the overall permeability of MMMs.

2. Experimental:

2.1 Membrane Preparation:

The silicone rubber membrane was prepared with Elastosil RT 601; supplied from the Walker Chemie, it consists of two components A and B. The two components mixed thoroughly at a 9:1 ratio to get a homogeneous mixture. To eliminate air trapped during mixing, a vacuum encapsulation done occasionally. Later on the mixture was put on a stainless steel plate for casting a membrane. The membrane was cured at room temperature for 24 hours and then striped out from casting plate. Zeolite (ZSM-5, from Tricat Zeolites GmbH) filled membranes are prepared by first mixing component A and zeolite thoroughly and then component B is added; finally the mixture was put on the stainless steel plate for casting a MMM of uniform thickness.

2.2 Gas permeation measurements:

The pure gas permeability was measured using a constant volume variable pressure apparatus as shown in the **Fig. 1**. A known pressure of gas was taken in a constant volume autoclave (B1) and then the gas was allowed to pass over the membrane surface while the permeate side was kept at atmospheric pressure (0 psig). The pressure difference across the membrane was measured and reported for the permeability measurement of single gases. For single gas experiments the retantate valve VR1 was kept closed.

The gas permeability was measured by the following (Eq.(1)):

$$P_o = \frac{\delta_M}{A_M(p_{iF} - p_{ip})} * \frac{V}{RT} * \frac{dp_{iF}}{dt} \tag{1}$$

The permeability P_o is reported in „Barrer"(10^{-10}cm^3 (STP) cm cm^{-2} s^{-1} cmHg^{-1}).

$\dfrac{dp_{iF}}{dt}$ feed pressure change of Component i with time (t), **T** is the operational temperature (K), **R** is the universal Gas constant, **V** is the volume of the autoclave (B1) i.e. 1.4 litre, A_M is the active permeation area of membrane (51.5 cm^2) of the membrane module (M), δ_M is the thickness of the membrane, and $(p_{iF} - p_{ip})$ is the pressure difference between feed side and the permeate side.

2

$$\alpha_{A/B} = \frac{P_A}{P_B} = \frac{D_A}{D_B} * \frac{S_A}{S_B} \qquad\qquad (2)$$

The ideal selectiviy $\alpha_{A/B}$ is the ratio of permeability coefficient of component A and B. While D_A, S_A and D_B, S_B are the solubility and diffusivity coefficients of individual components.

For mixture of gases permeate and retantate flow rates were measured by using bubble flow meters. Gas chromatogram (G-1530A) was used to measure permeate and feed side compositions.

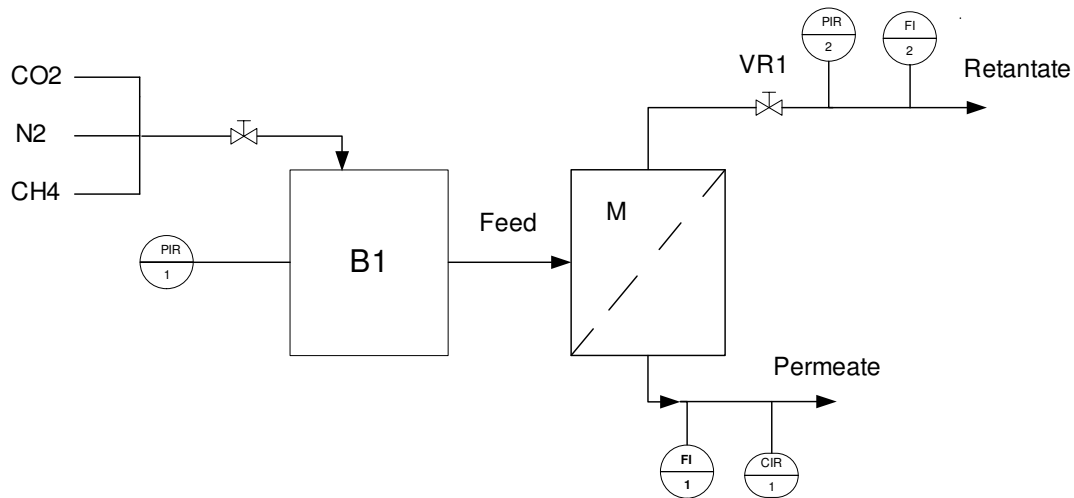**Fig.1: Experimental Setup for Gas Permeation measurements**

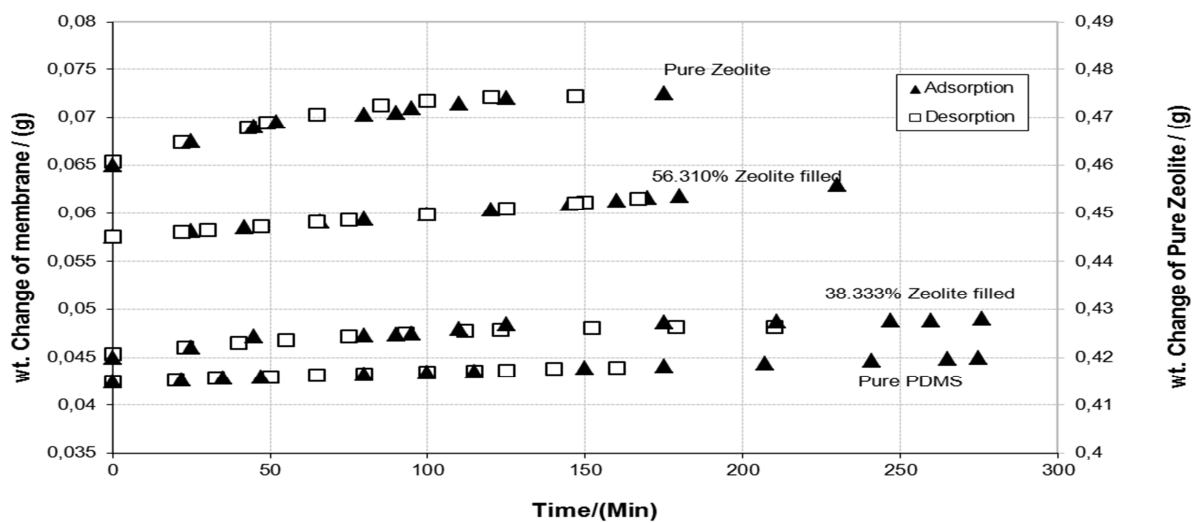## 3.Results and Discussion:

3.1 Adsorption Isotherms:

Fig. 2: Solubility data for different membranes reference to different zeolite loading in CO$_2$ environment (20bars and 300K)

3

The experimental results of adsorption and desorption behaviour dependency for different membranes were plotted and displayed in **Fig.2**. By filling membrane with zeolites, the solubility of the CO_2 increased as compare to pure polymer membrane. Moreover, the adsorption and desorption values are almost same for a particular membrane with different incorporated percentage of zeolite showing less hysteresis.
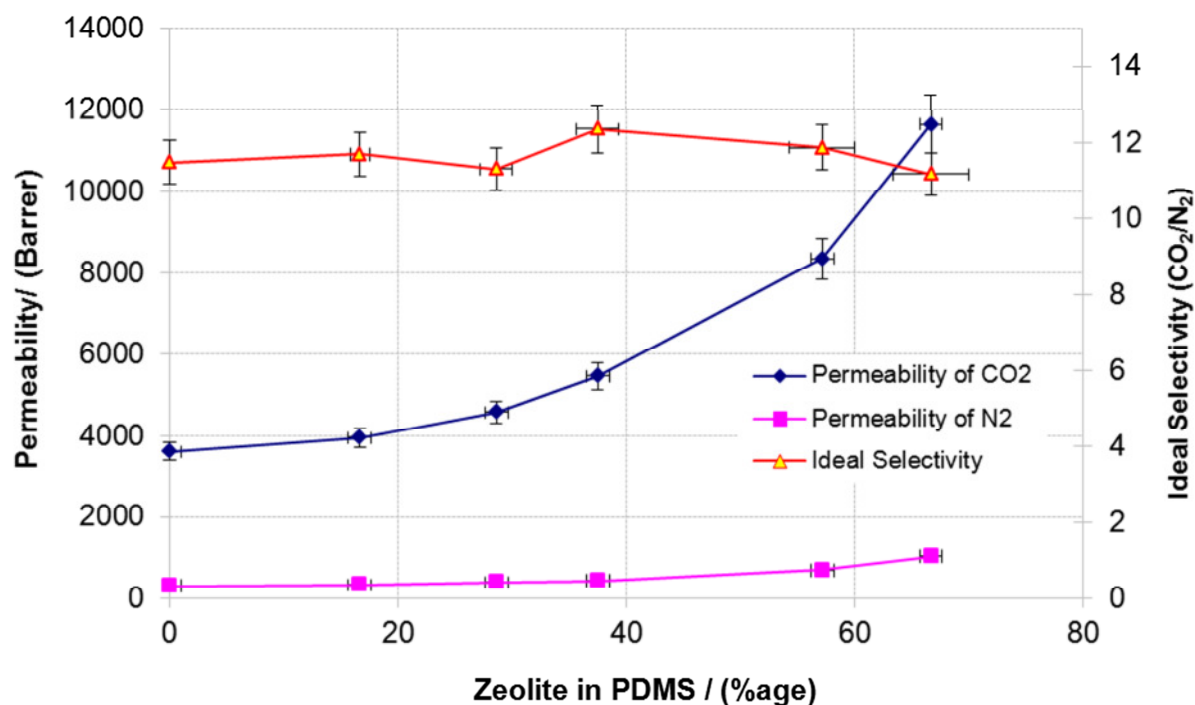
3.2 Single Gas Permeabilities:

Fig. 3: Single gas permeability and ideal separation factor for CO_2 and N_2 as a function of Zeolite Loading in PDMS

The variation in the permeability values of CO_2 and N_2 in PDMS membranes filled with zeolite (ZSM-5) with respect to the zeolite loading (wt.%) are shown in **Fig.3**. An increase of the permeability of CO_2 in the zeolite–PDMS mixed matrix membranes was observed in the cases investigated. By increasing the percentage of zeolite in PDMS the permeability coefficients increases gradually up to 38 % filled membranes and afterwards it increases strongly.

Furthermore, the increase in CO_2 and N_2 permeability could be elucidated by two different factors. The first one seems to prove the existence of positive adsorptive interactions between zeolite and gas molecules as was also indicated in adsorption isotherms **Fig2**. That leads to the higher adsorption of gas on the zeolite–polymer interfaces and this may provide a driving

4

force for the molecules, i.e. a reservoir effect, leading to an increase in the permeability of the mixed matrix membranes.

It might also be explained on the basis of 'Sieve-in-a-cage' morphology that means the interface exits beyond the dispersed phase. This zone of influence comprises of a void or high free volume phase or a rigidified/compressed region of the polymer matrix **[5]**. Frequent examples are available in literature regarding this undesirable morphology **[6]**.
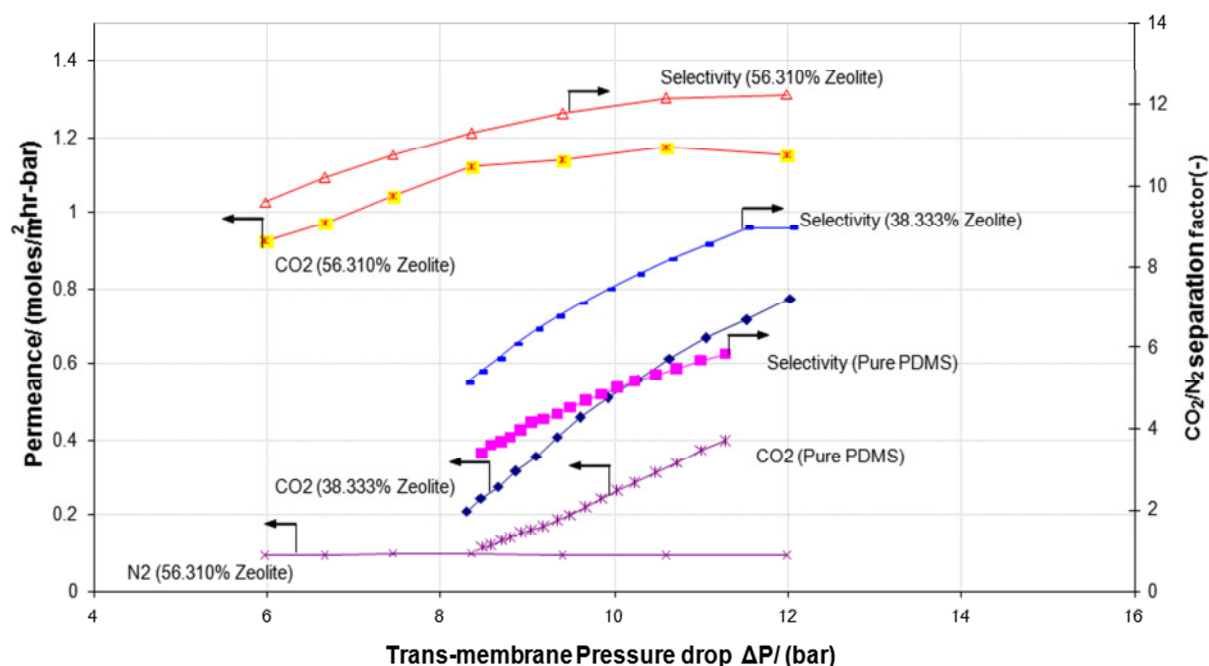
3.3 Mixtures of Gases:

Fig. 4: CO_2 and N_2 permeance and separation factor for different zeolite filled membranes as a function of trans-membrane pressure drop (Feed Composition 50 Vol% CO_2).

Fig.4 shows the effects of trans-membrane pressure drop on CO_2-N_2 permeance and separation factors (feed composition of 50 vol % CO_2) of different zeolite filled mixed matrix membranes. The pure gas permeabilities of non-adsorbable gases such as He, N_2, and O_2 are well described by Arrhenius plots corresponding to the activated diffusion model in micropores **[7]**.

Just as expected, all experimental data indicated an increase in the permeance of CO_2-N_2 with the rise of the feed pressure with corresponding increase in zeolite content in the membrane. It could be explained as increased mobility of the permeating molecules in the bulk feed solution, which results in higher partial pressure and provide greater driving force for the permeating components. Also, the increased mobility of the permeating molecules within the

5

membrane will facilitate the diffusion of the components. In the case of zeolite filled membranes, the variation of the interface between polymer–zeolite induced by the rise of pressure might play a role as well.
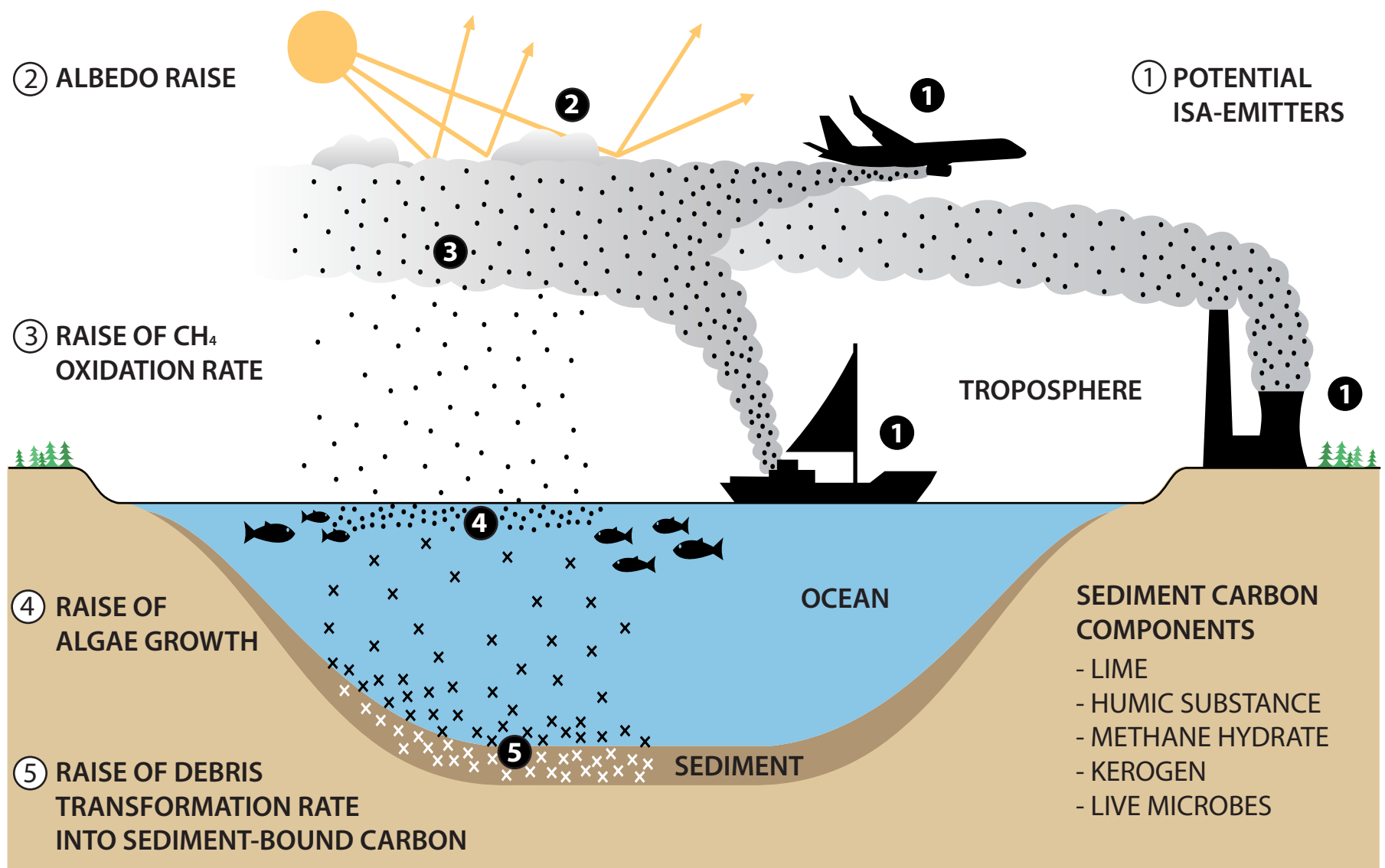
4. Conclusion:

Mixed matrix membranes have been prepared using zeolite (ZSM-5) and rubbery polymer PDMS (Polydimethylsiloxane) in different compositions. The ideal separation factor for CO_2/N_2 stays constant for all zeolite-filled membranes .However, the permeability of CO_2 and N_2 increased almost three times in case of 66 % zeolite filled membrane compare to pure silicone membrane. The effect of pressure on the permeance of CO_2 and N_2 is also investigated for mixture of gases, and an increasing effect with pressure on CO_2 permeance and separation factor has also been observed.

References :

[1]   W.J. Koros, G.K. Fleming, Membrane-based gas separation, J. Membr. Sci. 83 (1993) 1.

[2]   S.A Stern, Polymers for gas separation: The next decade, J. Membr.Sci. 94 (1994) 1.

[3]   B. Freeman, I. Pinnau, Separation of gases using solubility-selective polymers, Trends Polym. Sci 5 (1997) 167.

[4]   M. Jia, K.V. Pienemann and R.D Behling, Molecular sieving effect of the zeolite-filled silicon rubber membranes in gas permeation. In.: *Journal of Membrane Science, 57 (1991) 289-296.*

[5]   T. Moore, W. Koros, Non-ideal effects in organic-inorganic materials for gas   separation membranes. In.: *Journal of Molecular structure,* 739 (2005) 87-98.

[6]   R. Mahajan, W. Koros, Polym. Eng. Sci. 42 (2002) 1420.

[7]   R. J . R. UHLHORN, K. KEIZER and A. J . BURGGRAAF, *J. Membr. Sci.* **66** (1992) 241.
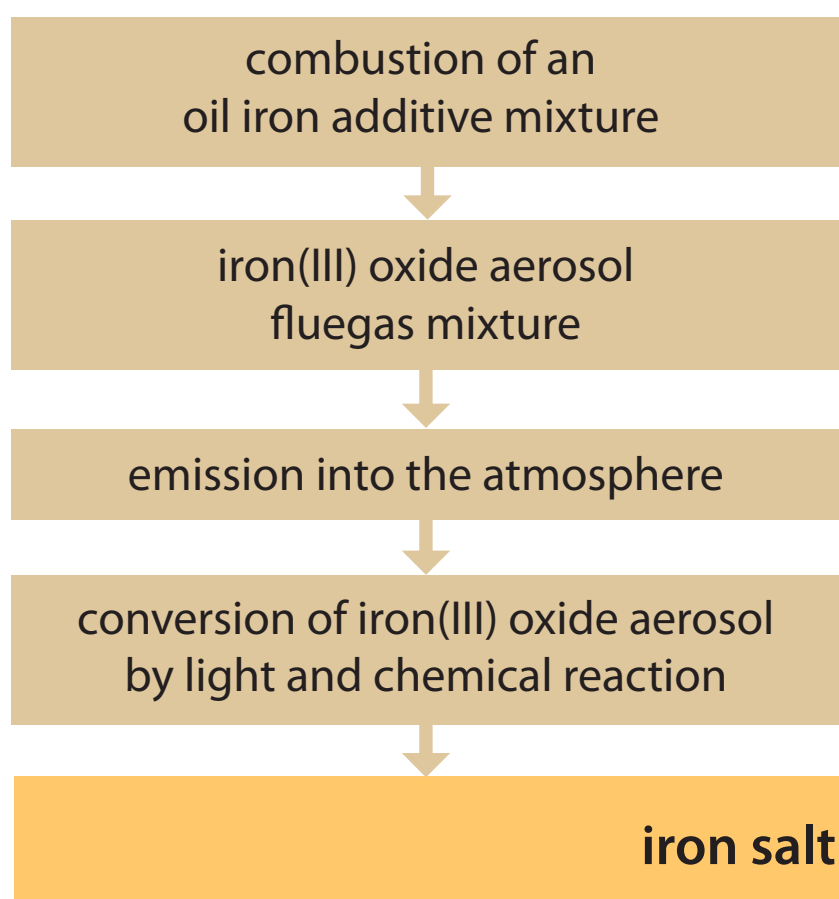
6

CO₂- and CH₄- CCS by Iron Salt Aerosol (ISA)

Introduction of a permanent raise of the CH₄ oxidation rate, cloud-albedo and
CO₂ -transformation into sediment-bound carbon by ISA

② **ALBEDO RAISE**

① **POTENTIAL ISA-EMITTERS**

③ **RAISE OF CH₄ OXIDATION RATE**

TROPOSPHERE

④ **RAISE OF ALGAE GROWTH**

OCEAN

SEDIMENT CARBON COMPONENTS
- LIME
- HUMIC SUBSTANCE
- METHANE HYDRATE
- KEROGEN
- LIVE MICROBES

⑤ **RAISE OF DEBRIS TRANSFORMATION RATE INTO SEDIMENT-BOUND CARBON**

SEDIMENT

ISA-Process

Technical Production of Atmospheric Iron Salt Aerosol (ISA)

Variant A

combustion of an
oil iron additive mixture

↓

iron(III) oxide aerosol
fluegas mixture

↓

emission into the atmosphere

↓

conversion of iron(III) oxide aerosol
by light and chemical reaction

↓

Variant B

salt water electrolysis

↓

reaction of chlorine gas
with hot iron scrap

↓

gaseous iron(III) chloride

↓

emission into the atmosphere

↓

conversion of gaseous iron(III) chloride
by condensation and hydrolysis

↓

iron salt aerosol (ISA)

CO$_2$ and CH$_4$ CCS by iron salt aerosol (ISA): Enduring carbon burial within the oceanic sediment by coal power plant fluegas, traffic systems and "cloud whitening"

Franz D. Oeste, gM-Ingenieurbüro, D-35274 Kirchhain, Germany
Ernst Ries, Ries Consulting GmbH u. Co. Betriebs KG, D-36154 Hosenfeld, Germany

The operation of the ISA process aims to capture and store the CO$_2$ and CH$_4$ carbon (CCS). With the exception of the of **i**ron **s**alt **a**erosol (ISA) generation step the technical ISA-Process is almost identical to the carbon sequestering process that determined the ice age carbon cycle. The ice age carbon cycle was accelerated by the increased transfer- and burial-rate of atmospheric CO$_2$ and CH$_4$ carbon into the oceanic sediments. The lowered greenhouse gas level dropped the climate temperature. The ice age climate was generated by excessive elevation of dust, developing in small parts into ISA. The technical ISA-Process mimics this ice age process by technical generation of ISA.

The ISA triggered the carbon burial and activated the glacial epoch. Data collected from Antarctic and Greenlandic ice core samples, dating back approximately 800,000 years, give transparency to definite correlations between the atmospheric contents of dust, both greenhouse gases CO$_2$ and CH$_4$ and the temperature:
High dust content epochs (up to 50x present day levels) pushed the concentration levels of CH$_4$, CO$_2$, as well the overall global temperature, down to glacial levels. Contrary, the warm inter-glacial periods are characterized by low dust or even dust-free periods. These periods are characterized by high CH$_4$- and CO$_2$-levels resulting in temperature increases within Europe and North America to subtropic conditions[1A]. In reference to the glacial-interglacial CO$_2$ change John C. Martin published his famous "Iron Hypothesis"[1B] concerning the biological activation of green plankton growth by iron.

The reasoning behind this phenomenon are small amounts of ISA contained within the dust. As powerful oxidation tool within the troposphere and fertilizing tool at the ocean surfaces ISA accelerated the transfer of the gaseous carbon phases from the planets atmosphere into the condensed carbon state within the oceanic sediments. The natural ISA-driven carbon burial process, may be devided into five definite steps:

1) ISA generation occurs through dust production within the troposphere as a result of aeolic movement of soil particles. Atmospheric ingredients, such as sulphur- and chlorine-compounds, NO$_x$, organic acids and water vapour change small reactive iron oxide fractions of every dust particle into photo-oxidant acting water soluble iron salts (ISA).

2) The ISA content triggers a drop of the atmospheric CH$_4$ concentration level by generation of hydroxyl and chlorine radicals. These are the only oxidants in the lower atmosphere with the ability to initiate methane oxidation. ISA generates the radicals mainly during daytime by the Photo Fenton oxidation cycle and during nighttime by the Fenton reaction. Essentials for the Fenton reaction beside ISA are tropospheric chloride, hydrogen, peroxide and sunlight. The Photo Fenton reaction is known as most powerful oxidizing tool. It has received much attention in different technical processes: Decomposition of resistant organics in drinking water, wastewater, tooth whitening, chlorine production, photography[2-8].
Additional, tropospheric organics of low vapour pressure adsorb on ISA and become photo-oxidized by ISA. In the absence of ISA these organics consume the radical oxidants hydroxyl and chlorine. This kind of ISA action lowers the atmospheric radical oxidant consumption followed by an increased radical level. This level elevation of the CH$_4$ radical oxidants hydroxyl and chlorine additional triggers the CH$_4$ level drop. Additional the elevated halogene radical level lowers the tropospheric concentration of ozone, a further greenhouse gas.
The main sources of the ISA-generated chlorine radicals are sea spray chloride and hydrogen chloride. Hydrogen chloride, produced by the CH$_4$ chlorine radical reaction, is washed out from the atmosphere by precipitation in the absence of ISA. During ISA epoches hydrogen chloride is re-oxidized to chlorine radicals by the ISA Photo-Fenton-Cycle preventing chlorine loss from the atmosphere by the wash-out of hydrogen chloride[9].

3) Dust and ISA content within the dust aerosol initiate a denser and wider spread cloud cover by multiplying the cloud condensation nuclei[10]. This initiates an additional climate cooling effect by increasing the level of sunshine reflection.

4) After several days and weeks the ISA has left the troposphere by sorption on cloude ice crystals precipitating as rain or snow all over the ocean surfaces. From the water surface the dissolved iron salt distributes within the oceanic photic zone. The ISA precipitation is quasi-continuous throughout extremely wide spread areas, generating very low specific iron input per ocean surface square by ISA. At this point CCS starts. As a consequence of the very high fertilization factor of dissolved iron on the mid-oceanic green plankton, however, due to the very low specific input per square, the following phyto plankton mass growth is small, and at fractions of lower than the 1 % level. Calculating the huge oceanic surfaces, where ISA realizes mass growth, 1 iron atom drives the transfer of up to 100,000 CO_2 carbon atoms from the gaseous phase into the condensed organic phase[11]. Even such low growth increase rates may transfer huge CO_2-carbon masses into condensed organic carbon. Phyto plankton represents the first link of the oceanic food chain; consequently the mass increase will cover the whole chain. Additional to the CO_2 carbon transfer increase into organic carbon the ISA fertilization generates an increase in CO_2 carbon transfer into carbonate carbon bound within skeletons, shells, corals and further carbonate bio-constructs.

5) The increase of sedimentation rate of the organic and carbonate carbon bound to dead organism on the ocean floor, from the former tropospheric CO_2 and CH_4 carbon will follow at least the same percentage that the iron-triggered oceanic food chain growth has increased. Due to its lower deep water concentration, the availability of free oxygen is restricted near the ocean floor. Due to the ISA-induced increase of the rain of oxygen consuming organic carbon the oxygen deficient anaerobic sediment localities at the ocean floor will spread. According to this fact anaerobic micro organisms will change sediment interior and even sediment surfaces of additional localities into anaerobic condition reducing the reoxidation of the organics. This again will increase the organic sediment load, changing it into kerogene, humic acids and CH_4 hydrate. Additional the anaerobic conditions increase the alkalinity to basic conditions by sulphate reduction to hydrogen sulfide and by nitrate reduction to ammonium and nitrogen. These pH changes to basic will trigger the Precipitation of additional CO_2 amounts within the anaerobic localities as lime. Reduction of every sulphate or nitrate ion will induce the transfer of at least one additional CO_2 molecule into this carbonate precipitate.

The technical ISA-Process

As mentioned above, except the ISA generation step, the world-wide patented ISA-Process runs on nearly identical tracks. The technical ISA generation may be realized by the variants 1a and 1b:

1a) A flow of a carrier gas like the flue gas of fossil power plants or of traffic vehicles or of any other carrier gas stream is enriched by iron oxide aerosol. This iron oxide aerosol is produced by the well known burning of mixtures of iron-organic oil additives, preferable ferrocene, with oil. The iron-organic oil additives are changed by combustion into iron oxide aerosol. This aerosol is composed of nanometer sized pure iron oxide particles of outstanding chemical reactivity. After emission into the atmosphere, this reactive iron oxide aerosol particles change quantitative and without any residue into water-soluble particulate and/or droplet ISA by reaction with the fluegas- and air-borne chemicals SO_2, NO_x, water, oxygen, chloride and organic acids like oxalic acid and catechols.

1b) A flow of carrier gas like the flue gas of fossil power plants or traffic vehicles or any other carrier gas stream is enriched by injection of gaseous iron(III) chloride. Within the carrier gas iron(III) chloride change into ISA by condensation and hydrolysation. Preferable the gaseous iron(III) chloride is produced at the emission locality by simple reaction of hot iron scrap with gaseous chlorine. This chlorine can be produced there by salt water electrolysis. This kind of ISA production may utilize the electric energy during day times of low electric power consumption.

All following steps of the technical ISA-Process are in principle the same as in the glacial ISA process described above. Differing to nature the efficiency of the technical ISA process is by orders of magnitude higher than that of natural dust. Some reasons why ISA shall have orders of magnitude higher efficiency than natural dust are:

- Artificial ISA is composed of nanometer-sized particles; natural dust particle diameters are of micrometer size. This effect raises the chemical activity of artificial ISA.
- Due to their low velocity free falling artificial ISA particles stay and react much longer than natural dust particles within the troposphere. This effect elongates the duration of chemical activity raising the oxidation capacity per ISA iron atom.
- Artificial ISA are composed of pure iron salt. The iron salt content of natural dust particles is much lower than 1 percent. This effect raises the chemical activity of artificial ISA.
- Artificial ISA are easy dissolvable as requirement for consumability by the phyto plankton. Only small parts of the iron mineral fraction within natural dust are soluble. This effect raises the fertilizing capacity of artificial ISA.

We have different clues to calculate rough estimations about the efficiency of the ISA-process[11-14]:

a) 1 Atom of ISA iron has the ability to sequester up to 100,000 Atoms of CO_2-carbon; corresponding to 1 kg ISA iron (=17.86 mol) sequestering up to 79 t CO_2 (=1,786,000 mol)

b) 1 Atom ISA iron has the ability to initiate the oxidation of up to 100,000 CH_4 molecules; corresponding to 1 kg ISA iron (= 17.86 mol) oxidizing 29 t CH_4 (=1,786,000 mol). Within this calculation it should be considered, that the global warming potential (GWP) of CH_4 is more than 21 times that of CO_2[15) 16)]. 29 t of CH_4 have a GWP of about 600 t CO_2.

From this estimation we can calculate the possible quantitative potential and economy of the order of magnitude of the ISA-Process concerning its ability to initiate the oxidation of CH_4 into CO_2 and its ability to bury CO_2-carbon. Taking the above calculation we come to the conclusion, that 1 kg of iron in the form of ferrocene may eliminate up to about 600 to 700 t of CO_2-equivalents. 1 kg of iron corresponds to about 3 kg ferrocen oil additive or to about 3 kg iron(III) chloride. Then 1 kg of ferrocen or 1 kg of iron(III) chloride shall bury the carbon of up to about 100 to 200 t CO_2 equivalents. Calculating the price of ferrocene to about 50 €/kg, and the price of iron(III) chloride to lower 5 €/kg, the costs to bury the carbon of 100 t CO_2 equivalents without any harm to the environment and to the health of men will be even lower than 100 € in the case of ferrocene as ISA educt and even lower than 10 € in the case of iron(III) chloride as ISA educt.

In the order to bury the whole of CO_2 emission quantity of a coal power plant by ISA the necessary concentration of the ISA precursor alternatives iron(III) oxide or iron(III) chloride within the flue gas may fall short of 1 mg/Nm³ Fe; this would even apply in a brown coal power plant flue gas. Because the carbon burial location is independent on the greenhouse gas emission location, the ISA Process may be carried out in remote areas on the ocean or within deserts to keep away any harm to human health.

Climate chamber and bench scale research will have to be done to realize stable and quantitative data as a base for certification of the ISA process as CCS process. Certified, the ISA process would be a very useful tool for potential process owners and licence holders by compensating or even selling eco credits.

The ISA process has even the potential to overcome the climate warming problem and may be defined as geo-engineering process. Combined with the off-shore "cloud whitening" geo-engineering process[17)] by unmanned sea salt spray ships, the ISA process could improve the physical cloud whitening cooling by addition of the chemical and biological carbon burial of greenhouse gas carbon within an enduring ocean sediment storage as fuel- and lime-carbon sediment. The sea salt aerosol carrier gas stream of the cloud whitening process additional may act as carrier gas for ISA as well. This combined ISA cloud whitening action shall result in an extraordinary improvement of both processes: By the enrichment of ISA with sea salt chlorine the ISA process would gain effectivity. The cloud whitening process to reduce the global temperature would gain drastic improvement of economy and even ecology; we estimate that this advantage could reduce the number of the proposed fleet of sea salt spray ships for cloud whitening from the proposed 1,500 ships to 10 or lower, gaining as well CCS extension plus extension of the albedo increase by cloud cover extension.

References

1) A) van der Pluijm, B.A & Sefcik, L.T. 2007: Inquiries in global change, Unit 8a. Analysis of Vostok ice core data; November 14, 2007: http://www.globalchange.umich.edu/globalchange1/current/labsLab9/Vostok.htm
   B) Martin, J.H. 1990: Glacial-interglacial CO_2 change: The iron hypothesis; Paleooceanography. 5(1), pp. 1-13

2) Sattler, C. 2003: SOWARLA Solare Wasserreinigung von der Entwicklung in die Praxis; Deutsches Zentrum für Luft- und Raumfahrt (DLR) Inst. F. Technische Thermodynamik Solarforschung, Köln-Porz; www.ttz-lampoldshausen.de/ximages/27763praesentat.pdf

3) Prousek, J. et al. 2007: Fenton and Fenton-like AOPs for wastewater treatment: From-laboratory-to-plant-scale-application; Separation Science and Technology; 42(7), pp. 1505-1520

4) Anonym - Chairside Zahnaufhellungssystem 2009: „Die beste Zahnaufhellung die wir je hatten"; Druckschrift der Diskus Dental Europe B.V., 76275 Ettlingen; www.discusdental.com/de

5) Ling M. et al. 2006: Photochemical synthesis of chlorine gas from iron(III) and chloride solution; Journal of Photochemistry and Photobiology A: Chemistry, 183(1-2), pp. 126-132

6) Eder, J.M. 1880: Über die Zersetzung des Eisenchlorids und einiger organischer Ferridsalze; Monatshefte für Chemie, 1, Dezember 1880, pp. 755-762

7) Eder, J.M. 1881: Decomposition of ferric chloride and some ferric salts of organic acids by light; J. Chem. Soc. Abstr. 40, pp. 670-671

8) von Hübl, A.F. 1895: Der Platindruck, 1. Abschnitt. Das Platinpapier und seine Herstellung; Druck und Verlag von Wilhelm Knapp

9) Oeste, F.D. 2004: Climate cooling by interaction of natural or artificial loess dust with tropospheric methane; GeoLeipzig 2004, Joint Conference on the German Geological Society (DGG) and the Society of Geo-Sciences (GGW), 29th Sept. – 1st Oct. 2004, Leipzig.

10) Rosenfeld, D. et al. 2008: Flood or drought: How do aerosols affect precipitation? Science, 321, pp. 1309-1313

11) Duggen, S. et al. 2007: Subduction volcanic ash can fertilize the surface ocean and stimulate plankton growth: Evidence from biogeochemical experiments and satellite data; Geophysical Research Letters, 34 L01612, doi:10.1029/2006GL027522, pp. 1-5

12) Fabian, P. 1984: Atmosphäre und Umwelt; pp. 72-73, Springer-Verlag; ISBN 3-540-55773-3 – Anmerkung: P. Fabian counts a methane growth rate of about 2 % per year. After eruption of the iron salt bearing ash from mount Pinatubo in 1991 the methane growth rate dropped to zero. Then again the growth rate changed to positive values.

13) Australian Greenhouse Office 2005: Australian Government Department of Environment and Heritage Australian Greenhouse Office: Have methane levels stabilized? Hot topics in climate change science, topic 10, fig. 1, www.greenhouse.gov.au/science/hottopics/pubs/topic10.pdf

14) Gauci, V. et al. 2008: Halving of the northern wetland CH_4 source by a large Icelandic volcanic eruption; J. Geophys. Res., 113, G00A11,doi:10.1029/2007JG000499

15) Fabian, P. 2002: Atmosphäre und Umwelt; pp. 24, Springer-Verlag; ISBN 3-540-43361-6

16) Völker-Lehmkuhl, K. 2005: Praxis der Bilanzierung und Besteuerung von Emissionsrechten, p. 9, Erich Schmidt Verlag; ISBN 978-3-505-09310-6

17) A) Latham, J. 2002: Amelioration of global warming by controlled enhancement of the albedo and longevity of low-level maritime clouds; Atmos. Sci. Lett. 3, pp. 52-58
    B) Salter, S., Sortino, G. Latham, J. 2008: Sea-going hardware for the cloud albedo method of revising global warming; Phil. Trans. R. Soc. A366(1882), pp. 3989-4006

Reducing CO₂-Capture Costs in Combined-Cycles by Replacing Excess Air by Water Injection into the Compressed Stoechiometric Air and Water Vapour Condensation

Prof. Dr. techn. Reinhard Leithner
Institut für Wärme und Brennstofftechnik, Technische Universität Braunschweig,
Germany (www.wbt.ing.tu-bs.de, E-Mail: r.leithner@tu-bs.de)

Abstract

A possibility to reduce Carbon Capture Costs in Combined Gas- and Steam Turbine Cycles is the injection of water into the compressed air and vaporization by low temperature heat instead of using a high amount of excess air. If only stoechiometric air is used for a gas turbine, the allowable inlet temperatures would be exceeded. Therefore an additional mass flow has to be used, e. g. water vapor. If water is injected into the compressed air, it can be evaporated at partial pressure, i. e. at low temperatures. This offers a possibility to use low temperature waste heat or solar heat or geothermal heat in a combined cycle. In addition it offers the possibility to reduce the CO_2-capture costs because the exhaust gas of such a combined cycle only consists of water vapor, CO_2, N_2 and a negligible amount of O_2. After the condensation of water vapor only CO_2 and N_2 remain. That means that the CO_2-capture plant has to deal with a much lower amount of exhaust gas with higher CO_2 content. Finally three advantages coincide namely the use of low temperature heat for the vaporization of water in the compressed air, an increase of efficiency and the low mass flow in the CO_2-post combustion capture plant. This will result in additional efficiency gains by the reduction of CO_2-capture losses in the CO_2- post combustion capture plant.

Introduction

The Humid Air Turbine [HAT] cycle uses a gas turbine with intercooling by water evaporation avoiding a steam cycle as well as the STIG- or Cheng Cycle [Jones 1985], which uses the steam produced in a Heat Recovery Steam Generator - HRSG for injection into the combustion chamber of the gas turbine . The intention of the Solar- and Low temperature Heat-Combined Cycle-Solico/ Lotheco is different. Condensate from the flue gas is injected into the compressed air and evaporated by low temperature or solar heat at changing partial pressure but at lower temperatures as in the HRSG of a Cheng Cycle. In addition the air flow through the compressor is reduced to nearly stoechiometric values. This is possible, because the steam produced by the low temperature or solar heat reduces the adiabatic combustion temperature to allowable values. The heat of the flue gas after the gas turbine is used as in a usual combined cycle HRSG i.e. for a steam turbine (Rankine) cycle.

Facilitation of CO2-Capture out of Gas turbine exhaust gas

Figure 1 shows the flow diagram of such a Lotheco/ Solico-Cycle. After the compressor an aftercooler is heating up the compressed air-steam mixture before this mixture enters the combustion chamber of the gas turbine. After the aftercooler condensate is injected into the compressed air and evaporated at increasing partial pressure. The water flow injected depends on the allowable gas turbine inlet temperatures as can be seen on figure 5.
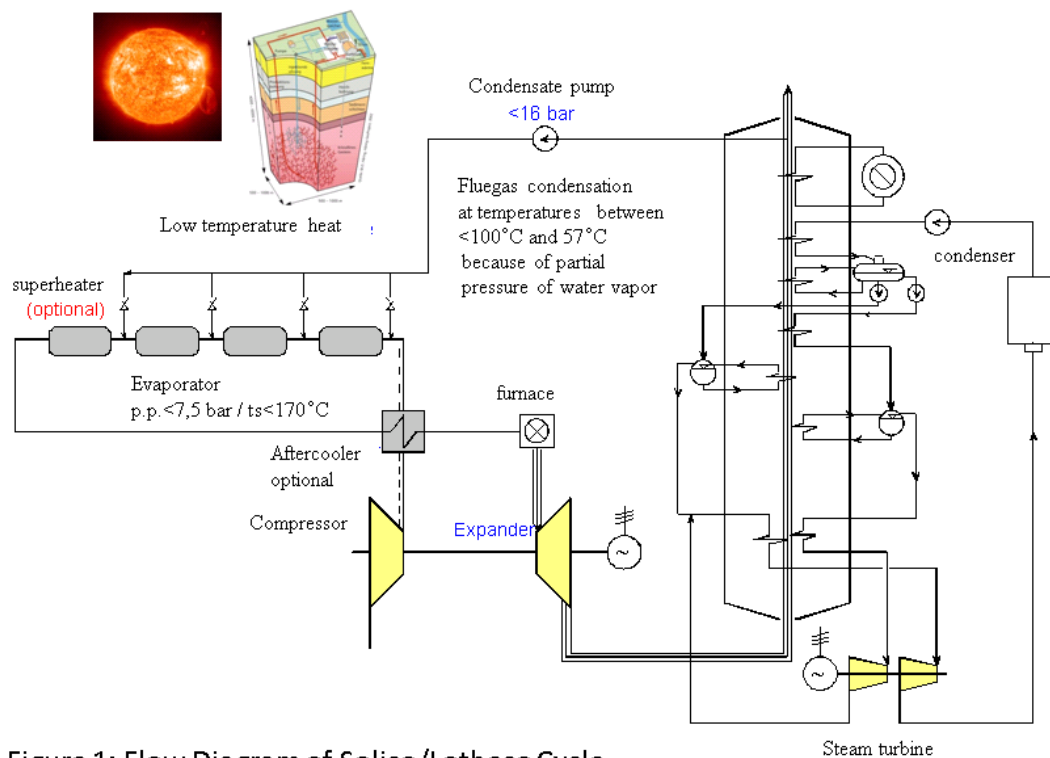

Figure 1: Flow Diagram of Solico/Lotheco Cycle

In Figure 2 a combined cycle using on Alstom GT10C gas turbine and a simple HRSG can be seen, which is used as basic cycle for the comparison.
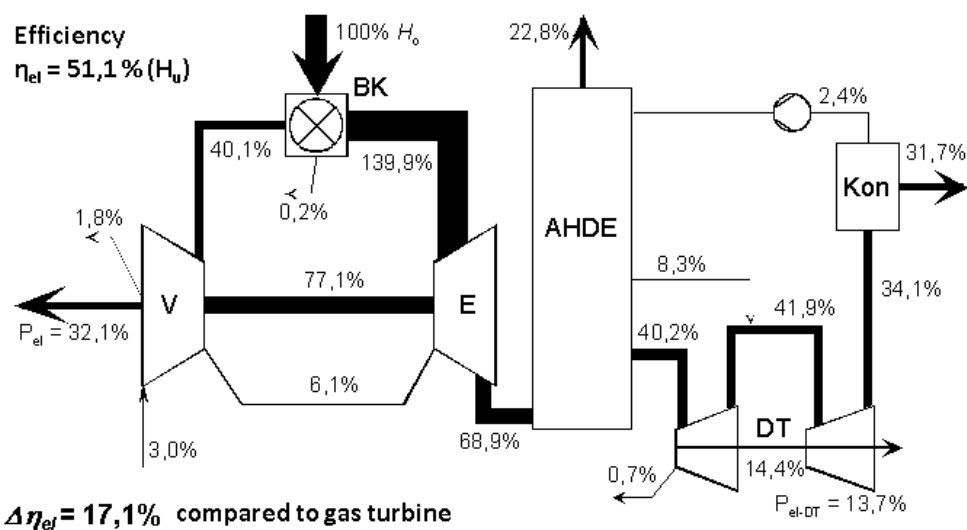

Figure 2: Flow Diagram of conventional Combined Cycle with Alstom GT 10C gas turbine

Figure 3 shows the Lotheco/ Solico-Cycle, which has an improved efficiency of 57.6 % related to the fuel flow compared with 51.1 % of the basic combined cycle.
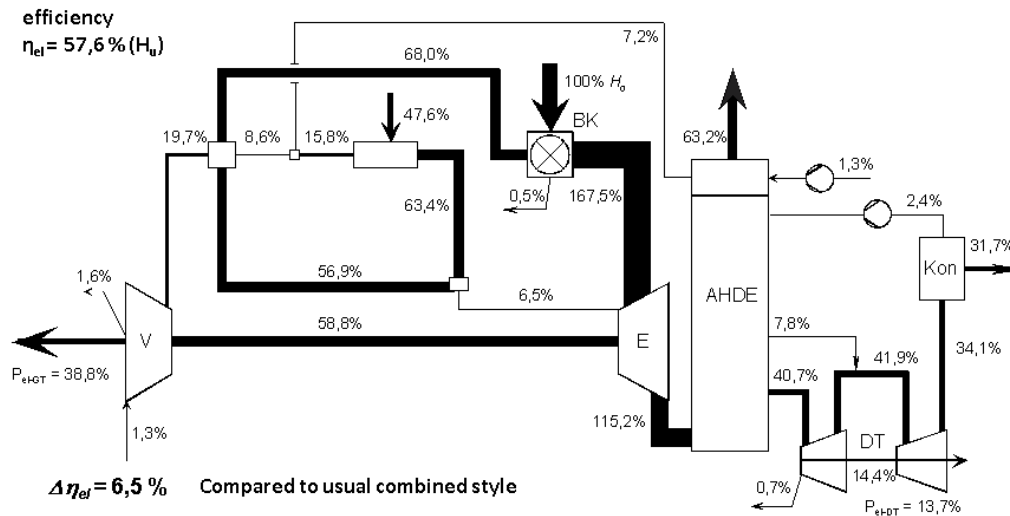

Figure 3: Energy Flow Diagram of Solico/Lotheco-Cycle using Alstom GT 10C gas turbine

In Figure 4 the adiabatic temperature at the combustion chamber outlet (= gas turbine inlet) is depicted over the excess air ratio. In addition the flue gas composition is given. The main part is N_2 followed by O_2 at excess air ratios above about 1.6 and then by CO_2 and water vapour.
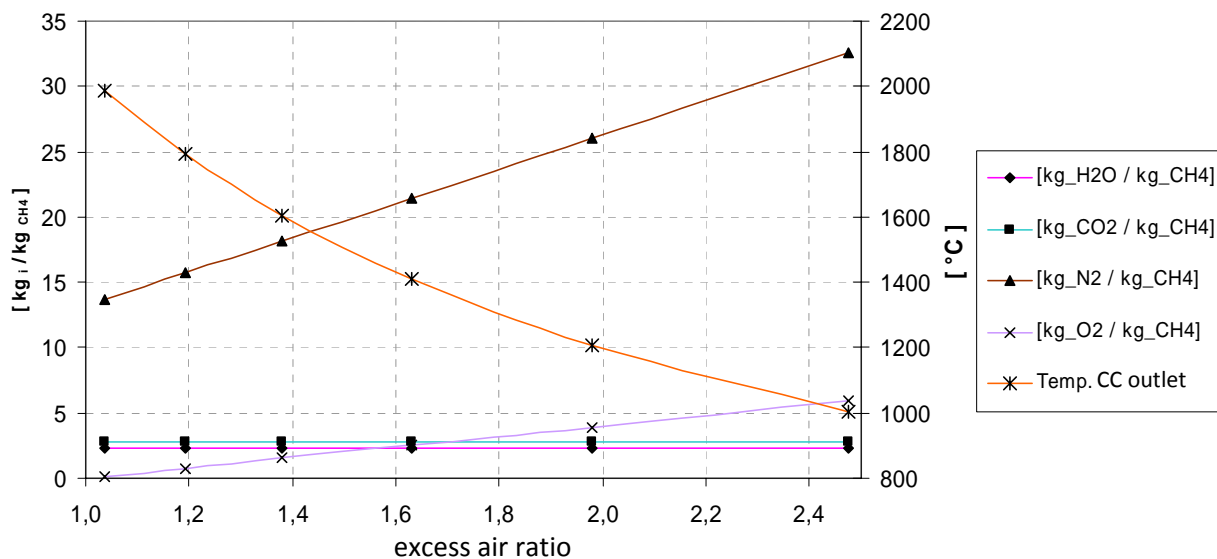

Figure 4: Concentrations of Flue Gas and Adiabatic Combustion Temperature Depending on Excess Air

Figure 5 reveals the advantage of using water vapour instead of excess air. N_2 is still the main part of the flue gas, but followed by high amounts of water vapour, which is at least partly condensed, so that CO_2 concentration is remarkably increased. O_2 is nearly negligible. So any CO_2-capture process starts at a much higher CO_2-concentration compared to a usual combined cycle with excess air.
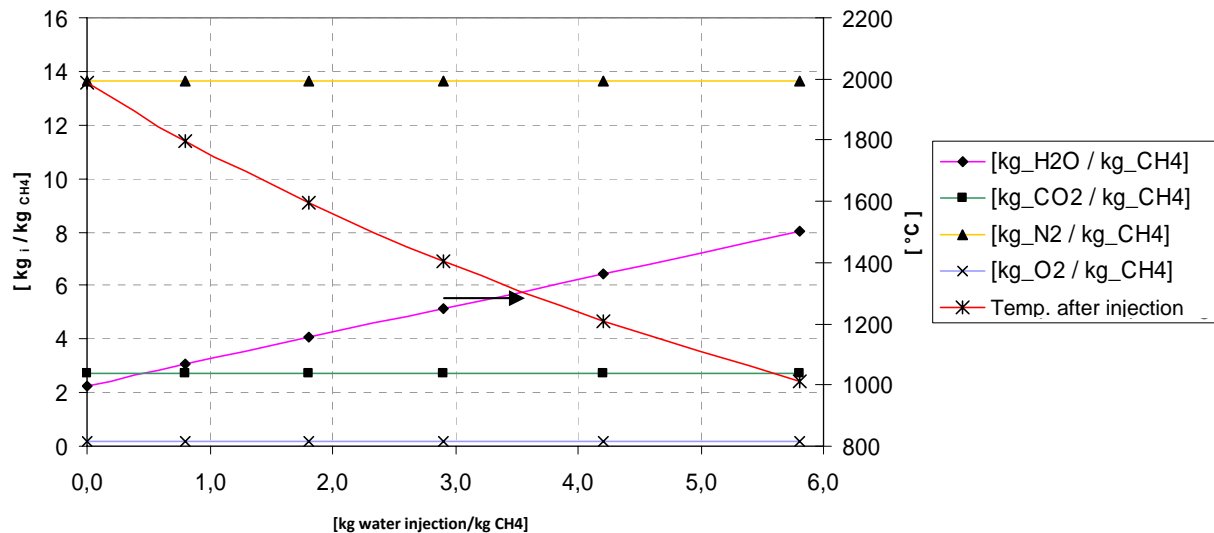
Figure 5: Concentrations of Flue Gas and Adiabatic Combustion Temperature Depending on Water Injection before Water Condensation

So water injection and evaporization by low temperature waste-, geothermal- or solar heat not only increases efficiency but also reduces penalty of CO_2-capture.

Literature

[Aronis 2005] Aronis N.: Analyse einer GuD-Anlage mit Wassereinspritzung und Einkopplung von Nieder-temperaturwärme. PhD-Thesis at IWBT, Technische Universität Braunschweig, VDI-Fortschrittberichte, Reihe 6, Energietechnik, 2005, ISBN: 3-18-352906-8

[Aronis 2004] Aronis, N., Leithner R.: Combined Cycle with low-quality heat integration and water injection into the compressed air, Energy, 2004

[Aronis 2003] Aronis, N., Leithner, R.: Thermodynamic analysis and economic evaluation of medium scale gas turbins based power plants, ECOS 2003 16th International Conference on Efficiency, Cost, Optimization, Simulation and Environmental Impact of Energy Systems, Kopenhagen, Dänemark

[Aronis 2002] Aronis,N., Leithner, R.: Combined Cycle with Low Quality Heat Integration and Water Injection into the Compressed Air, ECOS 2002, TU Berlin: ISBN: 3-00-009533-0, Berlin

[Leithner 2001] Leithner, R.Aronis, N.Kakaras, E.Doukelis, A.: Combined Cycle Power Plants with Integrated low-temperature Heat, VGB Conference "New Power Plant Concepts for Power and Heat Generation": Essen, 2001

[Aronis 2000] Aronis N., Leithner R. and Witkowski A.: New Combined Cycle with Integrated Low Temperature Heat or Solar Heat, International Conference on Efficiency, Cost, Optimisation, Simulation and Environmentel Aspects of Energy and: Process Systems, ECOS 2000, Enschede, Niederlande

[Leithner 1996] Leithner R.: Solar- und Niedertemperaturwärme-Kombianlage-Solico, DE 196 52 349.4

[HAT] United States Patent 5349810

[Jones 1985] J. Lloyo Jones, Dr. Chung-Nan Chang, Dr. Ramarao V. Digumarthi, Dr. William M Conlon: Design and Construction of the first commercial Cheng Cycle Series 7 Cogeneration Plant, ASME 85-IGT-122, 1985

Ni Hydrotalcites materials for catalytic reaction

F.Touahra[1], K. Bachari[2], A. Saadi[1], O. Cherifi[1], <u>D. Halliche</u>[1]*

[1]*Laboratoire de Chimie du Gaz Naturel, Faculté de Chimie, USTHB, BP32, El-Alia, Alger, Algeria.*
[2]*Centre de recherches scientifiques (CRAPC), BP 248, Alger, 16004, Algeria.*

1. Introduction

CO_2 reforming of methane shows a growing interest from both industrial and environmental viewpoint. From an environmental perspective, CO_2 and CH_4 are undesirable greenhouse gases and both are consumed by the proposed reaction. From the industrial point of view, the reaction allows to transform these invaluable gases into synthesis gas with a low H_2/CO ratio adequate for Fischer–Tropsch synthesis [1,2]. The CO_2 reforming reaction has been studied over numerous supported metal catalysts including Ni-based catalysts. The main drawback of this catalyst is its poor stability caused, mainly, by a high coking-rate. Thus, basic supports and highly dispersed Ni catalysts have been used to lower the rate of coke deposition [3].

In this context, the objective of this work is to study the influence of the catalyst composition on the catalytic properties of NiAl- R, or R=Ni^{2+}/Al^{3+} (R=2, 3, 5, 8 and 10) for CO2 reforming of methane.

The catalytic activity runs were carried out at atmospheric pressure, was carried out using an engine fixed-bed quartz U-tube, Before each catalytic test, the samples were reduced in situ at 600°C during 14h under hydrogen, After the reduction, a reactional mixture consisting of $CH_4/CO_2/Ar$ with a molar ratio of CH_4 and CO_2 in proportion 1:1 was used for the reaction tests, at a total flow rate of 1.5 l/h. (According to a speed of heating equal to 5°C/min). The water produced in the reaction was condensed out and the reacting gases and products were analyzed with TCD chromatograph.

2. Catalysts preparation

The corresponding NiAl-R samples were prepared prepared by a standard Co-precipitation procedure using two solutions. The first solution contained Ni $(NO_3)_2,6H_2O$ and Al $(NO_3)_2$, $9H_2O$, with a different molar ratio Ni:Al (R= 2,3,5,8 and 10) and total metal ion concentration of 1.0 mol.l^{-1}. The second solution contained NaOH and Na_2CO_3 in adequate concentrations to obtain the total precipitation of Al and Ni. Was controlled to maintain reaction pH = 12. When the addition was complete, the mixture was stirred for a further 1.5 h, durring which time the pH was still maintained constant.the product was then filtered off, washed thoroughly with distilled water and dried overnight at 60 °C. The dried and powdered product was formed into pellets and calcined at 800 °C for 6 h in air.

3. Characterizations

The Chemical composition of the calcined samples was determined by ICP method and the data obtained confirmed that the values of R were close to the intended value (Table-1).

Table-1: Chemical analysis and chemical formulas of Calcined catalysts NiAl-R with 800°C

Catalysts	M^{+2}/M^{+3}	Chemical formula
NiAl-2	1.94	$Ni_{0.66}Al_{0.34}$
NiAl-3	2.70	$Ni_{0.73}Al_{0.27}$
NiAl-5	4.88	$Ni_{0.83}Al_{0.17}$
NiAl-8	7.33	$Ni_{0.88}Al_{0.12}$
NiAl-10	9.00	$Ni_{0.90}Al_{0.10}$

X-Ray powder diffraction patterns were recorded in a X'PERT PRO MPD diffractometer using CuKα radiation and varying 2θ values from 5 to 70°C.   The XRD patterns of the NiAl-R (R=2, 3, 5, 8 and 10) non calcined are shown in fig.1. All these peaks when R ≤ 5
are characteristics of clay mineral (hydrotalcite) having a layered structure, which is not clearly evidenced for samples with R > 5.
The X-ray diffraction patterns of all calcined samples are shown in fig.2.

After calcinations at 800°C. The mixed oxides showed sharp diffraction peaks due to NiO

and $NiAl_2O_4$ spinel phase.

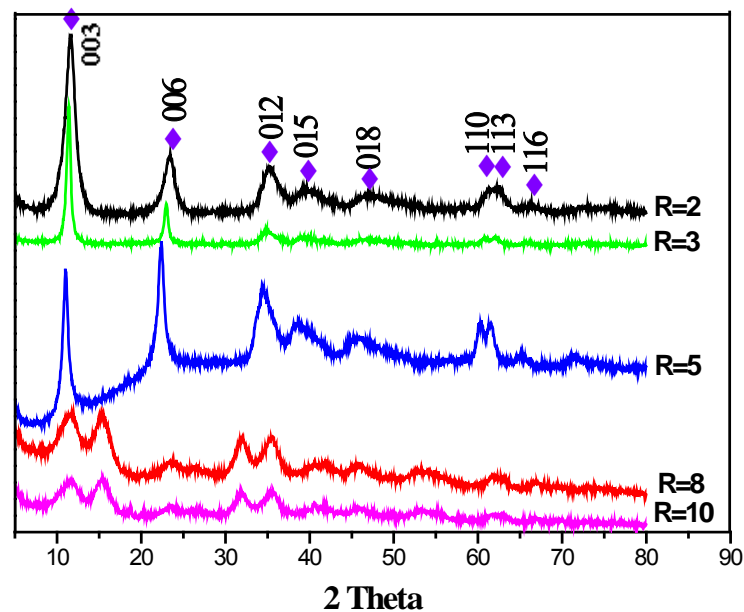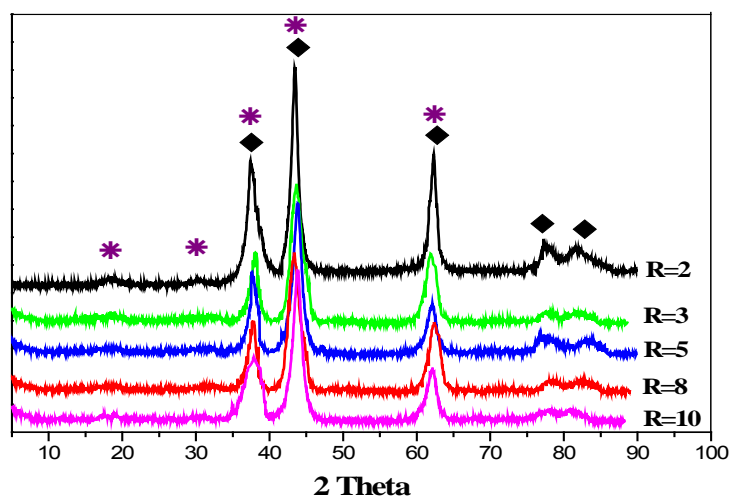Fig.1:   XRD patterns of the NiAl-R non calcined

Fig.2 X-ray diffraction patterns NiAl-R
after calcination at 800°C.

Surface area and mesoporous structure of the catalysts were determined by adsorption/ desorption of nitrogen at -196 C using the BET and BJH (Barret, Joyner, Hallenda) methods were used for evaluation of surface area and pore size distribution, respectively. The lower surface areas values were obtained for the samples with lower Ni^{2+}/Al^{3+} molar ratios.

FTIR spectra in the region 4000-400 cm^{-1} were obtained with PERKIN-Elmer spectrometer, using KBr pellet technique.
on the non-calcined samples (Fig.3), the obtained spectra reproduce the general features often reported for hydrotalcites –like compounds.
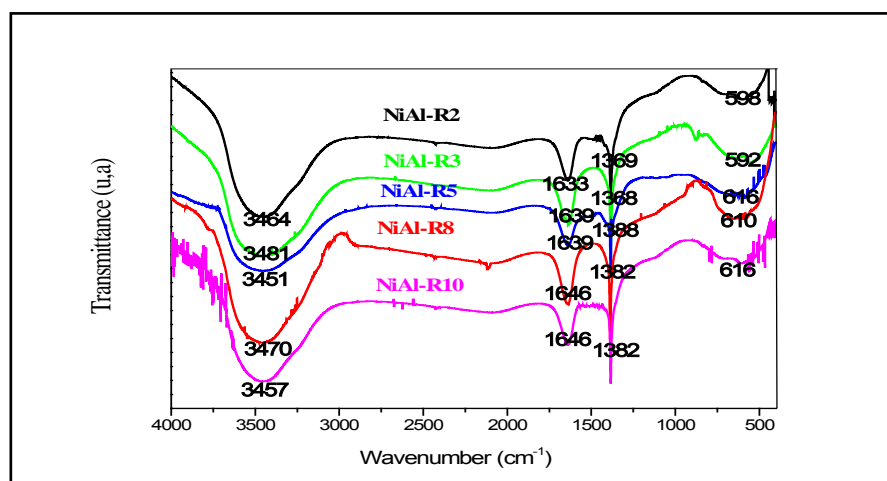

Fig. 3. FT-IR spectra of NiAl-R non calcined.

The calcined samples were analyzed by temperature programmed reduction (TPR) carried out at atmospheric pressure under H_2 atmosphere in the range of 25 to 900°C (fig.4) .TheTPR profiles of samples showed a reduction peaks (around 400-600 and 800°C) which were shifted at the highest temperatures when R-values increased. The reducibility may depend on the degree of aggregation of the nickel oxide.
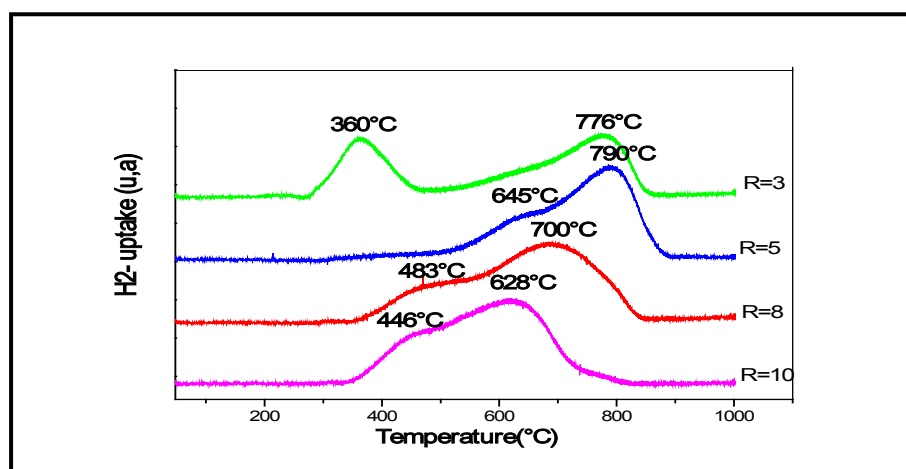

Fig.4. TPR profiles for NiAl–R samples calcined at 800 °C;

4. Catalyst characterization

Catalysts stability was carried out at 650°C and a 1:1 CO_2/CH_4 feed ratio. It was found that performances of catalysts after 8 h in reaction, within this period nor or little deactivation takes place and a relatively high CH_4 conversions were obtained such as: 69.8%, 70.0%, 70.3%, 71.1% and 75.4 % respectively on $Ni_{0.66}Al_{0.34}$, $Ni_{0.83}Al_{0.17}$, $Ni_{0.88}Al_{0.12}$, $Ni_{0.88}Al_{0.12}$ and $Ni_{0.90}Al_{0.10}$ catalysts. In another hand, the rate of CO formation obtained were about 10.7×10^{-2} mol/g.h, 10.8×10^{-2}, 13.8×10^{-2} mol/g.h, 14.0×10^{-2} mol/g and 17.9×10^{-2} mol/g.h respectively. As can be seen, the better catalytic performances were obtained when R > 5 which can be probably related to the higher nickel content in these cases.

References
[1]. Ross, J.R.H., Catal. Today ,vol. 100, 2005, p.151.
[2]. Wang, S., Lu G.Q., Millar G.J., Energy Fuels, vol. 10, 1996, p. 896.
[3]. Takehira, K., Shishido, T., Kondo, M., J.Catal., vol.207, 2002 , p.307.

Chemical looping combustion of syngas in packed beds

Paul Hamers, Stijn Smits, Fausto Gallucci, Martin van Sint Annaland,

Multiphase Reactors, Chemical Engineering and Chemistry, Eindhoven University of Technology, Eindhoven, The Netherlands;

Chemical-looping combustion (CLC) has been demonstrated as an interesting technology for energy production with great potential to integrate CO_2 capture with low energy penalties. CLC of methane carried out in dynamically operated packed beds has been developed in our previous work (Noorman, 2009). In this process the oxygen for combustion is provided by an oxygen carrier, which is oxidized when air is blown through the packed bed reactor. This oxidation reaction is an exothermic reaction and power is generated from the hot exhaust gas. The oxygen carrier is afterwards reduced via reaction with a fuel and a product gas mixture of CO_2/H_2O is obtained, circumventing energy intensive separation steps for the CO_2 capture.

In the present work, the fixed bed CLC process has been further developed by investigating the use of syngas (e.g. produced by coal or biomass gasification) as fuel. In particular, the performance of different oxygen carriers including naturally available ilmenite has been theoretically investigated and the maximum temperature rise during CLC in packed beds. It has been found that oxidation of ilmenite could give a temperature rise up to 500°C (depending on the composition of the material). Reduction of ilmenite with CO is an exothermic reaction and reduction with H_2 is an endothermic reaction. The temperature profile during reduction is thus dependent on the H_2/CO ratio and the kinetic rates of the two reduction reactions. Axial temperature profiles in packed bed CLC have been studied in detail using numerical reactor models.

The stability after many alternating reduction/oxidation cycles of ilmenite for CLC of syngas has been also investigated with TGA experiments.